Electronic Supplementary Information

Navigating Chemical Reaction Space – Application to DNA-encoded Chemistry

*Silvia Chines,[a] Christiane Ehrt,[b] Marco Potowski,[a,c] Felix Biesenkamp,[a] Lars Grützbach,[a] Susanne Brunner,[d] Frederik van den Broek,[e] Shilpa Bali,[e] Katja Ickstadt,[d] and Andreas Brunschweiger.[a]**

[a.] *TU Dortmund University, Department of Chemical Biology, Otto-Hahn-Str. 6, 44227, Dortmund, Germany.*

[b.] *Universität Hamburg, Bundesstr. 43, 20146, Hamburg, Germany.*

[c.] *Current address: Serengen GmbH, Emil-Figge-Str. 76a, 44227, Dortmund, Germany.*

[d.] *TU Dortmund University, Department of Statistics, Vogelpothsweg 87, 44227, Dortmund, Germany.*

[e.] *Elsevier B.V., Radarweg 29, 1043 NX Amsterdam, The Netherlands.*

Table of Contents Page

KNIME workflow

The final KNIME workflow for this project was executed on a machine with the following characteristics and it was fully processed in approximately two hours:

Memory: 7.6 GB
Processor: Intel® Core™ i7-6498DU CPU @ 2.50GHz × 4
Graphics: Mesa Intel® HD Graphics 510 (SKL GT1)

This ESI is intended for educational purposes, to help chemists with setting up or modifying the workflow according to their needs. Therefore, not only the link for the download is provided (https://kni.me/s/R8gFmu9rgDDqVxtp) but also the description with figures of each stage. Additionally, an initial sample of 100 reactions is provided with the workflow to test its functionalities at the same link. In the workflow, unique features of KNIME have been employed, such as *metanodes* and *components*, for compressing the length of the workflow and for the interactive views, respectively.

Input data

The first part of the algorithm includes a small workflow for a preliminary data curation. This workflow was processed at Reaxys[§] and included a selection according to completeness of reaction description and commercial availability of reaction components. Subsequently, the output table was used by a *Table Reader* and processed via the "temperature extraction" section. In this section, a combination of *String Replacer*, *Cell Splitter* and *Rule-based Row Splitter* nodes broke down the different delimiters in the column "Temperature (RXD.T)" and standardized the values (Figure S1).

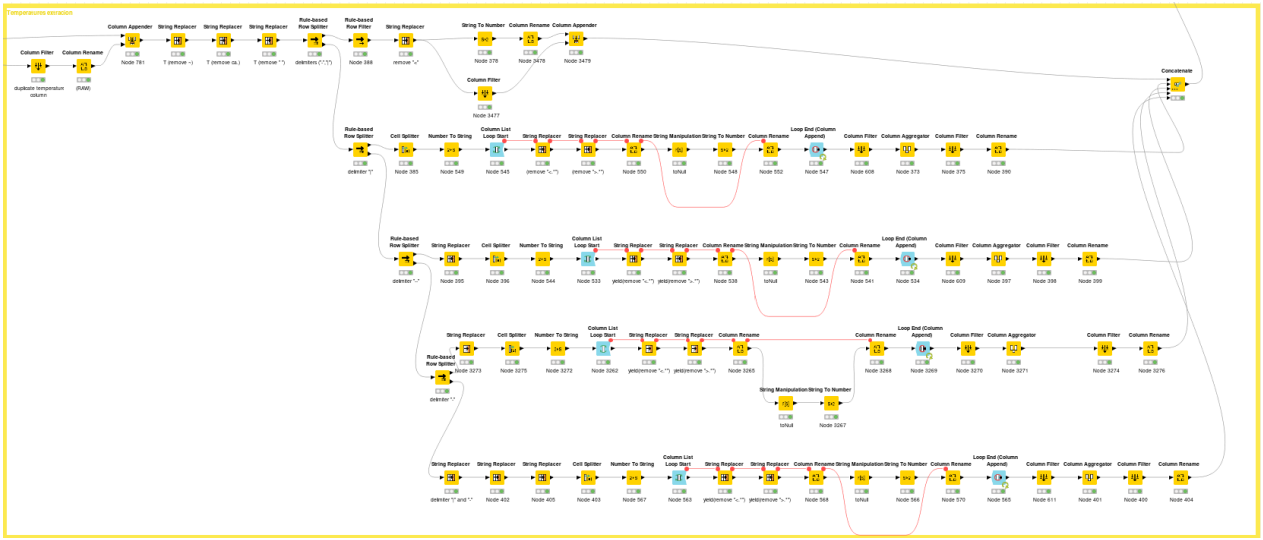

Fig. S1. KNIME workflow for the temperature extraction.

Module I – filter by condition

Reactions with temperature higher than 200°C were filtered out via a *Row Splitter* node. The next concern was about catalyst/reagents, which were merged together and named mediators by splitting and unpivoting them together. The workflow in Figure S2 was employed to score the reactions according to their mediator. For this all columns containing reagents or catalysts were looped using a *Column List Loop Start*, which subsequently processed all columns containing the pattern "*_Arr*". For this purpose, we compiled a list of reagents/catalysts based on the database and ranked the known ones according to literature-known DNA compatibility. One considered parameters in this step was the oxidation potential compared to the most sensible base Guanine, whose oxidation potential is 1.29 ± 0.03 V at neutral pH. The assigned scores ranged from 0 for proven incompatible mediators to 4 for proven compatible mediators. The values 1 and 3 were assigned to probable incompatible and compatible reagents/ catalysts, respectively, and the score 2 to unknow mediators. It is worth mentioning that mediators with mutagenic power were scored with 0 as well. An extract of the scored reactions according to their catalyst is listed in Table S1, while the complete list of scored reagents is available as KNIME report I in attachment to this ESI. Inside the loop, before and after the *Cell Replacer*, whose second input port was connected with the mediators table, we connected two *Column Rename* nodes. The

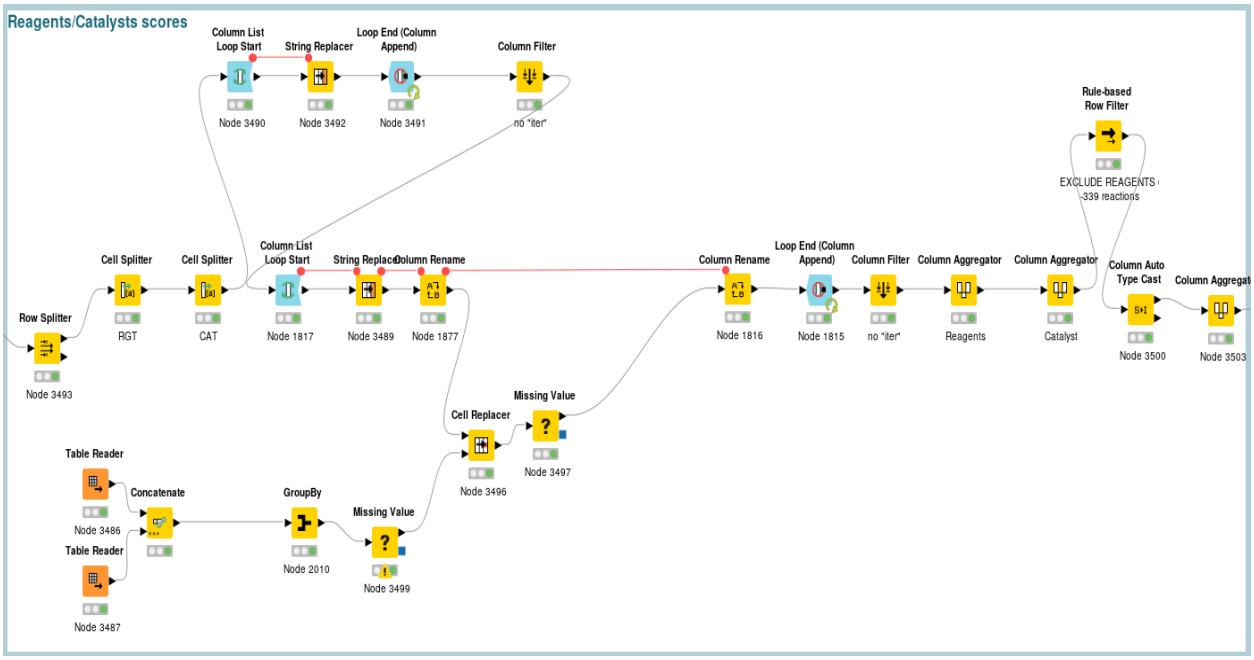

Fig. S2. KNIME workflow to score reactions according to their catalyst or reagent.

former always output the same column name "Arr", allowing the *Cell Replace* to actually process all columns, and the latter renamed the “Arr” column after the initial column name. After the loop, the iteration columns were filtered out, the column including the pattern **_Arr** were aggregated with a *Column Aggregator* using the “Minimum” as aggregation method and the reactions with reagent/catalyst score 0 were dismissed.

Table S1. Examples of scored reactions according to the respective mediator.[S1-S4]

reaction ID	score	names	reaction scheme	Ref.
34285291	4	acetic acid	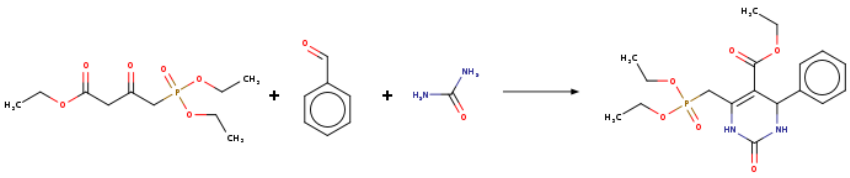	S1
38369343	4	L-proline	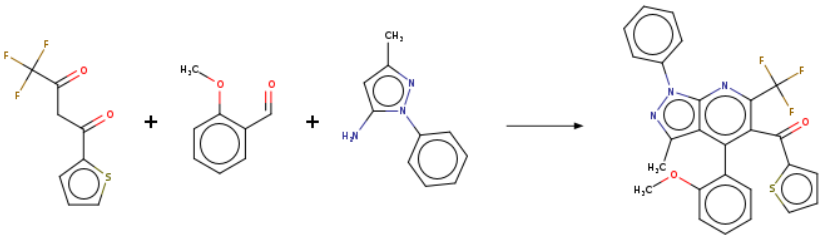	S2
47068944	0	2-mesityl-6,7-dihydro-5H-pyrrolo[2,1-c][1,2,4]triazol-2-ium chloride|potassium carbonate	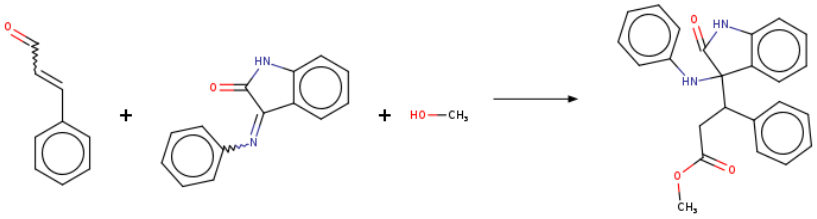	S3
5064401	0	potassium hydroxide|sodium hydroxide	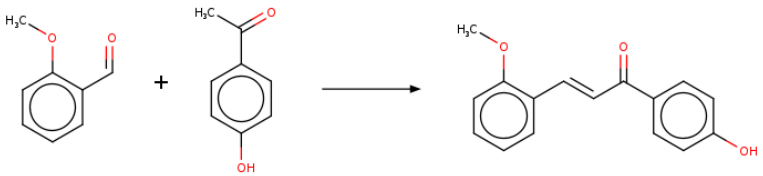	S4

The next step involved the prioritization of solvent by boiling point. Solvents with lower boiling points received a lower priority, because they are used less for the low volumes typically employed in DEL synthesis. For this purpose, a list of the identified solvent boiling points was compiled and a loop similar to the previous one was used to assign the respective boiling points to the reactions. Similarly, at the end the “Minimum” aggregation method was applied.
With all the conditions in hands, we firstly ordered the reactions by the Pareto Ranking node with the following settings:

- optimal range of temperature between 20°C and 80°C.
- maximize the mediators score
- maximize the solvents boiling point

The lack of the Pareto rank was a clear sign that at least one of these parameters was missing, so those reactions were excluded for safety. However, considering also those reactions could be a strategy to increase the size of the output.
A last Rule-based Row Splitter node was employed to filter out reactions with missing products or reactants.

Module II – filter by structure

The surviving 44178 reactions were unmapped via the Indigo *Reaction Automapper* node. After that, reactions yielding an acetal structure, which is less attractive in screening libraries due to questionable long-term storage stability, and reactions leaving the aldehyde moiety unreacted were excluded by a combination of the *MarvinSketch* and the *Substructure Matcher* node. For this purpose, the SMARTS patterns *[#8;X1]-[#6]-[#8;X1]* and *[#6H1]=[O;X1]* were generated by the *MarvinSketch* node and fed into the *Substructure Matcher* taking the "products" column into consideration and matching at least one query. The settings "Treat X as pseudoatom", "Ignore stereochemistry errors" and "Treat input query string as SMARTS" were flagged.

Complexes and salts removal

Reactions including metal complexes were excluded as well via a short loop based on a table of common metals in complexes (Table S2), matching them with a *String Replacer* node and excluding them with a *Row Splitter* node.

Table S2. Common metals in complexes.

Cu	*Mo*	*Co*
Fe	*W*	*Pt*
Mg	*Re*	*Y*
Mn	*Os*	*Ti*
Zn	*Rh*	*Zr*
Pd	*Ir*	*Hf*
Dy	*Au*	*V*
Ru	*Cd*	*Nb*
Ni	*Pb*	*Ta*
Ag	*Hg*	*Cr*

In order to have a correct description of each reaction, salts and other additives were removed via a small loop (Figure S3). Firstly, all reactants and products were separated by a *Cell Splitter*, generating the "X_Arr*" (where X corresponded to reactants or products and * to the number of reactants/products per each reaction) columns and each of those columns were matched to a list of salts and small additive molecules that we compiled according to the data (KNIME Report I). The loop in this case was very similar to the loop utilized to append the boiling points to the respective solvents: including two *Column Rename* and the *Cell Replacer* nodes. Additionally, in this case a *Column Auto Type Cast* was employed to ensure that empty cells were converted in missing values. After looping the process across all the “reactant” and “product” columns, we aggregated them with a *Column Aggregator* unflagging the "missing" option, so that the missing salts and additives were not included anymore.

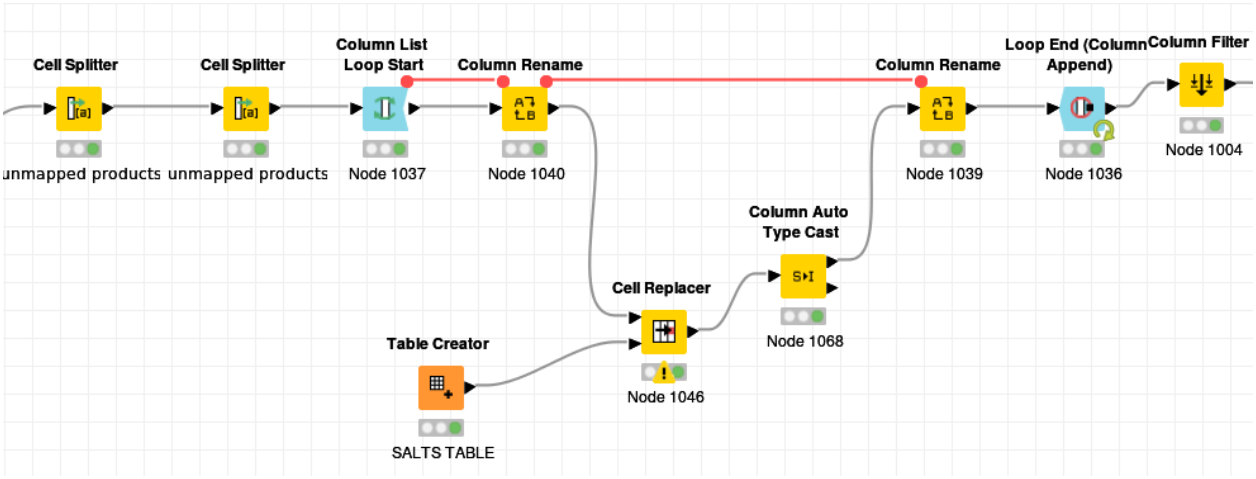

Fig. S3. KNIME workflow for solvents boiling point assignment.

Further refinement

On the treated reactions we performed further filtering, not related to conditions but to the utility in a chemical library context, in particular for DELs.

After the "Salts removal" *metanode* (grouped sequences of nodes are called *metanodes* in KNIME), the workflow continued into two parallel sections (Figure S4). The former involving the reactants and the latter the products. To remove the reactions involving duplicate reactants, we unpivoted the split reactants columns with the pattern **reactants_Arr** by the *Unpivoting* node. With this method, all reactants of all reactions were collected in one column called "ColumnValues". At this point, a *Missing Value* node removed the empty cells and a *String Manipulation* node was needed to standardize the reactants SMILES strings in terms of atom connectivity. The employed expression was the following: *replace(replace(replace($ColumnValues$, "[N]", "N"), "[cH]1", "c1"), "=[O]", "=O")*. With this step we ensured that the following grouping by the *Groupby* node gave reliable results. We grouped the reactions by Reaction ID, using at the same time the "Count" and "Unique count" aggregation methods for the "ColumnValues" column. Additionally, the reactants were concatenated utilizing the "Unique Concatenate" aggregation method and an additional column called "ColumnValues (Unique concatenate*)" was appended. Then, with a *Math Formula* node the count was divided by the unique count appending an additional column called "multi-react". The *Math Formula* was followed by a Row Splitter node to exclude reactions with only one reactant (2895 entries). These could be for example rearrangement reactions or oxidation reactions (Table S3 entry 4).

In the parallel part of the workflow, the same nodes sequence was repeated for the products column, with the difference that, after the *Unpivoting* node, a *Molecule Type Cast* and a *MolConverter* node were needed to take out the stereochemical information from the products to ensure uniqueness. Then, the same expression was applied by the *String Manipulation* and the *Groupby* was employed in the same manner. In this case, the products were concatenated under the name "Unique concatenate*(ColumnValues)". After the operation with the *Rule-based Row Splitter*, only reactions with one unique product were kept (1719 excluded entries). After joining the two tables according to the Reaction ID and the RXN column via a *Joiner node*, the *Number to String* node was used to convert the "multi-react" column into string and the ".0" was erased by a *String Manipulation*. In the following *Rule-based Row Splitter* node the expression was set to: *$multi-react$ = $Unique count*(ColumnValues)$ => TRUE*. The expression implied that the division of the total reactants count by the unique count was to be equal to the number of products for the reactions to be considered. To rescue reactions where the number of products equaled the number of reactants pairs another *Rule-based Row Splitter* node was used with the following expression: *$ColumnValues (Unique count*)$ = $Count*(ColumnValues)$ => TRUE*. The first output table was, then, concatenated with the first output of the previous Rule-based Row Splitter via a Concatenate node.

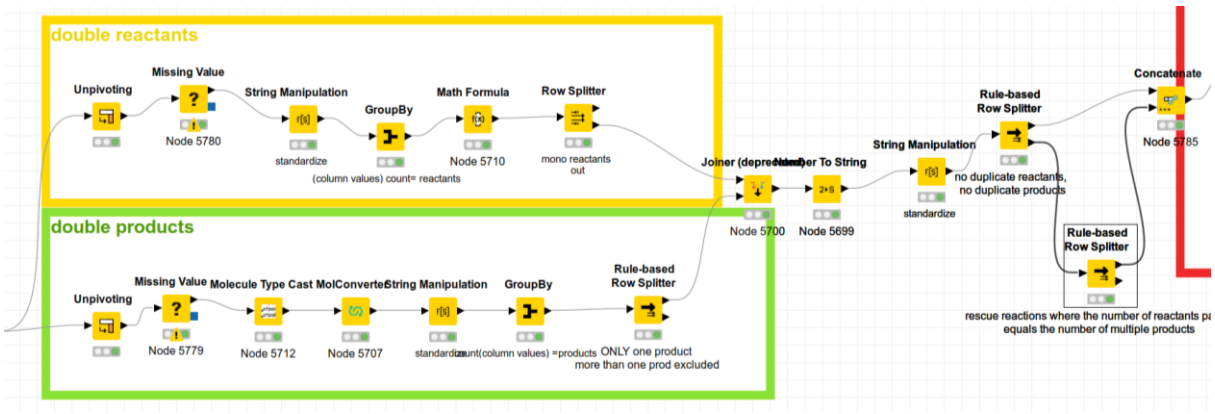

Fig. S4. KNIME workflow to exclude unsuitable reactions for DEL synthesis, namely with multiple identical reactants or yielding different side products.

Reactions including more than one aldehyde were removed as they would disturb the library construction. For this data curation step, a very simple workflow was used (Figure S5), starting with a *Cell Splitter* node, which split the "ColumnValues (Unique concatenate*)" by the delimiter "." and fed those "*Arr*" columns into the *Column List Loop Start / Loop End (Column append)* nodes for processing them one by one. Inside the loop, they were turned into smiles by the *Molecule type Cast* node and submitted to the *RDKit Substructure Counter* node, using the SMARTS pattern *[H][#6]=O*, generated by the *MarvinSketch* node. After the *Loop End (Column Append)* node, the *Column Aggregator* node summed the values up under the name “n.aldehydes” and the *Column Filter* node removed the "Iteration" columns. Within the next *Row Splitter* node, the threshold for the column "n.aldehydes" was set to 1 and therefore reactions with more than one aldehyde were excluded (sent to the second output port). The last node of this section was a *Column Aggregator* to concatenate all reactants under the name “reactants_desalt”. The reactions that were excluded by this step are depicted in Table S3.

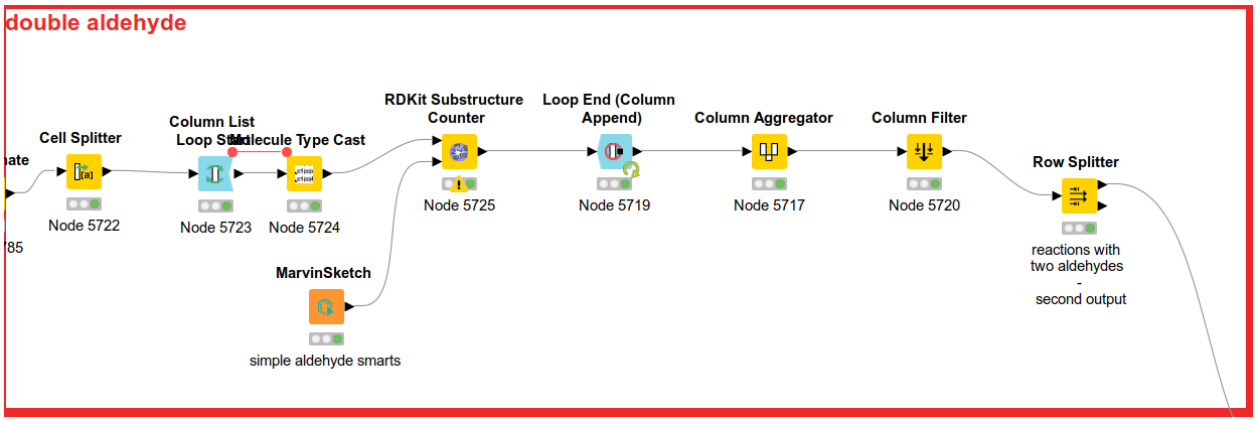

Fig. S5. KNIME workflow for excluding reactions with multiple aldehyde moieties.

Table S3. Excluded reactions with respective examples, counts and references.[S5-S15]

Entry	Category	Example	Count	Ref.
1	Metal complexes	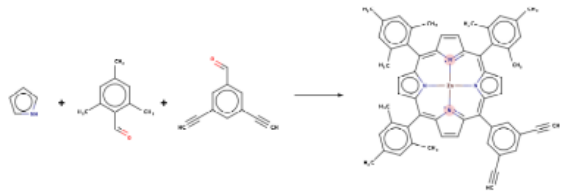	300	S5
2	Acetals-producing	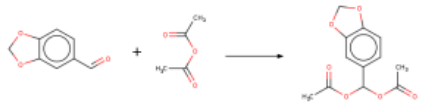	2904	S6
3	Unreacted aldehydes	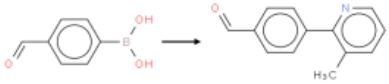	14	S7
4	Single reactant	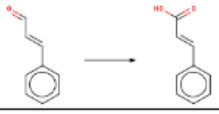	2895	S8
5	Multiple side products	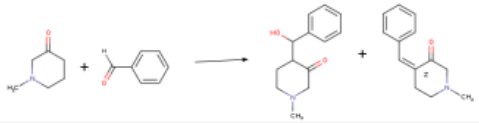	1712	S9
6	Identical reactants	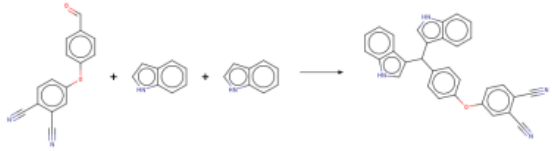	1431	S10
7	Di-aldehyde reactants	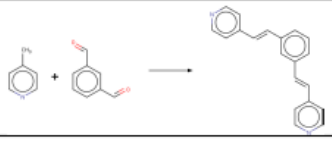	1100	S11
8	Positive difference in elemental analysis	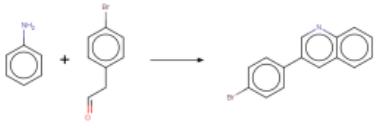	2796	S12
9	Unbalanced	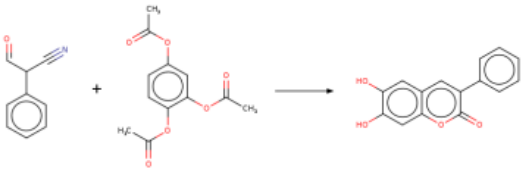	3894	S13
10	Reductive amination	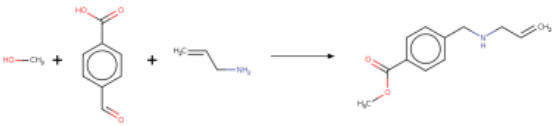	7727	S14
11	Aldehyde-ketone aldol reaction	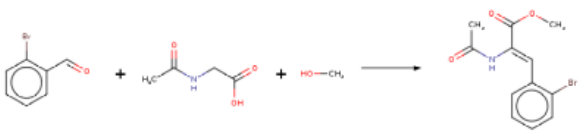	1618	S15
	Total of excluded reactions	**~27000**		

The following columns were excluded by a *Column Filter* node:
ColumnValues (Count*) (Number (integer));
ColumnValues (Unique count*) (Number (integer));
ColumnValues (Unique concatenate*) (String);
products (First*) (Smiles);
multi-react (String);
Count*(ColumnValues) (Number (integer));
Unique count*(ColumnValues) (Number (integer));
n.aldehydes (Number (integer)).
Moreover, the remaining columns were renamed, mostly to remove the aggregation methods deriving from the *Groupby* node, except for the column "Unique concatenate*(ColumnValues)" which was renamed as "product_unique".

Insertion of reference reactions

The *Column Rename* node was followed by a *Constant Value Column* node to append the column "type" with the value "Reaxys". This passage was necessary to distinguish between these reactions and the ones we tested in the lab, used as references (Figure S6). They were manually inserted to be used as landmarks in the final plot of the chemical reaction space. Those reactions were processed in a separate workflow but with the same procedure, after being sketched with *MarvinSketch* nodes. To the reference reactions the column "type" was appended as well, with the value "tested", via a *Constant Value Column* node. At this point they could be concatenated and further processed together.

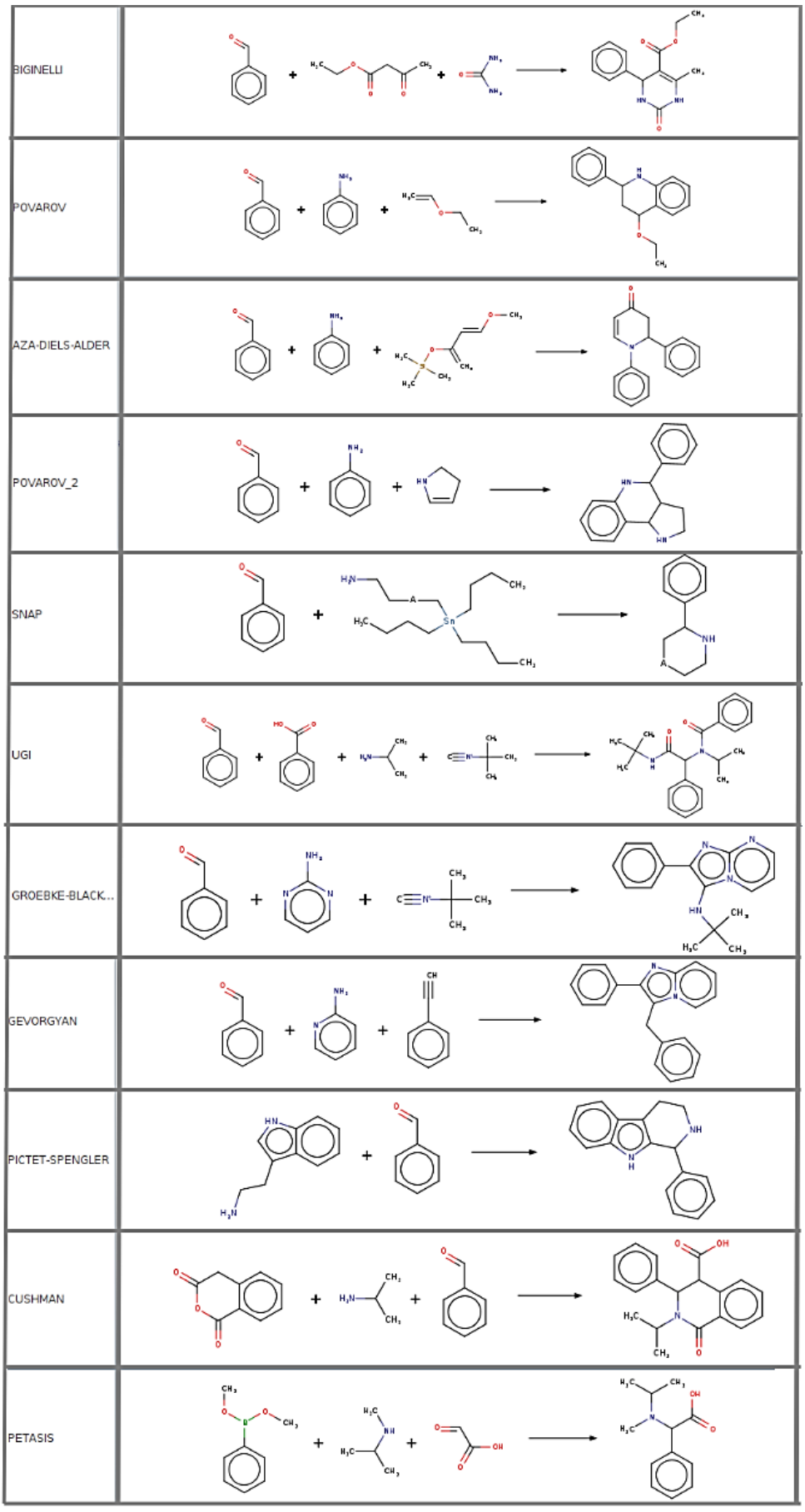

Fig. S6. Screenshot of the KNIME table containing the reference reactions which were drawn and inserted manually to function as landmarks in the final scatter plot of the chemical reaction space.[S16-S23]

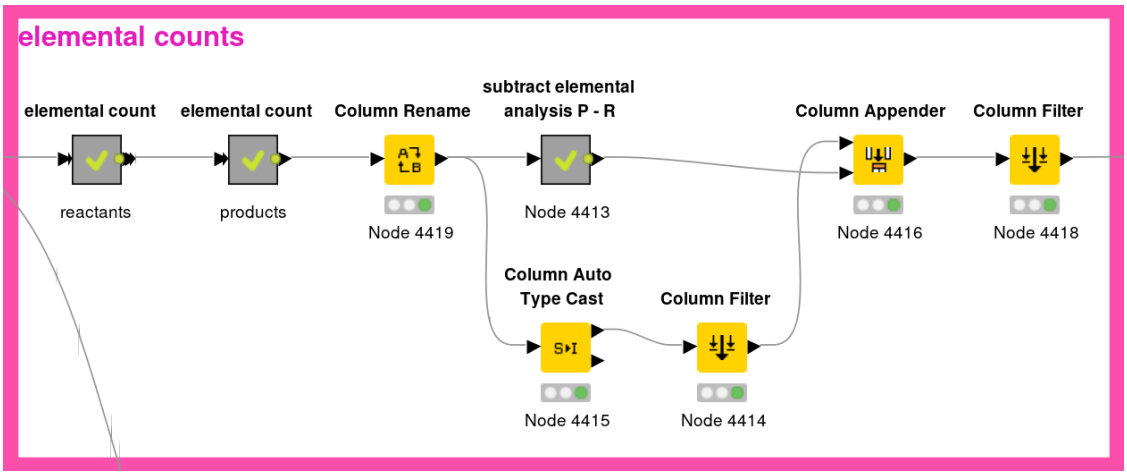

Fig. S7. KNIME workflow for elemental analysis. The grey nodes with the green check are called *metanodes* and they contain additional sequences of nodes.

Elemental analysis

An elemental analysis was performed on the reactants and the products, counting each element by String Manipulation nodes using the "count()" function (Figure S7). For some elements, such as carbon and chlorine ("C" and "Cl" respectively), to ensure that they were not mistaken, the expression *C_count - Cl_count* was employed in the Math Formula node, and the column "C_count" was substituted with the result. After performing this analysis on both reactants and products, the former was subtracted from the latter to make sure that no loss or addition of some elements occurred during the reactions. We set some reasonable thresholds: a loss of 1 or 2 oxygen (for condensation reactions), 1 halogen and/or a nitrogen (for elimination reactions) were allowed by a Rule-based Row Splitter node with the following rule: *S_count = 0 AND (O_count <= "0" OR O_count >= "-2" OR F_count <= 0 OR Cl_count <= 0 OR Br_count <= 0 OR I_count <= 0 OR N_count <= 0) AND C_count = 0 AND Sn_count = 0 AND Si_count = 0 AND B_count = 0 AND As_count = 0 AND Sb_count = 0 AND Se_count = 0 AND Te_count = 0 AND Zn_count = 0 AND Al_count = 0 => TRUE*. Reactions that obeyed those rules were fed into the descriptors calculation part of the workflow. The rest of the reactions were processed separately.

Module III – descriptor calculation

Reactants descriptors

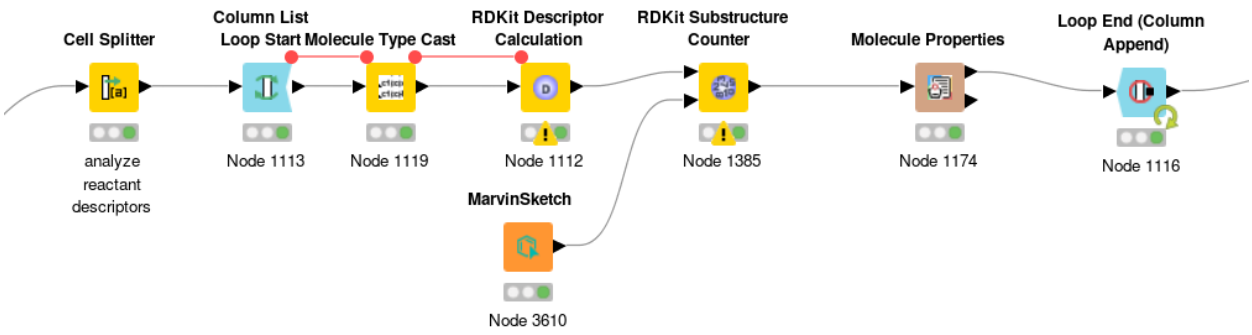

Fig. S8. Initial part of the KNIME workflow for descriptors calculation.

At first, to calculate the descriptors of the reactants, the column "reactant_desalt" was split by the delimiter "." generating one "*Arr*" column per each reactant. Then, the *Column List Loop Start* node circled around those columns to calculate the descriptors for each reactant of each reaction. The first node of the loop was the *Molecule Type Cast* to convert the reactant string into smiles, the “Structure Column” was set to the variable "currentColumnName" (one reactant per time) in the Flow Variables section (Figure S8).

The descriptors were calculated using the nodes *RDKit Descriptor Calculation* by RDKit[S20], the *Molecular Properties* by CDK[S21] and the *Molecule Properties* by Indigo[S22]. Additionally, we employed the count of some substructures as in-house descriptors. For this purpose, the combination of the *MarvinSketch* and the *RDKit Substructure Counter* nodes was adopted. Thus, the following 21 descriptors were obtained:
NumRings (Number (integer)): number of rings,
NumAromaticRings (Number (integer)): number of aromatic rings,
NumAliphaticRings (Number (integer)): number of aliphatic rings,
NumAromaticHeterocycles (Number (integer)): number of aromatic heterocylcles,
NumAliphaticHeterocycles (Number (integer)): number of aliphatic heterocycles,
NumAromaticCarbocycles (Number (integer)): number of aromatic carbocycles,
NumAliphaticCarbocycles (Number (integer)): number of aliphatic carbocycles,
NumRotatableBonds (Number (integer)): numer of rotatable bonds,
NumAmideBonds (Number (integer)): number of amide bonds,
NumAliphaticBonds (Number (integer)): number of aliphatic bonds,
NumAromaticBonds (Number (integer)): number of aromatic bonds,
NumCisTransBonds (Number (integer)): number of cis/trans bonds,
Csp3 (Number (integer)): number of sp3 carbons,
C-C (Number (integer)): number of carbon-carbon bonds,
C-N (Number (integer)): number of carbon-nitrogen bonds,
C-O (Number (integer)): number of carbon- oxygen,
C-S (Number (integer)): number of carbon-sulfur,
NumNInR (Number (integer)): number of nitrogen in rings,
NumOInR (Number (integer)): number of oxygen in rings,
NumPInR (Number (integer)): number of phosphor in rings,
NumSInR (Number (integer)): number of sulfur in rings.
The loop was completed by a *Loop End (Column Append)* node and the workflow carried on with a series of *Column Aggregator* nodes, one per each descriptor, summing up the values in order to have a total number for the reactants per each reaction. At the end of this section, we placed two *Column Filter* nodes to remove the Iteration columns and "Arr" columns with the regex patterns *^(?!.*(Iter)).*$* and *^(?!.*(Arr)).*$* respectively. Then, a *Column Aggregator* node determined the median absolute deviation of all so-far calculated descriptors and the reactions with a value higher than 4.0 were excluded via a *Row Splitter* node. The thus excluded reactions were considered outliers, mostly because of the bulky substituents. Indeed, we confirmed that the same reaction with simpler substituents could be detected in the rest of the database.

Product descriptors and reaction descriptors

The same workflow section was applied to the products, with the only difference that at this point the products were unique, so no loop was needed anymore. The sequence of *Column Aggregator* nodes after the loop, in this case, was substituted by 2 *metanodes*: one for renaming the SMARTS column headers into common names (according to Table S4) and one for adding the prefix "P_" to the products descriptors.

Table S4. Column headers name assignment.

SMARTS and RDKit name	Final name
[#7;R]	NInR
[#8;R]	OInR
[#16;R]	SInR
[#15;R]	PInR
[#6]~[#6]	C-C
[#6]~[#7]	C-N
[#6]~[#8]	C-O
[#6]~[#16]	C-S
[#6;X4]	Csp3
[#5]~[#8]	B-O_count
[#5]~Cl	B-Cl_count
[#5]~F	B-F_count
[#5]~[#6]	C-B_count
[#6]~[#14]	Si-C_count
[#8]~[#16]	S-O_count
F~[#14]	Si-F_count
[#6]~F	C-F_count
[#8]~[#15]	O-P_count
[#7]~[#16]	S-N_count
[#14]~Cl	Cl-Si_count
Number of aliphatic bonds	NumAliphaticBonds
Number of cis/trans bonds	NumCisTransBonds
Number of aromatic bonds	NumAromaticBonds

After calculating all descriptors for reactants and for products, a small loop was needed to subtract the descriptors and generate the difference descriptors (Figure S9). For this, firstly a *Column Filter* was needed to only include integer columns via the option "Type Selection". The output table was fed into the *Column List Loop Start* node which included only the products descriptors by the pattern Regex pattern *((?!(R_)).)**. In this way the workflow looped only through the product descriptors. The variable "currentColumnName" was used in the next three *String Manipulation (Variable)* node to create the formula, the output column name and the filter pattern for the following *Math Formula* node. The expression was created via the following code: *join("$",$${currentColumnName}$$, "$ - $", replace($${currentColumnName}$$, "P_", "R_"), "$")* under the variable name "formula", the output column name via the following code *replace($${currentColumnName}$$, "P_", "")* under the variable name "result" and finally the filter pattern was created via the following code: *join("*",replace($${currentColumnName}$$,"P_", ""), "*")* under the variable name "filter". By consequence, the *Math Formula* node was set to employ the variables "result" and "formula" for the "replaced_column" and "expression" parameters, respectively. The next *Column Filter* node used, instead, the variable "filter" as "pattern" parameter. The loop ended with the node *Loop End (Column Append)* node and finally with two *Column Filter* nodes the descriptors for the separate reactants and products were eliminated by the regex patterns: *^(?!.*(R_)).*$* and *^(?!.*(P_)).*$* respectively.

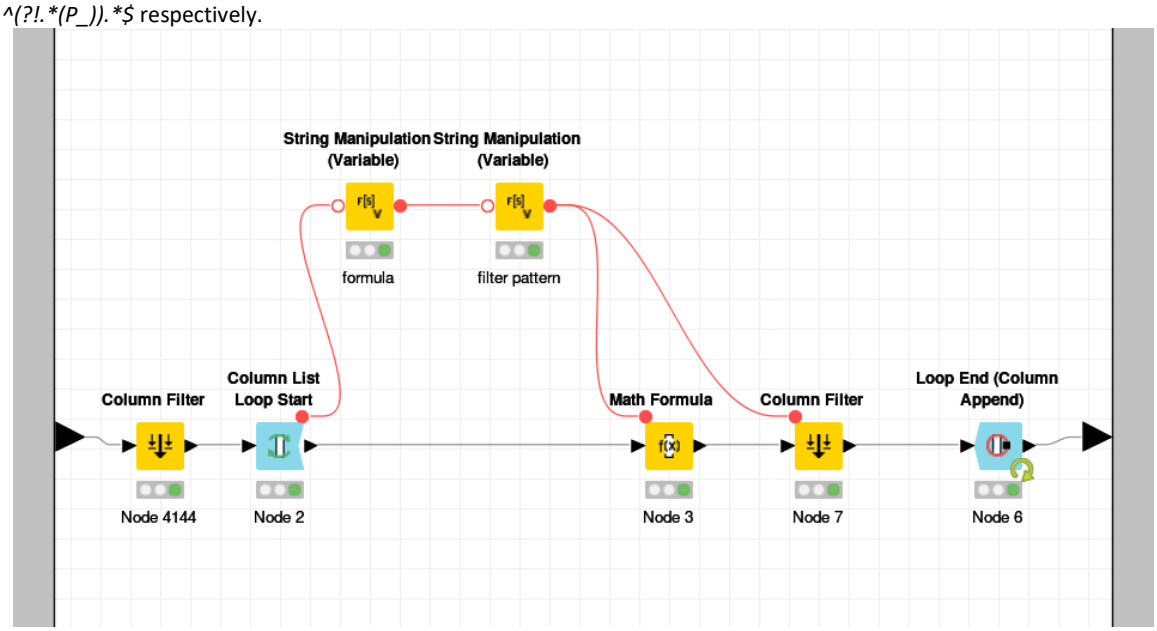

Fig. S9. KNIME workflow to calculate the difference descriptors.

Manual filter – reductive amination and aldol condensation

To improve the quality of the following clustering by reducing the size of the data set, we removed frequently occurring reactions such as reductive amination (or imine formation) and aldol condensation (Figure S10).

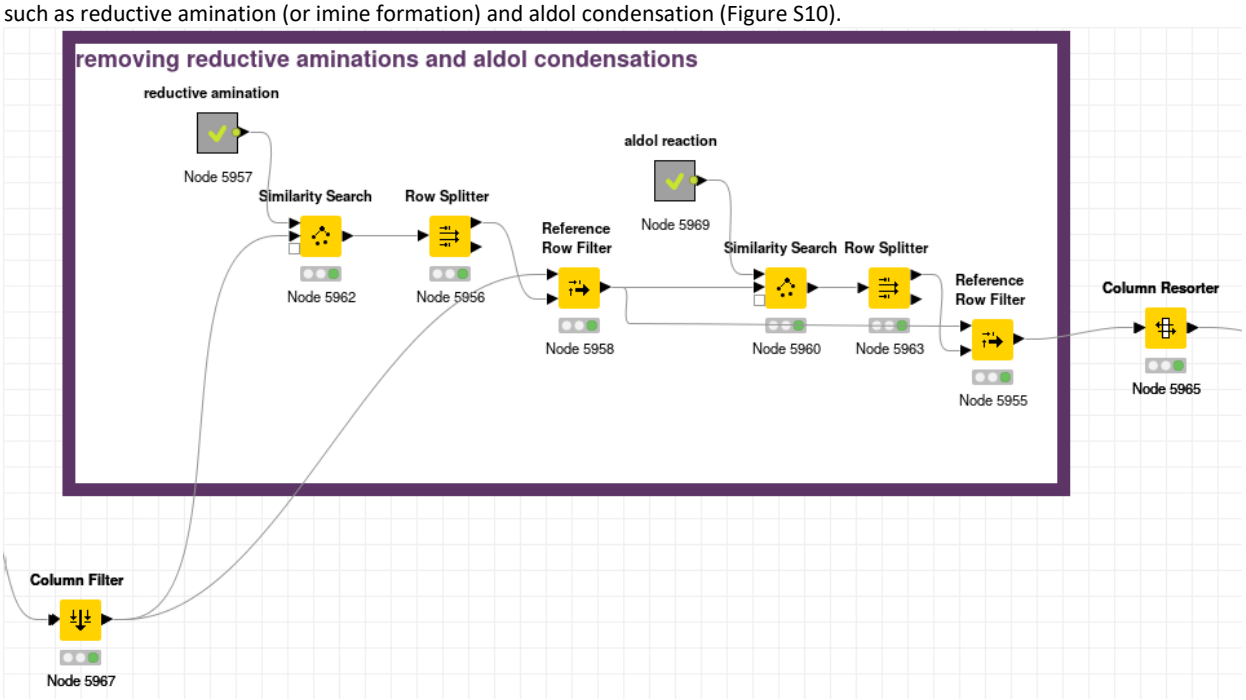

Fig. S10. KNIME workflow for similarity search of reductive amination and aldol condensation.

For this purpose, we sketched the simplest scheme for the reductive amination reaction via a *MarvinSketch* node: *[H][#6]=O.[#7]-[#7]-[#7]>>[#6]-[#7]*. The reactions were treated exactly like the rest of the reactions in the database: the *Cell Splitter* node split reactants and products, the column was renamed accordingly and the next *Cell Splitter* split the reactants to pass them through the above-mentioned descriptors calculation sub-workflow. The output was connected with the first input port of the *Similarity Search* node, whose second input port received the database reactions. The similarity search was performed using the descriptors as attributes for calculating the Euclidean distance. The coefficient type was set to "distance" and the neighbors' selection to "Nearest (most similar)", the neighbors count to 15000. Lastly, the representative column was set to "Reaction_smiles", to have a direct proof of the similarity for visual inspection. Then, we set the threshold for the distance to 1.4 with a *Row Splitter* node. Entries with distance smaller than 1.4 were sent to the first output port and the rest to the second one. Then, the reactions were tracked back with a *Reference Row Filter* node, which took the "Reaction_smiles" columns, excluding the matching entries. The same workflow was repeated for the aldol-condensation, this time applying the SMARTS pattern: *[H][#6:3]=O.[#6:4]-[#6:2](-[#6])=[O:1]>>[H]\[#6:3]=[#6:4]\[#6:2](-[#6])=[O:1]*.

Leaving groups treatment

Firstly, a Rule-based Row Splitter node was used to separate the reactions with mass gain (ca. 2000) from the reactions with mass loss (ca. 6000). The former group was ignored, mostly because those reactions contained errors or omissions in the reaction scheme, while the latter group was processed as reactions involving leaving groups. The first step was to compile a list of leaving groups, which were extracted manually from the database (see respective KNIME report). We started performing the elemental analysis and calculating the descriptors on the leaving groups following the same protocol for the reactions. We assigned the column names with a small series of nodes to change the column headers (Table S3). The leaving groups were sorted by descending molecular weight via the *Sorter* node, to ensure that smaller substructures would not be mistaken for the more complex counterparts. At this point the leaving groups' list was fed into the second input port of the *Recursive Loop Start (2 ports)* node, which allowed for processing matching data and re-process the rest. The 5834 reactions with mass loss were fed into the first input port of the same node. Inside the loop, the leaving groups were considered one-by-one by using the *Row Splitter* node, which was set to output only the first row to the first output table and the rest to the second output table. This second output table was connected to the third input port of the *Recursive Loop End (2 ports)* node, which ended the loop as shown in Figure S11.

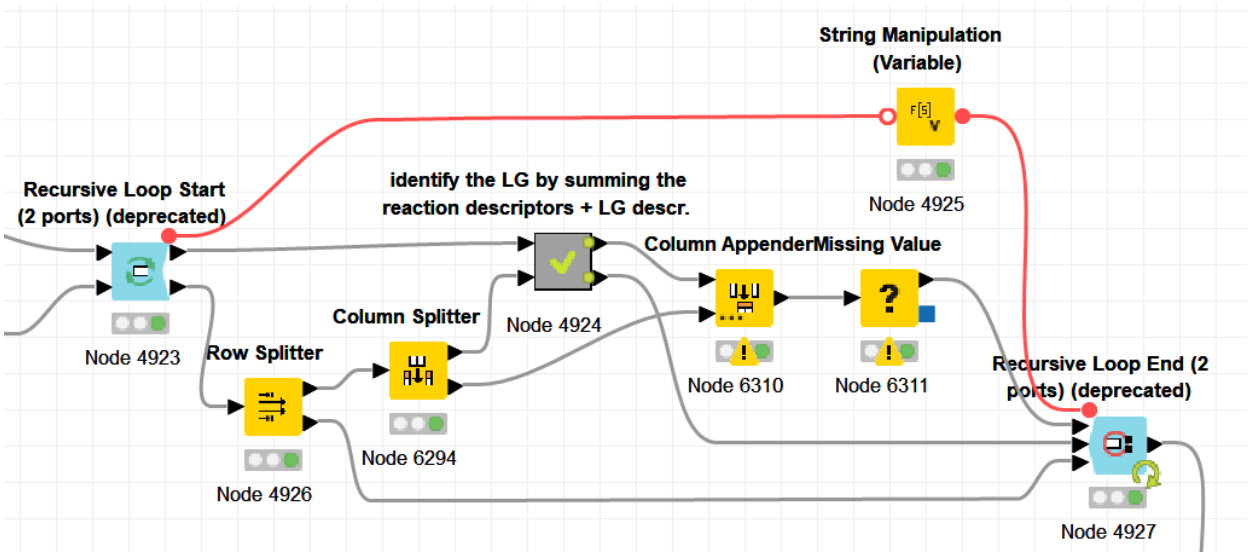

Fig. S11. KNIME workflow for leaving groups recognition and subtraction from the reactants' descriptors.

Subsequently, as the reactions elemental analysis in the case of reactions with leaving groups had a negative value, we summed the value for the reactions with the values for each leaving group in an automated fashion. The loop in this case was very similar to the one used for subtracting the reactant descriptors from the product descriptors. The main difference laid in the expression of the *String Manipulation (Variable)* nodes. The first expression was *join("$",$${ScurrentColumnName}$$, "$ + $", "LG_", $${ScurrentColumnName}$$, "$")*, the second was *join($${ScurrentColumnName}$$, "_sum")* and the third was simply *join($${ScurrentColumnName}$$, "*")*. Where this sum yielded a null result, the leaving group was believed to be disappearing in the considered reaction and, therefore, its descriptors were subtracted from the reactants' descriptors. For this purpose the "sum *metanode*" was followed by a *Rule-based Row Splitter* with the expression: *(O_count_sum =0 OR O_count_sum =-1 OR O_count_sum =-2) AND (S_count_sum = 0 AND N_count_sum = 0 AND C_count_sum = 0 AND Sn_count_sum = 0 AND Si_count_sum = 0 AND B_count_sum = 0 AND (F_count_sum = 0 OR F_count_sum = -1) AND (Cl_count_sum = 0 OR Cl_count_sum = -1) AND (Br_count_sum = 0 OR Br_count_sum = -1) AND I_count_sum = 0 AND As_count_sum = 0 AND Ti_count_sum = 0 AND Sb_count_sum = 0 AND Se_count_sum = 0 AND Te_count_sum = 0 AND Zn_count_sum = 0 AND Al_count_sum = 0 AND P_count_sum = 0)=> TRUE*. The first output port of the node was connected to a *Column Appender* node which added the respective leaving group to the table under the column name LG, followed by a *Missing Value* node which filled the empty cells of the column "LG" with the previous value, so that every reaction had its own leaving group. The output of the *Missing Value* node was fed into the first input port of the *Recursive Loop End (2 ports)*, the collection port. The second output port of the *Rule-base Row Splitter* was connected to the first recursive port of the *Loop End*. Finally, to the second recursive port of the *Loop End* node, the second output port of the *Row Splitter* that split the leaving groups was connected. Our approach was to remove the leaving groups from the reactants instead of adding them to the products. The thus processed reactants' descriptors were then subtracted from the products' descriptors with a very similar workflow. Around 2,000 reactions could be rescued with this method and were therefore reinserted in the main flow with a *Concatenate* node for a total number of ca. 26,000 entries.

Module IV - Features extraction

The dimensionality of the data was reduced by feature extraction (Figure S12). The correlation between the descriptors is illustrated in the heat map in Figure S13. First of all, with sequential Column Filters nodes the descriptors were grouped according to chemical features. In the first *Column Filter* node, only the descriptors for cyclic substructures, i.e. containing the keywords "ring" and "cycle", were considered. Then, the *Rank Correlation* node calculated the Spearmans Rho coefficient and in the following *Correlation Filter* node the threshold was set to 0.8, so that variables correlated for more than 80% would be removed. In this way some descriptors were lost and the remaining ones were summed via a *Column Aggregator* node generating the RINGS variable. The same process was repeated for the descriptors containing the keyword "bond" and heteroatom-describing keywords, generating the BONDS and the HETEROATOMS variables, respectively. The combination of features into the three new variable is illustrated in Figure 3 in the manuscript. The three new variables were normalized via a Normalizer node with the Z-score method and the normalized columns were used as attributes in the following *Fuzzy c-means* node for clustering.

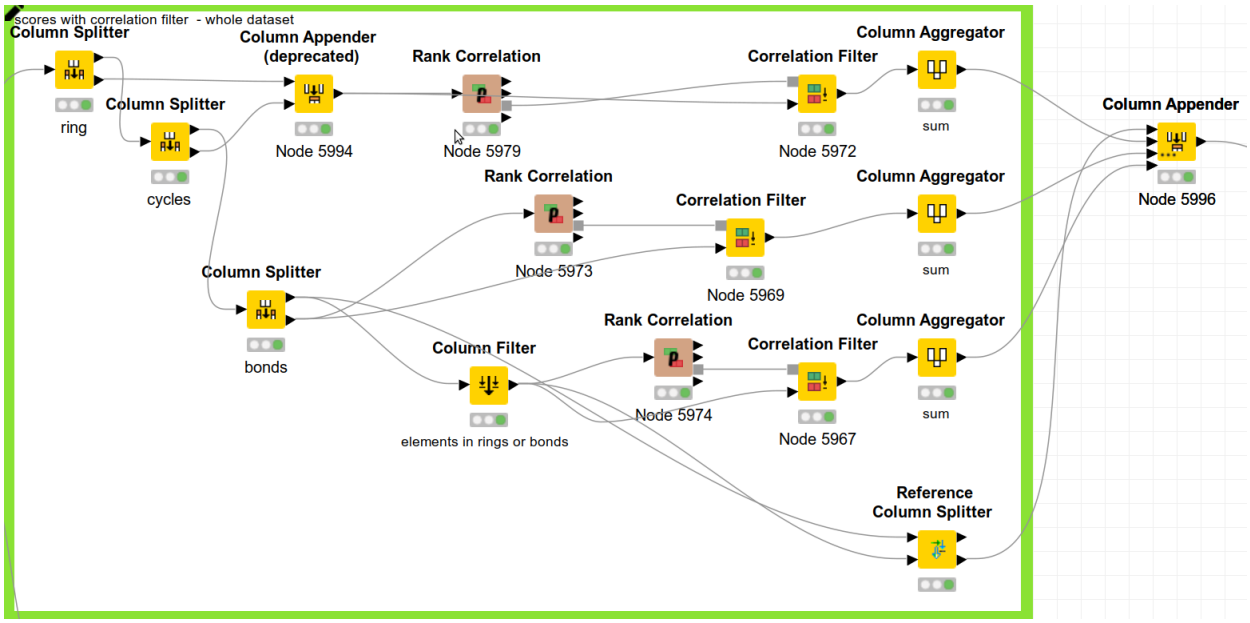

Fig. S12. KNIME workflow for the creation of the three new variables from the 21 descriptors, including the correlation filters.

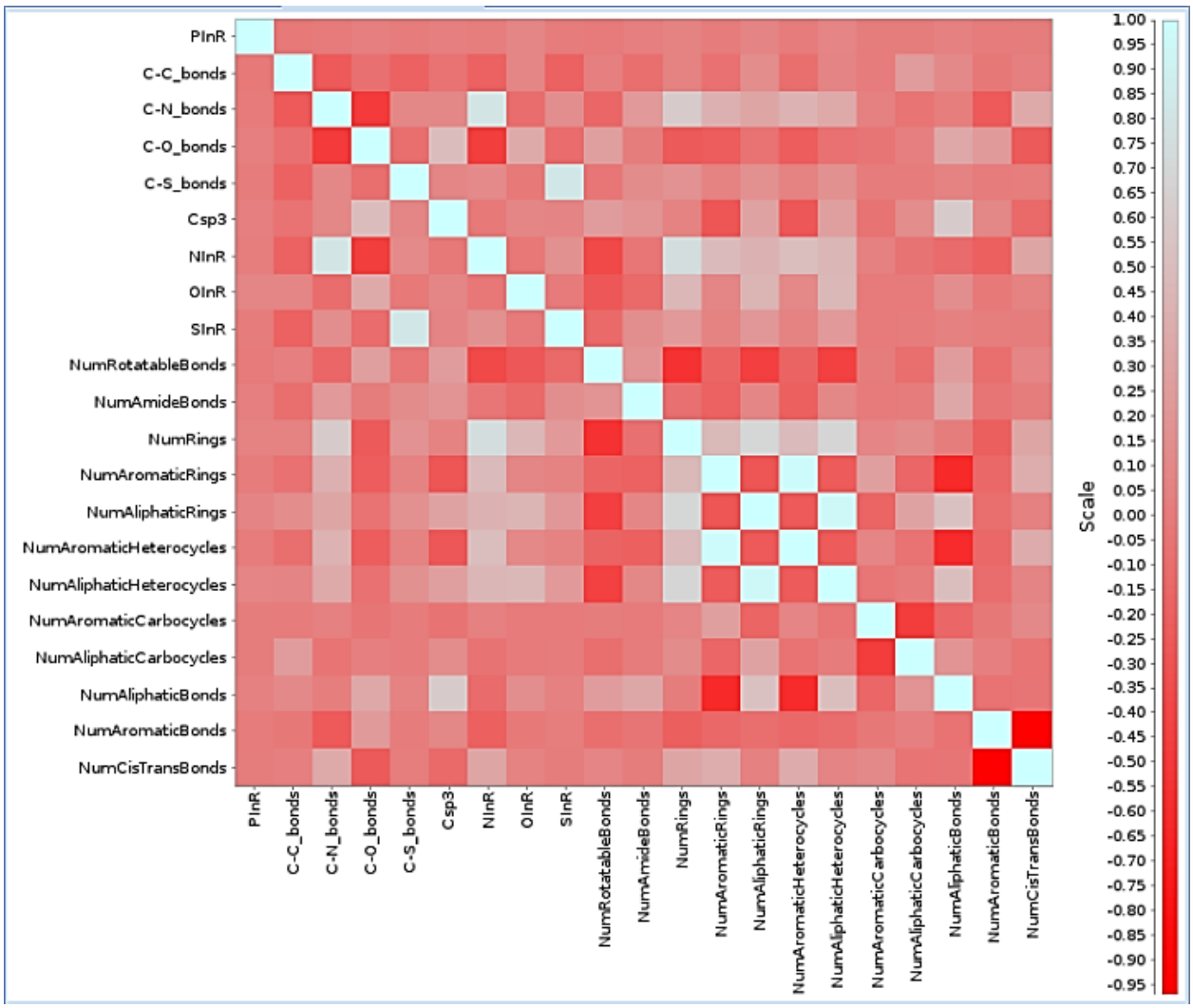

Fig. S13. Heat map of the correlation matrix *all vs. all* descriptors.

Clustering

The clustering parameters number of clusters and lambda were selected automatically in a separate *metanode*, depicted in Figure S14). Firstly, two tables were created with the *Table Creator* nodes. In the first table, the column header was set to "n. of clusters" and the values of 40, 45, 50, 55, 58 and 59 were assigned. In the second table, the column header was set to "lambda" and the values of 0.1, 0.3, 0.5 and 0.7 were assigned. Then, all possible combinations of the two parameters were generated via the *Cross Joiner* node and they were converted into variables with the *Table Row to Variable Loop Start* node. Those combinations were used one by one as parameters in the following *Fuzzy c-Means* node. After that, all reactions that were not clustered were considered "noise" and therefore assigned to the "noise cluster" which was ignored by employing the *Row Splitter* node and the Silhouette coefficient of the clusters (except the "noise cluster") was calculated with the homonym node. The Silhouette coefficient was used as quality measure for the clustering method, as we previously verified the correlation between the coefficient value and a good chemical clustering. The second output of the Silhouette Coefficient node was connected to a *Row Filter* node which extracted the "Overall" row. Before the *Loop End* node, the values for the overall Silhouette coefficient and the respective number of clusters and lambda were appended to the table with the *Variable to Table Column* node. After the loop, the table was sorted according to descending Silhouette Coefficient via the *Sorter* node and the optimized parameters were used in the *Fuzzy c-Means* node for the main workflow.

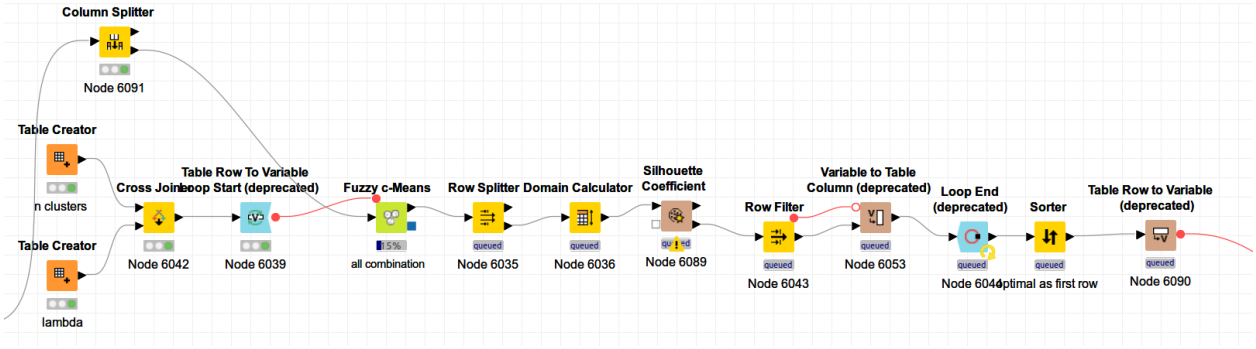

Fig. 14. KNIME workflow for the optimization of the clustering parameters *number of cluster* and *lambda*.

In this node, the fuzzifier was set to 1.1 and the option Automatic delta was flagged. The number of clusters and the lambda were controlled by the respective variables. Lastly, the options "Perform the Clustering in memory" and "Compute cluster quality measures" were checked. For the chemical analysis, that verified the efficacy of the Silhouette coefficient as quality measure, we extracted the cluster centers via the second PMML output of the Fuzzy c-means node with a small *metanode*[1] and then retrieved five central and five peripheral nearest neighbors per cluster by a Similarity Search node. This allowed us to check if reactions in one cluster were similar and reactions from different clusters were different.

Module V - output

Reactions classification

The reactions were classified according to combinations of the three factors and for that the factors were first split in two and then a recursive loop was created (Figure S15). First of all, the columns belonging to the clustering were excluded via a *Column Splitter*. Then, a *Column List Loop Start* node included only the three factors. Inside the loop, a *Row Splitter* node used the "currentColumnName" variable as column to test and split the value of the considered factor in positive and negative. Hence, a column was appended with a *Constant Value Column* node, which used the "currentColumnName" as replaced-column parameter. With this node the strings "breaking" and "forming" were assigned to negative and positive values, respectively. After that, the rows were unified again with a *Concatenate* node and the loop finished with the *Loop End (Column Append)* node. A *Column Filter* node excluded the iteration columns with the pattern: *^(?!.*Iter).*$*. At this point, the resulting table could enter the first input port of the *Recursive Loop Start* node and the Table S5 fed the second input port of the same node. The latter table was split via the *Row Splitter* node which separated the first entry in each iteration. The row was then converted into variable by the *Table Row to Variable* node and used in the Rule-based Row Splitter, which was fed with the first port of the *Recursive Loop Start* node. The *Row Splitter* node employed the variable "rule" and the following *Constant Value Column* appended the column "class" with the value given by the variable "class". The output of this last node was fed into the collecting port of the *Recursive Loop End* node, while the second output port was connected to the first recursion port of the *Loop End* and, finally, the second output port of the *Row Splitter* that divided the rule/class pairs was fed into the second recursion port of the same node. At the end, the *Joiner* node was utilized to append the numeric valued of the factors, to visualize the classes in the 3D scatter plot with the homonym node. Additionally, the *Pie/Donut Chart* node was used to summarize the proportion of such classes over the whole dataset. The output images of the two nodes are depicted in the manuscript (Figure 4 B and C in the manuscript).

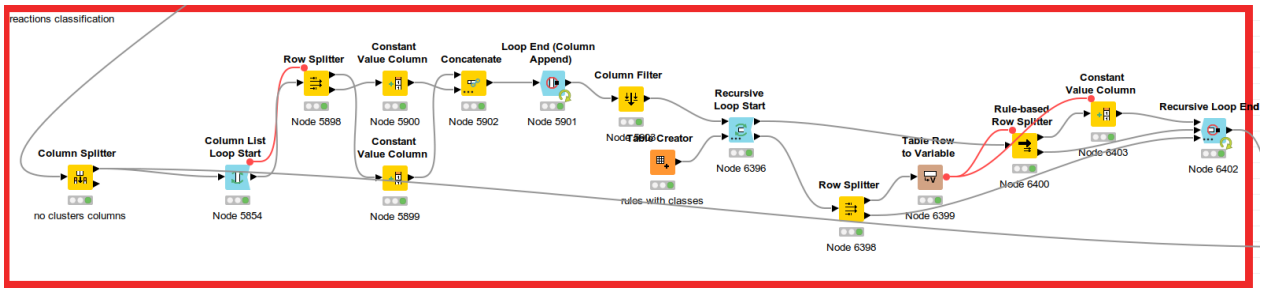

Fig. S15. KNIME workflow for reaction classification according to the breaking or forming connotation of the three variables.

[1] adapted from the workflow of *AlexanderFillbrunn* in the KNIME hub.

Table S5. Rules with the respective assigned class for reaction classification according to the "forming" or "breaking" three variables.

Rule	Class
$BONDS FACTOR$ = "breaking" AND $RINGS FACTOR$ = "forming" AND $HETEROATOMS FACTOR$ = "forming" => TRUE	Multi-rings or N-heterocycles formation
$BONDS FACTOR$ = "breaking" AND $RINGS FACTOR$ = "breaking" AND $HETEROATOMS FACTOR$ = "breaking" => TRUE	Aldol condensation, ring opening/closure
$BONDS FACTOR$ = "forming" AND $RINGS FACTOR$ = "breaking" AND $HETEROATOMS FACTOR$ = "breaking" => TRUE	Aldol condensation, ring opening/closure
$BONDS FACTOR$ = "breaking" AND $RINGS FACTOR$ = "forming" AND $HETEROATOMS FACTOR$ = "breaking" => TRUE	Ring formation
$BONDS FACTOR$ = "forming" AND $RINGS FACTOR$ = "forming" AND $HETEROATOMS FACTOR$ = "breaking" => TRUE	Ring formation
$BONDS FACTOR$ = "forming" AND $RINGS FACTOR$ = "forming" AND $HETEROATOMS FACTOR$ = "forming" => TRUE	Heterocycles formation
$BONDS FACTOR$ = "forming" AND $RINGS FACTOR$ = "breaking" AND $HETEROATOMS FACTOR$ = "forming" => TRUE	Grignard reaction, cyanation, aminoalkylation
$BONDS FACTOR$ = "breaking" AND $RINGS FACTOR$ = "breaking" AND $HETEROATOMS FACTOR$ = "forming" => TRUE	Aminoalkylation

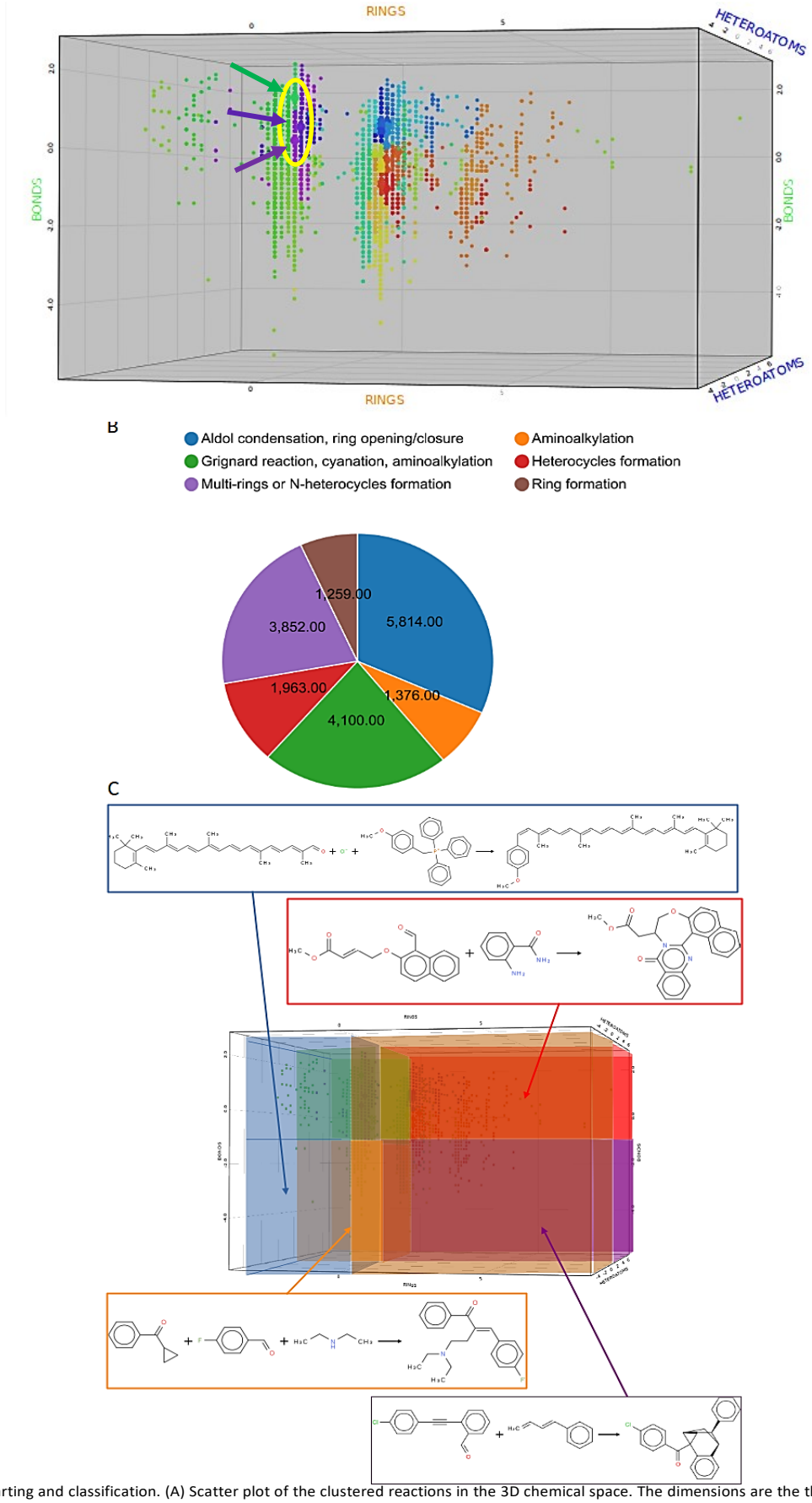

Fig. 4 (enlarged). Charting and classification. (A) Scatter plot of the clustered reactions in the 3D chemical space. The dimensions are the three variables RINGS, BONDS and HETEROATOMS and the colors of the dots depend on the cluster affiliation. The small dots belong to the Reaxys data set, while the big dots represent the reference reactions. The cluster affiliation confirms the chemical similarity as emphasized by the reference reactions circled in yellow: the two closer purple dots are the Ugi and the Cushman reactions, while the green dot is the Petasis reaction, slightly different then the first two. (B) Pie chart featuring the classes proportion in the data set. (C) Highlighted areas in the scatter plot, identified by the rule-based classes, with relative examples.
64-67

Reactants versatility

The versatility of one reactant or starting material was indicated by the number of clusters in which the reactant was present, as each cluster contained closely related a reaction type. To visualize this property, a *component* (a special feature of KNIME) was assembled in order to obtain an interactive view of the plot and the molecular structure of the reactants (Figure S16). First of all, the column "reactants_desalt" was split by the delimiter "." with the *Cell Splitter* node and then all reactants were collected in one column via the *Unpivoting* node. The generated column was converted into SMILES via the *Molecule Type Cast* node and the following *Groupby* node counted the number of clusters and the number of reactions per reactant. Starting materials that contained aldehyde and amine functionality were excluded from this analysis because they are known versatile building blocks. This was achieved with a combination of the *MarvinSketch* node with the SMARTS strings *[#6H1]=[O;X1]* and *[#7H2]* and the *RDKit Molecules Substructure* Filter, whose second output was connected to a *Row Filter* for missing values deletion. Then, the reactants were sorted by popularity and the first 15 were considered in this work as a proof of concept. A number was assigned to each of them via a *Counter Generation* node and the output table was fed into the *Renderer to Image* node and into the *Number to string* node. The first node converted the SMILES structures into pictures that were then fed to the *Tile View* node. The second node, instead, converted the "Counter" column into strings, to be used in the *Bar Chart* node as category column. Between these last two nodes, the *Sorter* node organized the table according to the column "Unique count*(Winner Cluster)" in descending order.

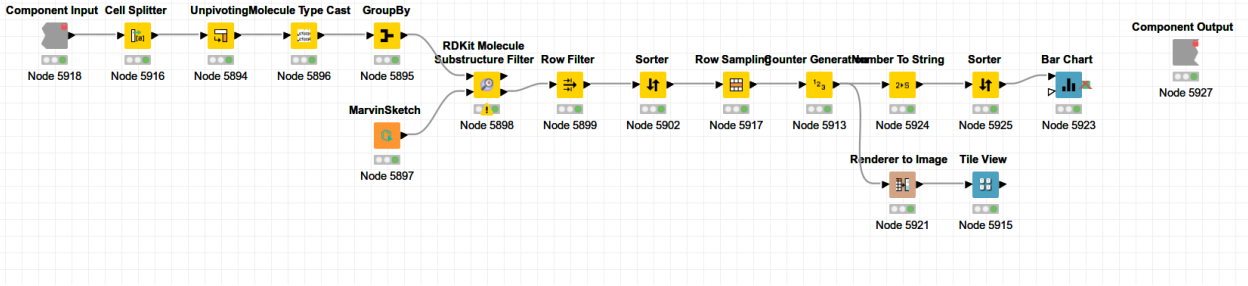

Fig. S16. Component for analysis of the reactants' versatility.

By right-click on the corresponding component and selecting the option "Interactive view: reactants versatility", it was possible to visualize the interactive view of the bar chart of the sorted reactants and the tile view table showing the selected reactants' structure. In the bar chart, the blue bar corresponded to the number of clusters and the orange bar to the number of reactions (Figure S17).

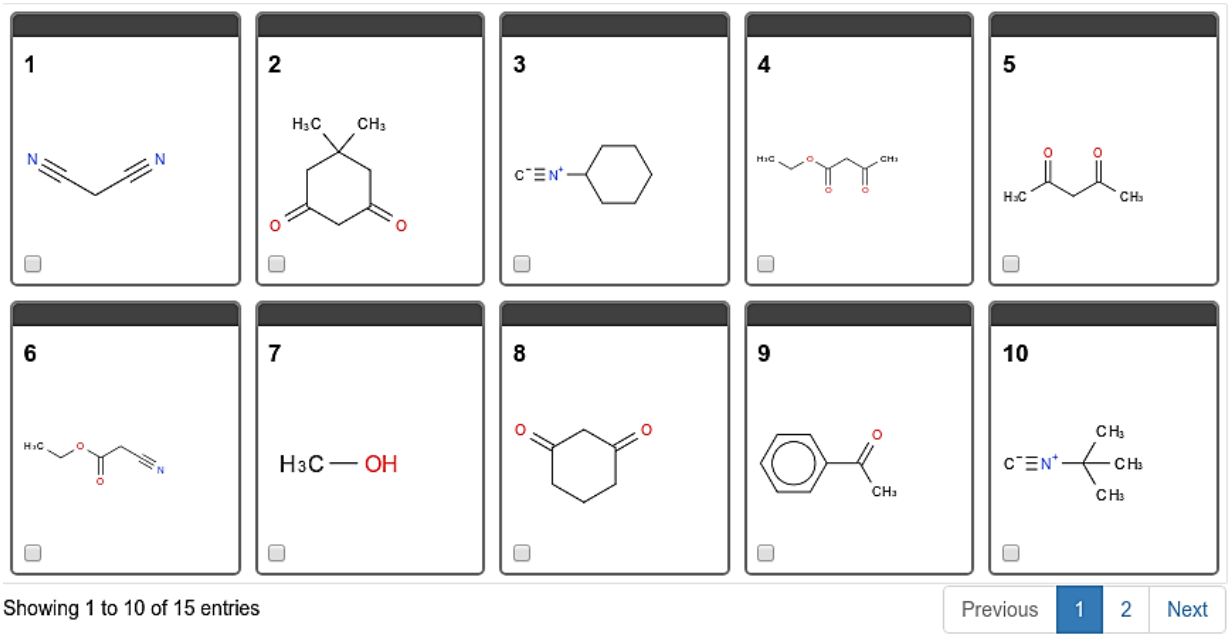

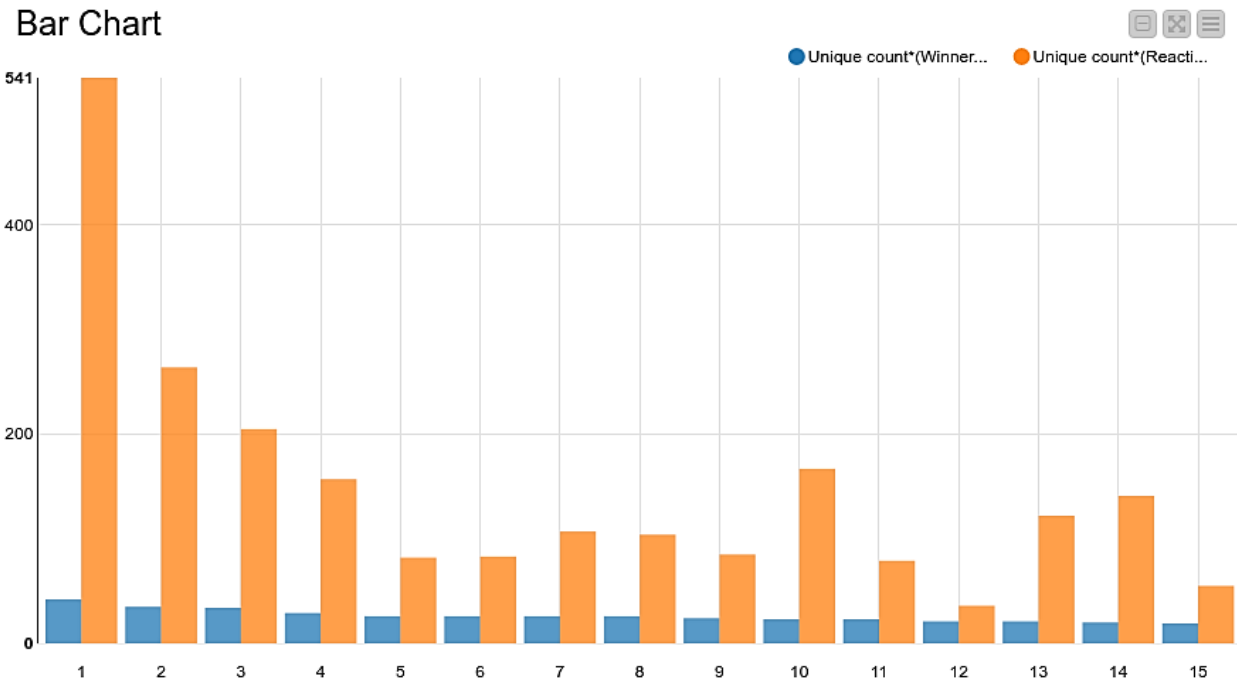

Fig. S17. KNIME interactive view for the reactants' versatility. In the bar chart, the numbers correspond to the reactants in the table above, the orange bars to the number of single reactions and the blue bars to the number of clusters where each reactant was found.

Correlation between clusters and metal centers

This analysis and the related part of the workflow considered only metal centers used as reaction promoters, excluding organocatalysts. This section started with two *Table Reader* nodes that opened the two tables of reagents and catalysts attached to the reactions table. These were the reagents and catalysts appearing in the dataset and they were provided by Reaxys®. The two tables were merged via a *Concatenate* node, because in the Reaxys® database there is no distinction between these two classes, so they were both defined as mediators. The column "Chemical Name (IDE.CN)" containing the mediators IUPAC names was then split by the "|" delimiter by the *Cell Splitter* node and all the single mediators were collected in one column via the *Unpivoting* node. In the initial table another important column was present, the "Reaxys Registry Number (IDE.XRN)" which connected the reagents and catalysts table with the reactions table. This column was converted into integer via a *String to Number* node and the missing values were removed via a *Row Filter* node. The chemical names in this output table were joined with the scored reagents via a *Joiner* node. This table entered then a loop to assign the reagents score to the respective reactions. For this, the table of clustered reactions coming from the *Fuzzy c- means* node was fed into two *Cell Splitter*, to separate reagents and catalysts by the "|" delimiter. The output of the last node was connected with a loop similar to the "salt removal" one, with

the difference that, in this case, three *Cell Replacer* nodes were inside the loop. The first to assign the score to the reactions, the second for the chemical names and the third to assign the metal queries relative to the reagents/catalysts. Following the loop, three *Column Aggregator* nodes joined again all the mediators per reaction, taking the minimum score per each reaction and concatenating the names accordingly. After that, a Joiner node appended the important columns there were not used during the loop from the table of clustered reactions. To analyze the shares of each mediator in the full data set, first of all the missing and unknown mediators were excluded via a *Row Filter* node. The remaining mediators in the "Query" column were split and unpivoted with the respective nodes and the filter was applied again for former combinations with unknown mediators. Subsequently, the *Pie/Donut Chart* node was used to illustrate the database composition (Figure 5 in the manuscript). The respective numbers are illustrated in Table S6. At this stage, the most common mediators were identified via a *GroupBy* node which grouped the "ColumnValues" column and counted the number of reactions by ID. According to this analysis, the most common metal centers promoting reactions in this data set resulted zinc with 365 reactions, followed by titanium, copper, silver and palladium with 280, 202, 197 and 181 reactions, respectively. In parallel, the output of the Joiner was connected to a *Cell Splitter* node and the *Unpivoting* node to separate the metal queries. Then, for reasons of technical compatibilities with the following nodes, in the column "Winner Cluster" the string "cluster_" was removed by a *String Manipulation* node and the number of the cluster was converted into integer via the *String to Number* node. The values were sorted in ascending order by a *Sorter* node and all columns not in focus in this part of the workflow were excluded by a *Column Filter* node. The *Pivoting* node was used to plot the clusters in the y-axis and the metals in the x-axis in the final heat map (Figure S18).

Table S6. All metal centers with the respective occurency counts in the dataset.

Query metal center	Occurency count
missing	8348
undefined	1712
[Zn]	365
[Ti]	280
[Cu]	202
[Ag]	197
[Pd]	181
[Al]	97
[Yb]	94
[Fe]	82
[Sn]	77
[Sb]	54
[Ce]	52
[Bi]	40
[In]	25
[Ni]	21
[Zr]	21
[Nb]	18
[W]	14
[Au]	12
[La]	10
[Co]	9
[As]	8
[Cr]	7
[Ga]	7
[Mn]	7
[Ru]	6
[Hf]	4
[Pb]	4
[V]	4
[Y]	4
[Mo]	3
[Nd]	3
[Pt]	3
[Lu]	2
[Pr]	2
[Re]	2
[Te]	2
[Er]	1
[Hg]	1
[Sm]	1
[Ta]	1
[U]	1

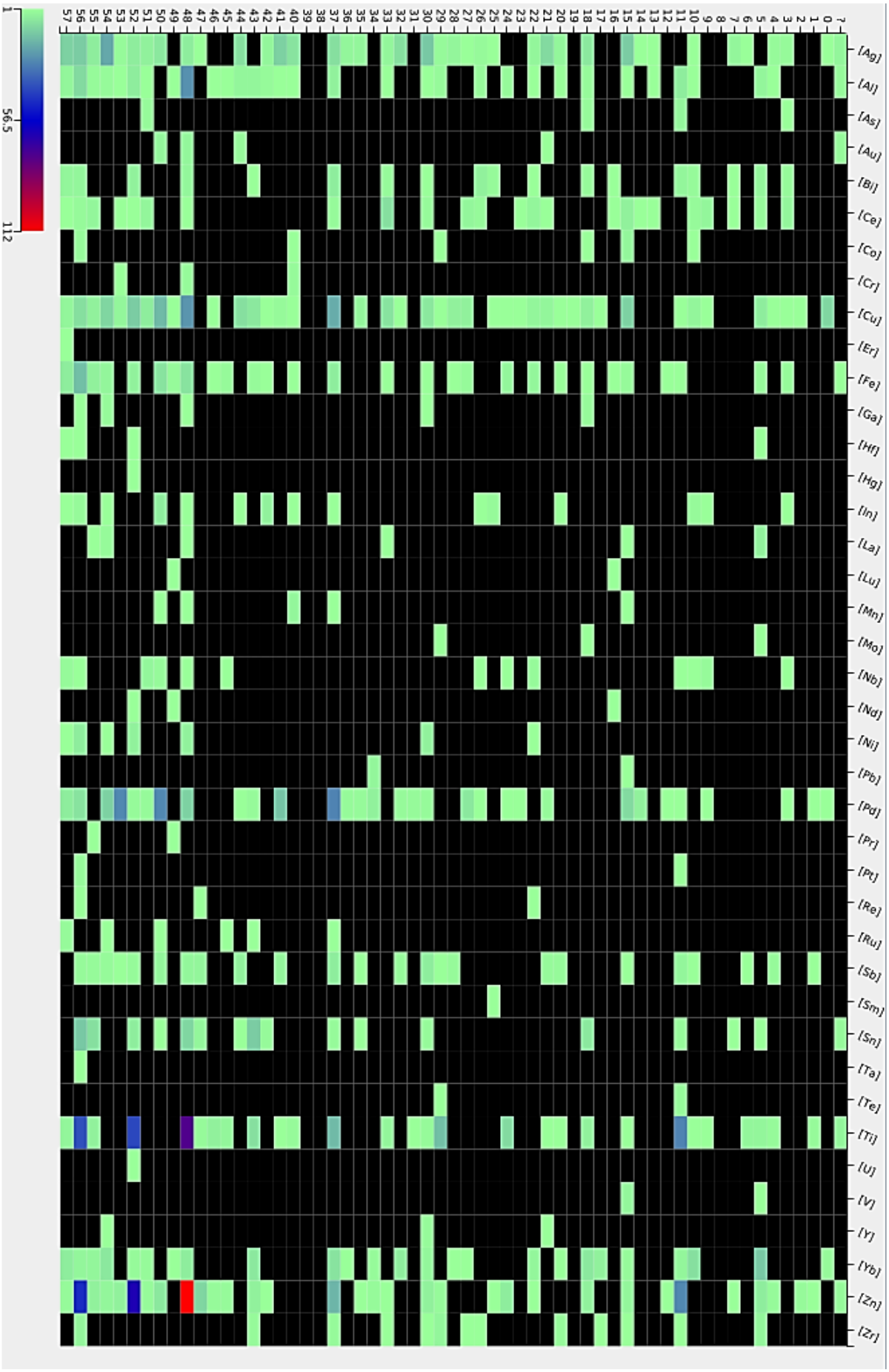

Fig. S18. Heat map relating mediators and clusters.

Visualization of the correlations by bar and pie charts

The heat map in Figure S18 gave an overview on possible interconnections between given metal centers and clusters, yet to analyze whether certain metal centers were overrepresented in certain reaction types, a deeper investigation was needed. Therefore, the bar chart of the metals and the pie chart of the clusters were generated via a parallel workflow starting from the same *Joiner* node. First of all, a numeric counter was assigned to each metal query via a *Counter Generation* node. Then, the metal query was substituted with the number by a *Cell Replacer* node. The *String Manipulation* node was employed to remove the brackets in the metals query, as they were listed as collection. The column "Winner Cluster" was renamed as "WinnerCluster" with a *Column Rename* node because the space would have disturbed the following nodes' settings.
After that, the workflow was split in 3 sections, one for the pie charts including the unknown mediators, one for the pie charts excluding the unknown mediators and the last for the bar charts per each mediator. The first one started with a *Group Loop Start* node, grouping the clusters via the pattern "WinnerCluster". This node was connected to a *Python View* node to generate the pie charts and then the loop was closed via a *Loop End* node. The script within the *Python view* node is listed in Figure S19.
For the pie charts per cluster excluding the unknown mediators, a *Row Filter* node was placed before the *Group Loop Start* to exclude the rows with the "unknown" pattern. The following *Python view* inside the loop ran the same script as the previous one. Finally, to generate the bar charts per each mediator, a similar loop was used starting with the *Group Loop Start* with the pattern "ColumnValues" and including a different script in the *Python view* node, visible in Figure S20.

```
# Load the Pandas libraries with alias 'pd'
import pandas as pd
import matplotlib.pyplot as plt

from io import BytesIO
#vars
colors = ['#C50B0D', '#E13342', '#6919DF', '#8474E7', '#1367E4', '#04ECDF', '#BC787A', '#A04D13'
df =  input_table.copy()

#preapring data

counts = df.groupby('ColumnValues')["WinnerCluster"].count()
df_plot = pd.DataFrame( counts.index.tolist(), columns = ['mediator'])

df_plot["count"]  = counts.values.tolist()

color_list = []
count_append = []
for value in df_plot["mediator"]:
    count_append.append( df.loc[(df.ColumnValues == value)]['count_append'].values.tolist()[0] )

for value in count_append:
    color_list.append(colors[int(value)])
# Label distance: gives the space between labels and the center of the pie
plt.title(flow_variables['WinnerCluster'])

plt.pie(values, labels=names, labeldistance=1.15, colors=color_list, wedgeprops = { 'linewidth'
# Create buffer to write into
buffer = BytesIO()
# Create plot and write it into the buffer
plt.savefig(buffer, format='png')

# The output is the content of the buffer
output image = buffer.getvalue()
```

Fig. S19. Script for the pie chart per each cluster, from the Python view node's configuration panel.

```
# Load the Pandas libraries with alias 'pd'
import pandas as pd
import matplotlib.pyplot as plt
import numpy as np

from io import BytesIO
#vars
colors = ['#C50B0D', '#E13342', '#6919DF', '#8474E7', '#1367E4', '#04ECDF', '#BC787A', '#A04D13'
df = input_table.copy()


#prepare data
df["WinnerCluster"] = df["WinnerCluster"].str.replace('cluster_','').str.replace('NoiseCluster',
counts = df.groupby('WinnerCluster')["ColumnValues"].count()
df_plot = pd.DataFrame( counts.index.tolist(), columns = ['cluster'])
df_plot["count"]  = counts.values.tolist()


# handle noice cluster
ids = df_plot.index[df_plot['cluster'] == 'NC'].tolist()
if len(ids) != 0:
    noice_cluster = df_plot.iloc[ids]
    noice_cluster = noice_cluster.assign(color = ['#000000']) # default color for noice cluster
    df_plot = df_plot.drop(ids)
else:
    noice_cluster = []

#sort bars
df_plot["cluster"]  = df_plot["cluster"].astype(int)
df_plot = df_plot.sort_values("cluster")

#add Colors
for value in df_plot["cluster"]:
        df_plot.loc[(df_plot.cluster == value),'color']= colors[int(value)]

if len(noice_cluster) != 0:
    df_plot = df_plot.append(noice_cluster)

if df_plot.empty == True:
    noice_cluster = noice_cluster.assign(color = ['#000000']) # default color for noice cluster
    df_plot = ""
    df_plot = noice_cluster


print(df_plot)
#ordinates
y = df_plot["count"]
x = df_plot["cluster"]
x_pos = np.arange(len(x))

# Create bars
plt.bar(x_pos, y, color=(df_plot["color"]) )
# Create names on the x-axis

plt.xlabel('Clusters')
plt.ylabel('Counts')
plt.title(flow_variables['ColumnValues'])
plt.xticks(x_pos, x)

plt.xticks(rotation = 89)

# Create buffer to write into
buffer = BytesIO()
# Create plot and write it into the buffer
plt.savefig(buffer, format='png')

# The output is the content of the buffer
output image = buffer.getvalue()
```

Fig. S20. Script to generate the bar charts per each mediator, from the Python View node's configuration panel. noice_cluster = noise cluster, i.e. reactions that could not be clustered and belong to the noise cluster.

The analysis of the correlation between mediators and clusters started with the heat map and then the pie charts for the clusters and the bar charts for the five most common mediators were compared to illustrate this part of the data analysis (Figure S21A-C).

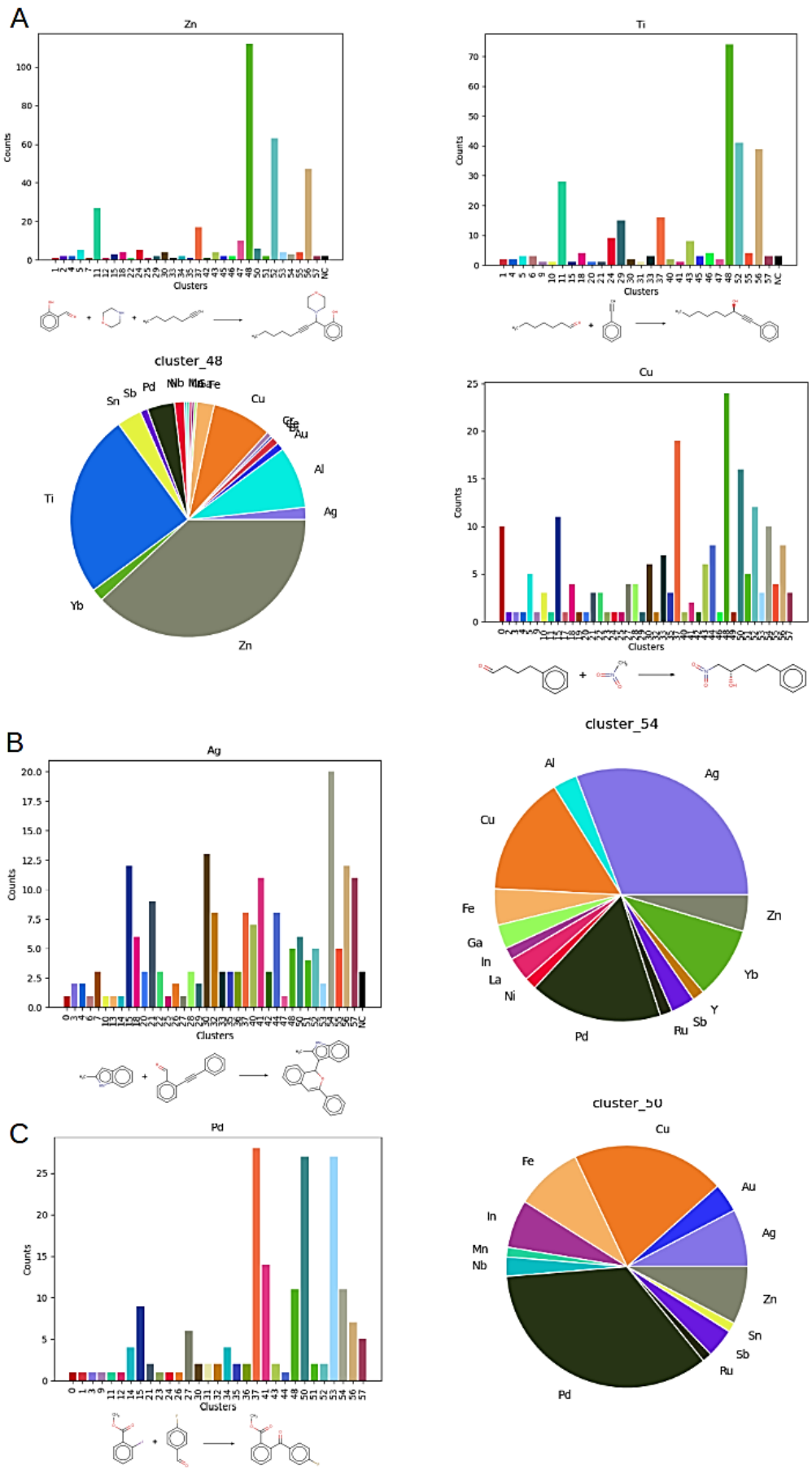

Fig. S21. Analysis of the most common metal centers, respective clusters and exemplary reactions. (A) Pie chart of cluster 48 and bar charts of its most prominent metal centers zinc, titanium and copper. (B) Bar chart of the silver metal center in comparison with cluster 54. (C) Bar chart of the palladium metal center in correlation with cluster 50.[S27-S31]

Occurrence of "privileged scaffolds" in medicinal chemistry

A component was designed to visualize the proportion of "privileged scaffolds" in medicinal chemistry within the provided data set and to assess their accessibility from the aldehyde functionality. First, the rings were firstly drawn in *MarvinSketch* resulting in the following SMILES strings:

- benzene: c1ccccc1 ,
- pyridine: c1ccncc1,
- piperidine: C1CCCNC1,
- piperazine: C1CNCCN1,
- cyclohexane: C1CCCCC1,
- tetrahydro-2H-pyran: C1CCOCC1,
- 1H-imidazole:c1c[nH]cn1,
- pyrrolidine: C1CCNC1,
- cephem: C1C=CN2C(S1)CC2=O,
- cyclopropane: C1CC1,
- tetrahydrofurane: C1CCOC1,
- thiazole: c1cscn1,
- indole: c1cc2ccccc2n1;
- pyrimidine: C1=CN=CN=C1,
- penam: C1CSC2N1C(=O)C2.

The list was fed into the "Query Molecule" port of the *RDKit Molecule Substructure Filter* node, while the "Molecules" port of the same node was fed with the clustered reactions. The "RDKit Mol" column was set to "reactants_desalt" and the option "At least one match" was checked. The second output port (excluded molecules) was connected to the *Molecule Type Cast* node which converted the products into SMILES. Then, the output table became the input of another *RDKit Molecule Substructure Filter* node, which this time considered the products. The first output port in this case was connected to the *Collection to String* node, which transformed the collection of matched scaffolds in the products into string. The following *String Manipulation* node removed the collection's delimiters "[," and "]." At this point, the matches were split by the comma delimiter and collected all in one column with the *Unpivoting* node. The output table constituted the data for the *Pie/Donut Chart* node. In parallel, the rings table from the *MarvinSketch* node was fed into the *Renderer to Image* node and then into the *Tile View* node. This combination of nodes constituted the body of the component and allowed to visualize the interactive view in Figure S22. In the view, the pie chart depicts the composition of the dataset in terms of drug scaffolds while it is possible to see the respective structures in the tile view below.

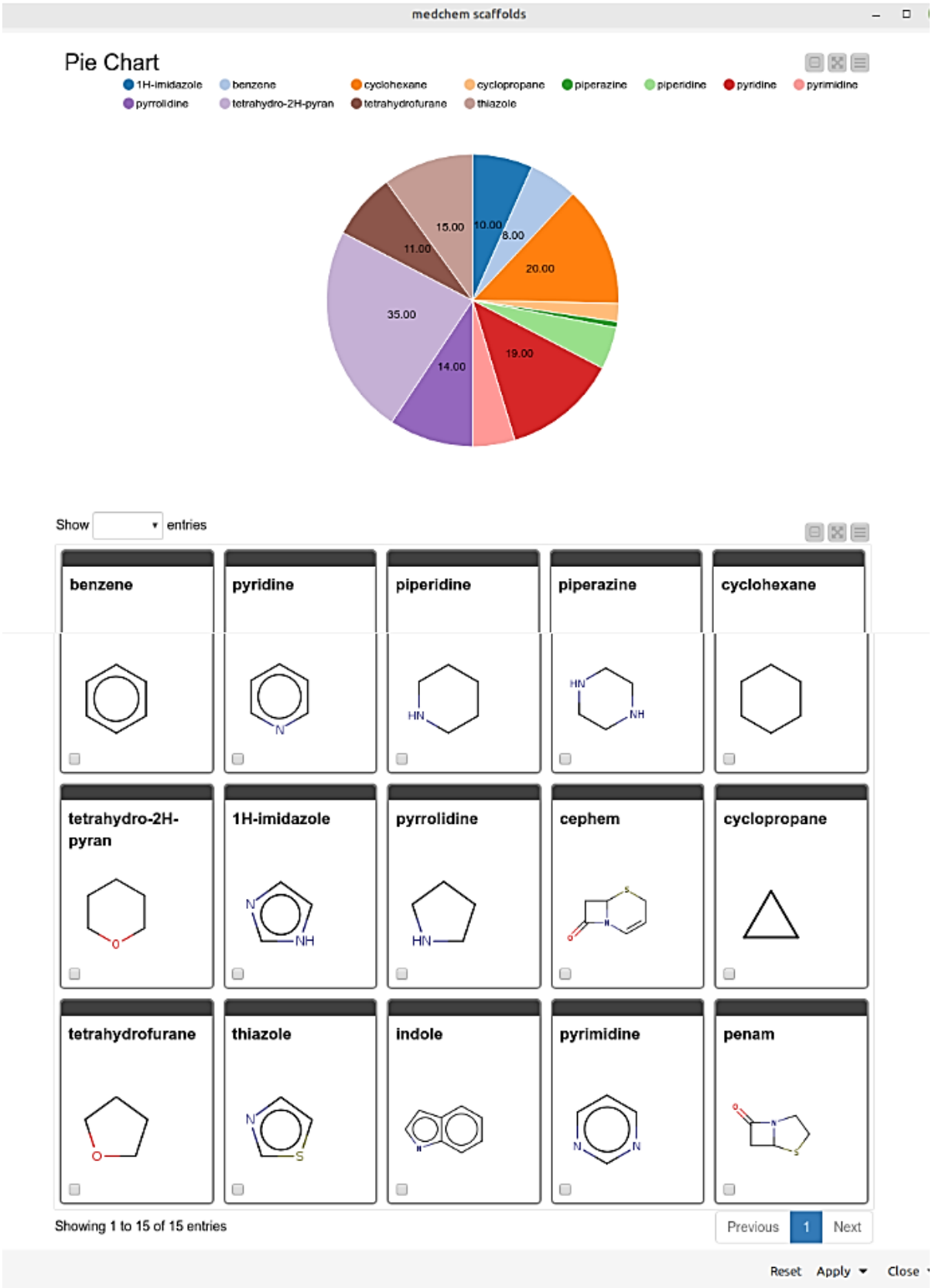

Fig. S22. KNIME view of the drug scaffolds' proportion.

Anti-reactions in DELs synthesis

The last result of our analysis was the identification of rections involving nucleosides (Figure S23), that would therefore affect the integrity of the DNA tag. In fact, if the nucleobases are modified by chemical reactions, the unique codes characterizing the encoded molecules could be read wrongly by the polymerase during the PCR (polymerase chain reaction) and the following sequencing experiments.

To identify those reactions the combinatin of the *MarvinSketch* node and the *RDKit Molecule Substructure Filter* was used, by simply drawing the nucleotides and search for those substructure among the reactants of the reactions.

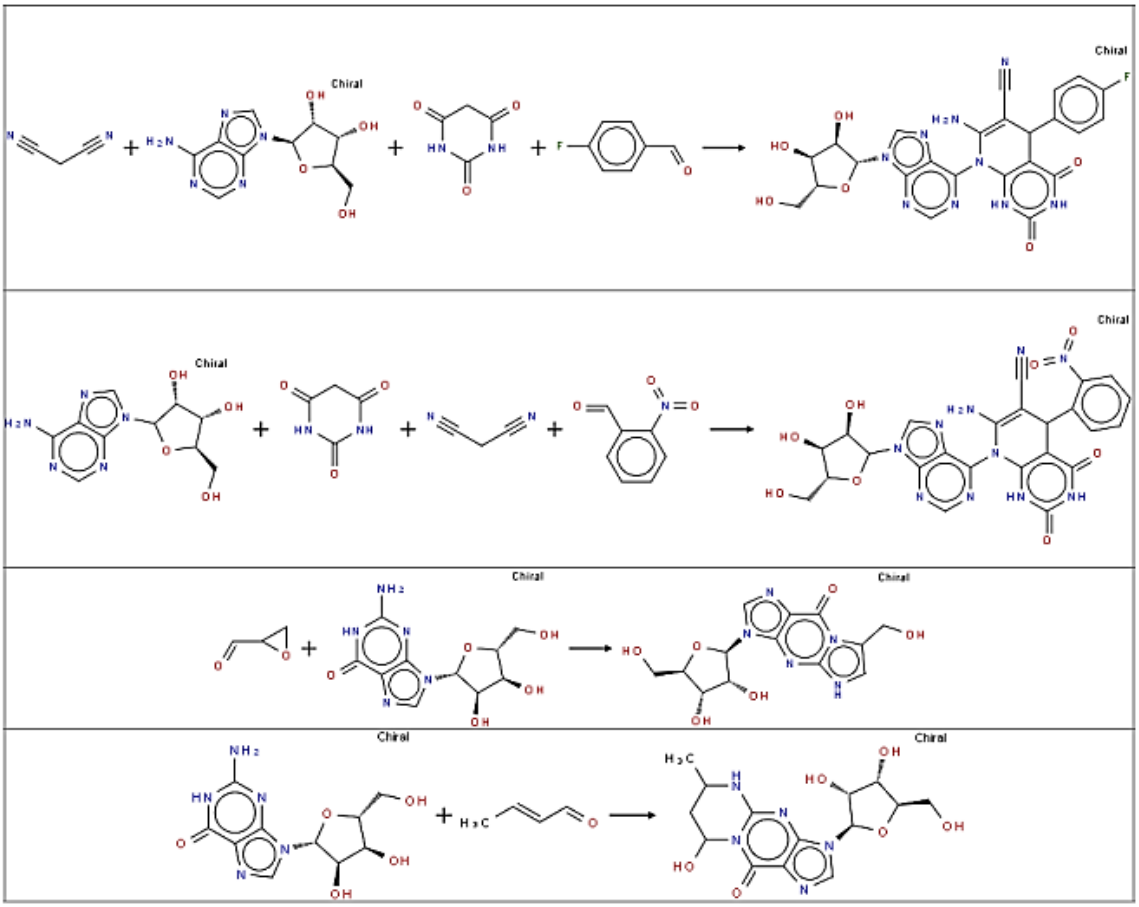

Fig. S23. *Anti-reactions*: reactions that would interfere with library synthesis as they involve nucleosides.[S32-S35]

Table S7. Highlighted reactions for the selection and experimental validation.

Reaction ID (RX.ID)	Reaction_smiles	Temper.	reagents score	solvent boiling point	LG	Winner Cluster
47150694	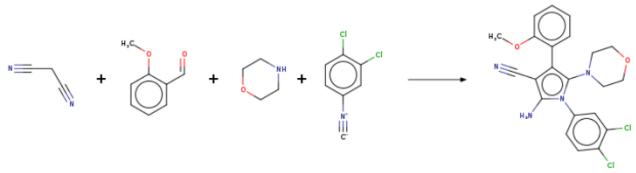	25	2	100		cluster_15
4778302	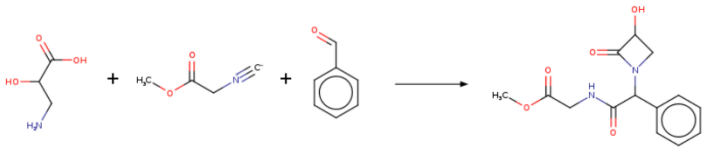		2	65		cluster_25
42227962	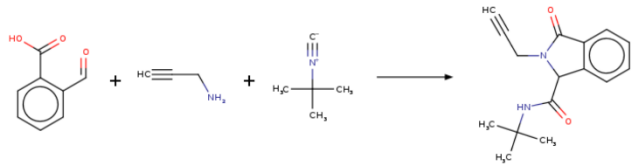	20	2	65		cluster_25
35906947	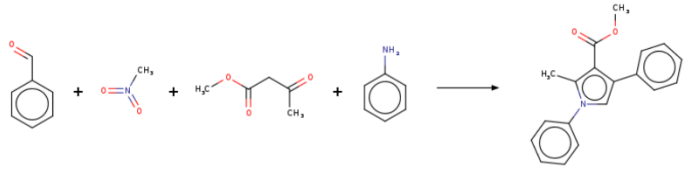	20	2	0		cluster_27
36212109	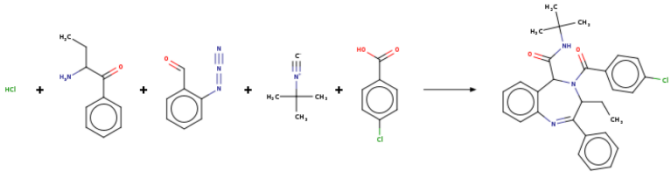	20	2	110		cluster_28
29158421	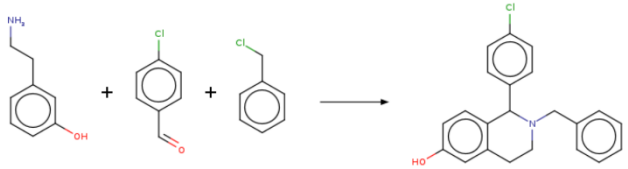	80	2	82		cluster_28
30976224	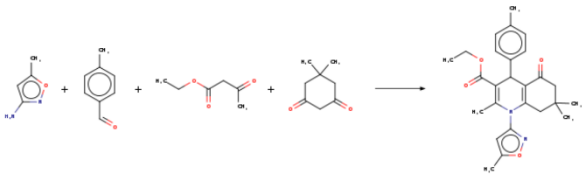		2	78		cluster_34
42819275	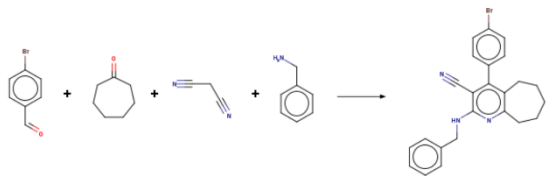		2	78		cluster_34
34309445	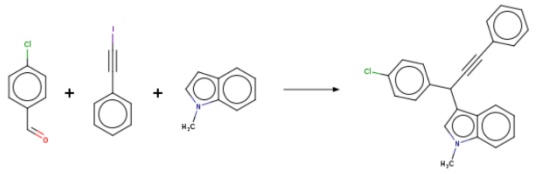	20	2	83		cluster_4
11257556	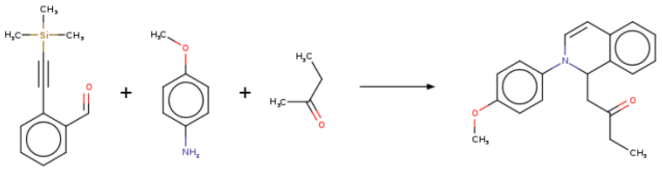				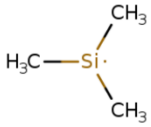	cluster_42

Reaction ID (RX.ID)	Reaction_smiles	Temper.	reagents score	solvent boiling point	LG	Winner Cluster
46804277	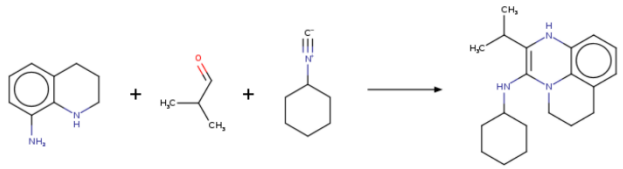	90	2	85		cluster_35
11149591	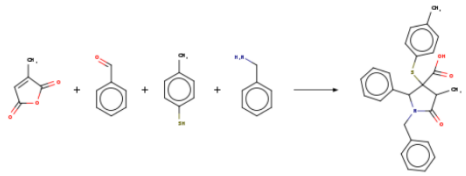	110	2	110		cluster_36
4811564	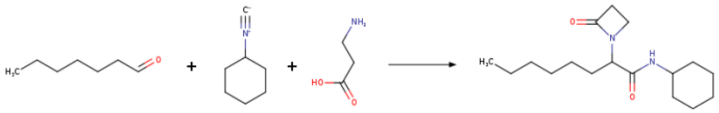		2	65		cluster_42
9084529	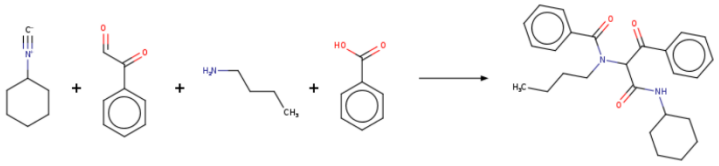	20	2	65		cluster_43
9379777	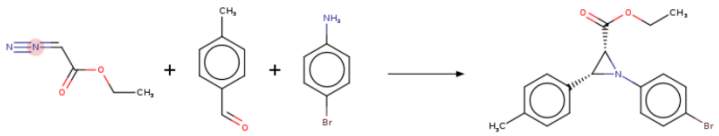	28	2	82		cluster_5
10306800	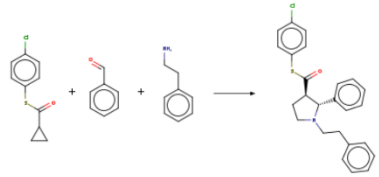	80	2	110		cluster_53
46247855	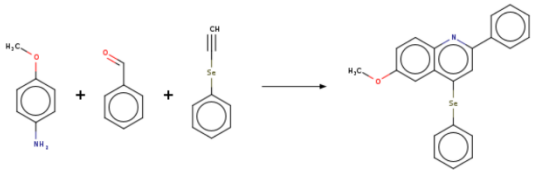	80	2	82		cluster_54
600252	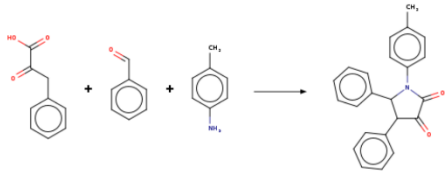		2			cluster_57
44639747	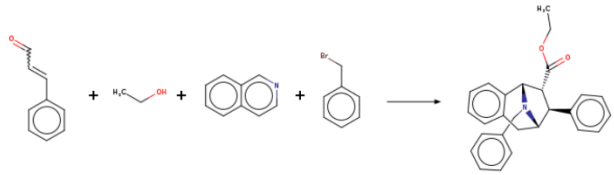	20	2	40		cluster_58
11203291	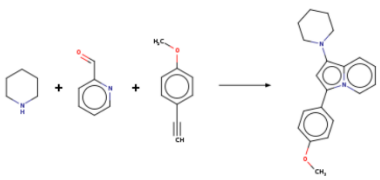	20	2	100		cluster_9

Experimental validation of selected reactions

General methods and materials

Unless otherwise noted, chemicals were purchased from *abcr, Acros Organics, Alfa Aesar, Fisher Scientific, Merck, Sigma Aldrich, TCI* and *VWR* and were used as provided without further purifications. Dry solvents (MeCN, DCE, DMA, DMF, DMSO, EtOH) were used as commercially available.

5'-Aminolinker-modified DNA oligonucleotides on controlled pore glass solid support (CPG, 1000 Å porosity) were synthesized by *Ella Biotech GmBH* (Planegg, Germany).

CPG (controlled pore glass) supported oligonucleotide-small molecule conjugates were filtered and washed through synthesis columns using a vacuum manifold (Vac-Man®) from *Sigma Aldrich*.

Semi-preparative ion pair RP-HPLC. Compound purification was performed on a *Shimadzu Prominence* HPLC System equipped with a C_{18} stationary phase (*Phenomenex*, Gemini, 5 µm, C_{18}, 110 Å, 100 x 4.6 mm). A gradient from 100 mM aqueous triethylammonium acetate (pH = 8.0, eluent A) to MeOH (eluent B) was used at a flow rate of 5 mL/min. Fractions containing the desired product were pooled and concentrated.

> **Method:** Step gradient of 20% to 70% B within 13 min, then 70% to 100% B within 1 min followed by 100% B for 3 min using 100 mM aqueous triethylammonium acetate (pH = 8.0, eluent A) and MeOH (eluent B) at a flow rate of 5 mL/min.

Analytical RP-HPLC I. HPLC analysis was performed on an *Agilent* 1100 series chromatograph equipped with 1100 Quaternary Pump (*G1311A*), a 1100 Multi-Wavelength Detector (G1365B) and an *Agilent* Eclipse Plus C_{18} (4.6 x 100 mm, 3.5 µm) column. The conversion and purity of DNA conjugates were determined by integration of peaks recorded at 254 nm wavelength.

> **Method:** Step gradient of 10% to 70% B within 10 min, then 70% to 100% B within 2 min followed by 100% B for 2 min using 10 mM aqueous triethylammonium acetate (pH = 8.0, eluent A) and MeOH (eluent B) at a flow rate of 0.6 mL/min.

Analytical RP-HPLC II. HPLC analysis was performed on a *Shimadzu Prominence* using a C_{18} stationary phase column (Phenomenex, Gemini; 4.6 x 100 mm, 110Å, 5 µm) and a gradient of 10mM aqueous triethylammonium acetate (pH=8.0)/MeOH. HPLC traces were recorded at 254nm wavelength.

> **Method:** Step gradient of 10% to 60% MeOH in 10mM aqueous triethylammonium acetate (pH=8.0) within 22 min at a flow rate of 0.6 mL/min.

MALDI-TOF. Mass analysis was performed on a MALDI TOF/TOF MS from *Bruker Daltonics* using 2',4',6'-trihydroxyacetophenone (THAP) matrix (*Dichrom*).

Representative Procedures

Amide coupling (RP-01)

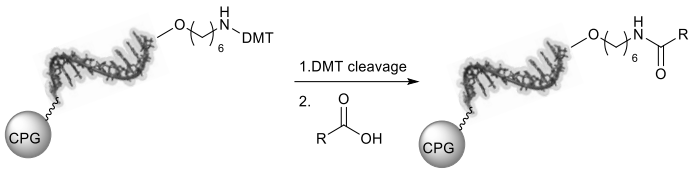

Step 1: DMT-protecting group of CPG-bound oligonucleotide (250 nmol, 9-10 mg of solid phase material) was removed by addition of 200 µL 3% trichloroacetic acid in CH_2Cl2 for 1 min. An orange coloring of the solution indicated successful removal of protecting group. The deprotection was repeated 3-5 times until no further coloring of the solution was observed. CPG-bound deprotected DNA was washed three times with each 200 µL of 1% TEA in ACN, DMF, MeOH, ACN and CH_2Cl_2 and dried in vacuo.
Step 2: CPG-coupled oligonucleotide, carboxylic acid and HATU were dried in vacuo for 30 min. Stock solutions of all reactants in dry DMF were prepared before the reaction was started. HATU (25 µmol, 100 equiv., 111 mM calculated for the final volume of 225 µL) dissolved in 75 µL dry DMF and DIPEA (62.5 µmol, 250 equiv. 277 mM calculated for the final volume of 225 µL) were added to the solution of carboxylic acid (25 µmol, 100 equiv., 111 mM calculated for the final volume of 225 µL) in 75 µL dry DMF. The mixture was shaken for 5 min and added to CPG-coupled DNA (250 nmol, 1 equiv.) suspended in 75 µL dry DMF. The amide coupling reaction was shaken at ambient temperature for 2 h. Next, the CPG-coupled conjugate was filtered over a filter column, washed three times with each 200 µL of DMF, MeOH, ACN and CH_2Cl_2 and dried in vacuo. Amide coupling was repeated two times. Completeness of amide coupling was controlled by cleaving off a small portion of CPG-coupled oligonucleotide conjugate (0.7–0.9 mg, ~20 nmol) with 500 µL AMA (AMA = aqueous ammonia (30%) / aqueous methylamine (40%), 1:1, vol/vol) for 30 min (TC) or 4 h (ATGC-sequences) at ambient temperature. Afterwards 20 µL of 1 M Tris buffer (pH = 7.5) were added, the mixture was dried under reduced pressure (SpeedVac) and DNA was dissolved in 200 µL distilled water. The crude reaction mixture was analyzed by analytical RP-HPLC and MALDI-MS. In case of uncompleted coupling (< 90%) the reaction was repeated a third time. Unreacted amines were capped with acetic acid anhydride (three times 200 µL, 30 s, 1:1 mixture of THF/methylimidazole, 9:1, vol/vol, and THF/pyridine/acetic acid anhydride 8:1:1, vol/vol). The capped CPG-coupled oligonucleotide conjugate was washed three times with each 200 µL of DMF, MeOH, ACN and CH_2Cl_2 and dried in vacuo.

Quinoline synthesis on CPG-bound oligonucleotide aldehyde conjugates (RP-02)

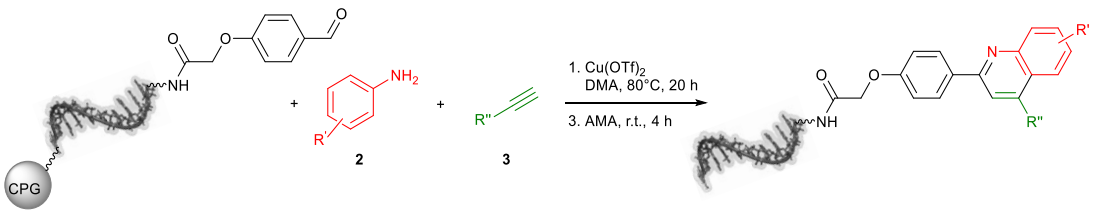

Prior to use, CPG-bound oligonucleotide aldehyde conjugate, solid aniline **2** and acetylenes **3**, as well as copper(II)triflate were dried in vacuo for 15 min. Aniline **2** (20 µmol, 200 mM), acetylene **3** (40 µmol, 400 mM and copper(II)triflate (0.5 µmol, 5 mM) were dissolved in 100 µL of dry DMA and were added to the CPG-bound oligonucleotide aldehyde conjugate (0.7 mg, 0.02 µmol). The suspension was shaken at 80 °C for 20 hours. Then the CPG-bound DNA conjugate was filtered over a filter column, washed three times with each 200 µL of 0.1 M EDTA solution, 0.1 M MgCl2 solution, water, DMF, MeOH, ACN and CH_2Cl_2 and dried in vacuo. CPG-bound oligonucleotide conjugated quinoline was cleaved from solid support and deprotected with 330 µL AMA for 4 h at ambient temperature. Then 20 µL of 1 M Tris buffer (pH = 7.5) were added, the mixture was dried under reduced pressure (SpeedVac) and afterwards dissolved in 45 µL of distilled water. 5 µL of 1,3,5-triazine-2,4,6-trithiol trisodium salt solution (15% in H2O) were added and the solution was shaken for 30 min at ambient temperature. Afterwards the sample was centrifuged at 4 °C for 30 min (13200 rpm; Centrifuge 5415 R, Eppendorf), the supernatant was taken off and diluted with 5 µL of a 3 M sodium acetate (pH = 5.2) and 200 µL 100% ethanol. The solution was incubated overnight at -80 °C. Afterwards the samples were centrifuged at 4 °C for 30 min (13200 rpm; Centrifuge 5415 R, Eppendorf), the supernatant was taken off, additional 100 µL of 100% ethanol were added to the pellet and the solution was incubated again for 1 h at -80 °C. Afterwards the sample was centrifuged at 4 °C for 30 min (13200 rpm; Centrifuge 5415 R, Eppendorf), the supernatant was taken off, and the DNA pellets were dried at 37 °C. The DNA samples were dissolved in 100 µL ddH2O. The crude was analyzed by analytical RP HPLC I and MALDI-MS. The product was purified by preparative RP-HPLC.

Pyrrole synthesis on CPG-bound oligonucleotide aldehyde conjugates (RP-03)

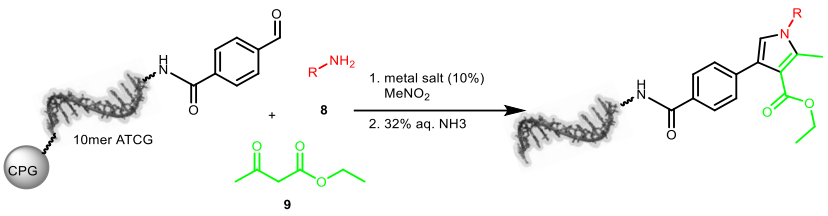

The amine **8** (200 eq., 4 µmol), the ethylacetoacetate **9** (200 eq., 4 µmol), and the given reaction promoter (10%, 20 eq., 0.4 µmol) were dissolved in nitromethane and added to 20 nmol of the CPG-bound DNA for a final volume of 40 µL and a concentration of 250 mM for all reagents except the metal salt whose concentration was 25 mM. The reaction mixtures were stirred, then transferred to a filter column and washed with dimethylformamide. Firstly, the samples were incubated with EDTA for 30 seconds and then washed 3 times with 200 µL dimethylformamide, metanol, acetonitrile and dichloromethane. Finally, the DNA-conjugates were cleaved from the solid support by dispersion in 32% aq. solution of ammonia, which was stirred for four hours. Subsequently, 20 µL of 1 M Tris buffer (pH = 7.5) were added and the mixture was dried under reduced pressure (SpeedVac). After re-dispersion in ddH2O and filtration, the samples were further purified by adding 5µL of 1,3,5-Triazine-2,4,6-trithiol trisodium salt solution to 45 µL of sample and stirring for 30 minutes. Then, the dispersion was centrifuged for 30 min at 4 °C at 11000 rpm and to the supernatant 5 µL of 3% sodium acetate aq. solution and 220 µL ethanol were added. The solution was then incubated at -80 °C overnight, then centrifuged, decanted and the pellet was re-dispersed in 200 µL of ethanol, incubated for 1 hour at -80°C and then centrifuged and decanted. The pellet was dissolved in water and analyzed by RP HPLC II and MALDI-TOF.

Pyrrolidine synthesis on CPG-bound oligonucleotide amine conjugate (RP-04)

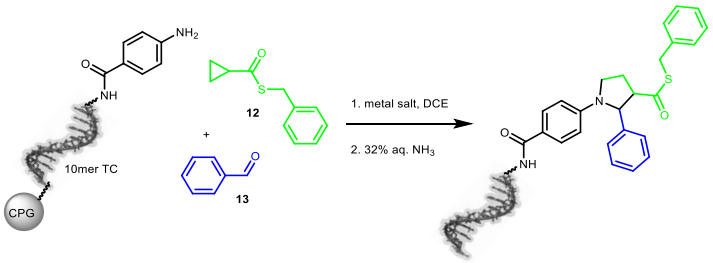

The oligonucleotide amine conjugate on CPG (20 nmol) and the thioester **12** (1000 eq., 20 µmol) were dried under low pressure for three hours. Then, they and the benzaldehyde **13** (1000 eq., 20 µmol) were separately solved in dichloroethane. The reagents including the metal salt (1000 eq., 20 µmol) were added to the DNA/dichloroethane dispersion, and the reaction was shaken for one hour. Afterwards, the reaction was stopped by washing the CPG-bound DNA three times with 200 µL dimethylformamide, methanol, acetonitrile and dichloromethane. For the analysis, the DNA conjugate was cleaved from the CPG by dispersion in a 32% aq. solution of ammonia and incubation for 30 minutes. Then, 20 µL of 1 M Tris buffer (pH = 7.5) were added, the mixture was dried under reduced pressure (SpeedVac) and redissolved in water to filter the CPG. The water phase was analyzed by MALDI-TOF to assess the presence of product.

Quinoline synthesis

Optimization of quinoline synthesis on CPG-bound DNA aldehyde conjugates

Table S8. Optimization of quinoline synthesis on a CPG-coupled pyrimidine DNA-aldehyde conjugate **5**.[a]

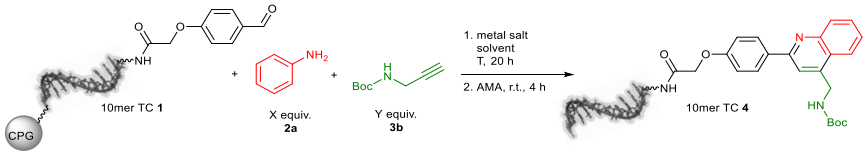

Entry	2a [mM]	3b [mM]	metal salt	[mM]	solvent	T [°C]	Conversion [%][b]
1	200	600	---	---	DMA/TEOF 4:1	50	n.d.
2	200	600	$FeCl_3$	40	DMA/TEOF 4:1	50	n.d.
3	200	600	$Yb(OTf)_3$	40	DMA/TEOF 4:1	50	n.d.
4	200	600	$Sc(OTf)_3$	40	DMA/TEOF 4:1	50	n.d.
5	200	600	$Cu(OTf)_2$	40	DMA/TEOF 4:1	50	59 (32)
6	100	600	$Cu(OTf)_2$	40	DMA/TEOF 4:1	50	41 (27)
7	400	600	$Cu(OTf)_2$	40	DMA/TEOF 4:1	50	45 (22)
8	200	200	$Cu(OTf)_2$	40	DMA/TEOF 4:1	50	36 (18)
9	200	400	$Cu(OTf)_2$	40	DMA/TEOF 4:1	50	57 (27)
10	200	1200	$Cu(OTf)_2$	40	DMA/TEOF 4:1	50	58 (31)
11	200	400	$Cu(OTf)_2$	20	DMA/TEOF 4:1	50	57 (18)
12	200	400	$Cu(OTf)_2$	20	DMA	50	65 (32)
13	200	400	$Cu(OTf)_2$	20	MeCN	50	<5 (11)
14	200	400	$Cu(OTf)_2$	20	EtOH	50	55 (36)
15	200	400	$Cu(OTf)_2$	20	DMF	50	43 (17)
16	200	400	$Cu(OTf)_2$	20	DMSO	50	<5 (<5)
17	200	400	$Cu(OTf)_2$	20	DCE	50	27 (44)
18	200	400	$Cu(OTf)_2$	20	DMA	80	75 (16)

[a] The suspension of DNA-aldehyde conjugate **1** (20 nmol), aniline **2a** (X mM), *N*-Boc-propargylamine **3a** (Y mM), metal salt (Z mM) in solvent (100 µL) was shaken at the given temperature. DNA cleavage with AMA (30% aqueous ammonia / 40% aqueous methylamine, 1:1 (vol/vol)) at ambient temperature for 0.5 h. [b] Determined by RP-HPLC I analysis based on the ratios of **1** to **4**; the fraction of byproducts is given in brackets. DCE = 1,2-dichloroethane, DMSO = dimethyl sulfoxide, DMA = dimethylacetamide, DMF = dimethylformamide, MeCN = acetonitrile, TEOF = triethyl orthoformate n.d. = not detected, 10mer TC = 5'-TTC CTC TCC T-3'-CPG, changed parameters are written in red and italic.

Table S9. Optimization of quinoline synthesis on a CPG-coupled 10mer ATGC-oligonucleotide conjugate **5**.[a]

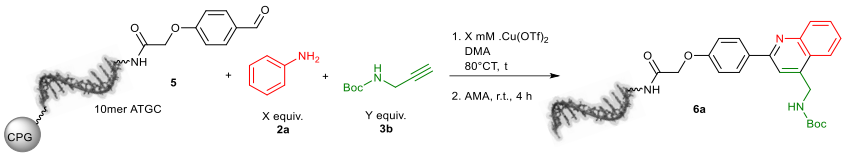

Entry	X [mM]	T [h]	Conversion [%][b]	DNA degradation [%][c]
1	20	20	60 (28)	33
2	10	20	65 (27)	19
3	5	20	67 (21)	14
4d	20	4	58 (30)	19

[a] The suspension of DNA-aldehyde conjugate **5** (20 nmol), aniline **2a** (200 mM), *N*-Boc-propargylamine **3a** (400 mM), $Cu(OTf)_2$ (Z mM) in dimethylacetamide (100 µL) was shaken at 80°C. DNA cleavage with AMA (30% aqueous ammonia / 40% aqueous methylamine, 1:1 (vol/vol)) at ambient temperature for 4 h. [b] Determined by RP-HPLC I analysis based on the ratios of **5** to **6a**; the fraction of byproducts is given in brackets. [c] Determined by RP-HPLC I analysis in ratio to the purity of the CPG-coupled DNA-aldehyde conjugate **5**. 10mer ATGC = 5′-NH_2-C_6-GTCATGATCT-3′-CPG

Table S10. Optimization of $CuOTf_2$-mediated quinoline synthesis on CPG-coupled 10mer TC-aldehyde conjugate.[a]

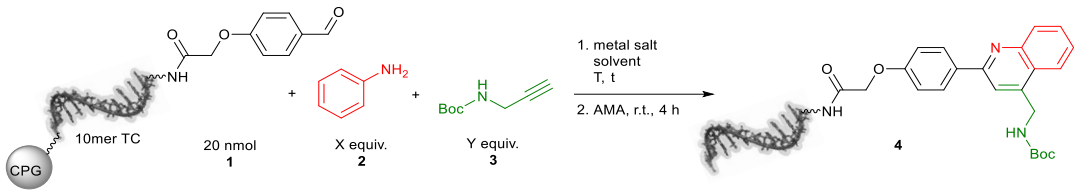

Entry	Reaction conditions	HPLC I trace of crude reaction mixture[c]
1	10mer TC aldehyde conjugate 1	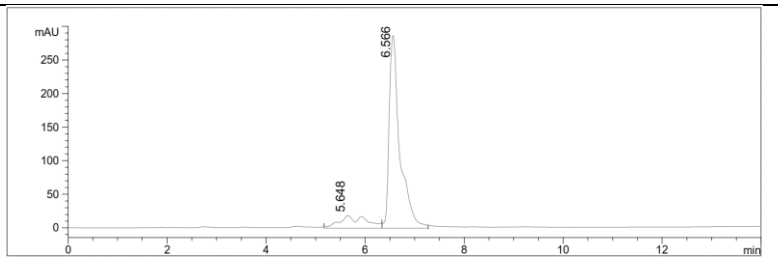
2	10mer TC quinoline conjugate 4	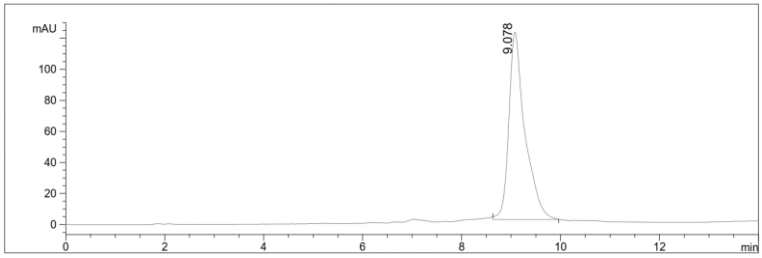
3	200 mM 2° 600 mM 3a DMA/TEOF (4:1) 50 °C, 20 h => conversion <5 %[b]	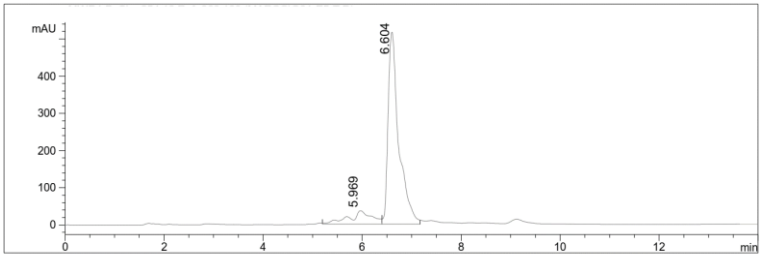
4	200 mM 2° 600 mM 3a 40 mM *FeCl₃* DMA/TEOF (4:1) 50 °C, 20 h => conversion <5 %	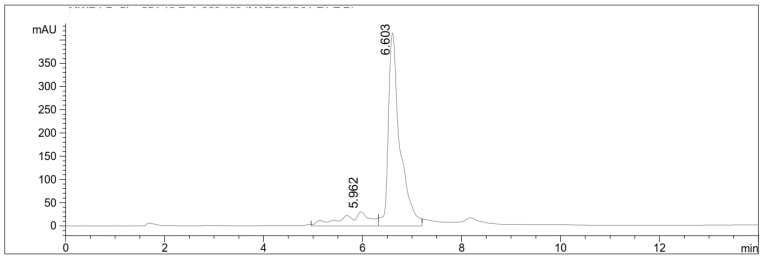

Peak list:

Ret. Time	Width min	Height	Area	Area %
5.648	0.625	18.791	704.358	14.051
6.566	0.250	286.865	4308.501	85.949

Peak list:

Ret. Time	Width min	Height	Area	Area %
5.969	0.530	35.810	1139.284	12.877
6.604	0.249	516.171	7707.861	87.123

Peak list:

Ret. Time	Width min	Height	Area	Area %
5.962	0.669	30.140	1209.639	15.324
6.603	0.268	415.001	6684.129	84.676

5

200 mM 2a
600 mM 3a
40 mM *Yb(OTf)₃*
DMA/TEOF (4:1)
50 °C, 20 h

=> conversion <5 %

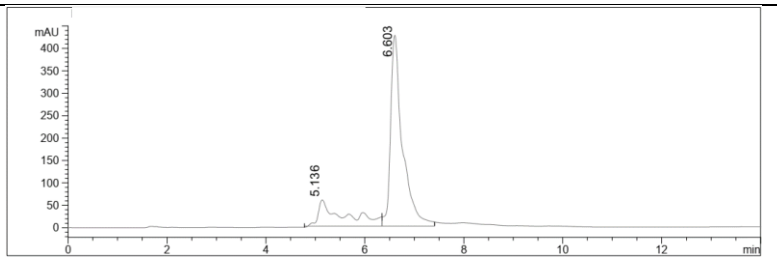

Peak list:

Ret. Time	Width min	Height	Area	Area %
5.136	0.594	58.416	2080.459	22.518
6.603	0.280	426.036	7158.791	77.482

6

200 mM 2°
600 mM 3a
40 mM *Sc(OTf)₃*
DMA/TEOF (4:1)
50 °C, 20 h

=> conversion <5 %

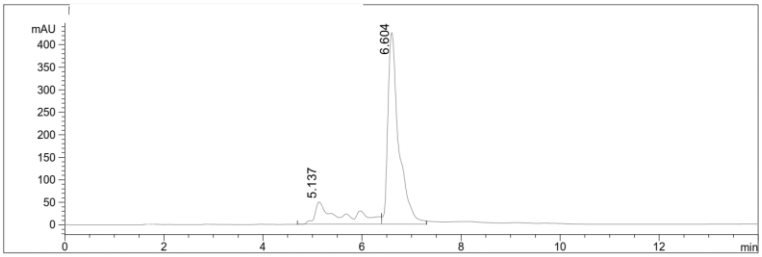

Peak list:

Ret. Time	Width min	Height	Area	Area %
5.137	0.631	48.993	1854.377	22.229
6.604	0.254	425.377	6487.964	77.771

7

200 mM 2°
600 mM 3a
40 mM *Cu(OTf)₂*
DMA/TEOF (4:1)
50 °C, 20 h

=> conversion 59 (32) %

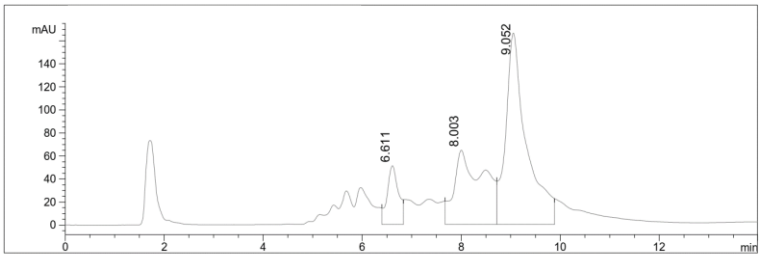

Peak list:

Ret. Time	Width min	Height	Area	Area %
6.611	0.264	50.932	805.665	9.789
8.003	0.673	64.461	2603.920	31.639
9.052	0.483	166.233	4820.618	58.572

8

100 mM 2°
600 mM 3a
40 mM $Cu(OTf)_2$
DMA/TEOF (4:1)
50 °C, 20 h

=> conversion 41 (27) %

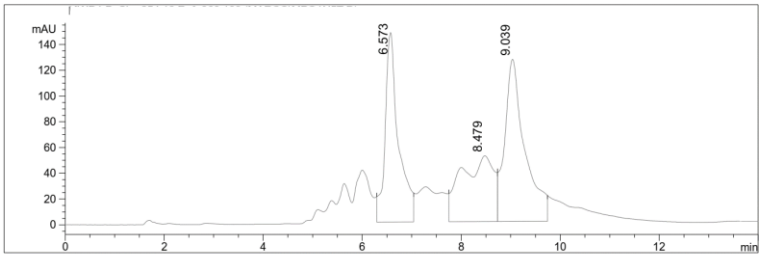

Peak list:

Ret. Time	Width min	Height	Area	Area %
6.573	0.311	146.993	2740.156	31.939
8.479	0.751	51.136	2305.110	26.868
9.039	0.468	125.972	3534.163	41.193

9

400 mM 2°
600 mM 3a
40 mM $Cu(OTf)_2$
DMA/TEOF (4:1)
50 °C, 20 h

=> conversion 45 (22) %

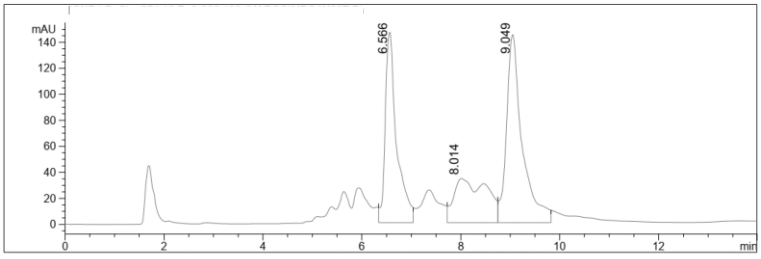

Peak list:

Ret. Time	Width min	Height	Area	Area %
6.566	0.266	146.374	2338.189	33.106
8.014	0.767	33.897	1559.224	22.077
9.049	0.365	144.540	3165.399	44.818

10

200 mM 2°
200 mM 3a
40 mM $Cu(OTf)_2$
DMA/TEOF (4:1)
50 °C, 20 h

=> conversion 36 (18) %

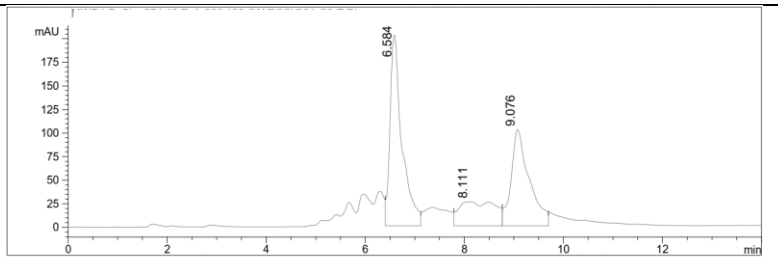

Peak list:

Ret. Time	Width min	Height	Area	Area %
6.584	0.277	202.475	3369.059	46.323
8.111	0.851	25.485	1300.706	17.884
9.076	0.425	102.016	2603.178	35.793

11

200 mM 2°
400 mM 3a
40 mM $Cu(OTf)_2$
DMA/TEOF (4:1)
50 °C, 20 h

=> conversion 57 (27) %

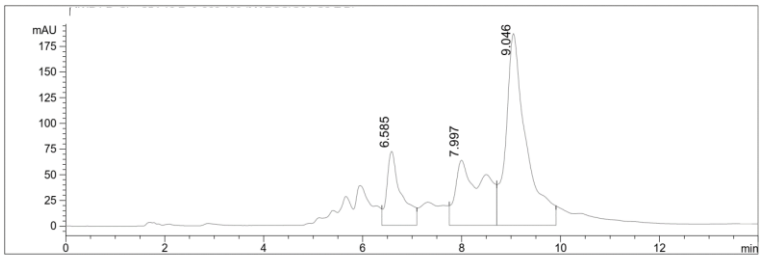

Peak list:

Ret. Time	Width min	Height	Area	Area %
6.585	0.337	71.894	1452.336	15.812
7.997	0.656	63.226	2487.612	27.083
9.046	0.469	186.552	5245.255	57.105

12

200 mM 2°
1200 mM 3a
40 mM $Cu(OTf)_2$
DMA/TEOF (4:1)
50 °C, 20 h

=> conversion 58 (31) %

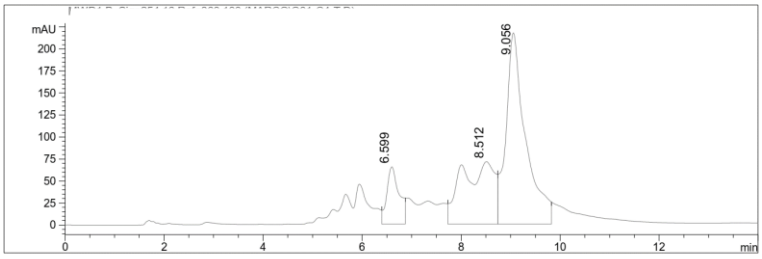

Peak list:

Ret. Time	Width min	Height	Area	Area %
6.599	0.290	64.865	1127.677	10.942
8.512	0.758	70.758	3217.046	31.215
9.056	0.458	217.166	5961.500	57.844

13

200 mM 2°
400 mM 3a
20 mM $Cu(OTf)_2$
DMA/TEOF (4:1)
50 °C, 20 h

=> conversion 57 (18) %

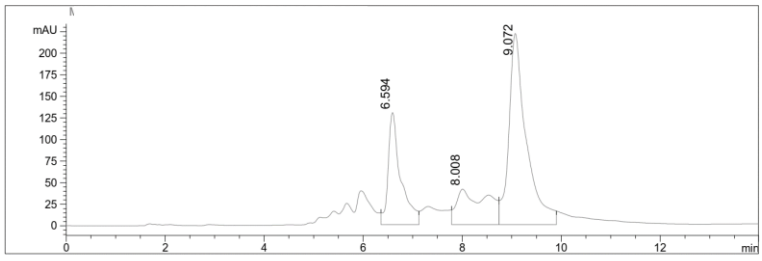

Peak list:

Ret. Time	Width min	Height	Area	Area %
6.594	0.293	129.929	2287.365	24.231
8.008	0.700	41.225	1731.817	18.346
9.072	0.408	221.648	5420.718	57.423

14

200 mM 2°
400 mM 3a
20 mM $Cu(OTf)_2$
DMA
50 °C, 20 h

=> conversion 65 (32) %

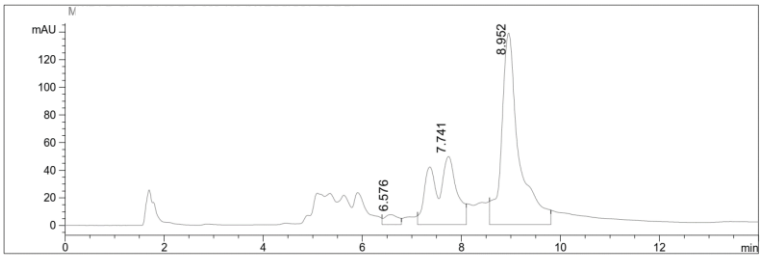

Peak list:

Ret. Time	Width min	Height	Area	Area %
6.576	0.319	7.205	138.030	2.671
7.741	0.565	49.271	1671.060	32.332
8.952	0.404	138.566	3359.381	64.998

15

200 mM 2°
400 mM 3a
20 mM $Cu(OTf)_2$
MeCN
50 °C, 20 h

=> conversion <5 (11) %

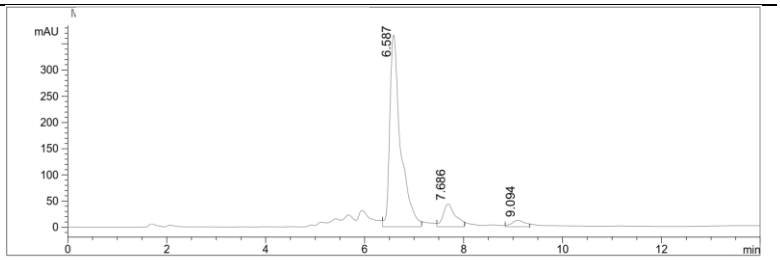

Peak list:

Ret. Time	Width min	Height	Area	Area %
6.587	0.254	365.708	5571.806	85.207
7.686	0.287	43.217	744.274	11.382
9.094	0.312	11.900	223.042	3.411

16

200 mM 2°
400 mM 3a
20 mM $Cu(OTf)_2$
EtOH
50 °C, 20 h

=> conversion 55 (36) %

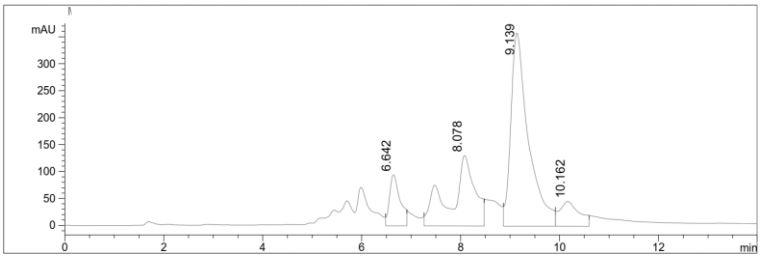

Peak list:

Ret. Time	Width min	Height	Area	Area %
6.642	0.248	94.793	1407.840	8.798
8.078	0.564	130.973	4433.256	27.705
9.139	0.412	358.533	8867.799	55.418
10.162	0.468	46.020	1292.898	8.080

17

200 mM 2°
400 mM 3a
20 mM $Cu(OTf)_2$
DMF
50 °C, 20 h

=> conversion 43 (17) %

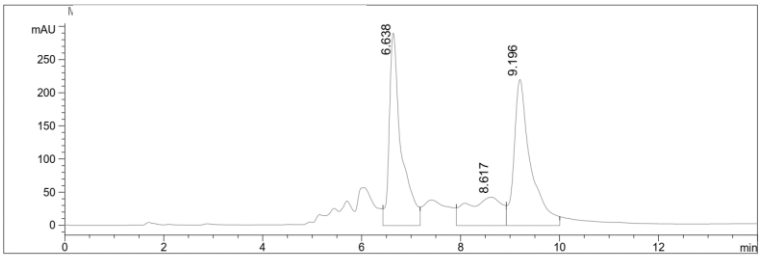

Peak list:

Ret. Time	Width min	Height	Area	Area %
6.638	0.278	290.248	4846.276	40.268
8.617	0.809	42.846	2080.016	17.283
9.196	0.387	220.270	5108.799	42.449

18

200 mM 2°
400 mM 3a
20 mM $Cu(OTf)_2$
DMSO
50 °C, 20 h

=> conversion <5 (<5) %

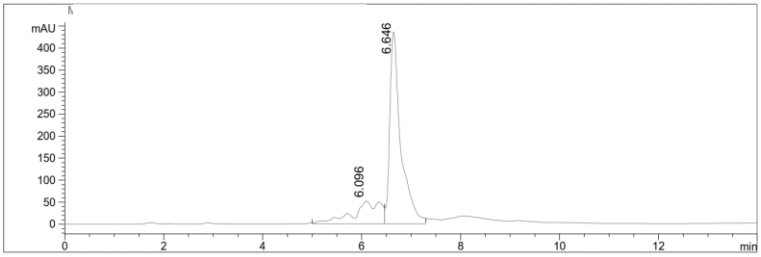

Peak list:

Ret. Time	Width min	Height	Area	Area %
6.096	0.642	51.295	1975.266	22.664
6.646	0.258	435.484	6740.172	77.336

19

200 mM 2°
400 mM 3a
20 mM $Cu(OTf)_2$
DCE
50 °C, 20 h

=> conversion 27 (44) %

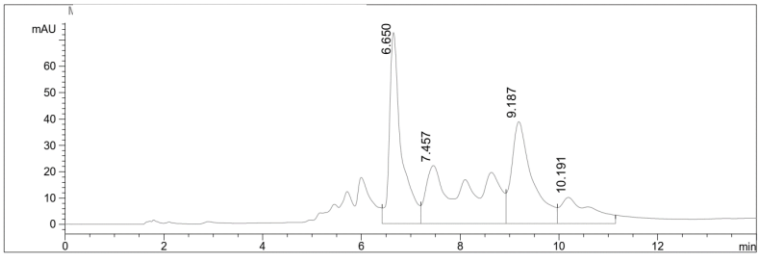

Peak list:

Ret. Time	Width min	Height	Area	Area %
6.650	0.277	72.490	1205.462	28.789
7.457	1.079	22.015	1425.766	34.051
9.187	0.487	38.620	1127.944	26.938
10.191	0.720	9.901	427.986	10.221

20	200 mM 2° 400 mM 3a *20 mM* $Cu(OTf)_2$ DMA *80 °C*, 20 h => conversion 75 (16) %	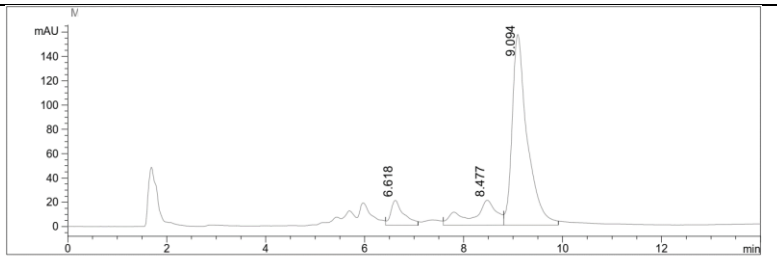 Peak list: Ret. Time Width min Height Area Area % 6.618 0.306 20.461 375.586 8.516 8.477 0.585 20.572 721.997 16.370 9.094 0.352 156.889 3312.889 75.114

[a] The suspension of DNA-aldehyde conjugate **1** (20 nmol), aniline **2a** (X mM), *N*-Boc-propargylamine **3a** (Y mM), promotor (Z mM) in solvent (100 µL) was shaken at temperature. DNA cleavage with AMA (30% aqueous ammonia / 40% aqueous methylamine, 1:1 (vol/vol)) at ambient temperature for 0.5 h. [b] Determined by RP-HPLC I analysis based on the ratios of **1** to **4**; the fraction of byproducts is given in brackets. DCE = 1,2-dichloroethane, DMSO = dimethyl sulfoxide, DMA = dimethylacetamide, DMF = dimethylformamide, MeCN = acetonitrile, n.d. = not detected, 10mer TC = 5'-TTC CTC TCC T-3'-CPG, changed parameters are written in red and italic.

Table S11. Optimization of $CuOTf_2$-mediated quinoline synthesis on CPG-coupled 10mer ATGC-aldehyde conjugate.[a]

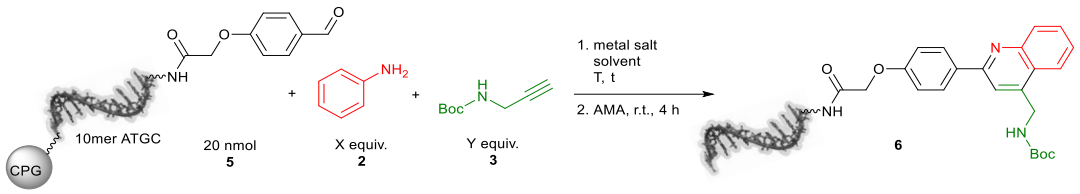

Entry	Reaction conditions	HPLC I trace of crude reaction mixture[c]
1	10mer ATGC aldehyde conjugate **5**	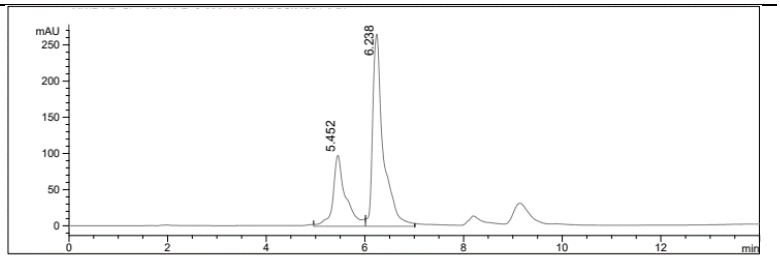

Peak list:

Ret. Time	Width min	Height	Area	Area %
5.452	0.297	98.111	1750.915	30.533
6.238	0.250	265.618	3983.549	69.467

2	10mer ATGC quinoline conjugate **6**	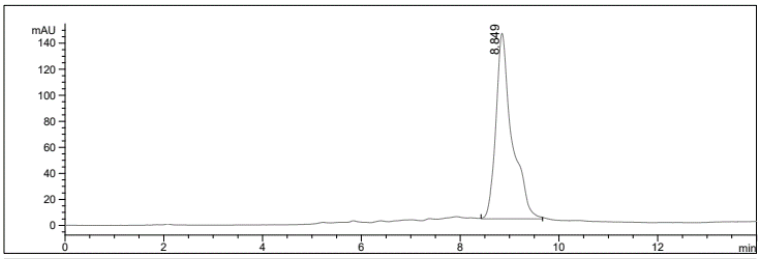
3	200 mM **2°** 400 mM **3a** *20 mM* $Cu(OTf)_2$ DMA 80 °C, 20 h => conversion 60 (28)%[b] => DNA damage 33%[c]	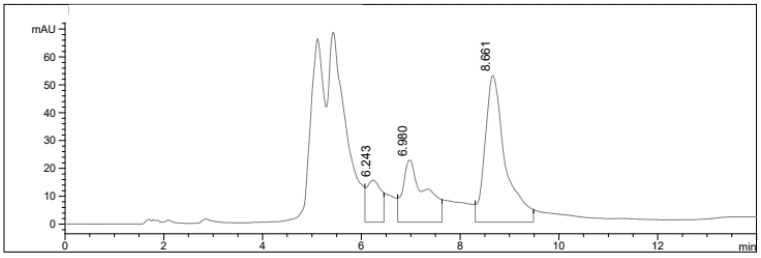

Peak list:

Ret. Time	Width min	Height	Area	Area %
6.243	0.338	15.015	304.659	12.230
6.980	0.522	22.235	696.197	27.947
8.661	0.472	52.667	1490.257	59.823

4	200 mM **2°** 400 mM **3a** *10 mM* $Cu(OTf)_2$ DMA 80 °C, 20 h => conversion 65 (27)% => DNA damage 19%	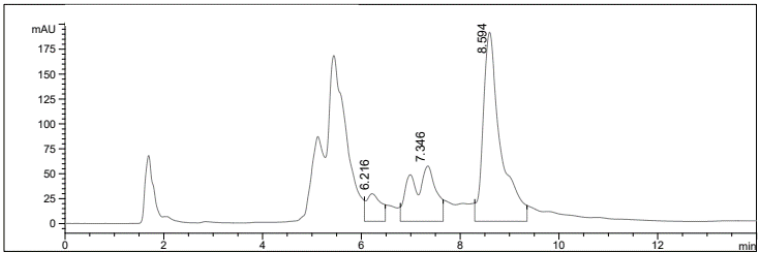

Peak list:

Ret. Time	Width min	Height	Area	Area %
6.216	0.341	27.592	564.592	7.988
7.346	0.567	55.430	1885.314	26.674
8.594	0.406	189.745	4618.081	65.338

5	200 mM **2°** 400 mM **3a** *5 mM* $Cu(OTf)_2$ DMA 80 °C, 20 h => conversion 67 (21)% => DNA damage 14%	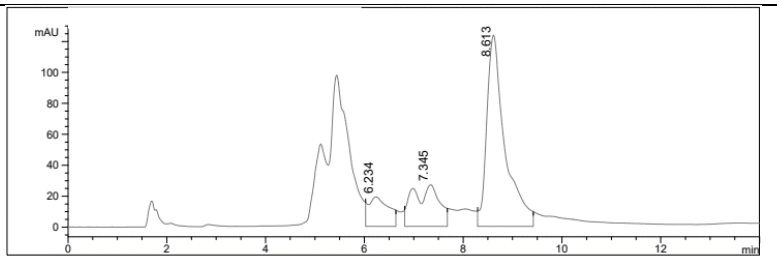 Peak list: Ret. Time | Width min | Height | Area | Area % 6.234 | 0.475 | 19.055 | 543.492 | 11.594 7.345 | 0.614 | 26.876 | 990.223 | 21.124 8.613 | 0.425 | 123.565 | 3153.875 | 67.281
6	200 mM **2°** 400 mM **3a** *20 mM* $Cu(OTf)_2$ DMA 80 °C, *4 h* => conversion 58 (30) % => DNA damage 19%	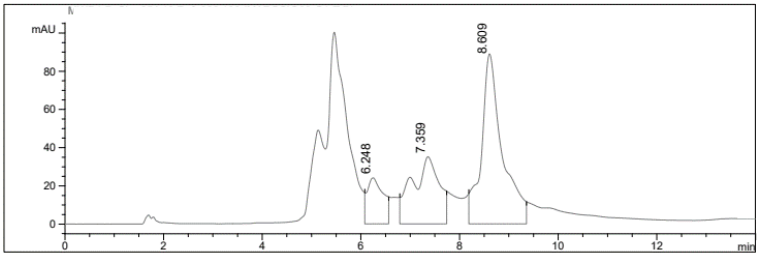 Peak list: Ret. Time | Width min | Height | Area | Area % 6.248 | 0.376 | 24.076 | 542.880 | 12.222 7.359 | 0.627 | 35.090 | 1319.314 | 29.702 8.609 | 0.484 | 88.897 | 2579.678 | 58.076

[a] The suspension of DNA-aldehyde conjugate **5** (20 nmol), aniline **2a** (200 mM), *N*-Boc-propargylamine **3a** (400 mM), $Cu(OTf)_2$ (Z mM) in dimethylacetamide (100 µL) was shaken at 80°C. DNA cleavage with AMA (30% aqueous ammonia / 40% aqueous methylamine, 1:1 (vol/vol)) at ambient temperature for 4 h. [b] Determined by RP-HPLC I analysis based on the ratios of **5** to **6**; the fraction of byproducts is given in brackets. [c] Determined by RP-HPLC I analysis in ratio to the purity of the CPG-coupled DNA-aldehyde conjugate **5**. 10mer ATGC = 5'-NH2-C6-GTCATGATCT-3'-CPG, changed parameters are written in red and italic.

Scope of quinoline synthesis

Table S12. Scope of quinoline synthesis on a CPG-coupled DNA-aldehyde conjugate 5 using various anilines **2**.[a]

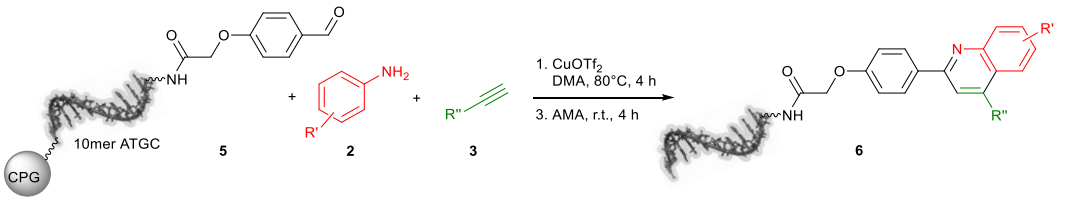

Entry	Product	Aniline 2	Alkyne 3	Conversion [%][b]	DNA degradation [%][c]	$Mass_{calc.}$ $Mass_{found}$[d]
1	6a	 **2a**	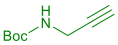 **3a**	80 (12)	8	3587.6 3589.4
2	6b	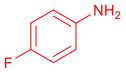 **2b**	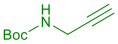 **3a**	77 (12)	4	3605.6 3608.0
3	6c	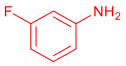 **2c**	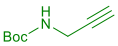 **3a**	74 (17)	10	3605.6 3609.0
4	6d	 **2d**	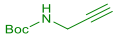 **3a**	39 (0)	15	3605.6 3608.3
5	6e	 **2e**	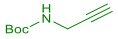 **3a**	26 (0)	27	3623.6 3627.1
6	6f	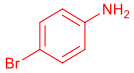 **2f**	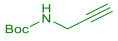 **3a**	83 (5)	11	3666.5 3668.7
7	6g	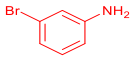 **2g**	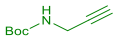 **3a**	87 (7)	5	3666.5 3669.4
8	6h	 **2h**	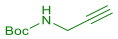 **3a**	<5	11	3666.5 n.d.
9	6i	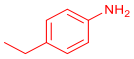 **2i**	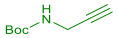 **3a**	70 (25)	8	3615.7 3616.2
10	6j	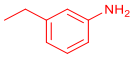 **2j**	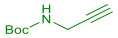 **3a**	63 (31)	18	3615.7 3618.5
11	6k	 **2k**	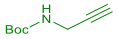 **3a**	38 (10)	6	3615.7 3618.7
12	6l	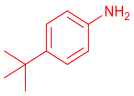 **2l**	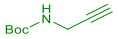 **3a**	62 (24)	0	3643.7 3645.1
13	6m	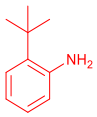 **2m**	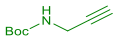 **3a**	<5	0	3643.7 n.d.

14	**6n**	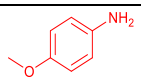 **2n**	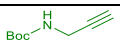 **3a**	61 (25)	18	3617.6 3620.1
15	**6o**	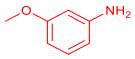 **2o**	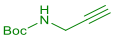 **3a**	65 (29)	13	3617.6 3618.3
16	**6p**	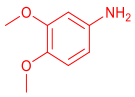 **2p**	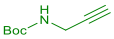 **3a**	63 (20)	0	3647.7 3648.9
17	**6q**	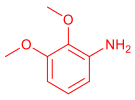 **2q**	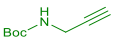 **3a**	54 (28)	7	3647.7 3649.0
18	**6r**	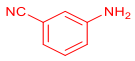 **2r**	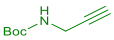 **3a**	19	7	3612.6 3615.8
19	**6s**	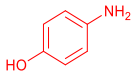 **2s**	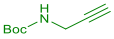 **3a**	54	10	3603.6 3605.1
20	**6t**	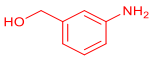 **2t**	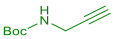 **3a**	68 (16)	2	3617.6 3619.0
21	**6u**	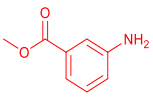 **2u**	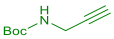 **3a**	69 (10)	15	3645.7 3648.3
22	**6v**	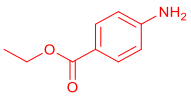 **2v**	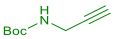 **3a**	36 (12)	11	3659.7 3663.3
23	**6w**	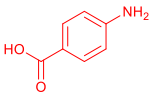 **2w**	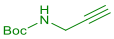 **3a**	51	16	3631.6 3634.8
24	**6x**	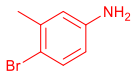 **2x**	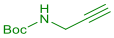 **3a**	82 (9)	3	3680.5 3682.3
25	**6y**	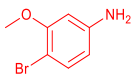 **2y**	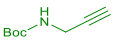 **3a**	75 (21)	3	3696.5 3697.5
26	**6aa**	 **2a**	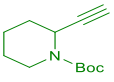 **3b**	18	4	3641.7 3645.0
27	**6ab**	 **2a**	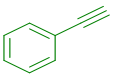 **3c**	61 (27)	9	3532.7 3537.5

[a] A suspension of Cu(OTf)2 (5 mM), aniline **2** (400 mM), alkyne **3** (800 mM) and DNA conjugate **5** (20 nmol) in DMA (100 µL) was shaken at 80°C for 20 h. DNA cleavage with AMA (30% aqueous ammonia / 40% aqueous methylamine, 1:1 (vol/vol)) at ambient temperature for 4 h. [b] Determined by RP-HPLC I analysis based on the ratios of **5** to **6**; additional amounts of unidentified byproducts in brackets. [c] Determined by RP-HPLC analysis in relation to the purity of **5**. [d] Measured by MALDI-MS. 10mer ATGC = 5'-NH2-C6- GTC ATG ATC T-3'-CPG.

DNA conjugate 1: CPG-bound 10mer TC-(CH_2)-NH_2 conjugate was reacted with 4-formyl-phenoxyacetic acid according to RP-01. HPLC trace of crude reaction mixture **1** (Analytical RP-HPLC I)

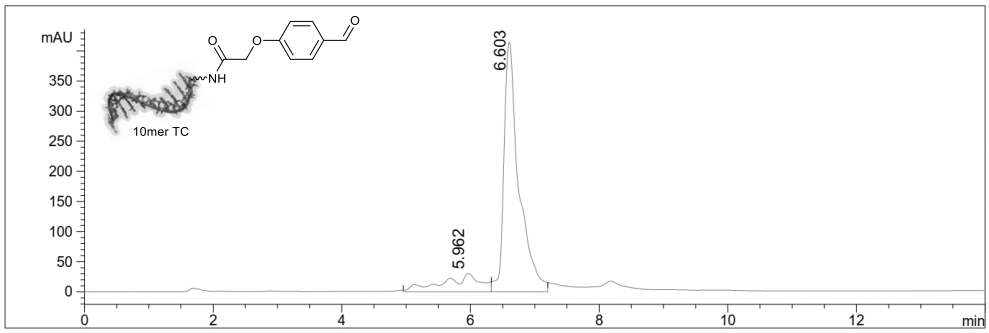

Peak list:

Ret. Time	Width min	Height	Area	Area %
5.962	0.669	30.140	1209.639	15.324
6.603	0.268	415.001	6684.129	84.676

MALDI-MS spectrum of crude reaction mixture 1

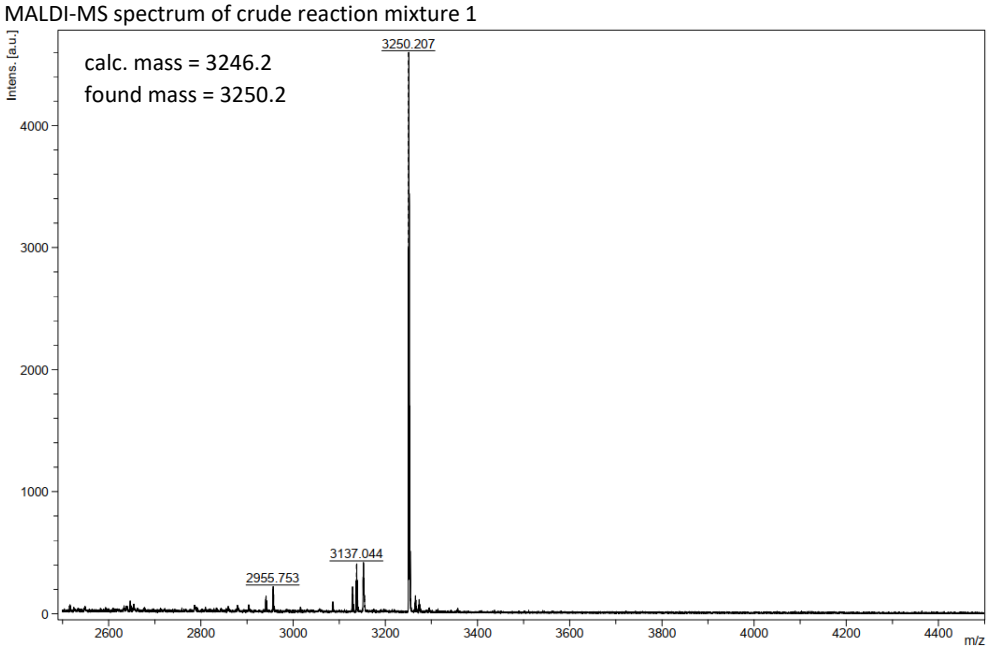

DNA conjugate 4: CPG-bound 10mer TC-aldehyde conjugate **1** was reacted with aniline **2a** and *N*-Boc-propargylamine **3a** according to RP-02.

HPLC trace of crude reaction mixture **4** (Analytical RP-HPLC I)

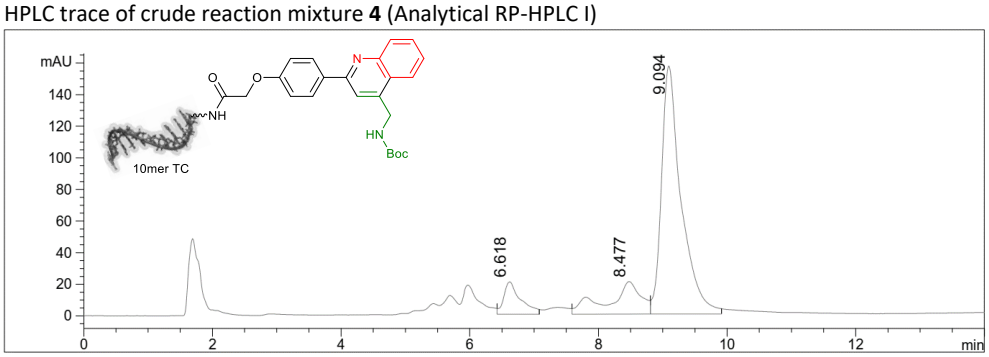

Peak list:

Ret. Time	Width min	Height	Area	Area %
6.618	0.306	20.461	375.586	8.516
8.477	0.585	20.572	721.997	16.370
9.094	0.352	156.889	3312.889	75.114

HPLC trace of isolated product **4** (Analytical RP-HPLC I)

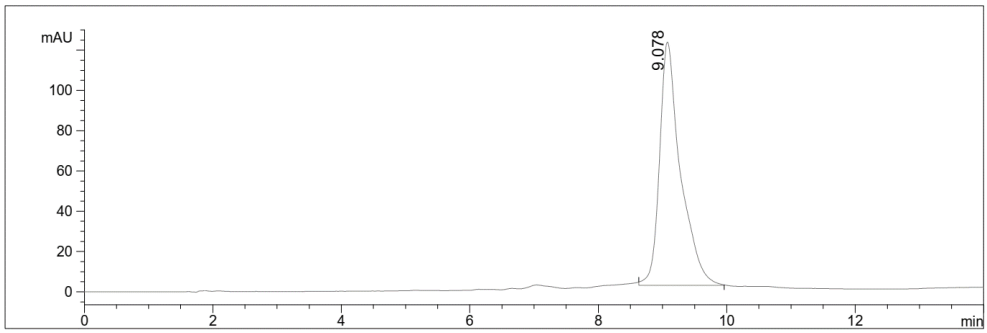

MALDI-MS spectrum of isolated product **4**

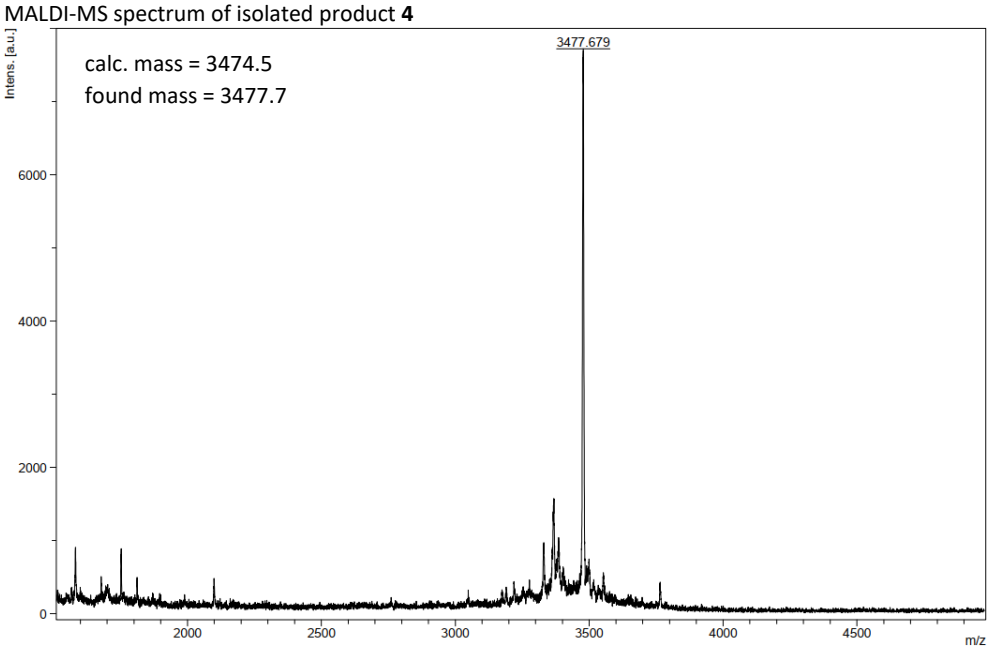

DNA conjugate 5: CPG-bound 10mer TC-(CH_2)-NH_2 conjugate was reacted with 4-formyl-phenoxyacetic acid according to RP-01.

HPLC trace of crude reaction mixture **5** (Analytical RP-HPLC I, **Batch A**)

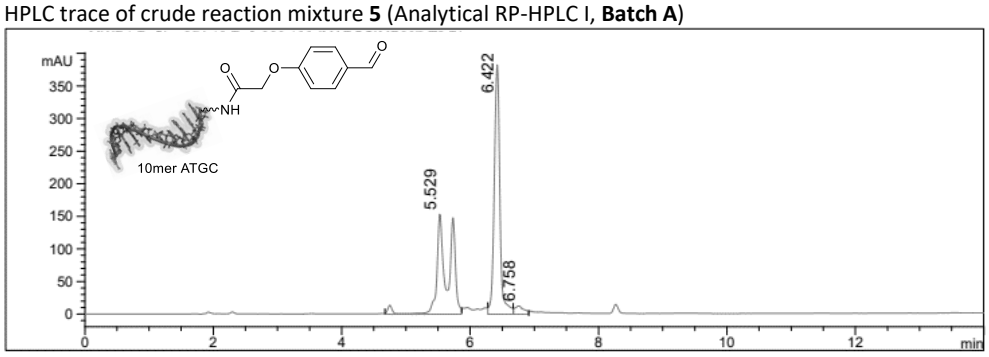

Peak list:

Ret. Time	Width min	Height	Area	Area %
5.529	0.213	153.544	1964.411	44.467
6.422	0.101	383.324	2323.022	52.585
6.758	0.169	12.849	130.228	2.948

HPLC trace of crude reaction mixture **5** (Analytical RP-HPLC I, **Batch B**)

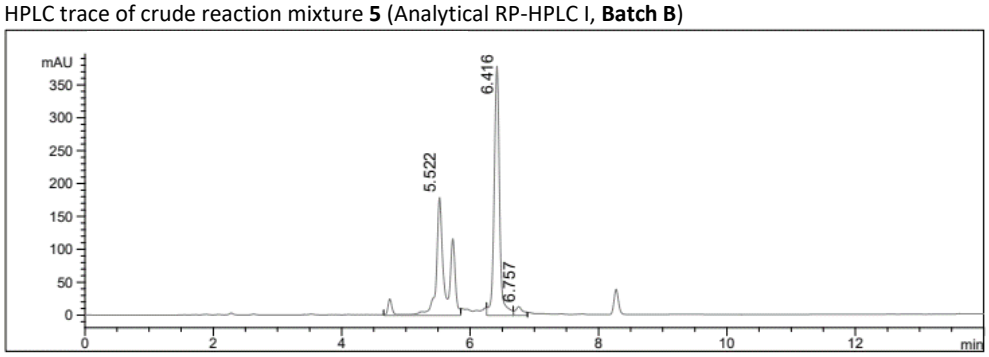

Peak list:

Ret. Time	Width min	Height	Area	Area %
5.522	0.183	180.062	1978.085	46.044
6.416	0.097	380.503	2207.682	51.388
6.757	0.139	13.214	110.337	2.568

HPLC trace of crude reaction mixture 5 (Analytical RP-HPLC I, Batch C)

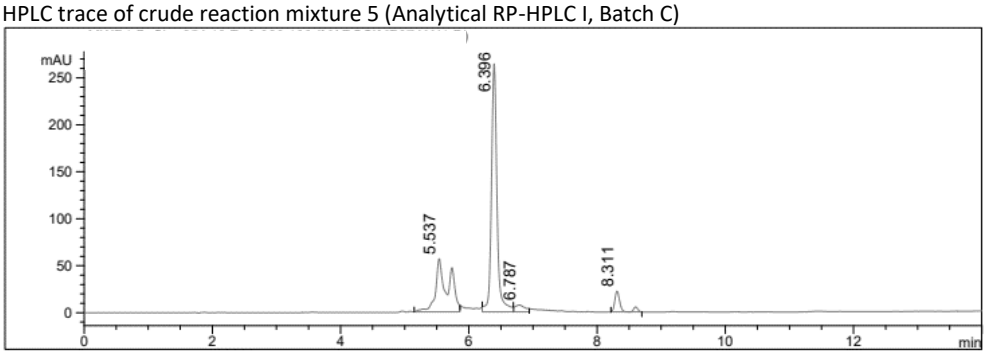

Peak list:

Ret. Time	Width min	Height	Area	Area %
5.537	0.232	56.711	791.055	30.438
6.396	0.100	264.378	1589.024	61.142
6.787	0.186	7.309	81.514	3.136
8.311	0.104	21.979	137.304	5.283

MALDI-MS spectrum of crude reaction mixture **5**

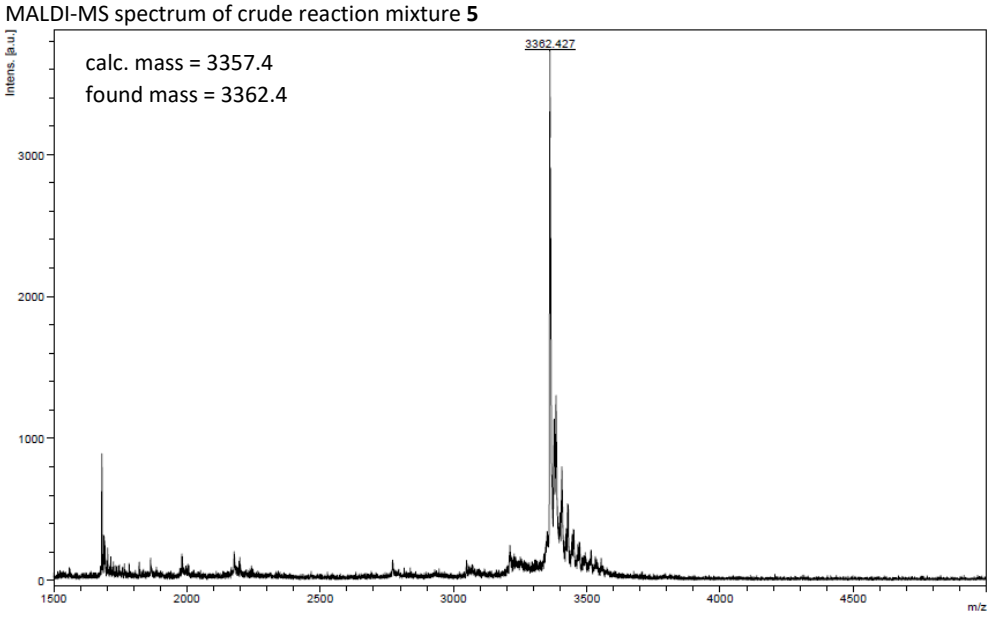

DNA conjugate 6a: CPG-bound 10mer ATGC-aldehyde conjugate (Batch A) 5 was reacted with aniline 2a and *N*-Boc-propargylamine 3a according to RP-02.

HPLC trace of crude reaction mixture 6a (Analytical RP-HPLC I)

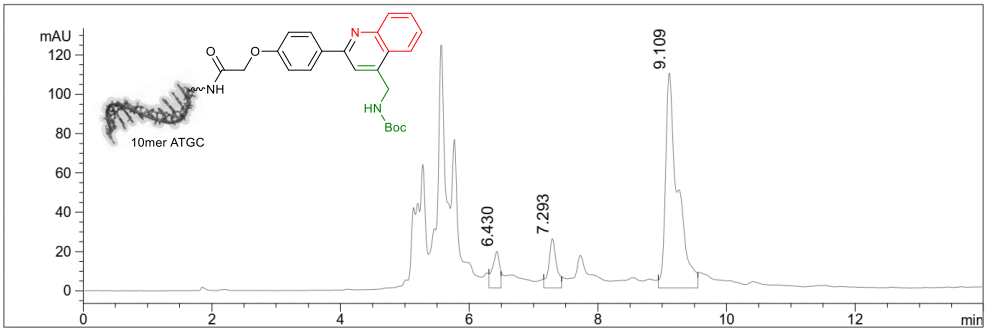

Peak list:

Ret. Time	Width min	Height	Area	Area %
6.430	0.129	18.569	143.314	8.042
7.293	0.138	25.075	206.964	11.613
9.109	0.218	109.406	1431.899	80.345

HPLC trace of isolated product **6a** (Analytical RP-HPLC I)

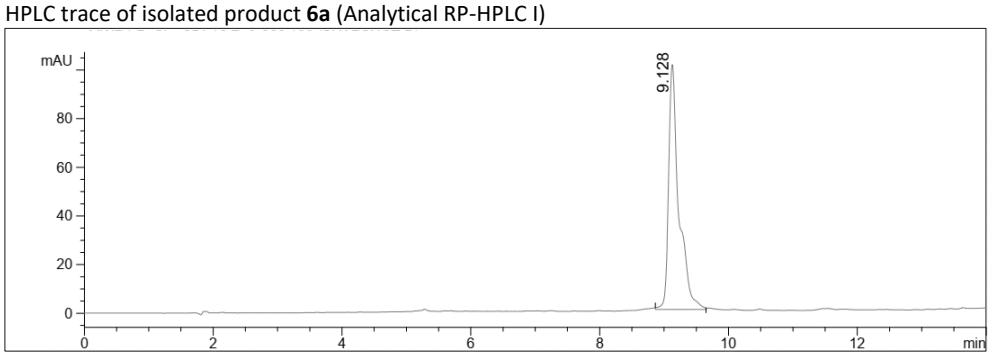

Peak list:

Ret. Time	Width min	Height	Area	Area %
9.128	0.184	100.731	1111.009	100.000

MALDI-MS spectrum of isolated product **6a**

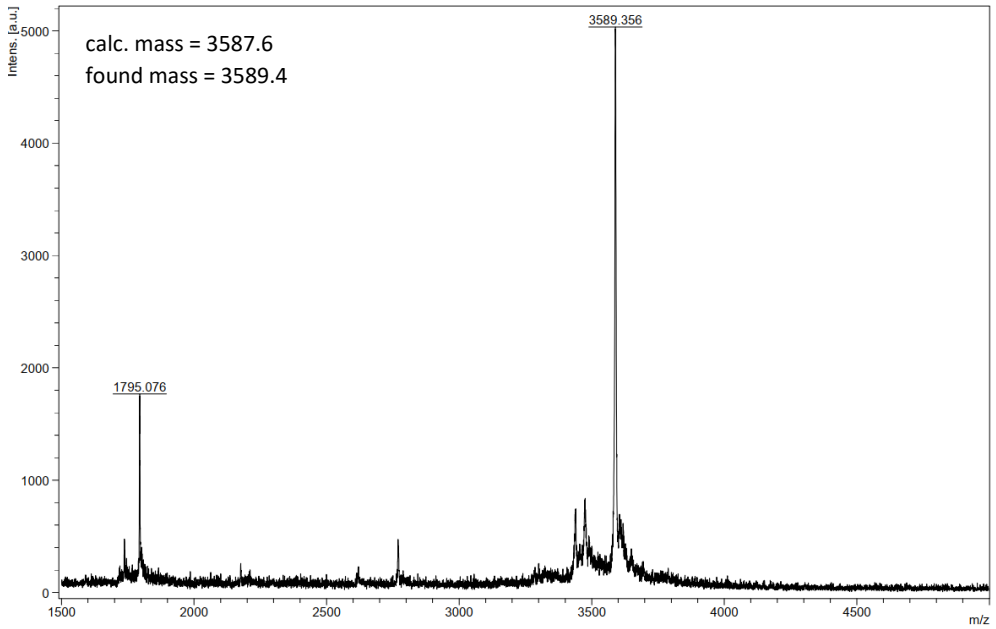
calc. mass = 3587.6
found mass = 3589.4
3589.356
1795.076
Intens. [a.u.]
5000
4000
3000
2000
1000
0
1500
2000
2500
3000
3500
4000
4500
m/z

DNA conjugate 6b: CPG-bound 10mer ATGC-aldehyde conjugate (Batch B) **5** was reacted with 4-fluoroaniline **2b** and *N*-Boc-propargylamine **3a** according to RP-02.

HPLC trace of crude reaction mixture **6b** (Analytical RP-HPLC)

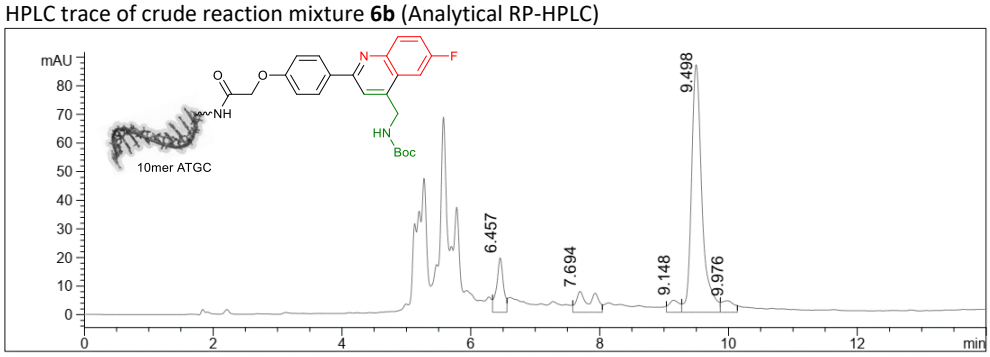

Peak list:

Ret. Time	Width min	Height	Area	Area %
6.457	0.122	19.057	139.190	10.346
7.694	0.286	7.288	125.141	9.301
9.148	0.192	4.195	48.414	3.598
9.498	0.188	86.565	978.276	72.713
9.976	0.225	4.035	54.374	4.041

HPLC trace of isolated product 6b (Analytical RP-HPLC I)

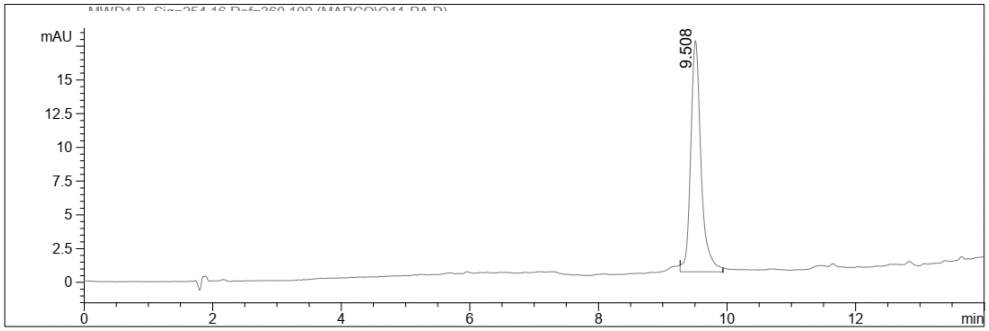

Peak list:

Ret. Time	Width min	Height	Area	Area %
9.508	0.185	17.135	190.338	100.000

MALDI-MS spectrum of isolated product **6b**

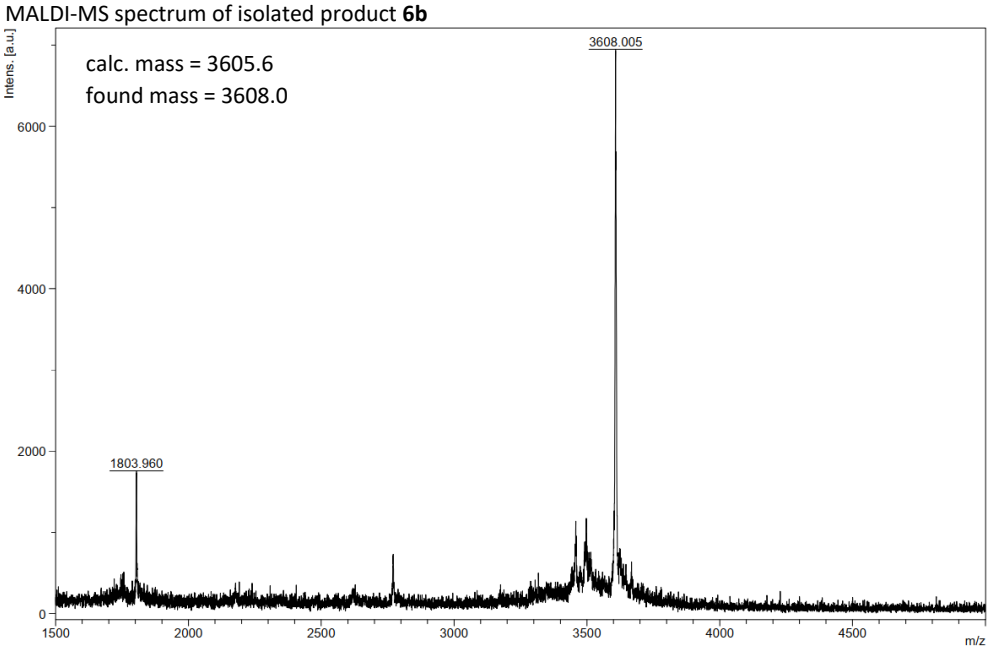

DNA conjugate 6c: CPG-bound 10mer ATGC-aldehyde conjugate (Batch B) **5** was reacted with 3-fluoroaniline **2c** and *N*-Boc-propargylamine **3a** according to RP-02.

HPLC trace of crude reaction mixture **6c** (Analytical RP-HPLC I)

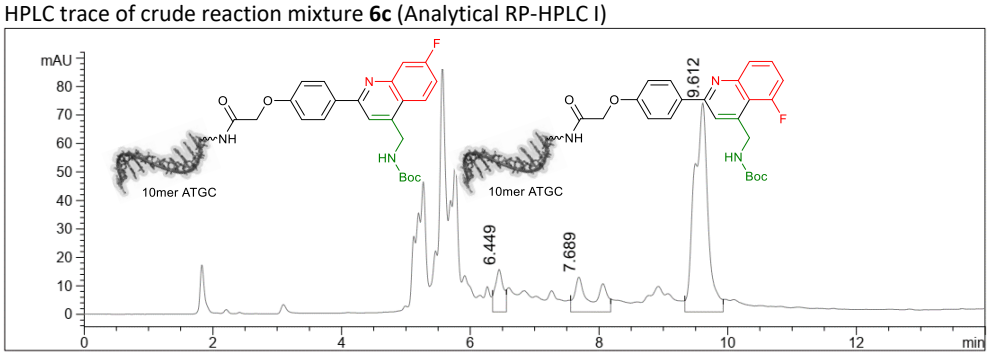

Peak list:

Ret. Time	Width min	Height	Area	Area %
6.449	0.148	14.887	132.506	9.154
7.689	0.326	12.207	238.940	16.507
9.612	0.244	73.443	1076.049	74.339

HPLC trace of isolated product 6c (Analytical RP-HPLC I)

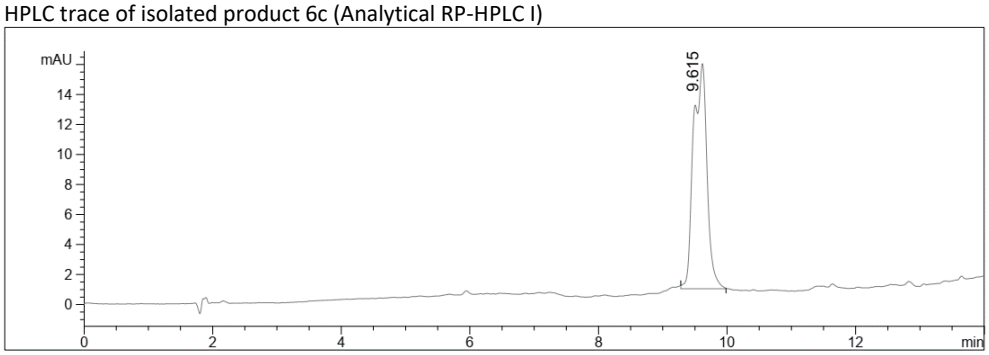

Peak list:

Ret. Time	Width min	Height	Area	Area %
9.615	0.243	15.003	218.574	100.000

MALDI-MS spectrum of isolated product **6c**

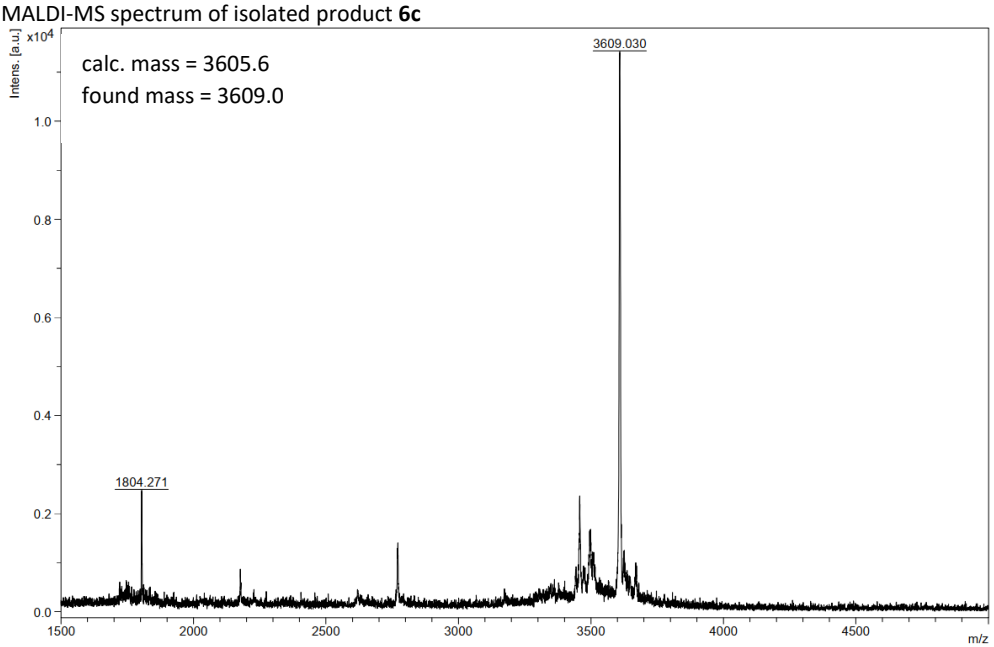

DNA conjugate 6d: CPG-bound 10mer ATGC-aldehyde conjugate (Batch C) **5** was reacted with 2-fluoroaniline **2d** and *N*-Boc-propargylamine **3a** according to RP-02.

HPLC trace of crude reaction mixture **6d** (Analytical RP-HPLC I)

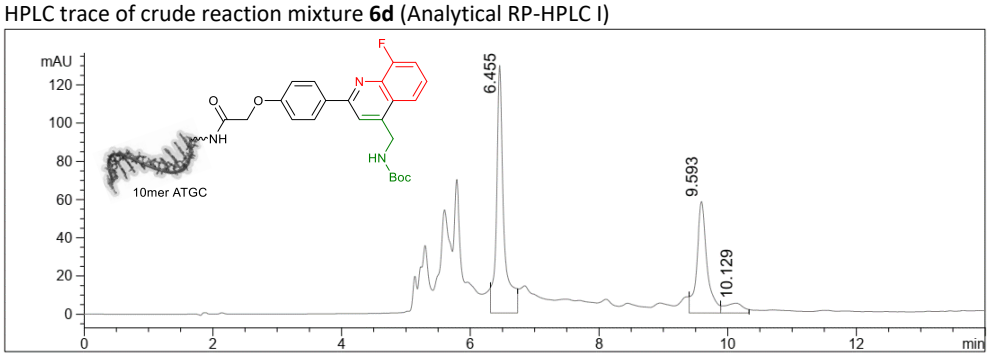

Peak list:

Ret. Time	Width min	Height	Area	Area %
6.455	0.130	129.792	1010.963	57.617
9.593	0.183	58.369	640.964	36.530
10.129	0.335	5.114	102.702	5.853

HPLC trace of isolated product **6d** (Analytical RP-HPLC I)

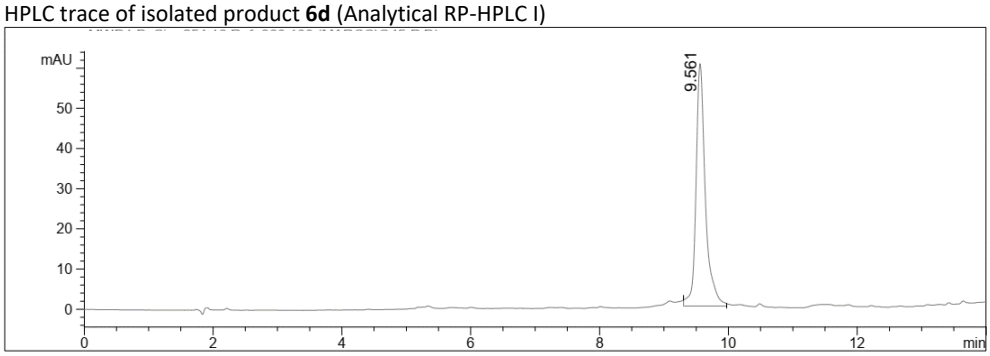

Peak list:

Ret. Time	Width min	Height	Area	Area %
9.561	0.167	60.388	606.000	100.000

MALDI-MS spectrum of crude reaction mixture **6d**

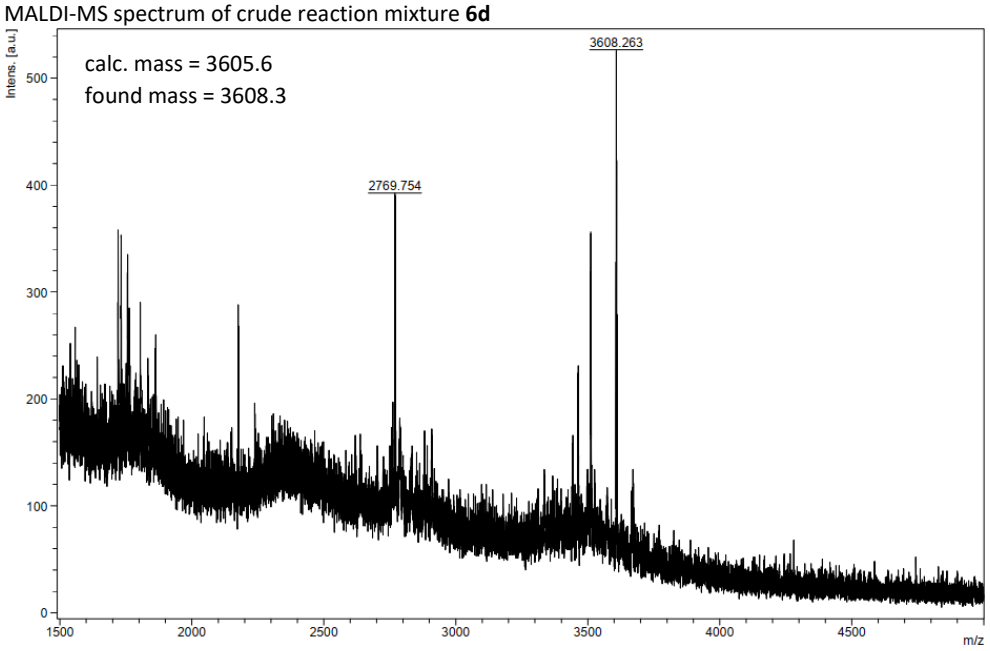

DNA conjugate 6e: CPG-bound 10mer ATGC-aldehyde conjugate (Batch B) **5** was reacted with 2,4-difluoro-aniline **2e** and *N*-Boc-propargylamine **3a** according to RP-02.

HPLC trace of crude reaction mixture **6e** (Analytical RP-HPLC I)

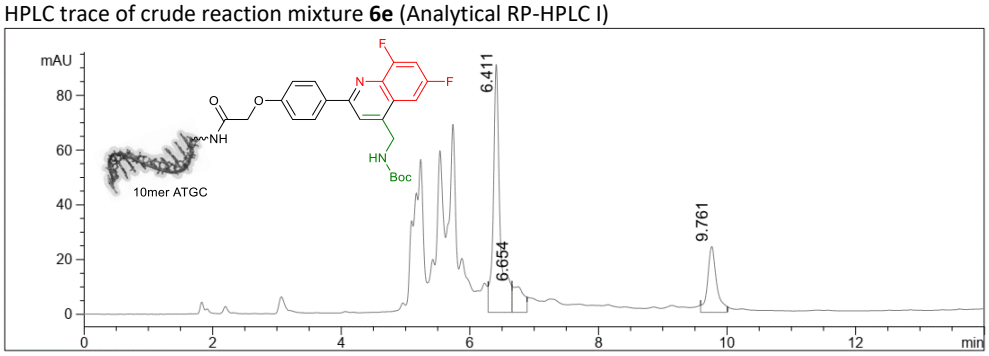

Peak list:

Ret. Time	Width min	Height	Area	Area %
6.411	0.122	90.938	663.625	65.432
6.654	0.156	9.639	112.984	11.140
9.761	0.165	24.025	237.605	23.427

HPLC trace of isolated product 6e (Analytical RP-HPLC I)

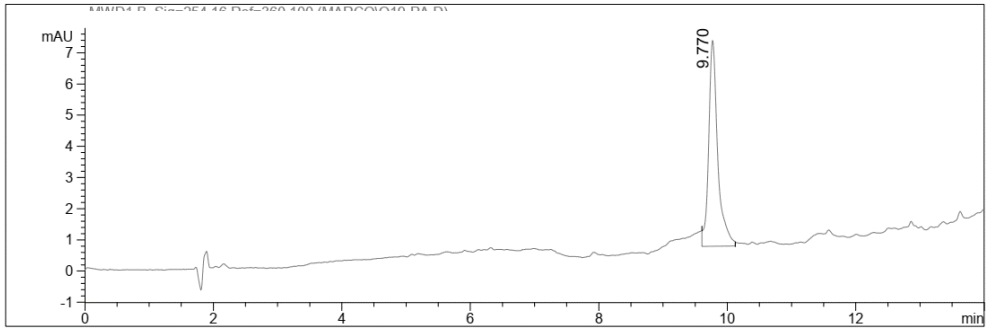

Peak list:

Ret. Time	Width min	Height	Area	Area %
9.770	0.162	6.602	64.326	100.000

MALDI-MS spectrum of isolated product **6e**

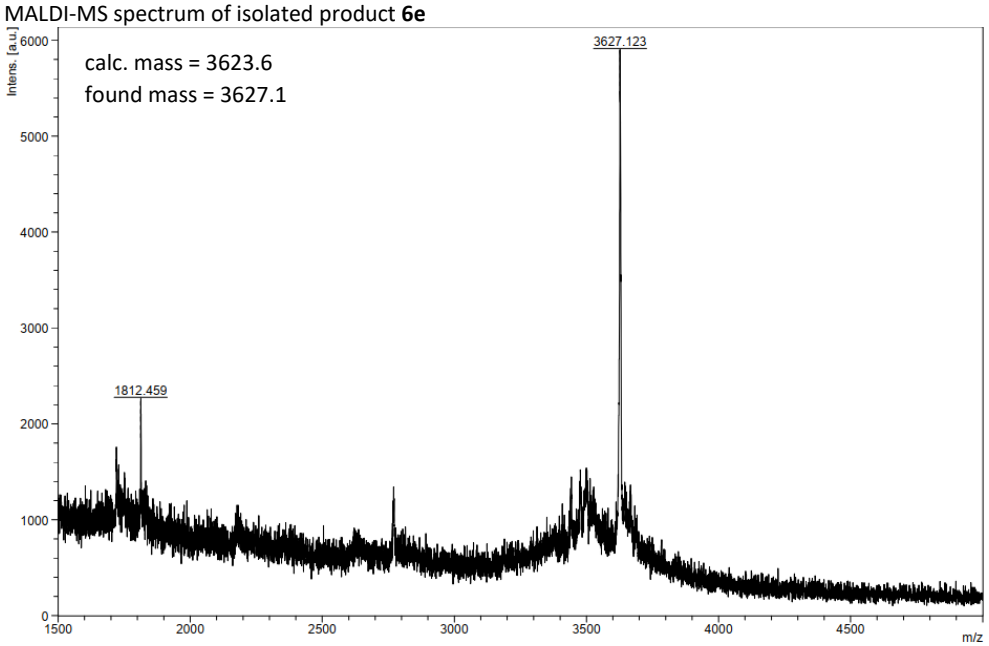

DNA conjugate 6f: CPG-bound 10mer ATGC-aldehyde conjugate (Batch C) **5** was reacted with 4-bromoaniline **2f** and *N*-Boc-propargylamine **3a** according to RP-02.

HPLC trace of crude reaction mixture **6f** (Analytical RP-HPLC I)

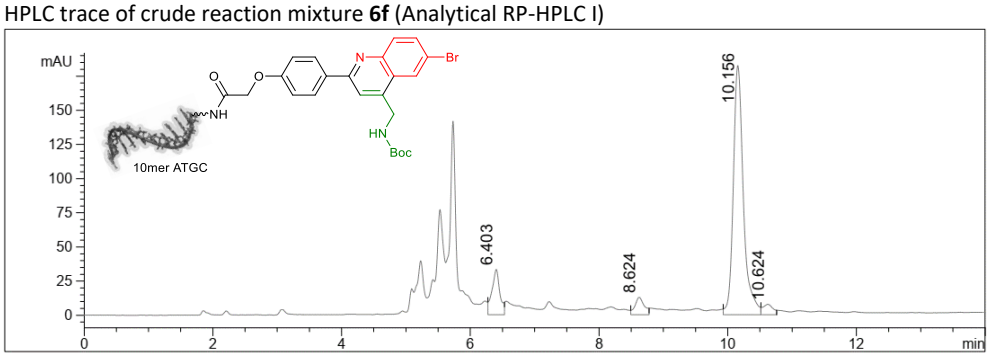

Peak list:

Ret. Time	Width min	Height	Area	Area %
6.403	0.142	33.170	282.733	11.415
8.624	0.169	12.728	129.326	5.221
10.156	0.181	182.480	1980.230	79.950
10.624	0.185	7.615	84.535	3.413

HPLC trace of isolated product **6f** (Analytical RP-HPLC I)

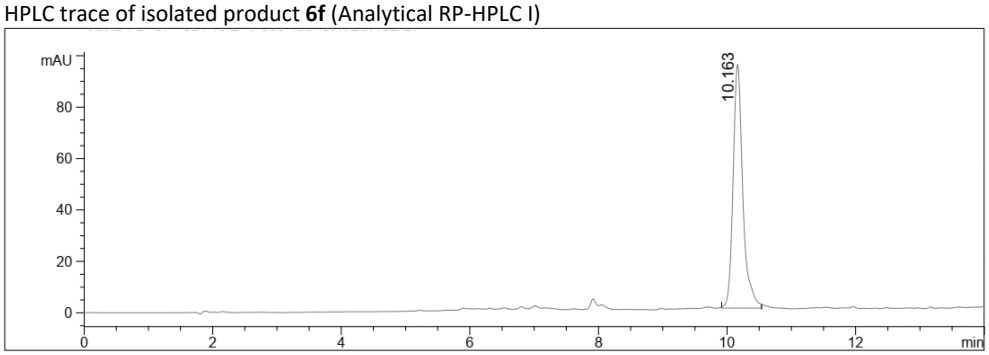

Peak list:

Ret. Time	Width min	Height	Area	Area %
10.163	0.175	94.770	993.030	100.000

MALDI-MS spectrum of isolated product **6f**

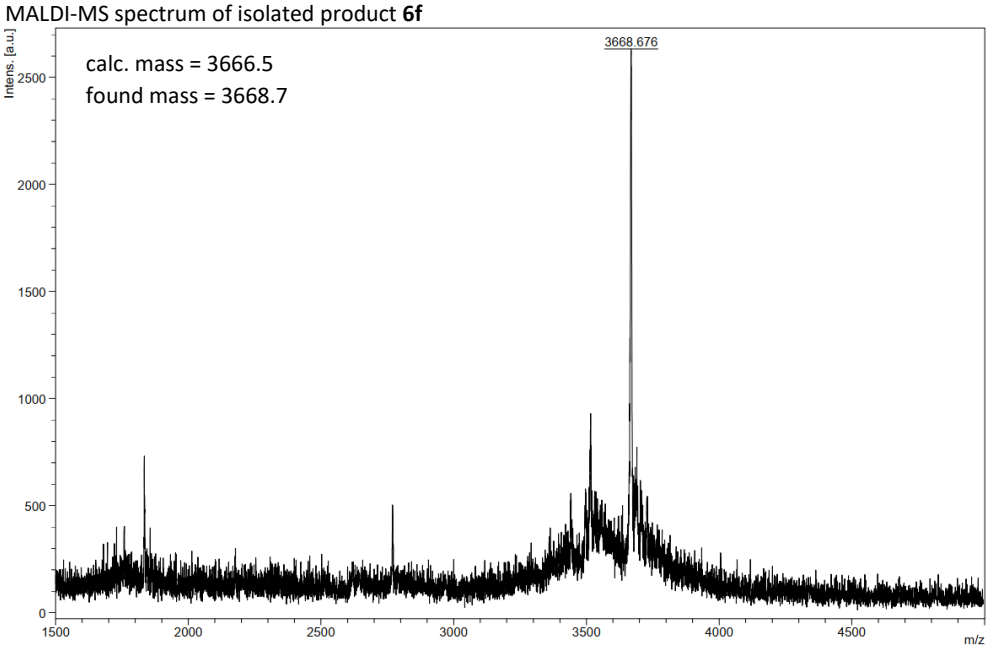

DNA conjugate 6g: CPG-bound 10mer ATGC-aldehyde conjugate (Batch C) **5** was reacted with 3-bromoaniline **2g** and *N*-Boc-propargylamine **3a** according to RP-02.

HPLC trace of crude reaction mixture **6g** (Analytical RP-HPLC I)

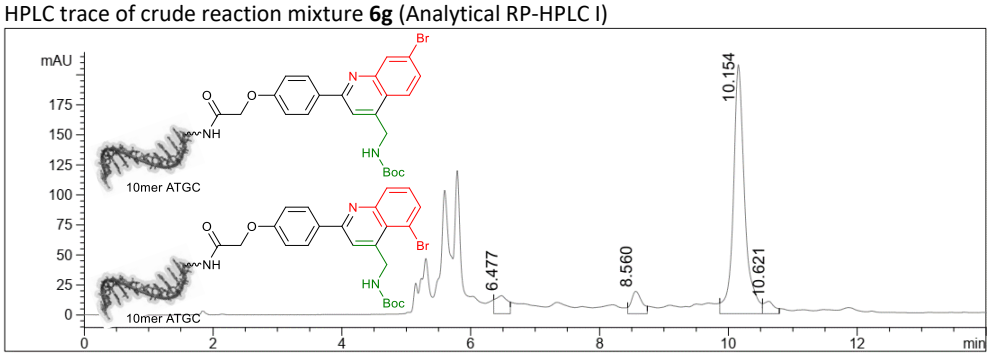

Peak list:

Ret. Time	Width min	Height	Area	Area %
6.477	0.220	15.010	197.921	6.408
8.560	0.190	18.578	211.990	6.864
10.154	0.206	207.557	2560.117	82.888
10.621	0.192	10.295	118.607	3.840

HPLC trace of isolated product **6g** (Analytical RP-HPLC I)

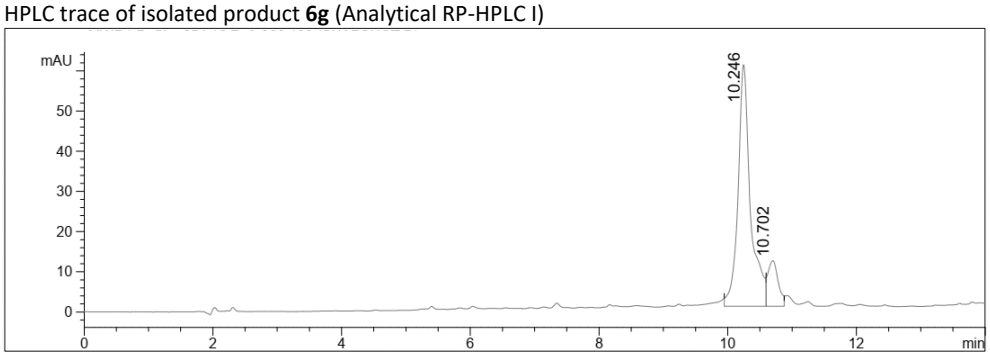

Peak list:

Ret. Time	Width min	Height	Area	Area %
10.246	0.224	60.126	807.665	86.512
10.702	0.185	11.345	125.918	13.488

MALDI-MS spectrum of isolated product **6g**

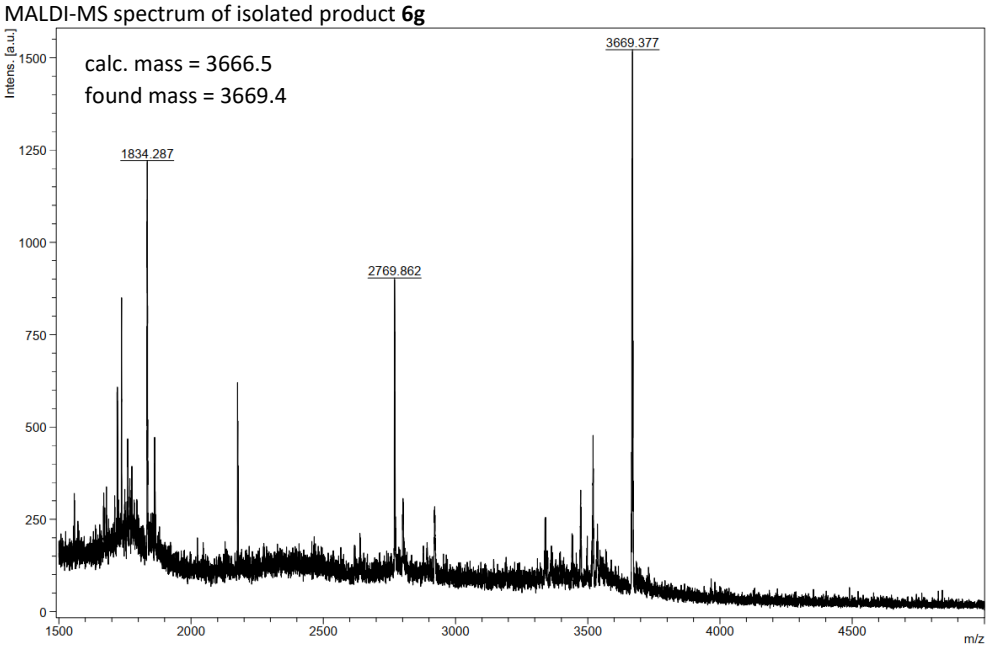

DNA conjugate 6h: CPG-bound 10mer ATGC-aldehyde conjugate (Batch C) **5** was reacted with 2-bromoaniline **2h** and *N*-Boc-propargylamine **3a** according to RP-02.

HPLC trace of crude reaction mixture **6h** (Analytical RP-HPLC I)

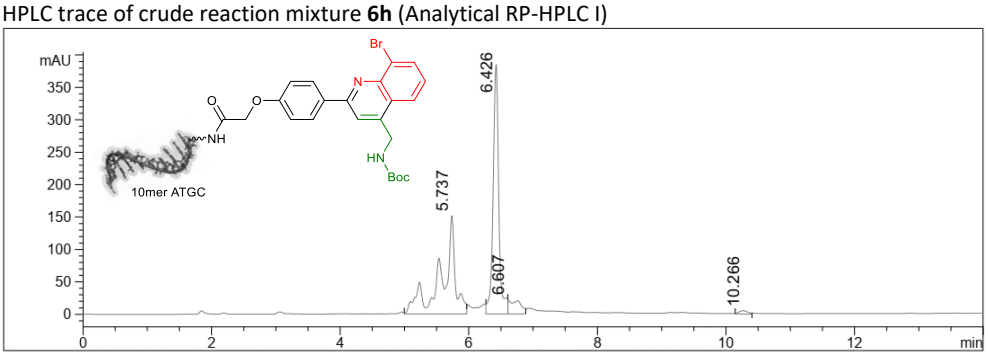

Peak list:

Ret. Time	Width min	Height	Area	Area %
5.737	0.244	151.936	2220.919	45.535
6.426	0.101	386.169	2338.165	47.939
6.607	0.196	22.804	267.684	5.488
10.266	0.161	5.225	50.570	1.037

MALDI-MS spectrum of crude reaction mixture **6h**

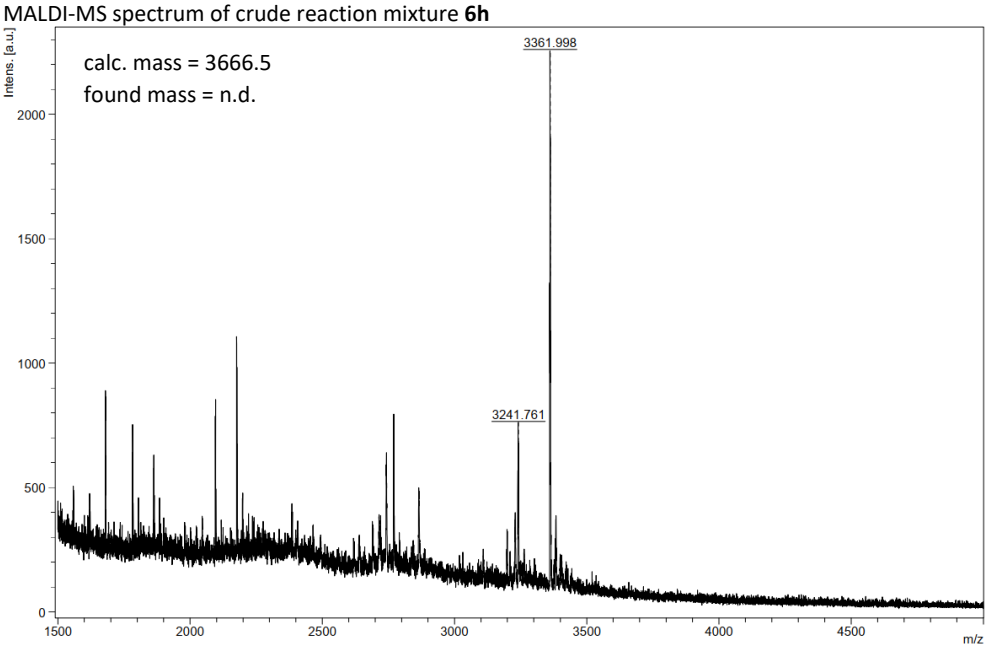

DNA conjugate 6i: CPG-bound 10mer ATGC-aldehyde conjugate (Batch B) 5 was reacted with 4-ethylaniline 2i and N-Boc-propargylamine 3a according to RP-02.

HPLC trace of crude reaction mixture 6i (Analytical RP-HPLC I)

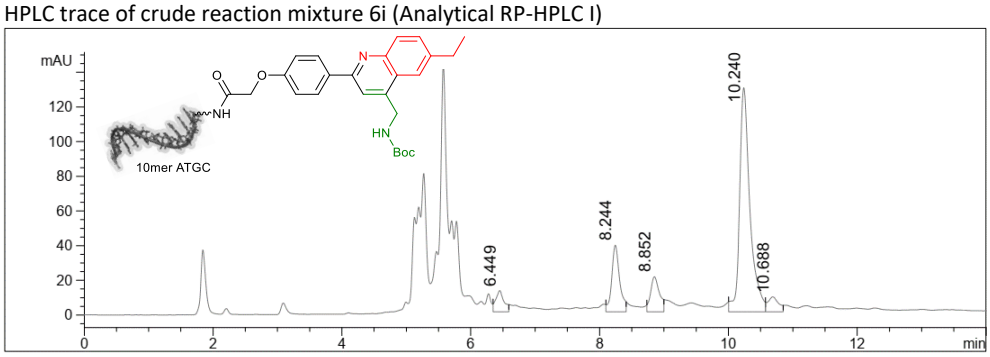

Peak list:

Ret. Time	Width min	Height	Area	Area %
6.449	0.150	12.264	110.335	5.062
8.244	0.142	38.443	327.847	15.041
8.852	0.159	20.311	193.979	8.900
10.240	0.186	129.323	1446.190	66.350
10.688	0.194	8.691	101.303	4.648

HPLC trace of isolated product 6i (Analytical RP-HPLC I)

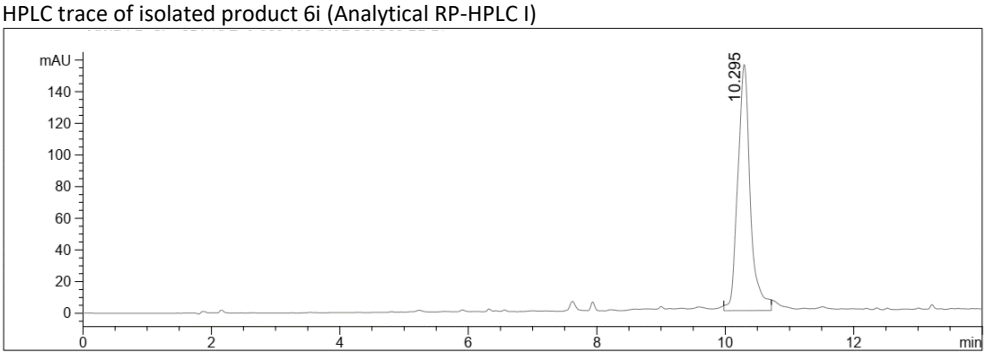

Peak list:

Ret. Time	Width min	Height	Area	Area %
10.295	0.224	155.491	2088.268	100.000

MALDI-MS spectrum of isolated product **6i**

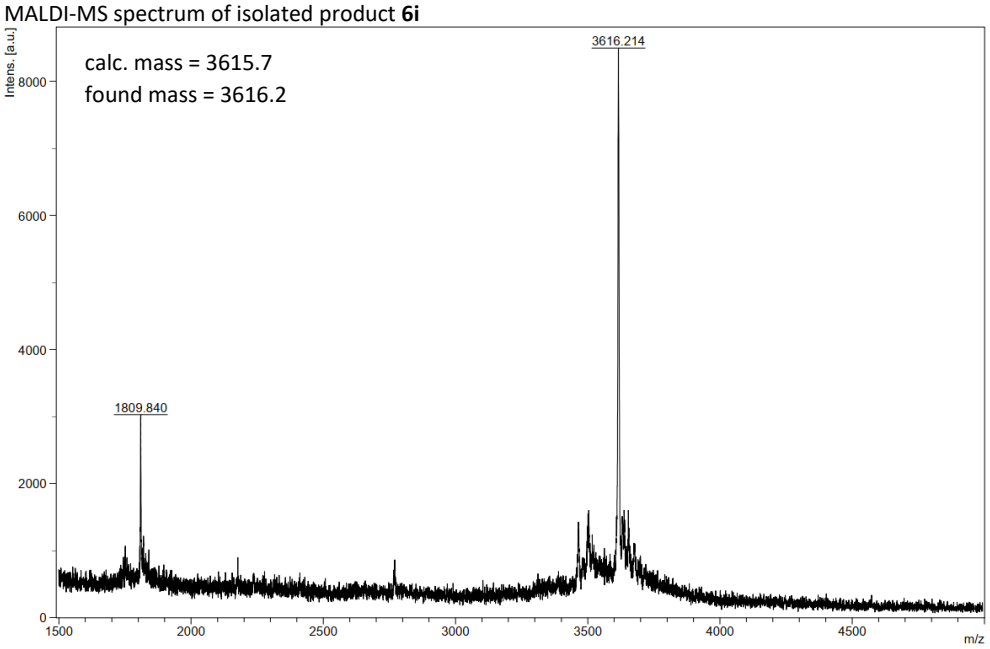

DNA conjugate 6j: CPG-bound 10mer ATGC-aldehyde conjugate (Batch B) **5** was reacted with 3-ethylaniline **2j** and *N*-Boc-propargylamine **3a** according to RP-02.

HPLC trace of crude reaction mixture **6j** (Analytical RP-HPLC I)

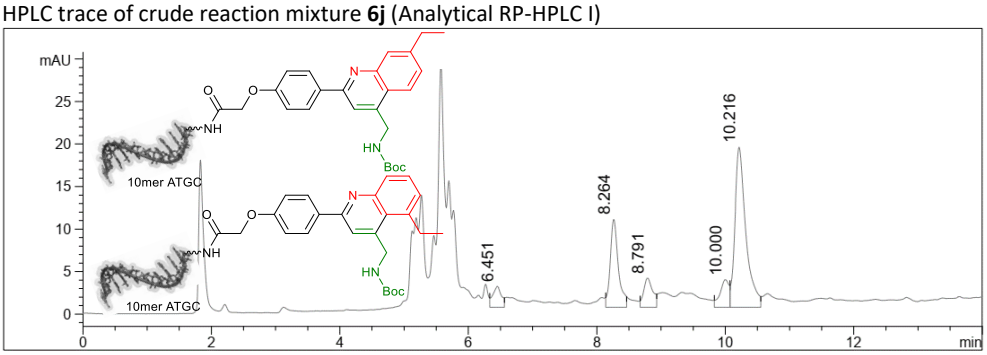

Peak list:

Ret. Time	Width min	Height	Area	Area %
6.451	0.156	2.458	23.048	5.730
8.264	0.145	10.347	90.090	22.399
8.791	0.164	3.432	33.841	8.414
10.000	0.162	3.251	31.514	7.835
10.216	0.198	18.798	223.716	55.622

HPLC trace of isolated product 6j (Analytical RP-HPLC I)

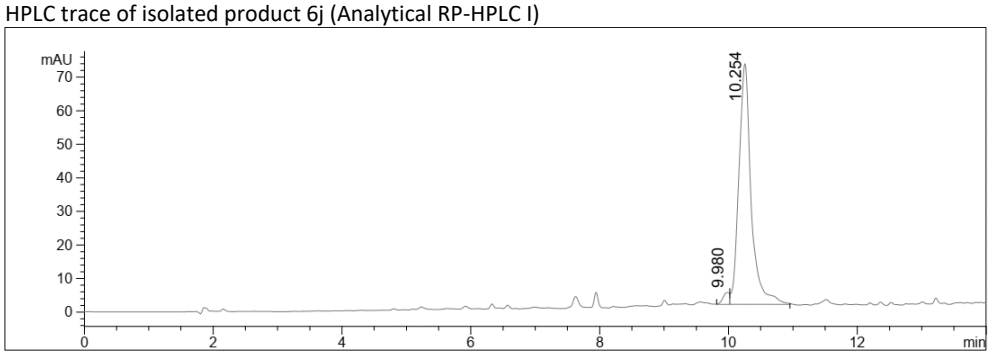

Peak list:

Ret. Time	Width min	Height	Area	Area %
9.980	0.116	3.571	24.775	2.551
10.254	0.220	71.727	946.446	97.449

MALDI-MS spectrum of isolated product **6j**

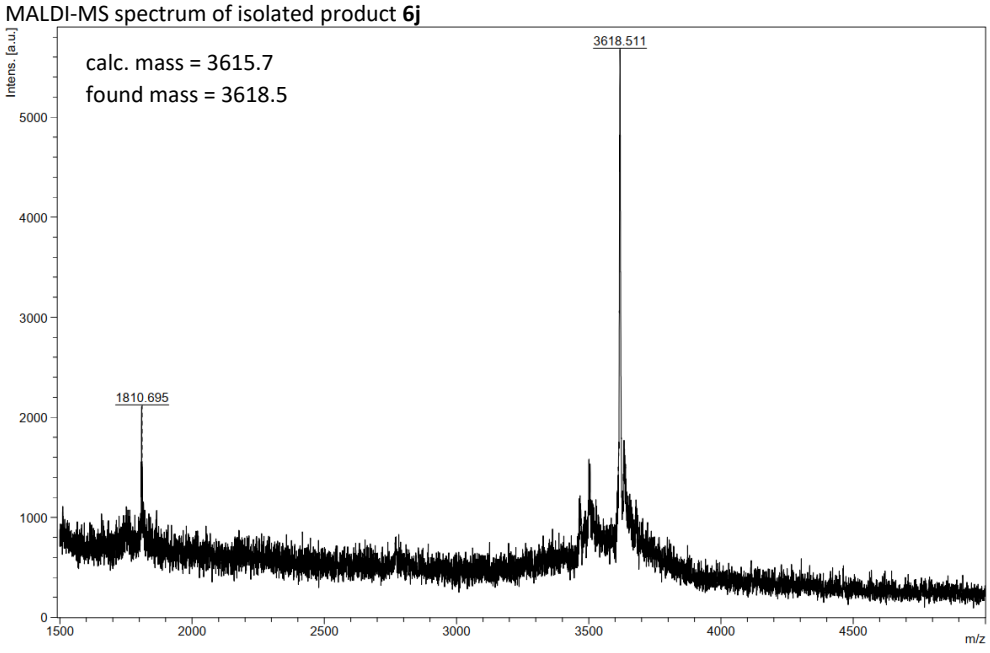

DNA conjugate 6k: CPG-bound 10mer ATGC-aldehyde conjugate (Batch B) **5** was reacted with 2-ethylaniline **2k** and *N*-Boc-propargylamine **3a** according to RP-02.

HPLC trace of crude reaction mixture **6k** (Analytical RP-HPLC I)

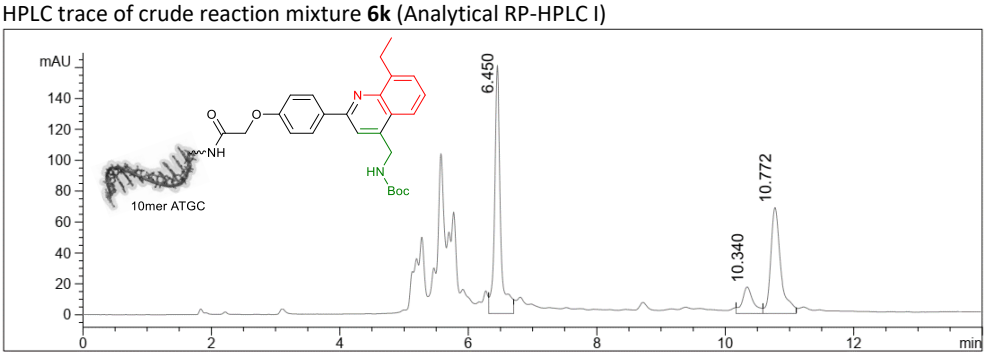

Peak list:

Ret. Time	Width min	Height	Area	Area %
6.450	0.106	160.987	1020.213	51.975
10.340	0.198	17.142	203.228	10.354
10.772	0.180	68.545	739.438	37.671

HPLC trace of isolated product **6k** (Analytical RP-HPLC I)

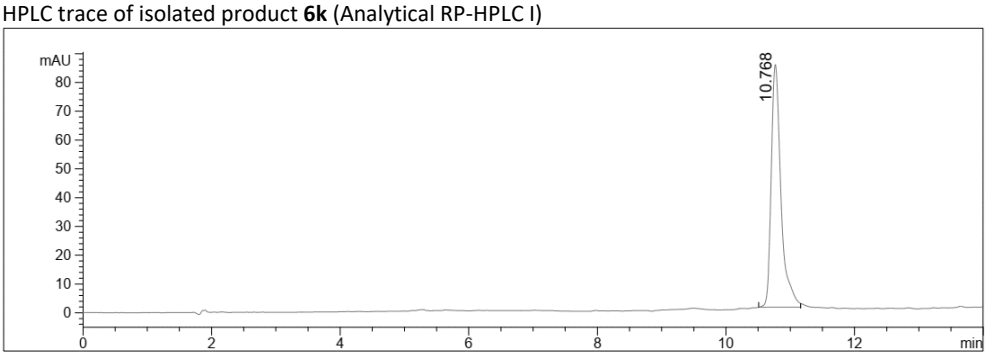

Peak list:

Ret. Time	Width min	Height	Area	Area %
10.768	0.175	84.323	885.384	100.000

MALDI-MS spectrum of isolated product **6k**

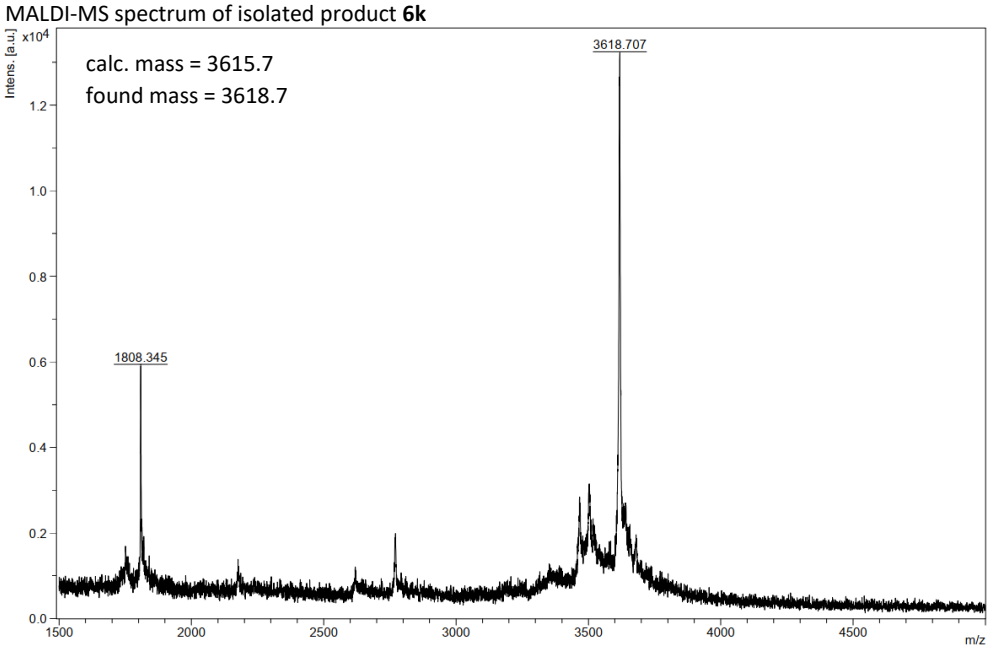

DNA conjugate 6l: CPG-bound 10mer ATGC-aldehyde conjugate (Batch C) **5** was reacted with 4-*tert*-butyl-aniline **2l** and *N*-Boc-propargylamine **3a** according to RP-02.

HPLC trace of crude reaction mixture **6l** (Analytical RP-HPLC I)

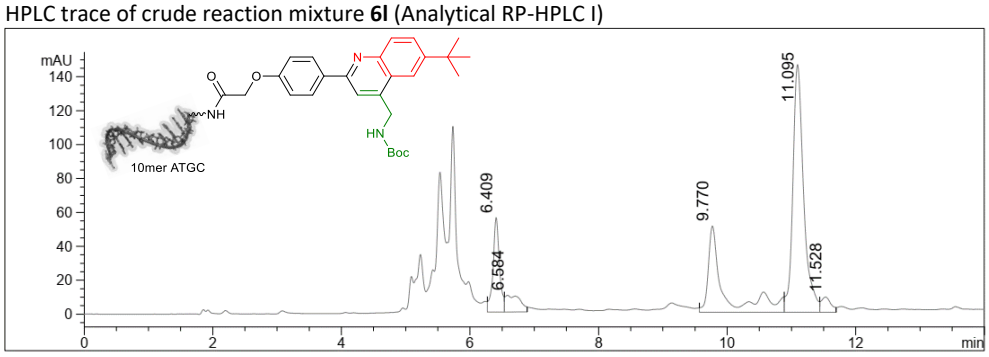

Peak list:

Ret. Time	Width min	Height	Area	Area %
6.409	0.118	55.718	393.121	12.294
6.584	0.270	9.850	159.292	4.981
9.770	0.279	50.808	851.177	26.618
11.095	0.194	146.028	1700.463	53.176
11.528	0.175	8.944	93.739	2.931

HPLC trace of isolated product 6l (Analytical RP-HPLC I)

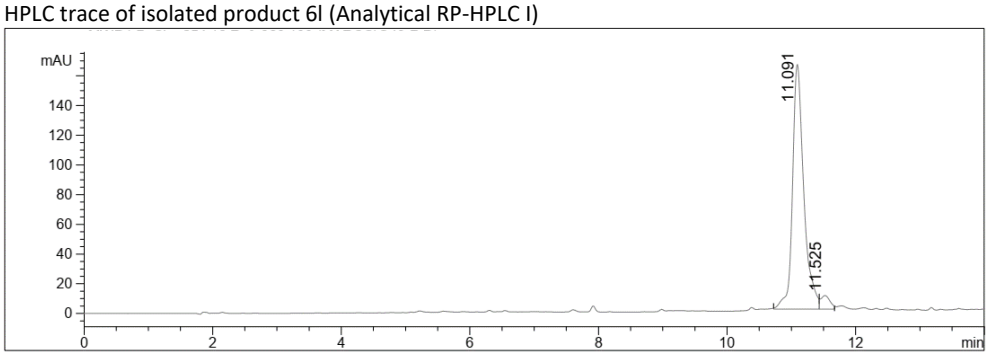

Peak list:

Ret. Time	Width min	Height	Area	Area %
11.091	0.203	164.733	2008.670	95.627
11.525	0.167	9.163	91.849	4.373

MALDI-MS spectrum of isolated product **6l**

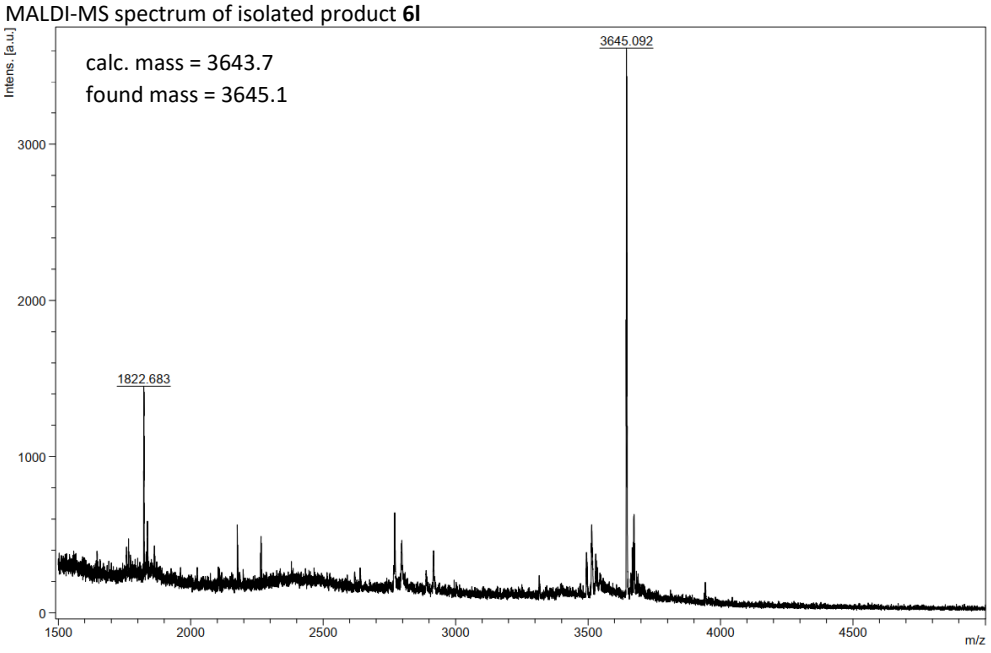

DNA conjugate 6m: CPG-bound 10mer ATGC-aldehyde conjugate (Batch A) **5** was reacted with 2-*tert*-butyl-aniline **2m** and *N*-Boc-propargylamine **3a** according to RP-02.

HPLC trace of crude reaction mixture **6m** (Analytical RP-HPLC I)

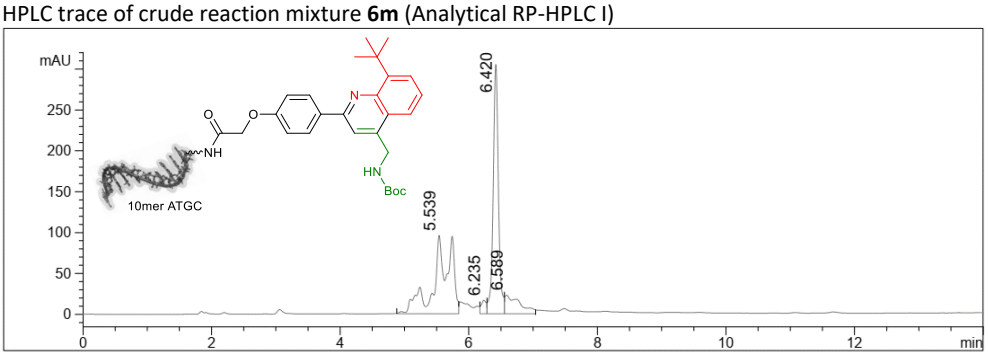

Peak list:

Ret. Time	Width min	Height	Area	Area %
5.539	0.305	95.913	1753.742	44.480
6.235	0.090	16.349	88.714	2.250
6.420	0.094	306.524	1735.034	44.006
6.589	0.269	22.591	365.249	9.264

MALDI-MS spectrum of crude reaction mixture 6m

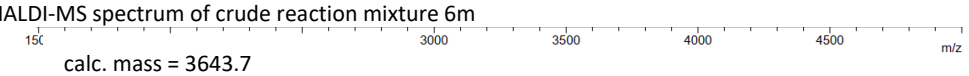

calc. mass = 3643.7

found mass = n.d.

DNA conjugate 6n: CPG-bound 10mer ATGC-aldehyde conjugate (Batch B) **5** was reacted with 4-methoxy-aniline **2n** and *N*-Boc-propargylamine **3a** according to RP-02.

HPLC trace of crude reaction mixture **6n** (Analytical RP-HPLC I)

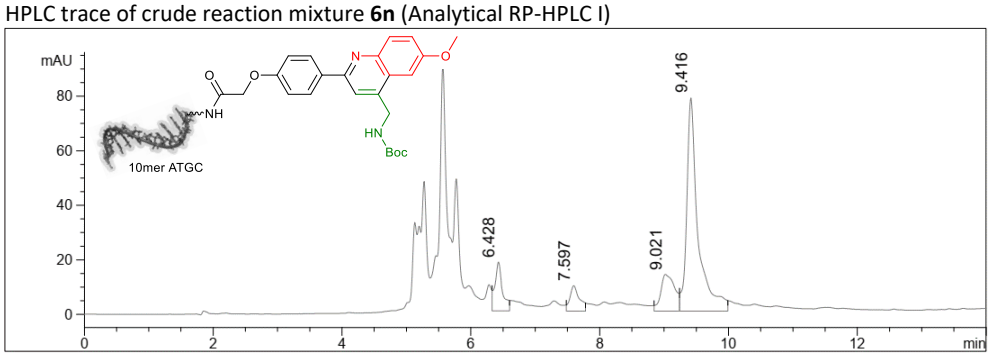

Peak list:

Ret. Time	Width min	Height	Area	Area %
6.428	0.136	17.958	146.250	10.445
7.597	0.170	9.330	95.197	6.799
9.021	0.252	13.441	203.419	14.528
9.416	0.203	78.255	955.322	68.228

HPLC trace of isolated product 6n (Analytical RP-HPLC I)

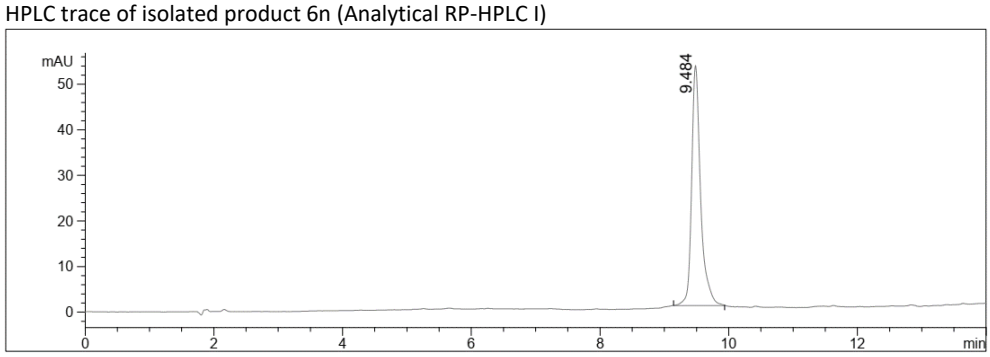

Peak list:

Ret. Time	Width min	Height	Area	Area %
9.484	0.161	52.719	509.151	100.000

MALDI-MS spectrum of isolated product **6n**

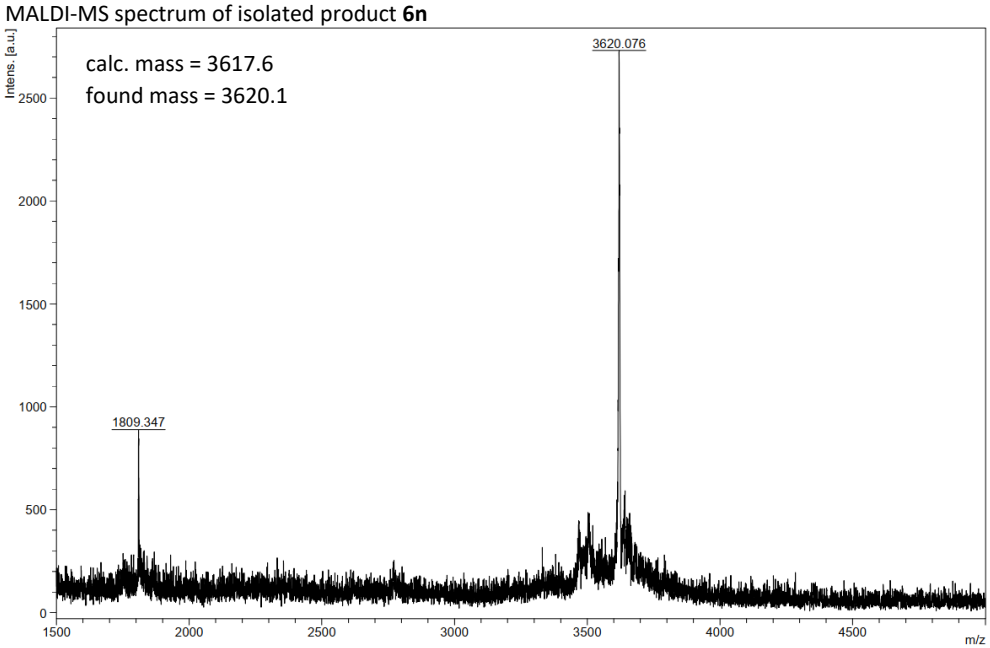

DNA conjugate 6o: CPG-bound 10mer ATGC-aldehyde conjugate (Batch A) **5** was reacted with 3-methoxy-aniline **2o** and *N*-Boc-propargylamine **3a** according to RP-02.

HPLC trace of crude reaction mixture **6o** (Analytical RP-HPLC I)

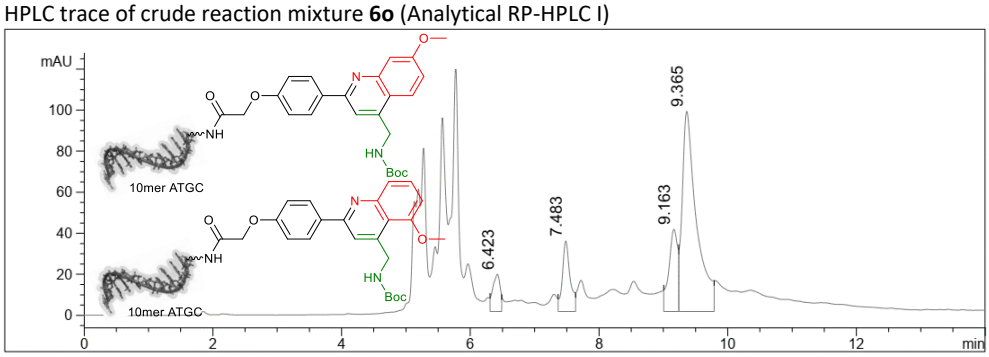

Peak list:

Ret. Time	Width min	Height	Area	Area %
6.423	0.131	18.168	142.982	6.200
7.483	0.139	34.435	286.729	12.433
9.163	0.159	40.075	381.159	16.527
9.365	0.255	97.611	1495.405	64.841

HPLC trace of isolated product 6o (Analytical RP-HPLC I)

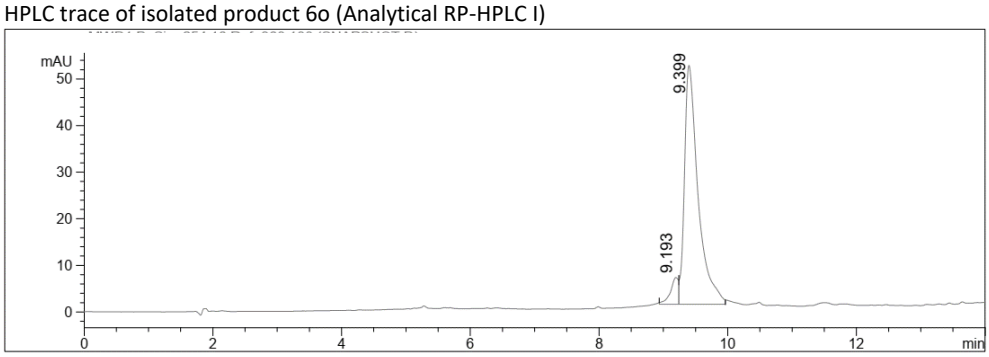

Peak list:

Ret. Time	Width min	Height	Area	Area %
9.193	0.146	5.736	50.212	6.285
9.399	0.243	51.279	748.659	93.715

MALDI-MS spectrum of isolated product **6o**

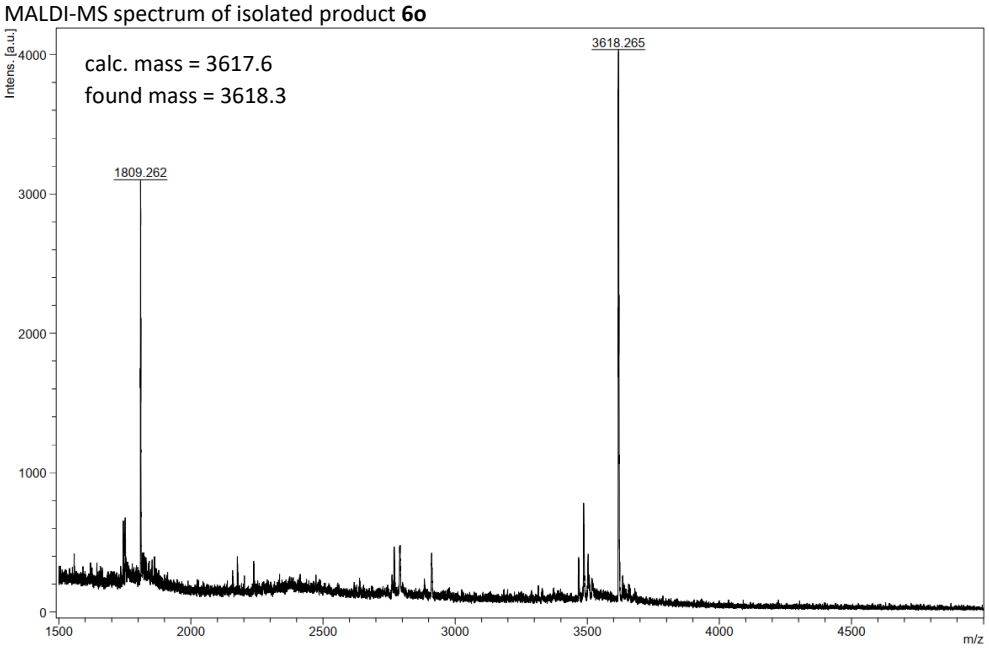

DNA conjugate 6p: CPG-bound 10mer ATGC-aldehyde conjugate (Batch C) **5** was reacted with 3,4-dimethoxy-aniline **2p** and *N*-Boc-propargylamine **3a** according to RP-02.

HPLC trace of crude reaction mixture 6p (Analytical RP-HPLC I)

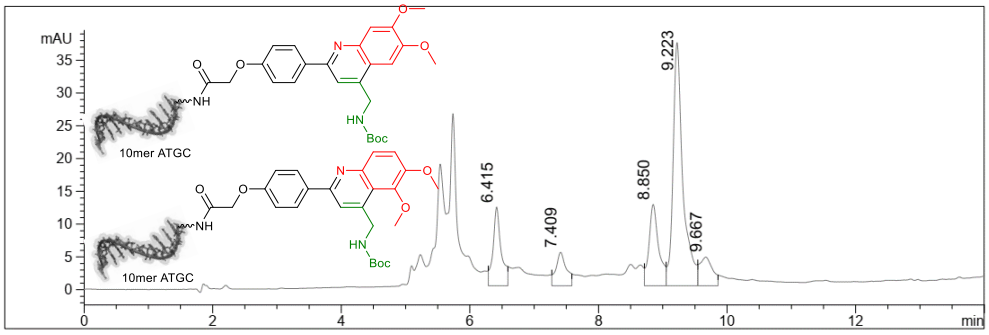

Peak list:

Ret. Time	Width min	Height	Area	Area %
6.415	0.146	12.023	105.550	14.096
7.409	0.186	5.116	57.004	7.613
8.850	0.175	12.409	130.436	17.420
9.223	0.177	37.116	395.100	52.767
9.667	0.231	4.369	60.681	8.104

HPLC trace of isolated product **6p** (Analytical RP-HPLC I)

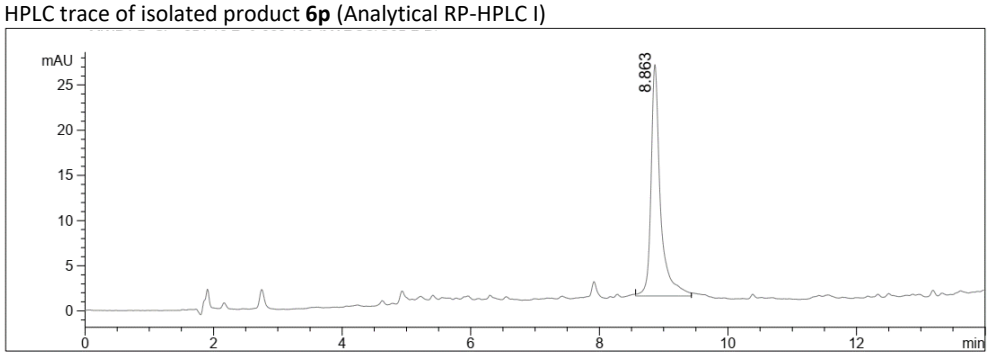

Peak list:

Ret. Time	Width min	Height	Area	Area %
8.863	0.169	25.609	259.614	100.000

MALDI-MS spectrum of isolated product **6p**

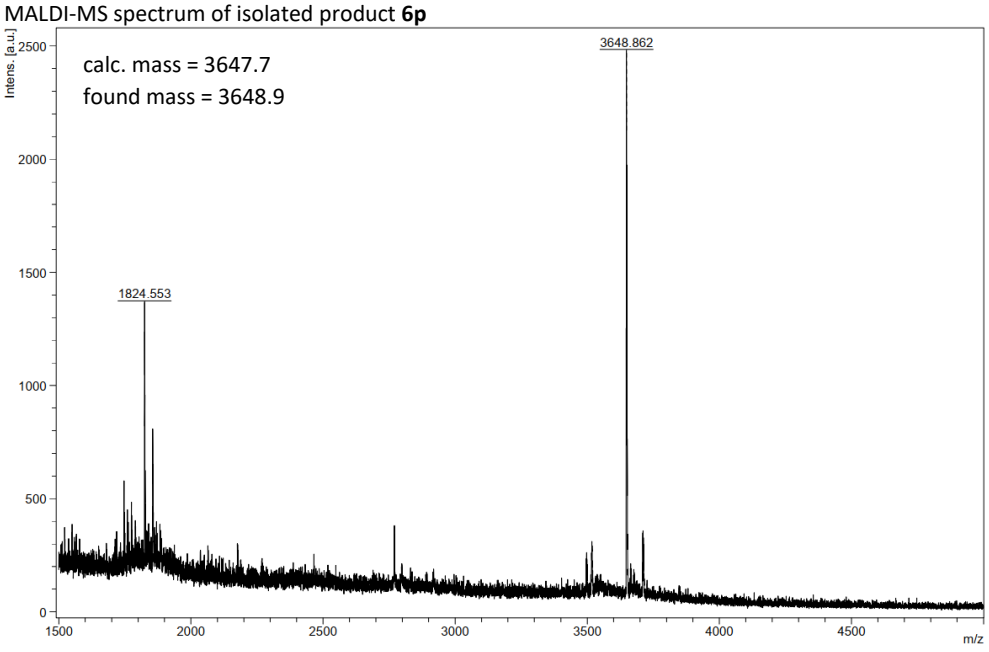

DNA conjugate 6q: CPG-bound 10mer ATGC-aldehyde conjugate (Batch C) **5** was reacted with 2,3-dimethoxy-aniline **2q** and *N*-Boc-propargylamine **3a** according to RP-02.

HPLC trace of crude reaction mixture **6q** (Analytical RP-HPLC I)

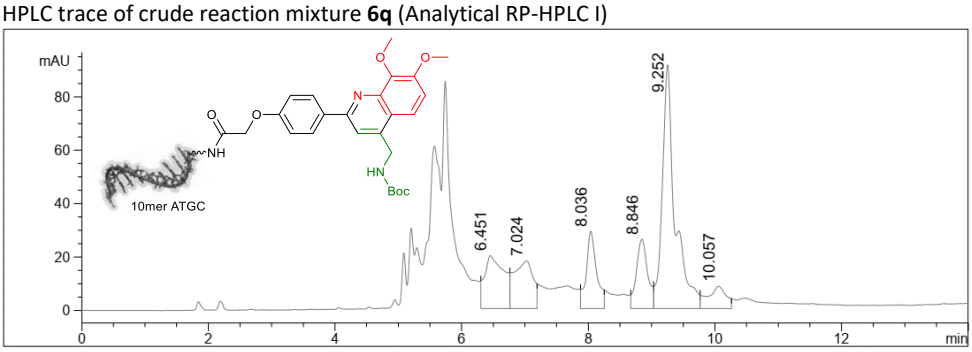

Peak list:

Ret. Time	Width min	Height	Area	Area %
6.451	0.354	19.826	420.999	14.622
7.024	0.346	17.846	370.579	12.871
8.036	0.189	28.991	328.717	11.417
8.846	0.208	25.978	323.795	11.246
9.252	0.232	91.259	1268.644	44.063
10.057	0.332	8.357	166.401	5.780

HPLC trace of isolated product 6q (Analytical RP-HPLC I)

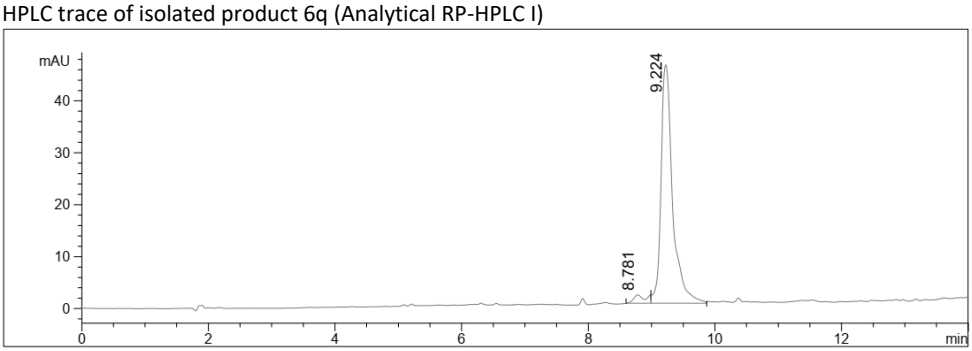

Peak list:

Ret. Time	Width min	Height	Area	Area %
8.781	0.223	1.578	21.147	3.477
9.224	0.213	45.883	587.083	96.523

MALDI-MS spectrum of isolated product 6q

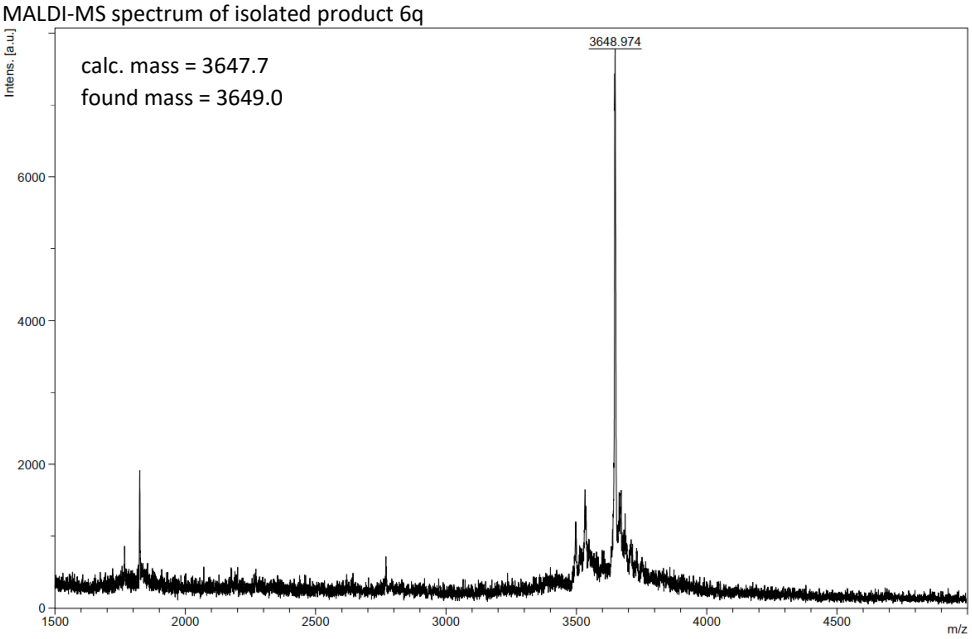

DNA conjugate 6r: CPG-bound 10mer ATGC-aldehyde conjugate (Batch C) **5** was reacted with 3-aminobenzo-nitrile **2r** and *N*-Boc-propargylamine **3a** according to RP-02.

HPLC trace of crude reaction mixture **6r** (Analytical RP-HPLC I)

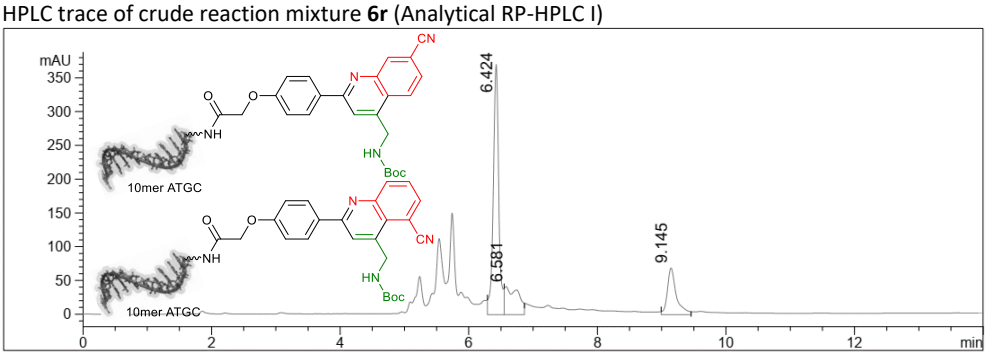

Peak list:

Ret. Time	Width min	Height	Area	Area %
6.424	0.100	371.025	2221.325	63.681
6.581	0.240	41.479	598.495	17.158
9.145	0.161	68.997	668.394	19.162

HPLC trace of isolated product 6r (Analytical RP-HPLC I)

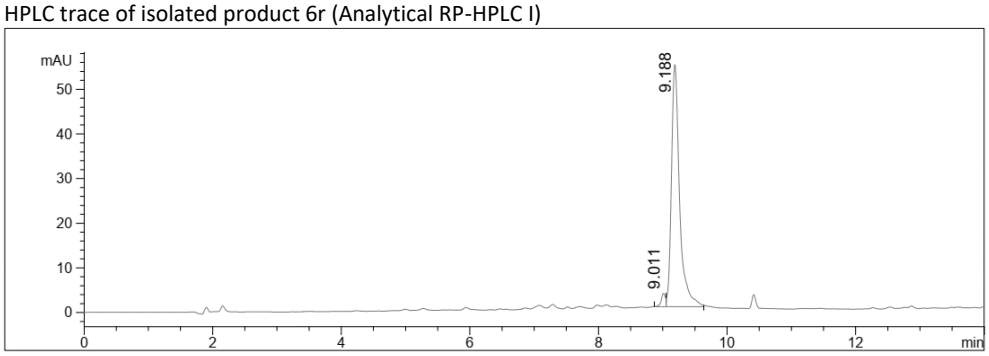

Peak list:

Ret. Time	Width min	Height	Area	Area %
9.011	0.078	2.997	14.085	2.879
9.188	0.146	54.294	475.068	97.121

MALDI-MS spectrum of isolated product **6r**

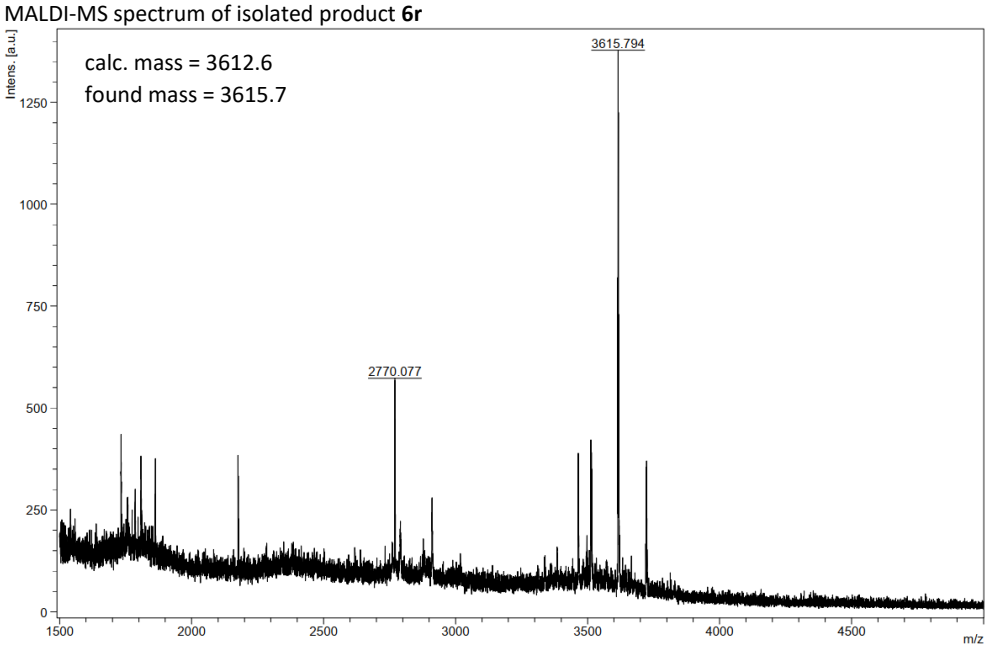

DNA conjugate 6s: CPG-bound 10mer ATGC-aldehyde conjugate (Batch C) **5** was reacted with 4-aminophenol **2s** and *N*-Boc-propargylamine **3a** according to RP-02.

HPLC trace of crude reaction mixture **6s** (Analytical RP-HPLC I)

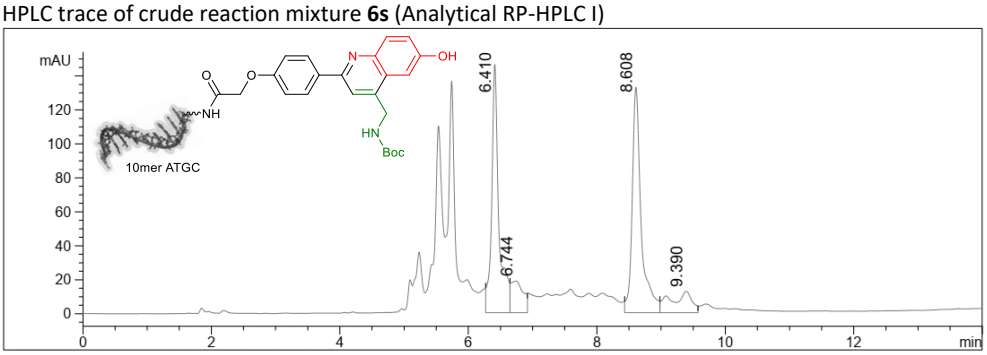

Peak list:

Ret. Time	Width min	Height	Area	Area %
6.410	0.129	146.695	1138.358	38.494
6.744	0.222	18.646	248.431	8.401
8.608	0.161	132.912	1286.739	43.512
9.390	0.374	12.658	283.684	9.593

HPLC trace of isolated product **6s** (Analytical RP-HPLC I)

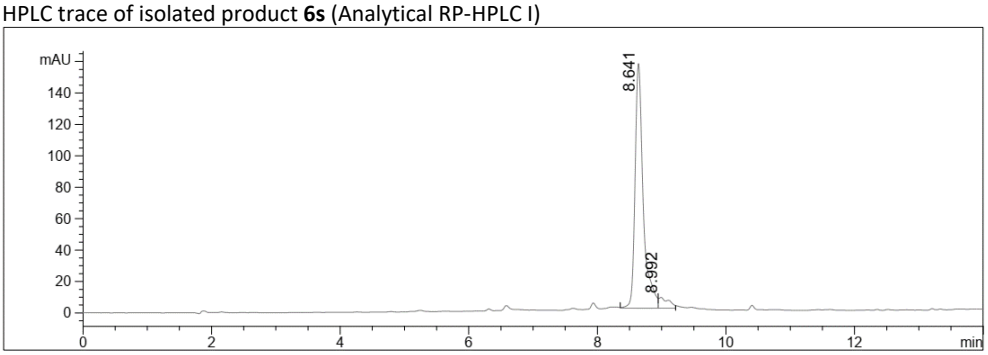

Peak list:

Ret. Time	Width min	Height	Area	Area %
8.641	0.147	155.789	1372.368	94.840
8.992	0.181	6.874	74.663	5.160

MALDI-MS spectrum of isolated product **6s**

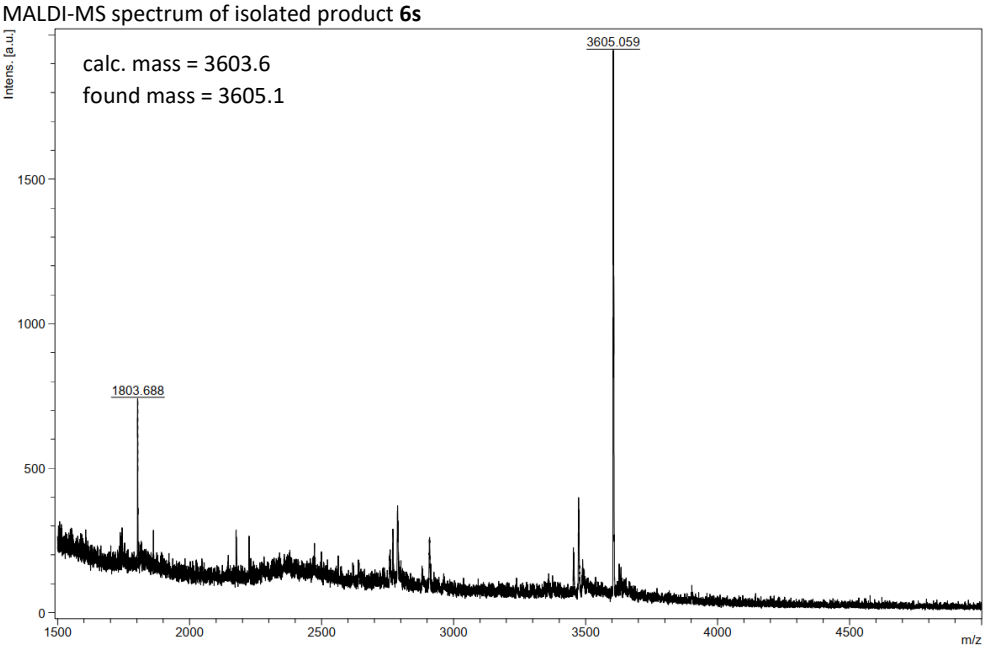

DNA conjugate 6t: CPG-bound 10mer ATGC-aldehyde conjugate (Batch C) **5** was reacted with (3-aminophenyl)methanol **2t** and *N*-Boc-propargylamine **3a** according to RP-02.

HPLC trace of crude reaction mixture **6t** (Analytical RP-HPLC I)

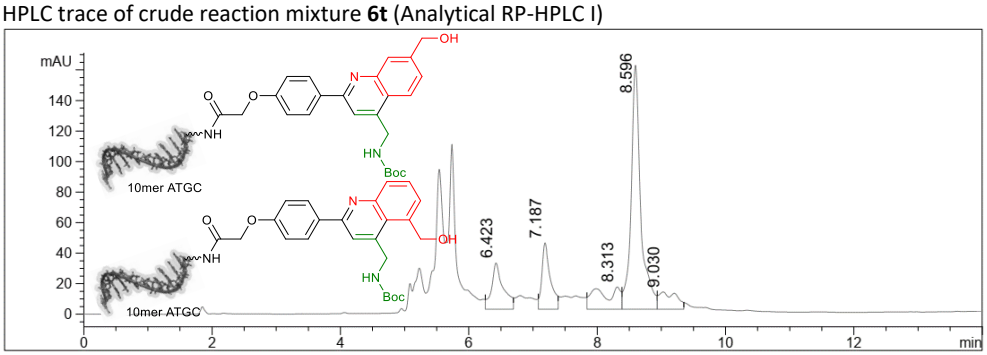

Peak list:

Ret. Time	Width min	Height	Area	Area %
6.423	0.211	30.252	382.237	12.730
7.187	0.153	43.397	399.531	13.306
8.313	0.389	14.485	338.245	11.265
8.596	0.174	159.719	1667.396	55.530
9.030	0.318	11.286	215.306	7.170

HPLC trace of isolated product **6t** (Analytical RP-HPLC I)

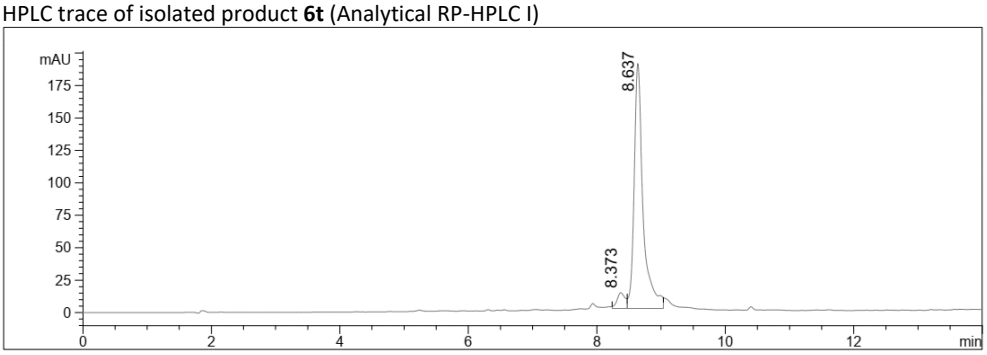

Peak list:

Ret. Time	Width min	Height	Area	Area %
8.373	0.148	12.174	107.916	5.554
8.637	0.162	188.960	1835.280	94.446

MALDI-MS spectrum of isolated product **6t**

calc. mass = 3617.6

found mass = 3619.0

DNA conjugate 6u: CPG-bound 10mer ATGC-aldehyde conjugate (Batch C) **5** was reacted with methyl 3-aminobenzoate **2u** and *N*-Boc-propargylamine **3a** according to RP-02.

HPLC trace of crude reaction mixture **6u** (Analytical RP-HPLC I)

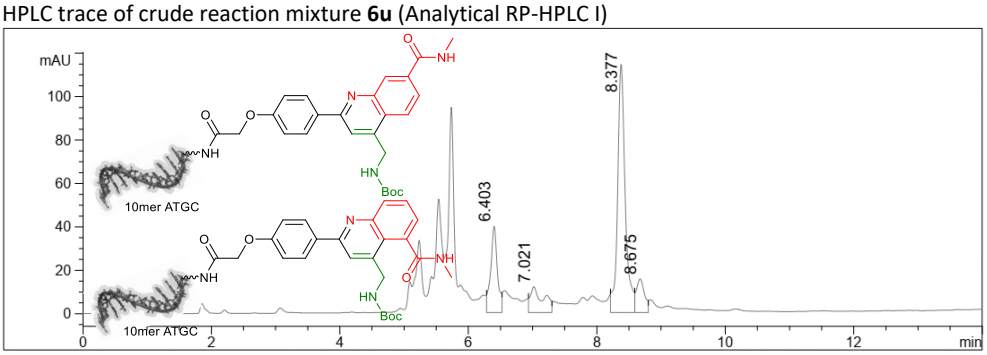

Peak list:

Ret. Time	Width min	Height	Area	Area %
6.403	0.121	39.748	289.111	18.960
7.021	0.233	11.853	165.516	10.854
8.377	0.137	114.292	936.129	61.391
8.675	0.145	15.438	134.108	8.795

HPLC trace of isolated product **6u** (Analytical RP-HPLC I)

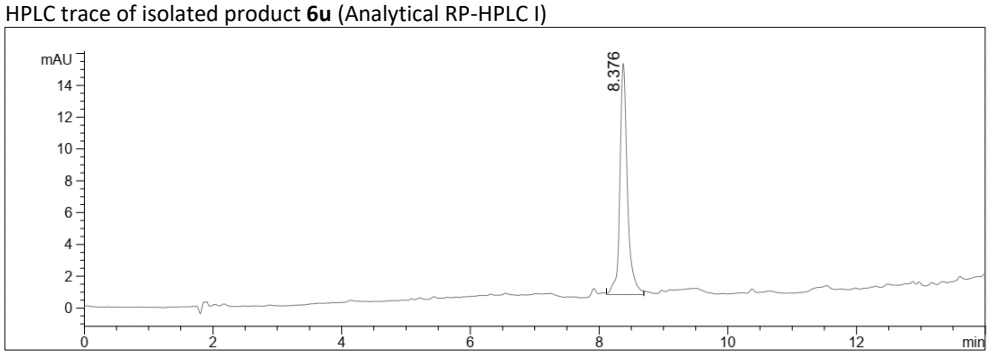

Peak list:

Ret. Time	Width min	Height	Area	Area %
8.376	0.136	14.520	118.059	100.000

MALDI-MS spectrum of isolated product **6u**

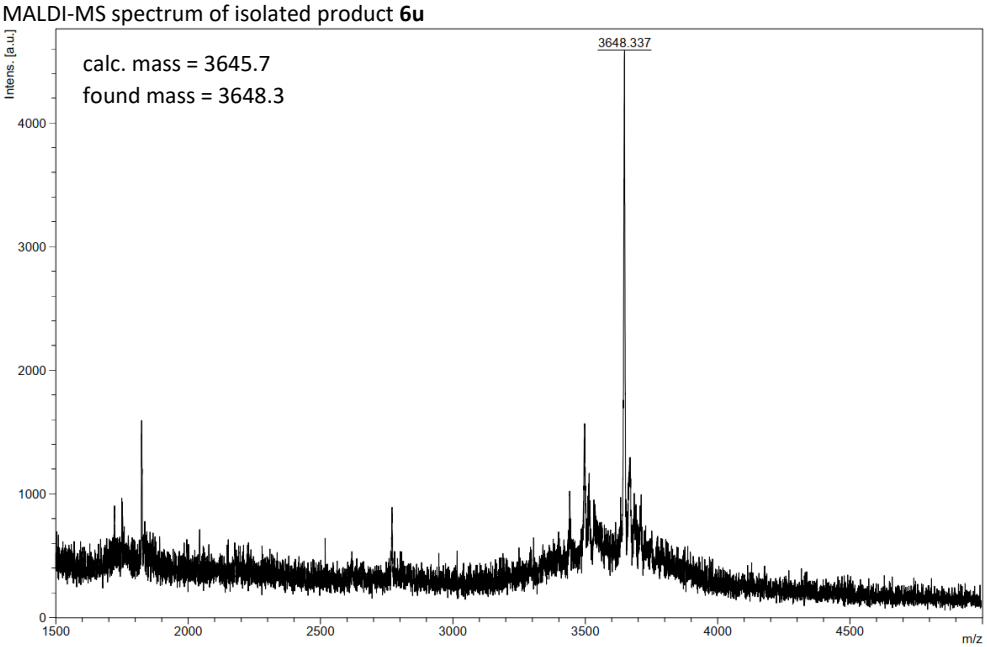

DNA conjugate 6v: CPG-bound 10mer ATGC-aldehyde conjugate (Batch C) **5** was reacted with ethyl 4-aminobenzoate **2v** and *N*-Boc-propargylamine **3a** according to RP-02.

HPLC trace of crude reaction mixture **6v** (Analytical RP-HPLC I)

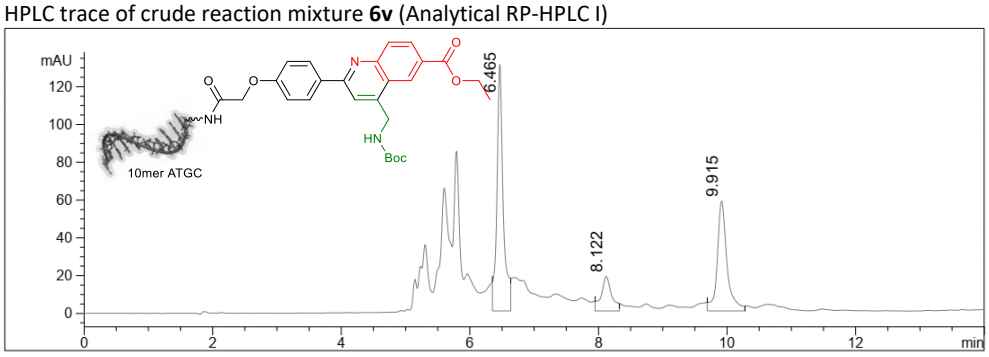

Peak list:

Ret. Time	Width min	Height	Area	Area %
6.465	0.115	130.748	899.938	52.472
8.122	0.187	18.262	204.557	11.927
9.915	0.175	58.206	610.589	35.601

HPLC trace of isolated product **6v** (Analytical RP-HPLC I)

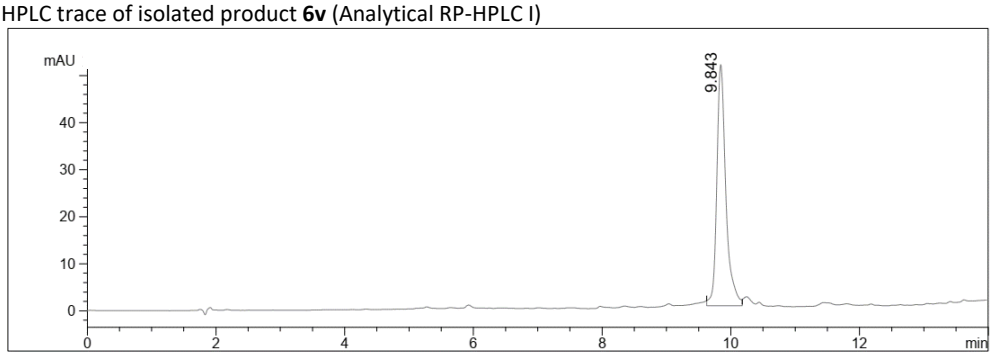

Peak list:

Ret. Time	Width min	Height	Area	Area %
9.843	0.162	51.248	497.612	100.000

MALDI-MS spectrum of isolated product **6v**

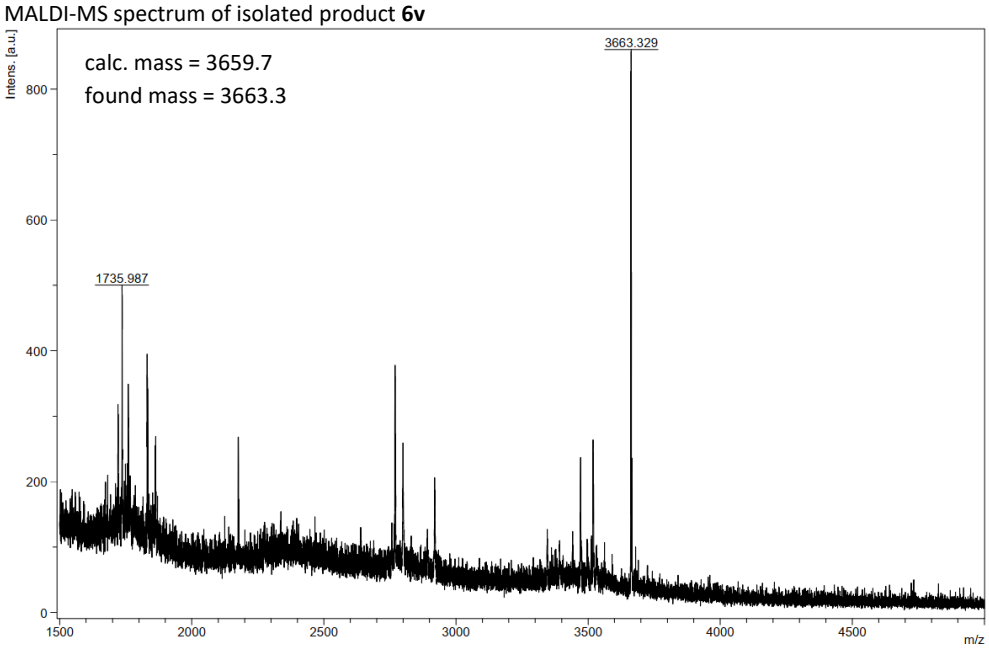

DNA conjugate 6w: CPG-bound 10mer ATGC-aldehyde conjugate (Batch C) **5** was reacted with 4-amino-benzoic acid **2w** and *N*-Boc-propargylamine **3a** according to RP-02.

HPLC trace of crude reaction mixture **6w** (Analytical RP-HPLC I)

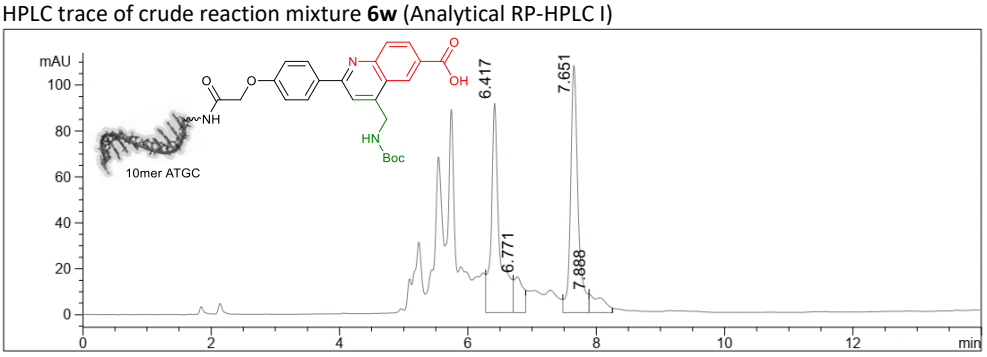

Peak list:

Ret. Time	Width min	Height	Area	Area %
6.417	0.151	91.171	826.177	42.079
6.771	0.166	15.508	154.314	7.860
7.651	0.134	107.681	868.729	44.247
7.888	0.237	8.032	114.161	5.815

HPLC trace of isolated product **6w** (Analytical RP-HPLC I)

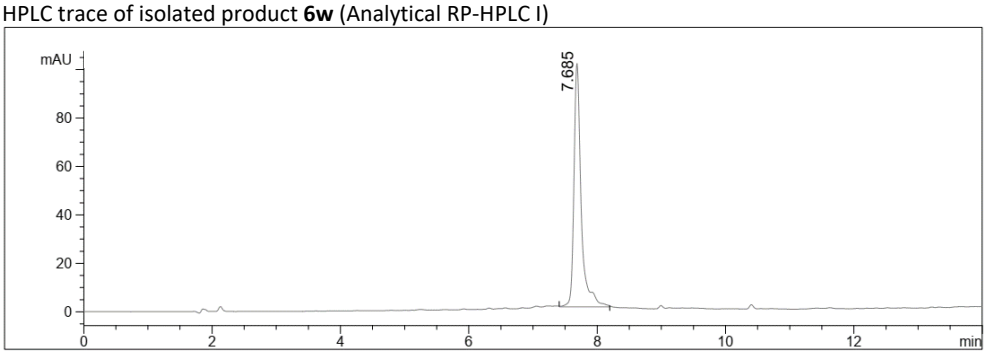

Peak list:

Ret. Time	Width min	Height	Area	Area %
7.685	0.130	100.536	784.956	100.000

MALDI-MS spectrum of isolated product **6w**

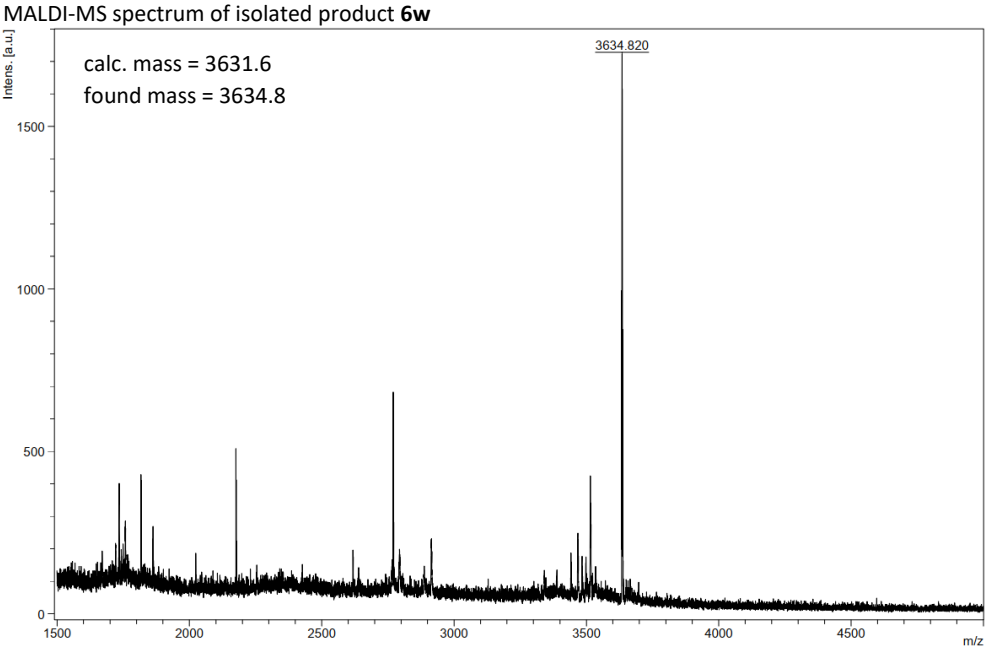

DNA conjugate 6x: CPG-bound 10mer ATGC-aldehyde conjugate (Batch C) **5** was reacted with 4-bromo-3-methylaniline **2x** and *N*-Boc-propargylamine **3a** according to RP-02.

HPLC trace of crude reaction mixture **6x** (Analytical RP-HPLC I)

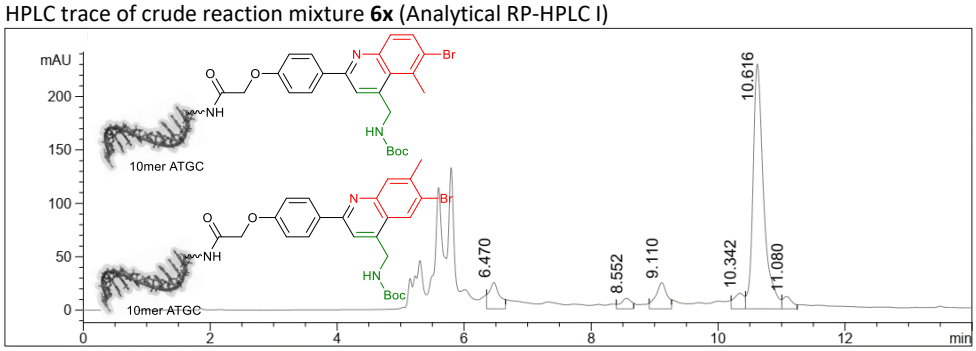

Peak list:

Ret. Time	Width min	Height	Area	Area %
6.470	0.191	24.725	282.971	7.797
8.552	0.196	9.803	115.125	3.172
9.110	0.204	24.552	300.768	8.288
10.342	0.187	14.643	164.705	4.539
10.616	0.192	229.391	2647.604	72.956
11.080	0.170	11.525	117.890	3.249

HPLC trace of isolated product 6x (Analytical RP-HPLC I)

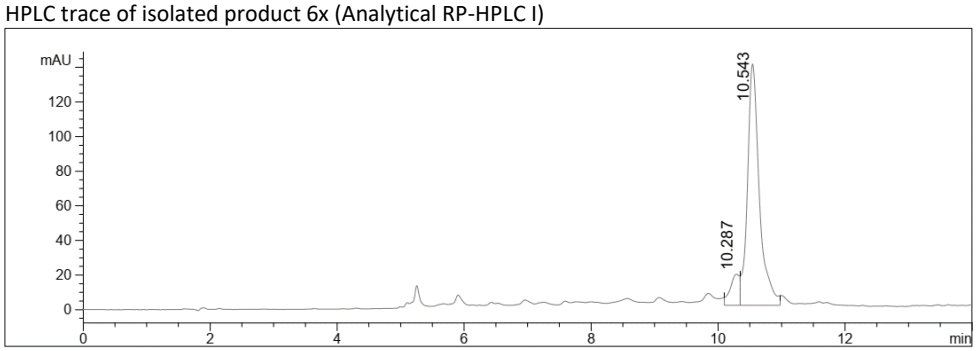

Peak list:

Ret. Time	Width min	Height	Area	Area %
10.287	0.174	17.956	187.081	9.383
10.543	0.216	139.446	1806.766	90.617

MALDI-MS spectrum of isolated product 6x

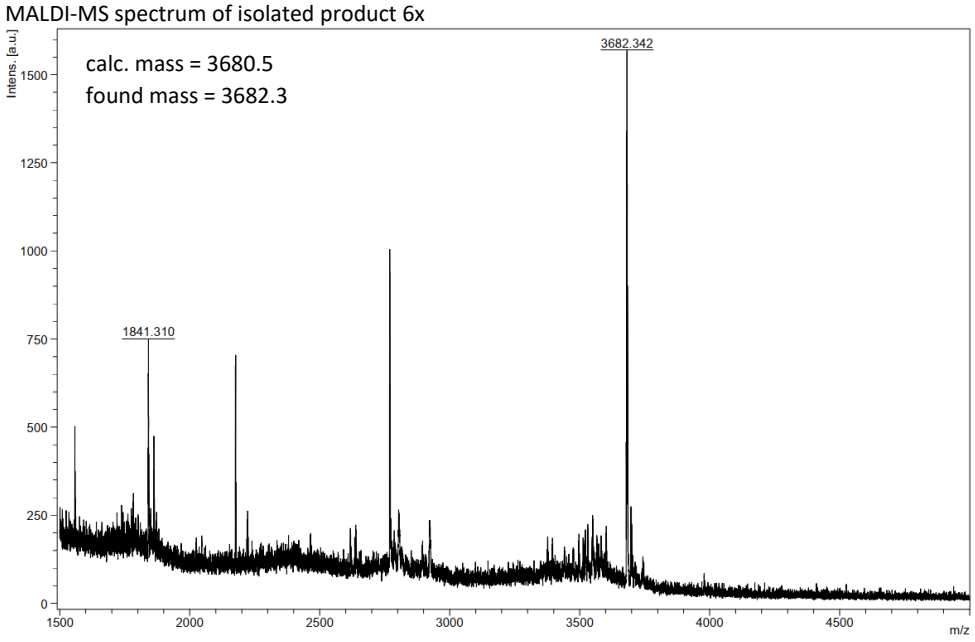

DNA conjugate 6y: CPG-bound 10mer ATGC-aldehyde conjugate (Batch C) **5** was reacted with 4-bromo-3-methoxyaniline **2y** and *N*-Boc-propargylamine **3a** according to RP-02.

HPLC trace of crude reaction mixture **6y** (Analytical RP-HPLC I)

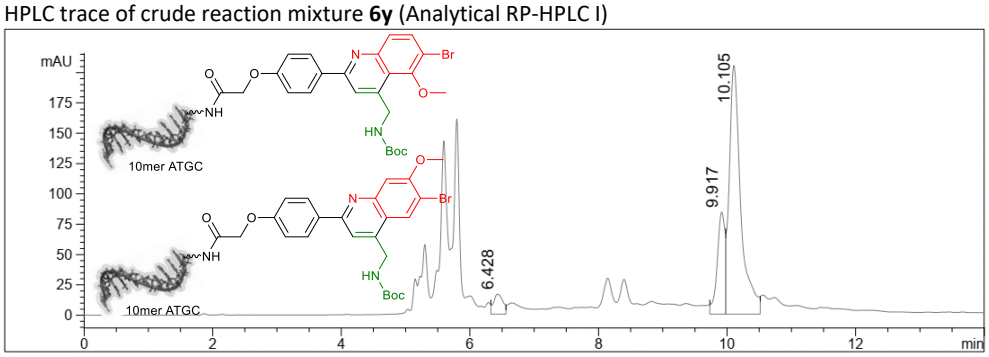

Peak list:

Ret. Time	Width min	Height	Area	Area %
6.428	0.170	16.336	166.211	4.867
9.917	0.139	84.108	701.400	20.539
10.105	0.207	204.933	2547.301	74.593

HPLC trace of isolated product **6y** (Analytical RP-HPLC I)

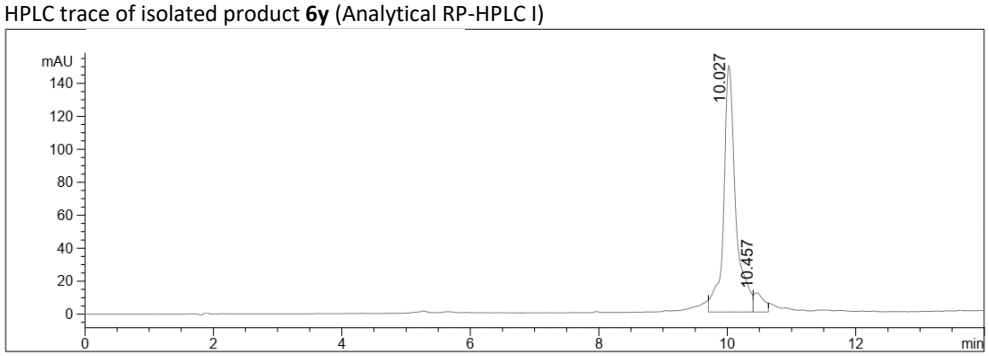

Peak list:

Ret. Time	Width min	Height	Area	Area %
10.027	0.219	149.472	1962.377	94.033
10.457	0.179	11.571	124.527	5.967

MALDI-MS spectrum of isolated product **6y**

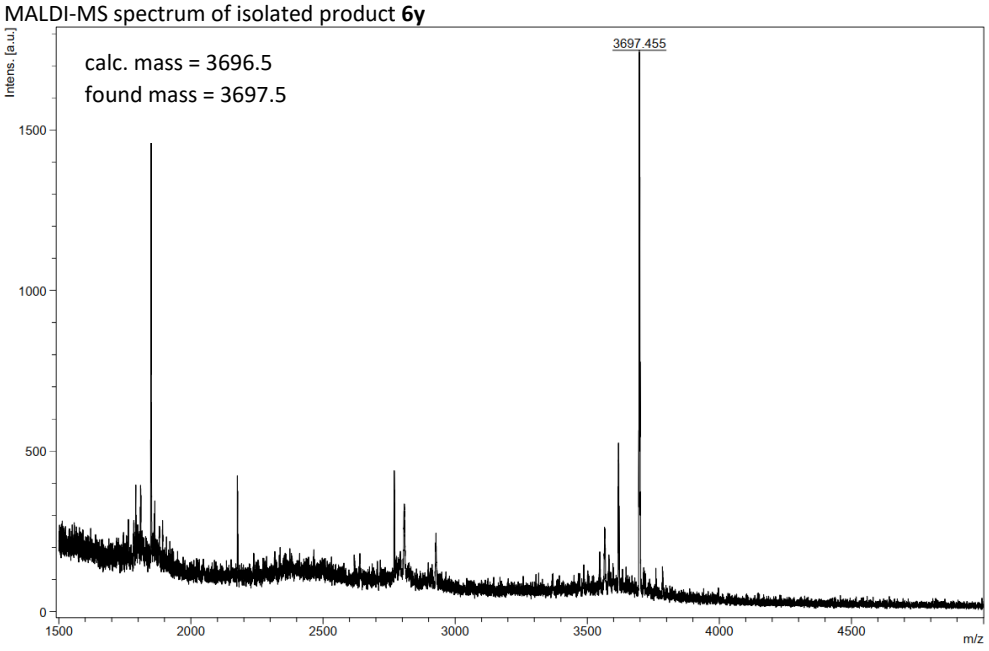

DNA conjugate 6aa: CPG-bound 10mer ATGC-aldehyde conjugate (Batch B) **5** was reacted with aniline **2q** and *tert*-butyl (S)-2-ethynylpiperidine-1-carboxylate **3b** according to RP-02.

HPLC trace of crude reaction mixture **6aa** (Analytical RP-HPLC I)

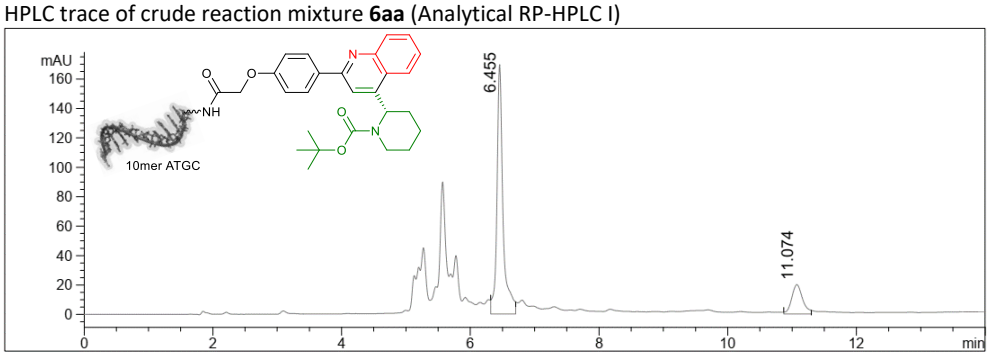

Peak list:

Ret. Time	Width min	Height	Area	Area %
6.455	0.108	170.032	1103.283	82.130
11.074	0.200	20.019	240.063	17.870

HPLC trace of isolated product **6aa** (Analytical RP-HPLC I)

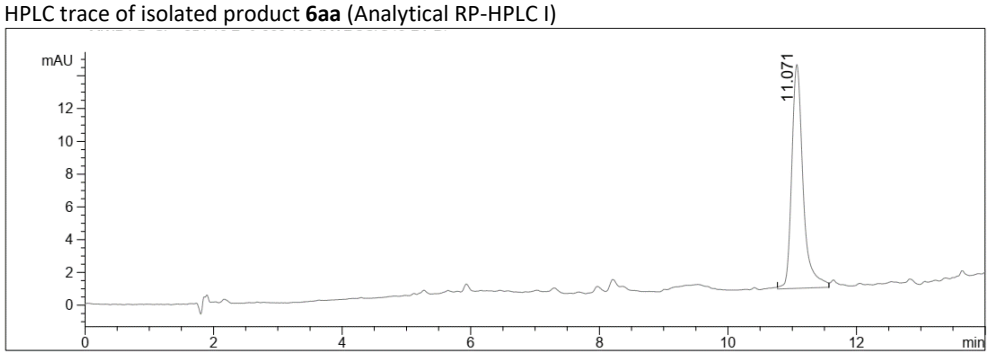

Peak list:

Ret. Time	Width min	Height	Area	Area %
11.071	0.187	13.650	166.880	100.000

MALDI-MS spectrum of isolated product **6aa**

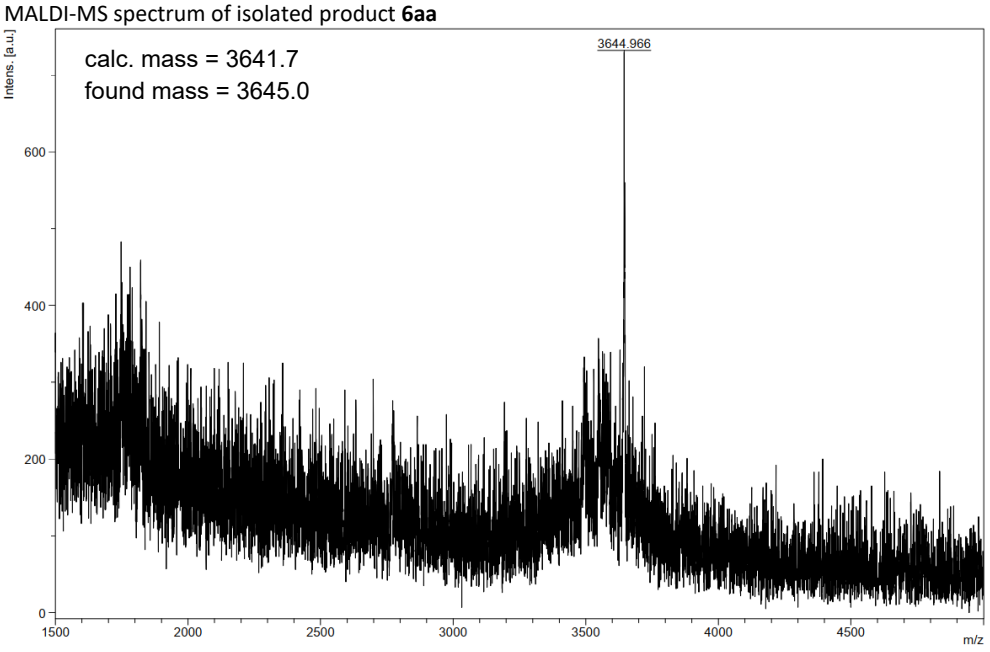

DNA conjugate 6ab: CPG-bound 10mer ATGC-aldehyde conjugate (Batch A) **5** was reacted with aniline **2q** and phenylacetylene **3b** according to RP-02.

HPLC trace of crude reaction mixture **6ab** (Analytical RP-HPLC I)

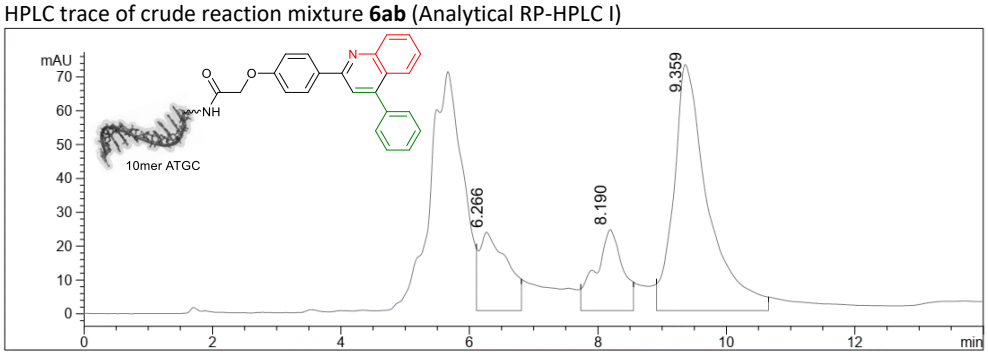

Peak list:

Ret. Time	Width min	Height	Area	Area %
6.266	0.502	23.137	697.527	17.196
8.190	0.482	23.908	691.132	17.039
9.359	0.612	72.673	2667.617	65.765

HPLC trace of isolated product **6ab** (Analytical RP-HPLC I)

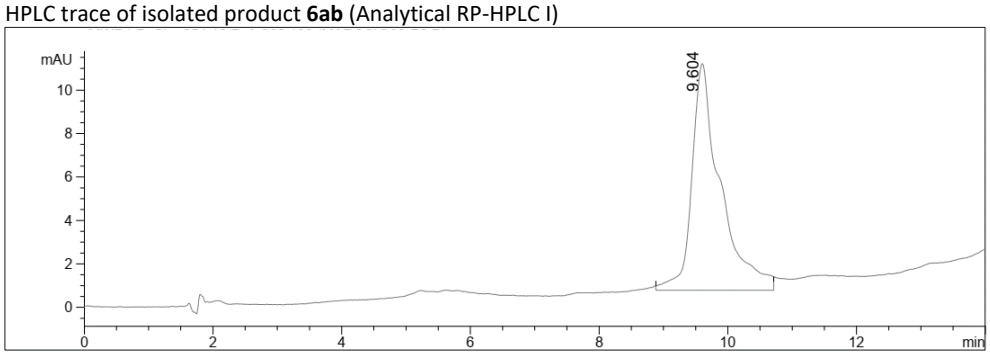

Peak list:

Ret. Time	Width min	Height	Area	Area %
9.604	0.517	10.430	323.348	100.000

MALDI-MS spectrum of isolated product **6ab**

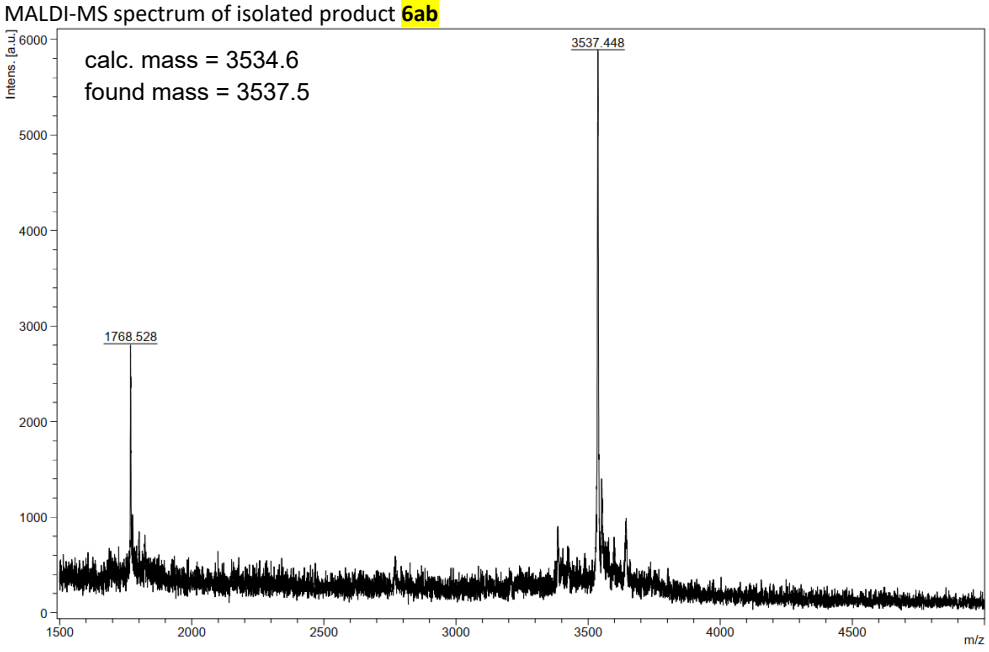

Pyrrole synthesis

Optimization of pyrrole synthesis on CPG-bound DNA-aldehyde conjugates

Table S13. Optimization of pyrrole synthesis on a CPG-bound DNA-aldehyde conjugate **7**.[a]

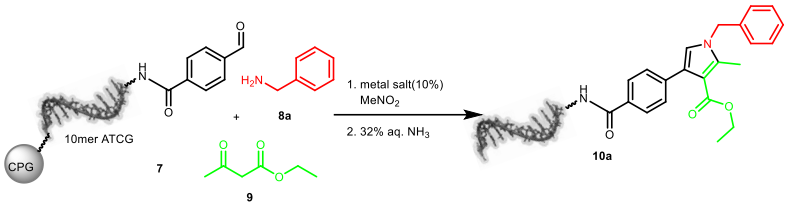

Entry	Metal salt	T (°C)	Time (h)	Conversion [%][b]	Degradation [%][c]
1	$FeCl_3$	60	6	0	20-33
2	$FeCl_3$	60	8	N.d.	N.d.
3	$FeCl_3$	80	6	21	37
4	$FeCl_3$	80	8	14	45
5	$NiCl_2$	60	6	4	25
6	$NiCl_2$	60	8	N.d.	N.d.
7	$NiCl_2$	80	6	19	52
8	$NiCl_2$	80	8	11	27

[a] The suspension of DNA-aldehyde conjugate **7** (20 nmol), benzylamine **8a** (250 mM), ethylcetoacetate **9** (250 mM) and metal salt (25 mM) in solvent (40 µL) was shaken at the given temperature for the given time. DNA cleavage with 32% aq. Ammonia solution at ambient temperature for 4 h. [b] Determined by RP-HPLC II analysis based on the ratios of **7** to **10a**. [c] Determined by RP-HPLC II analysis in ratio to the purity of the CPG-coupled DNA-aldehyde conjugate **7**, MeNO2 = nitromethane. N.d. = not detected, 10mer ATGC = 5'-NH2-C6-GTCATGATCT-3'-CPG.

DNA conjugate 7: CPG-bound 10mer ATCG-$(CH_2)_6$-NH_2 conjugate was reacted with 4-formyl-benzoic acid according to **RP-01**. HPLC trace of crude reaction mixture **7** (Analytical RP-HPLC II).

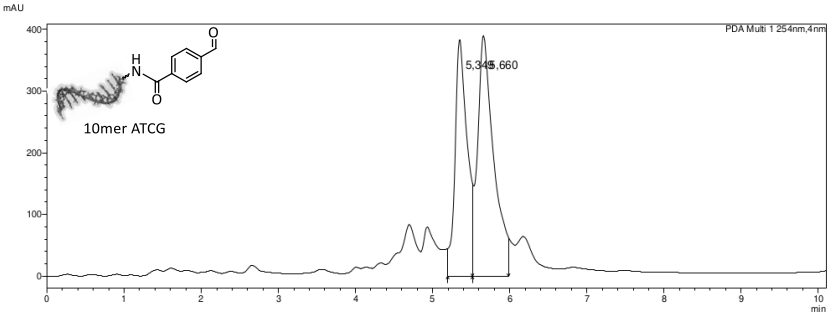

MALDI-MS spectrum of crude reaction mixture 7

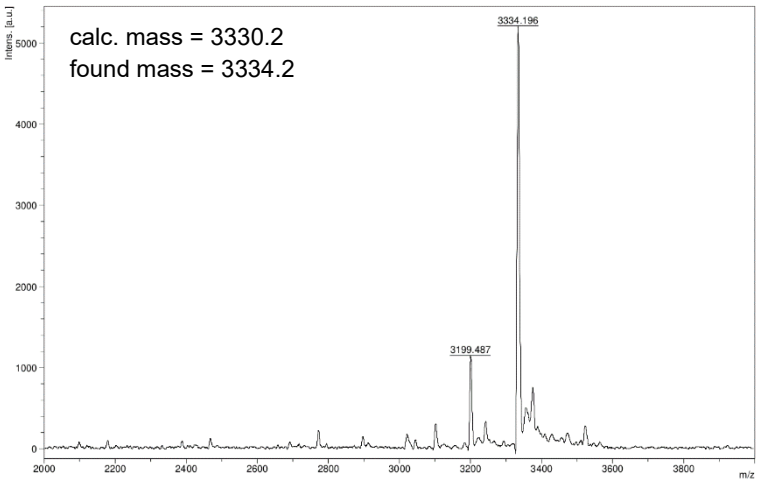

DNA conjugate 10a: CPG-bound 10mer ATCG-aldehyde conjugate **7** was reacted with benzylamine **8a** and ethylcetoacetate **9** according to RP-03.

Table S14. Optimization of pyrrole synthesis on a CPG-bound DNA-aldehyde conjugate **7**.[a]

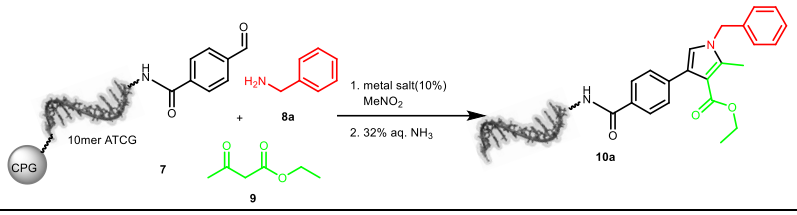

Entry	Reaction conditions	MALDI spectrum of the crude reaction mixture RP-HPLC II trace of the crude reaction mixture
1	$FeCl_3$ 60 °C 6 h => conversion 0% => degradation 20%	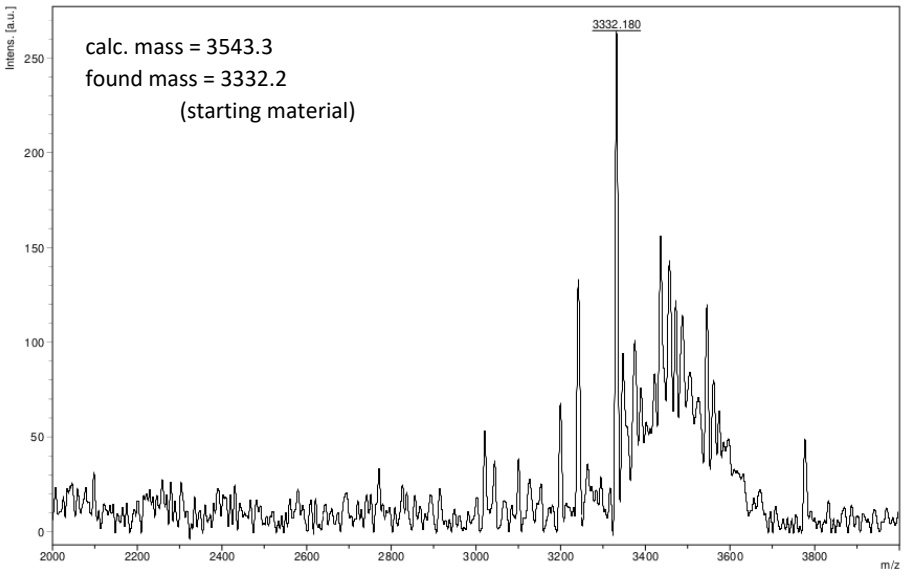 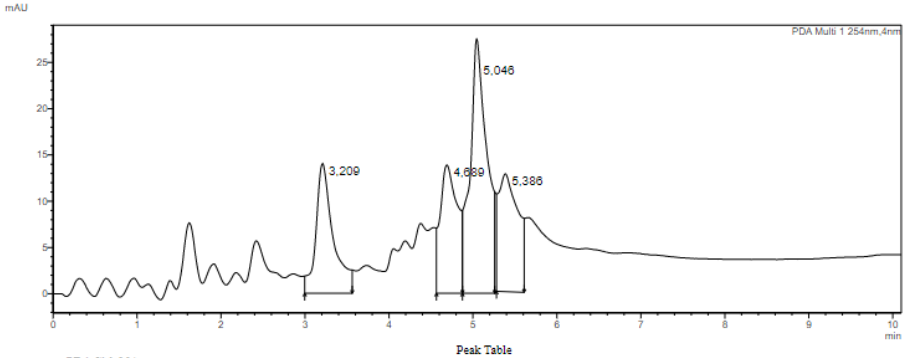 Peak Table PDA Ch1 254nm

Peak#	Ret. Time	Area	Area%	Height	Height%
1	3.209	200735	20.355	14033	20.580
2	4.689	197985	20.077	13858	20.324
3	5.046	381407	38.676	27551	40.405
4	5.386	206023	20.892	12745	18.691
Total		986151	100.000	68186	100.000

3	$FeCl_3$ 80 °C 6 h => conversion 25% => degradation 54%	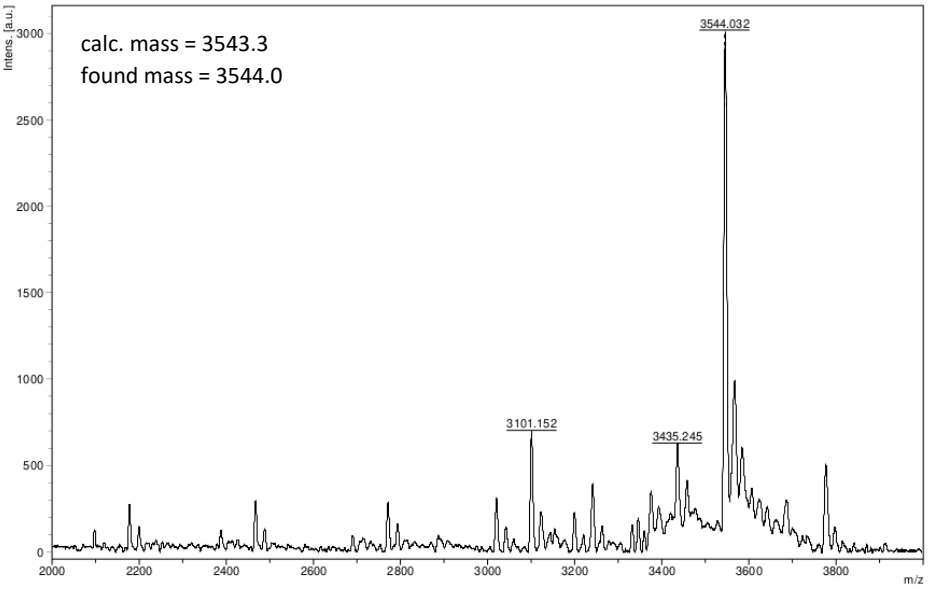 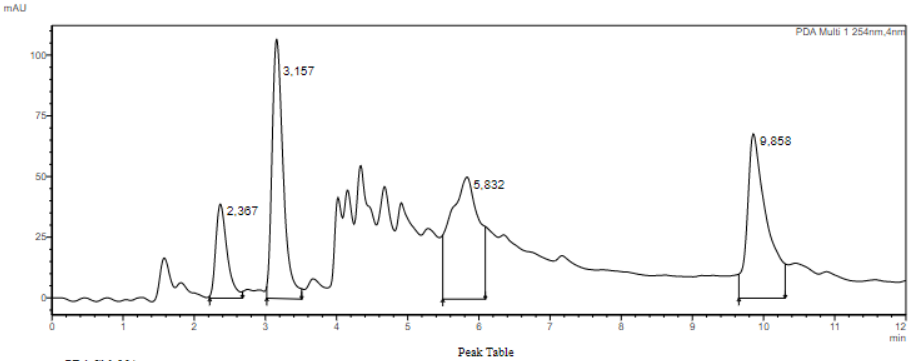 Peak Table PDA Ch1 254nm Peak# | Ret. Time | Area | Area% | Height | Height% 1 | 2,367 | 430322 | 10,096 | 38700 | 14,684 2 | 3,157 | 1162440 | 27,272 | 106953 | 40,582 3 | 5,832 | 1373941 | 32,234 | 50282 | 19,079 4 | 9,858 | 1295688 | 30,398 | 67614 | 25,655 Total | | 4262392 | 100,000 | 263549 | 100,000

4	$FeCl_3$ 80 °C 8 h => conversion 13% => degradation 72%	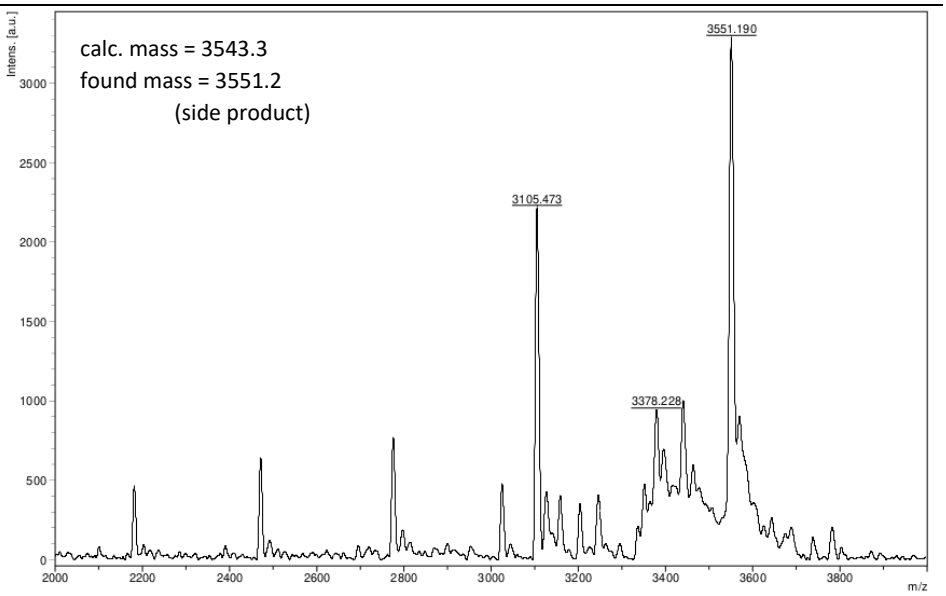 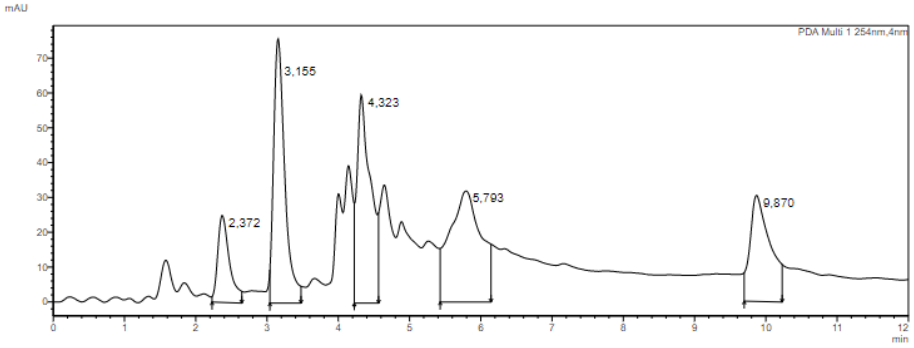 Peak Table PDA Ch1 254nm Peak# | Ret. Time | Area | Area% | Height | Height% 1 | 2,372 | 286896 | 8,208 | 24954 | 11,198 2 | 3,155 | 826557 | 23,648 | 75859 | 34,039 3 | 4,323 | 809281 | 23,154 | 59740 | 26,807 4 | 5,793 | 970377 | 27,763 | 31868 | 14,300 5 | 9,870 | 602075 | 17,226 | 30435 | 13,657 Total | | 3495187 | 100,000 | 222855 | 100,000

5	$NiCl_2$ 60 °C 6 h => conversion 6% => degradation 39%	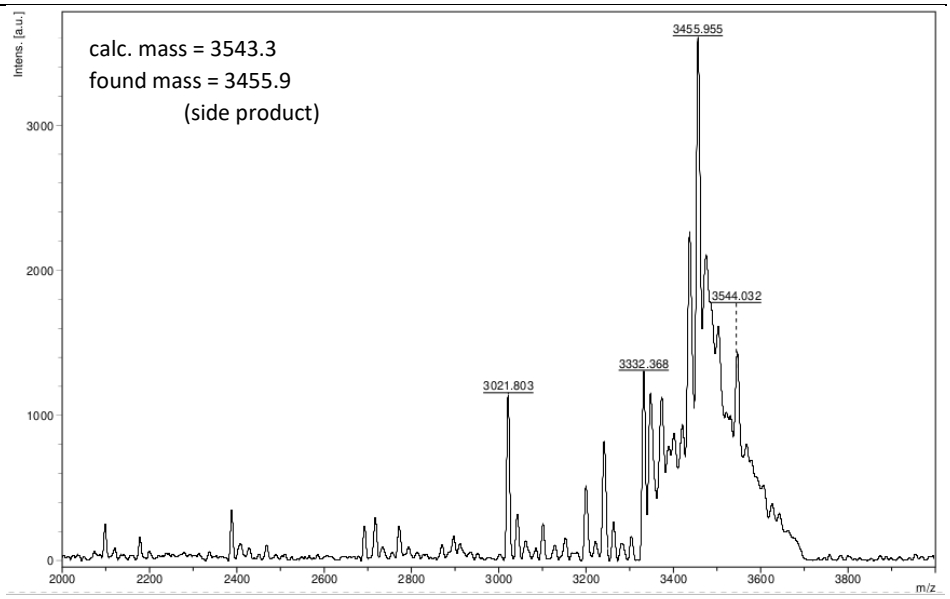 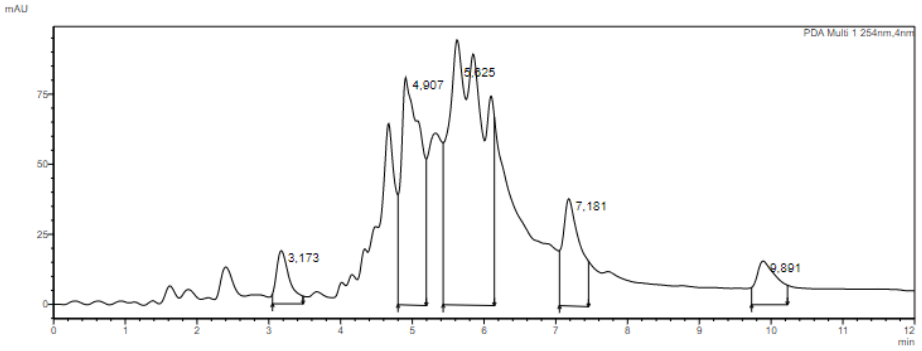 Peak Table PDA Ch1 254nm Peak# | Ret. Time | Area | Area% | Height | Height% 1 | 3.173 | 240911 | 4.055 | 18869 | 7.599 2 | 4.907 | 1526805 | 25.697 | 81090 | 32.657 3 | 5.625 | 3208665 | 54.004 | 94555 | 38.079 4 | 7.181 | 639576 | 10.765 | 38233 | 15.397 5 | 9.891 | 325558 | 5.479 | 15563 | 6.268 Total | | 5941515 | 100.000 | 248311 | 100.000

7

$NiCl_2$
80 °C
6 h

=> conversion
11%
=> degradation
37%

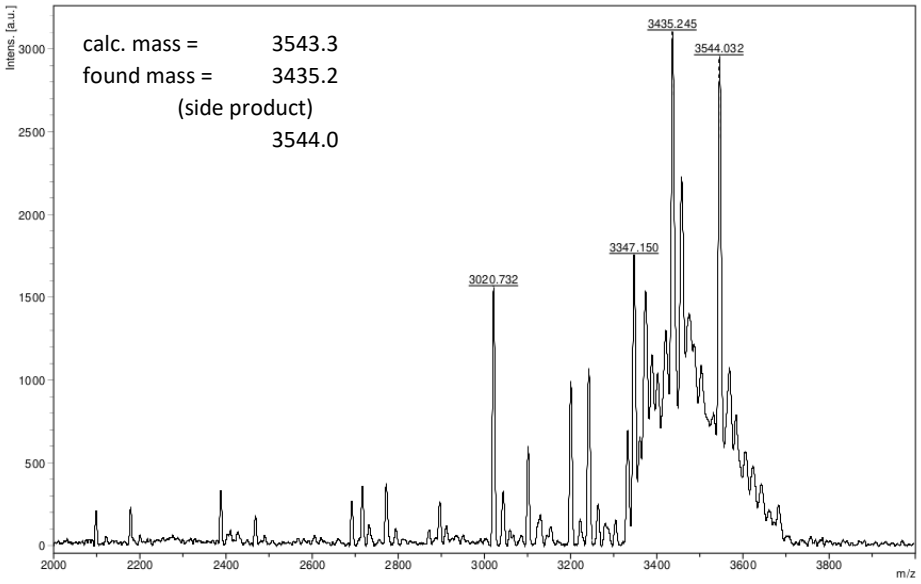

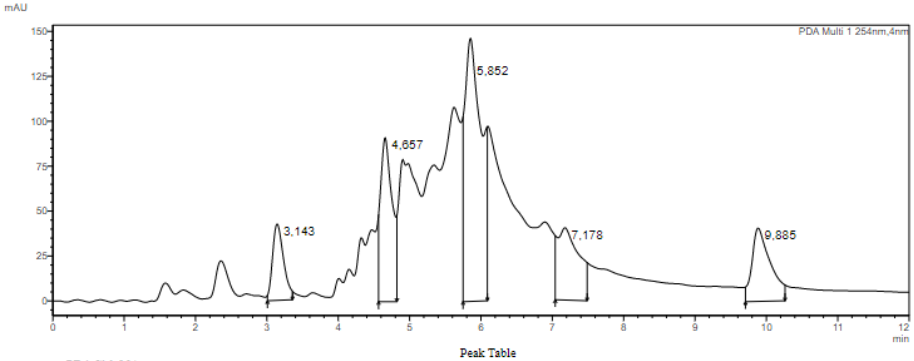

Peak Table

PDA Ch1 254nm

Peak#	Ret. Time	Area	Area%	Height	Height%
1	3,143	458938	8,454	42459	11,760
2	4,657	1038729	19,134	91206	25,261
3	5,852	2351465	43,315	146379	40,542
4	7,178	841015	15,492	40246	11,147
5	9,885	738561	13,605	40763	11,290
Total		5428709	100,000	361053	100,000

8	$NiCl_2$ 80 °C 8 h => conversion 19% => degradation 26%	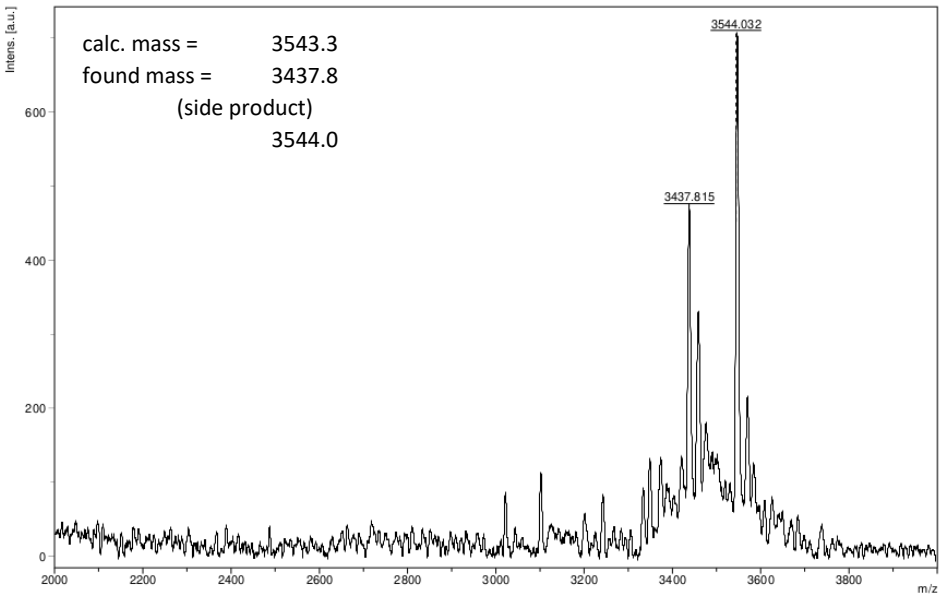 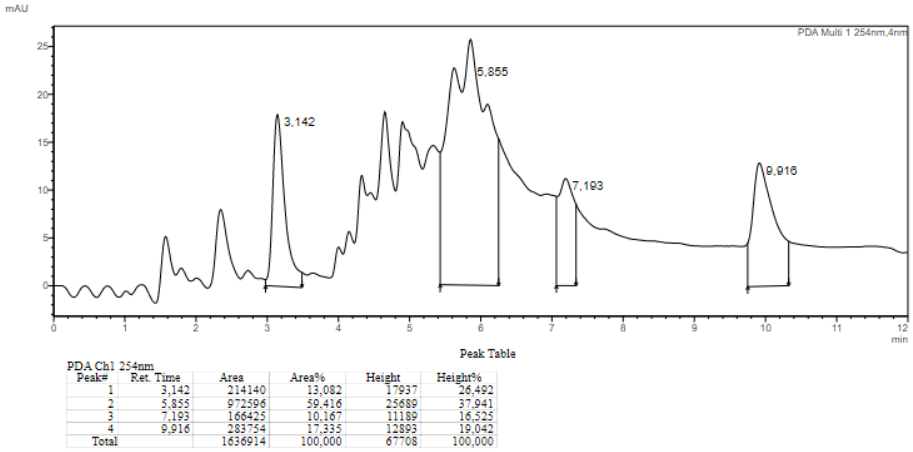 Peak Table PDA Ch1 254nm Peak# | Ret. Time | Area | Area% | Height | Height% 1 | 3,142 | 214140 | 13,082 | 17937 | 26,492 2 | 5,855 | 972596 | 59,416 | 25089 | 37,041 3 | 7,193 | 166425 | 10,167 | 11189 | 16,525 4 | 9,916 | 283754 | 17,335 | 12893 | 19,042 Total | | 1636914 | 100,000 | 67708 | 100,000

[a] The suspension of DNA-aldehyde conjugate **7** (20 nmol), benzylamine **8a** (250 mM), ethylcetoacetate **9** (250 mM) and metal salt (25 mM) in MeNO2 (40 µL) was shaken at the given temperature for the given time. DNA cleavage with 32% aq. Ammonia solution at ambient temperature for 4 h. [b] Determined by RP-HPLC II analysis based on the ratios of **7** to **10**. MeNO2 = nitromethane. N.d. = not detected, 10mer ATGC = 5'-NH2-C6-GTCATGATCT-3'-CPG.

Small scope for pyrrole synthesis

Table S15. Small amine scope for pyrrole synthesis on a CPG-bound DNA-aldehyde conjugate **7**.[a]

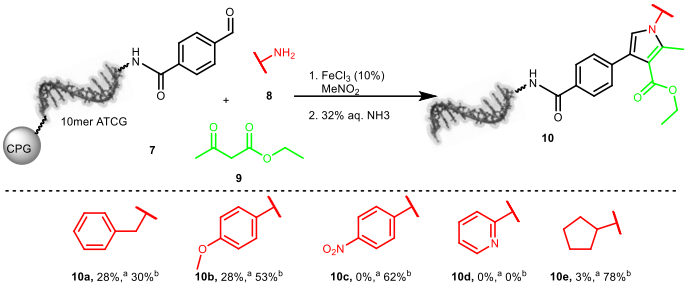

Entry	Product 10	Amine 8	Conversion [%][b]	Degradation [%]
1	**10a**	**8a**	28	30
2	**10b**	**8b**	28	53
3	**10c**	**8c**	0	62
4	**10d**	**8d**	0	0
5	**10e**	**8e**	3	78

[a] The suspension of DNA-aldehyde conjugate **7** (20 nmol), benzylamine **8** (250 mM), ethylcetoacetate **9** (250 mM) and $FeCl_3$ (25 mM) in $MeNO_2$ (40 µL) was shaken at 80 °C for 6 h. DNA cleavage with 32% aq. Ammonia solution at ambient temperature for 4 h. [b] Determined by RP-HPLC II analysis based on the ratios of **7** to **10**. $MeNO_2$ = nitromethane. 10mer ATGC = 5′-NH2-C6-GTCATGATCT-3′-CPG.

Table S16. Small amine scope for the pyrrole synthesis on the CPG- bound DNA-aldehyde conjugate **7**.[a]

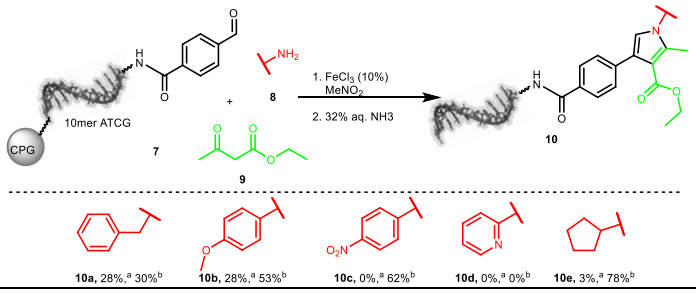

Entry	Product Amine	MALDI spectrum of the crude reaction mixture RP-HPLC II trace of the crude reaction mixture
1	Product **10a** Amine **8a** => conversion 45%	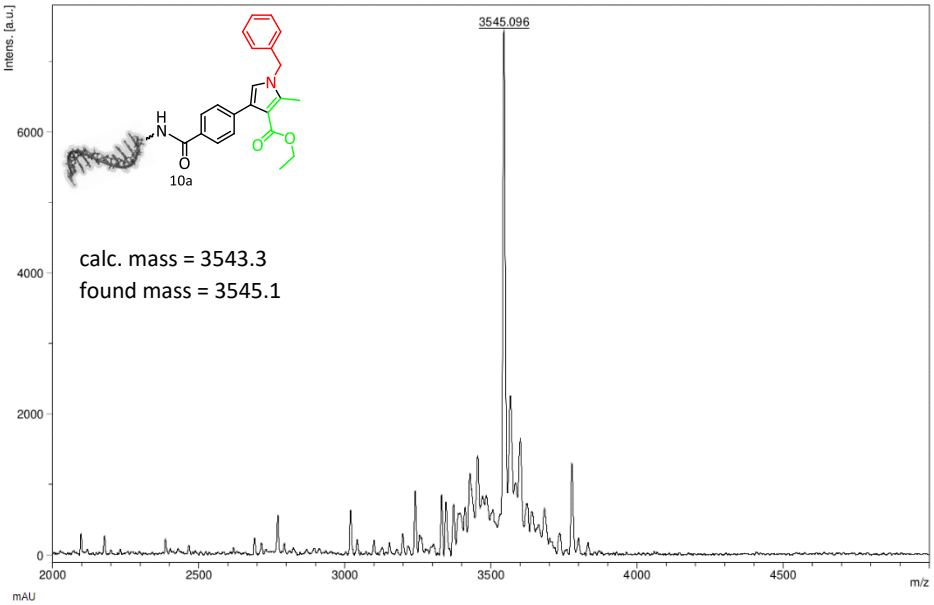 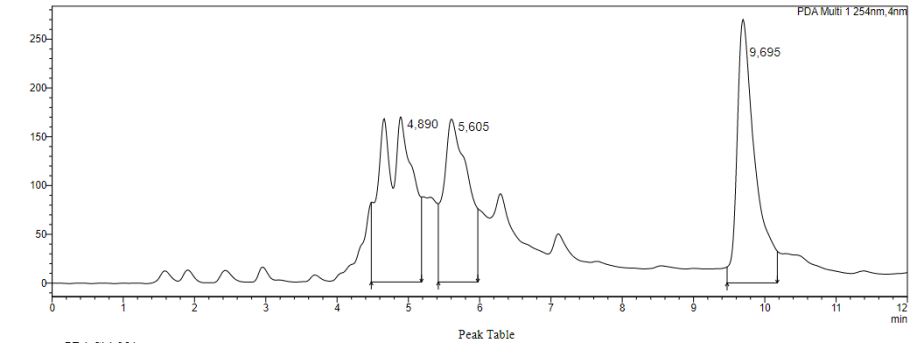 Peak Table PDA Ch1 254nm

Peak#	Ret. Time	Area	Area%	Height	Height%
1	4,890	5115941	36,995	168885	27,881
2	5,605	3948656	28,554	166840	27,544
3	9,695	4764290	34,452	270002	44,575
Total		13828887	100,000	605727	100,000

2	Product **10b** Amine **8b** => conversion 45%	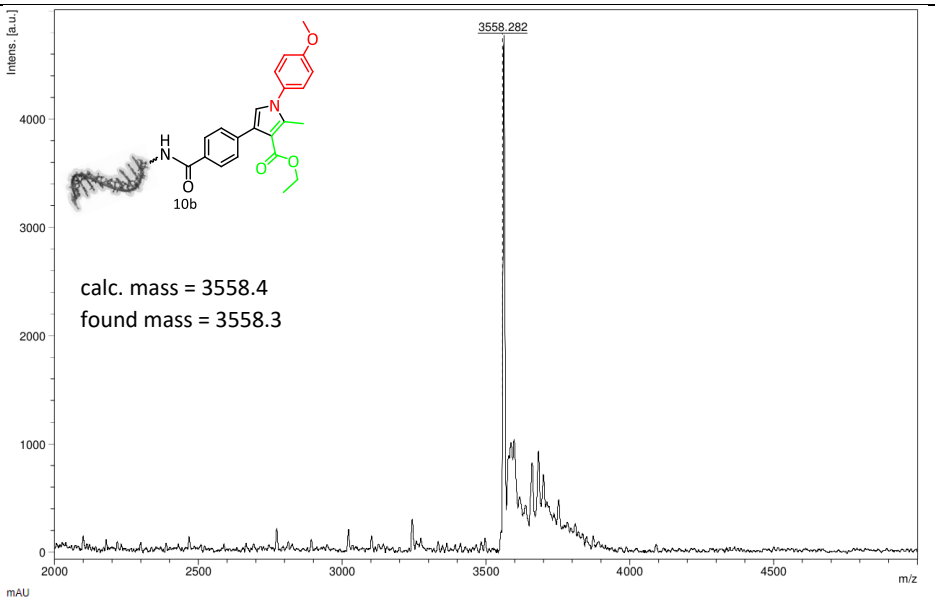 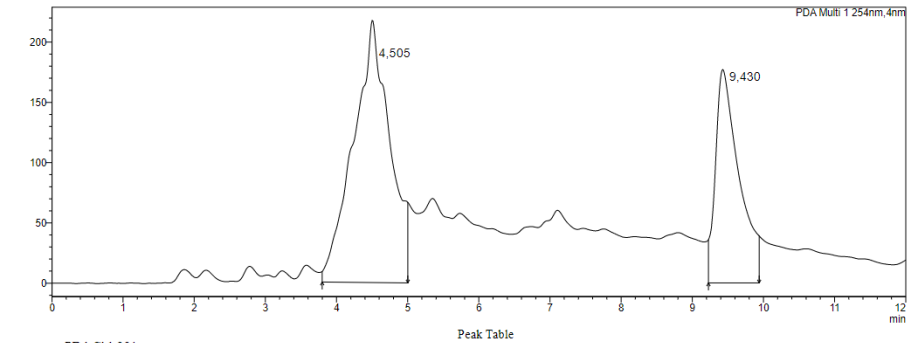 Peak Table PDA Ch1 254nm

Peak#	Ret. Time	Area	Area%	Height	Height%
1	4,505	7744353	65,533	217439	55,114
2	9,430	4073106	34,467	177083	44,886
Total		11817459	100,000	394522	100,000

3	Product **10c** Amine **8c** => conversion 0%	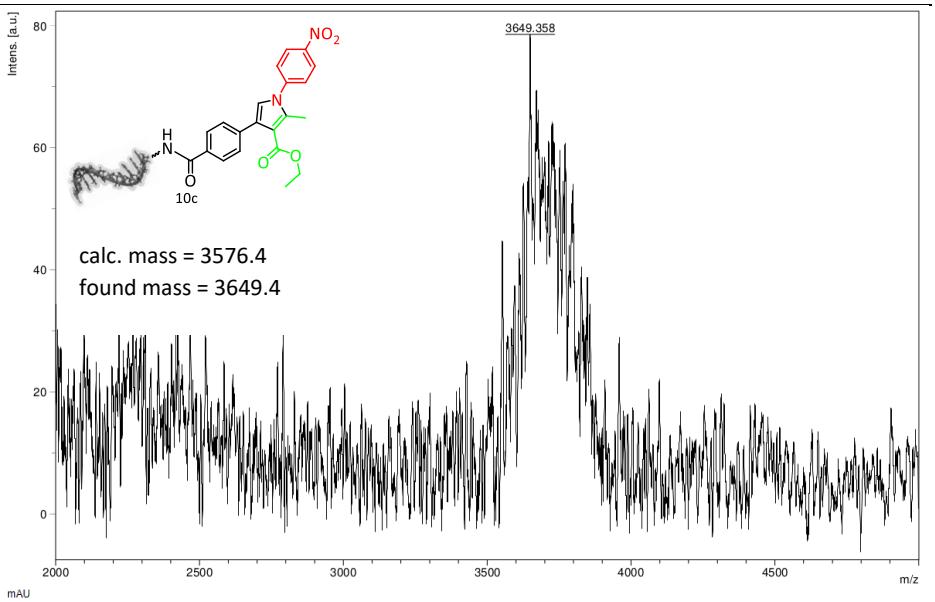 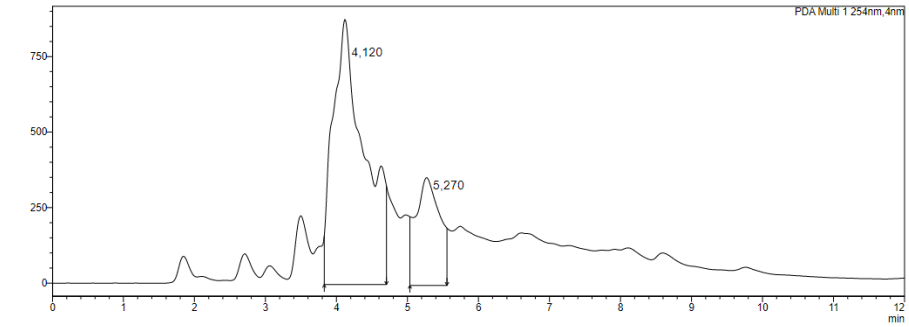 Peak Table PDA Ch1 254nm

Peak#	Ret. Time	Area	Area%	Height	Height%
1	4,120	26955094	76,241	877160	71,078
2	5,270	8400238	23,759	356928	28,922
Total		35355331	100,000	1234089	100,000

4	Product **10d** Amine **8d** => conversion 0%	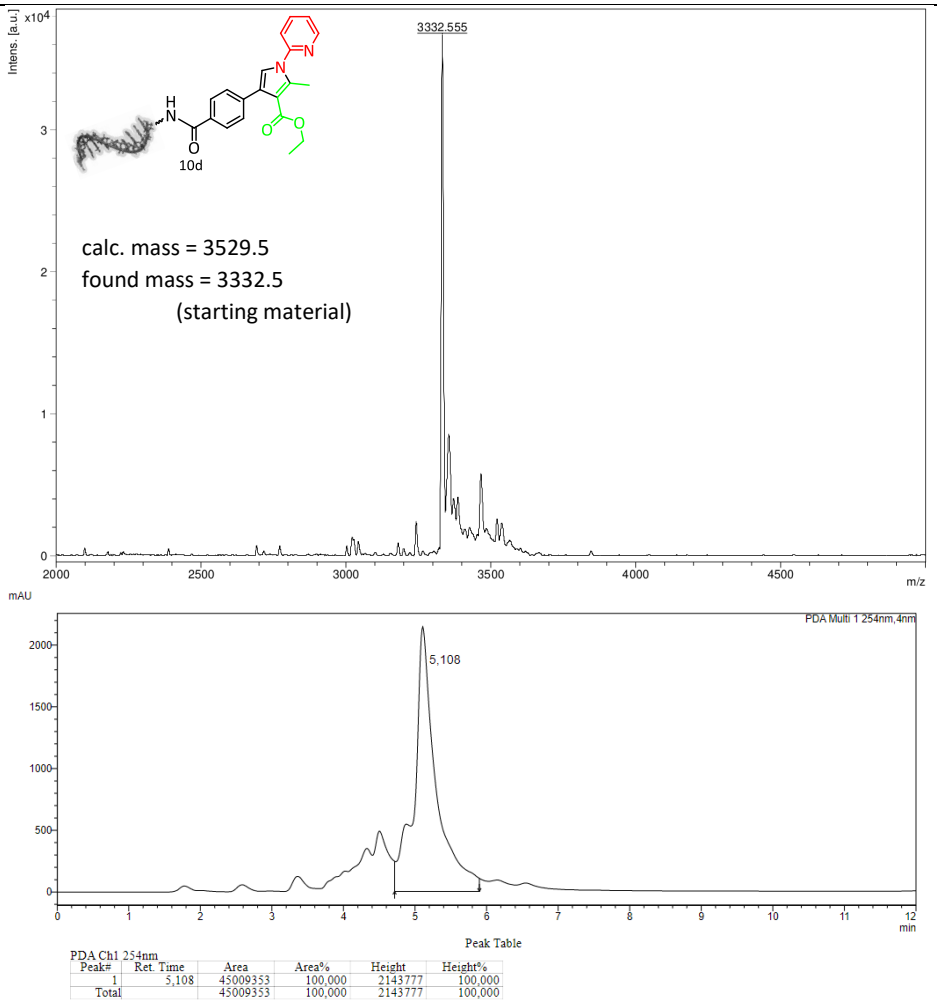 Peak Table PDA Ch1 254nm Peak# | Ret. Time | Area | Area% | Height | Height% 1 | 5,108 | 45009353 | 100,000 | 2143777 | 100,000 Total | | 45009353 | 100,000 | 2143777 | 100,000

5	Product **10e** Amine **8e** => conversion 0%	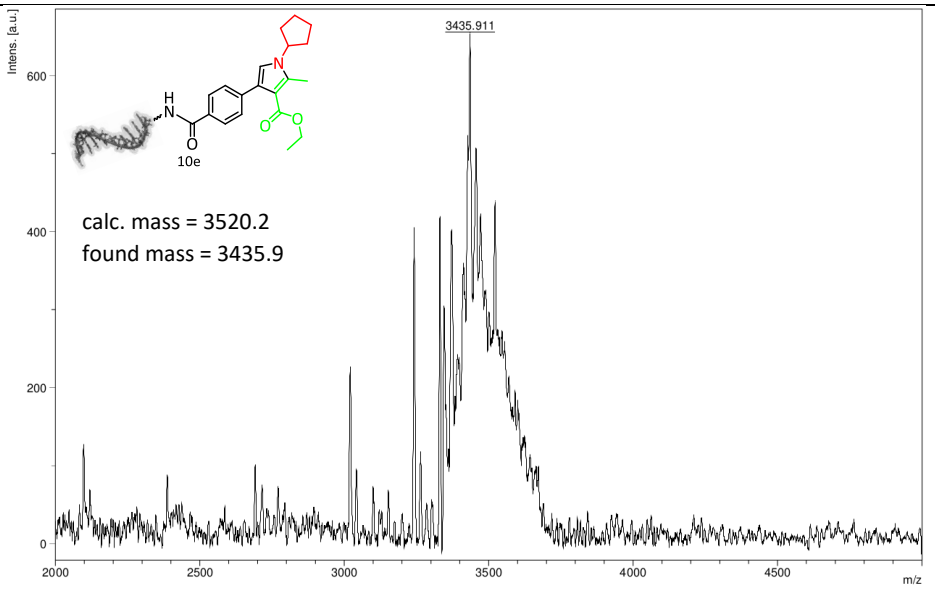 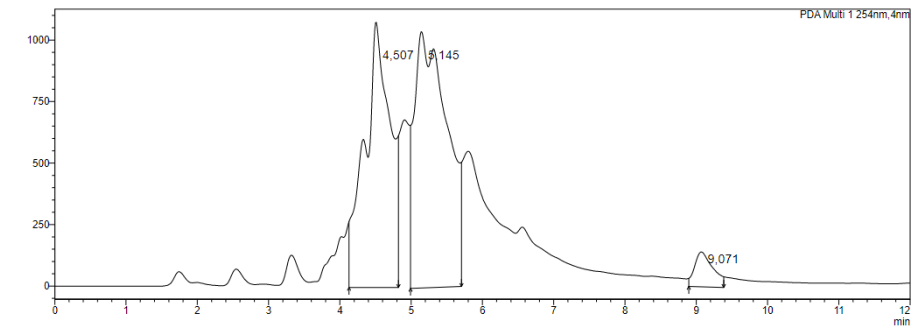 Peak Table PDA Ch1 254nm

Peak#	Ret. Time	Area	Area%	Height	Height%
1	4.507	27007875	43.020	1077464	47.653
2	5.145	33218450	52.912	1041784	46.075
3	9.071	2553931	4.068	141800	6.271
Total		62780256	100.000	2261049	100.000

[a] The suspension of DNA-aldehyde conjugate **7** (20 nmol), benzylamine **8** (250 mM), ethylcetoacetate **9** (250 mM) and $FeCl_3$ (25 mM) in $MeNO_2$ (40 µL) was shaken at 80°C for 6 h. DNA cleavage with 32% aq. Ammonia solution at ambient temperature for 4 h. [b] Determined by RP-HPLC II analysis based on the ratios of **7** to **10**. $MeNO_2$ = nitromethane. N.d. = not detected, 10mer ATGC = 5'-NH_2-C_6-GTCATGATCT-3'-CPG.

Pyrrolidine synthesis

Table S16. Test reaction for pyrrolidine synthesis on a CPG-bound pyrimidine DNA-amine conjugate **11**.[a]

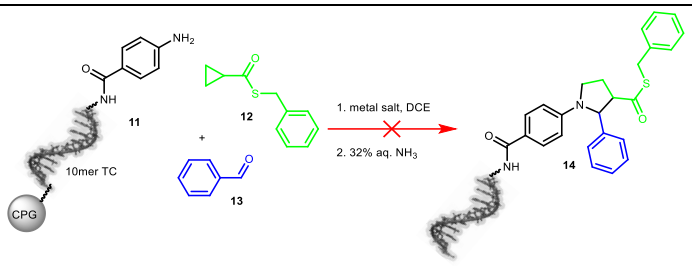

Entry	Metal salt	Conversion[b]	Identified side product[b]
1	Et_2AlI	n.d.	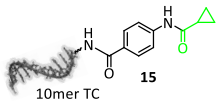
2	MgI_2	n.d.	

[a] The suspension of DNA-aldehyde conjugate **11** (20 nmol), thioester **12** (200 mM) and benzaldehyde **13** (200 mM) and metal salt (200 mM) in DCE (40 µL) was shaken at ambient temperature for 1 h. DNA cleavage with 32% aq. ammonia solution at ambient temperature for 30 min. [b] Determined by MALDI-TOF analysis, DCE = dichloroethane. n.d. = not detected, 10mer TC = 5'-TTC CTC TCC T-3'-CPG.

DNA conjugate 11: CPG-bound 10mer ATCG-$(CH_2)_6$-NH_2 conjugate was reacted with 4-amino-benzoic acid according to **RP-01**. HPLC trace of crude reaction mixture **11** (Analytical RP-HPLC II).

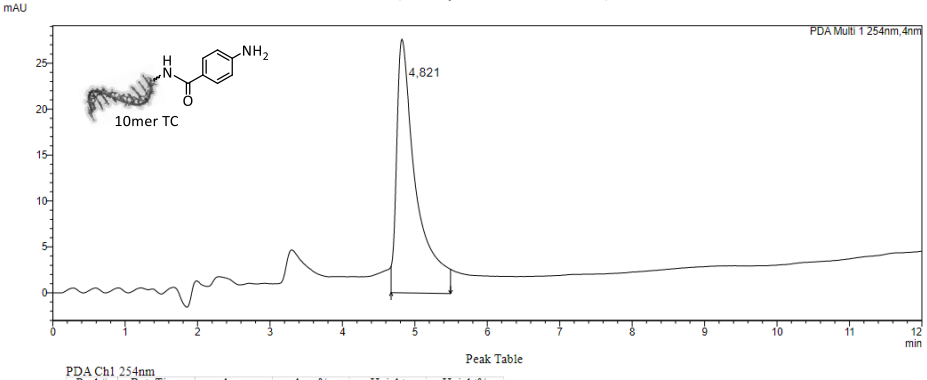

PDA Ch1 254nm

Peak#	Ret. Time	Area	Area%	Height	Height%
1	4,821	512866	100,000	27610	100,000
Total		512866	100,000	27610	100,000

MALDI-MS spectrum of crude reaction mixture 11

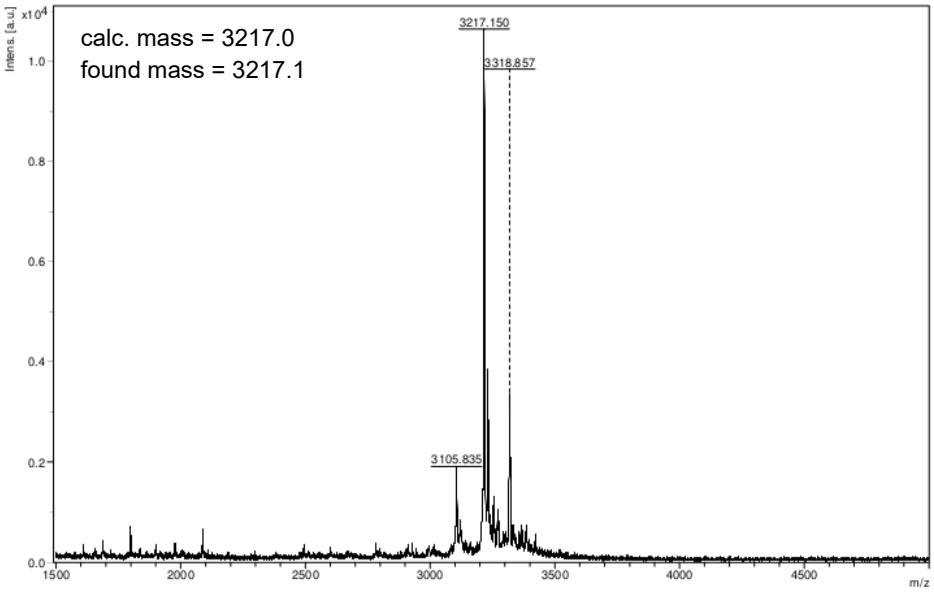

Table S17. Test reaction for pyrrolidine synthesis on a CPG-bound pyrimidine DNA-amine conjugate **11**.[a]

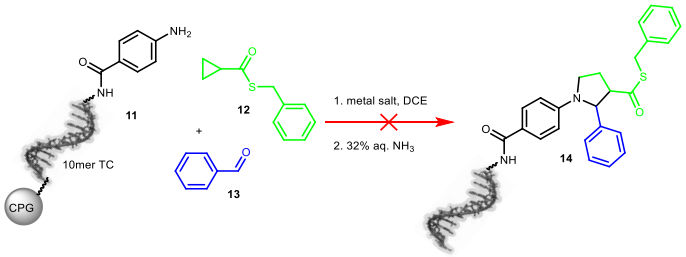

Entry	Reaction conditions	MALDI spectrum of the crude reaction mixture
1	thioester **12** (200 mM) benzaldehyde **13** (200 mM) *Et₂AlI* (200 mM) => conversion n.d.[b]	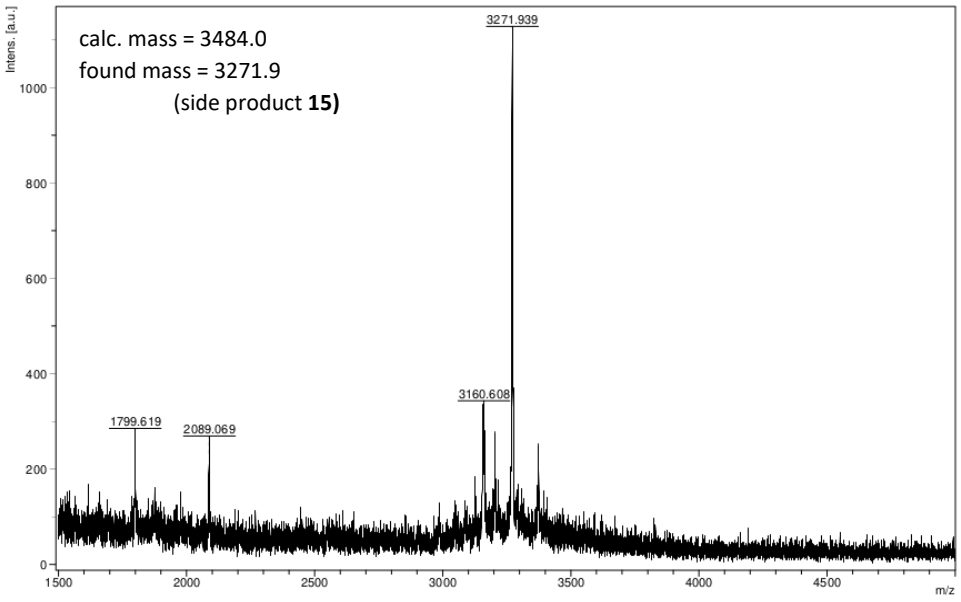

2	thioester **12** (200 mM) benzaldehyde **13** (200 mM) *MgI_2* (200 mM) => conversion n.d.[b]	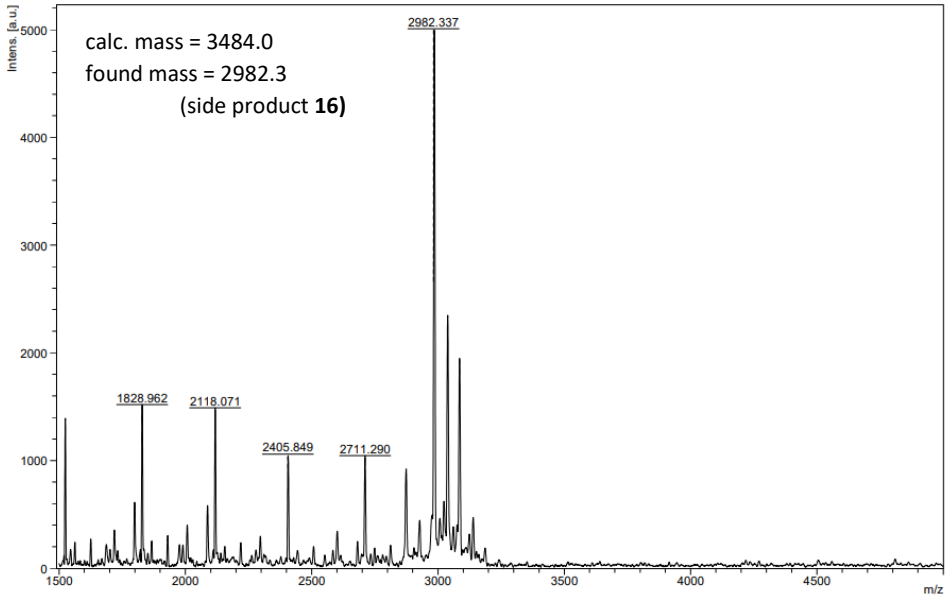

a The suspension of DNA-aldehyde conjugate 11 (20 nmol), thioester 12 (200 mM) and benzaldehyde 13 (200 mM) and metal salt (200 mM) in DCE (40 µL) was shaken at ambient temperature for 1 h. DNA cleavage with 32% aq. ammonia solution at ambient temperature for 30 min. [b] Determined by MALDI-TOF analysis, DCE = dichloroethane. n.d. = not detected, 10mer TC = 5'-TTC CTC TCC T-3'-CPG, changed parameters are written in red and italic.

Adaptability of the *Reaction Navigator*

The workflow was applied to different data sets to test its versatility.

Application to solution-phase strategies

At first, the filtering cascade was modified according to the solution phase strategy, which involve water and water-soluble solvents. This application requires reactions that are tolerant to water or use water as solvent. Therefore, this filter was applied to the "Solvent XRN" column by using the respective Reaxys ID as pattern in the *Row Filter* node. The number of reactions drastically dropped from 44,000 to 4,000, highlighting that such reactions are rare in the organic chemistry landscape. The *Reaction Navigator* was applied to the 4,000 reactions and the remaining 1,900 reactions were clustered, as depicted by the chemical reaction space in Figure S24.[S36]

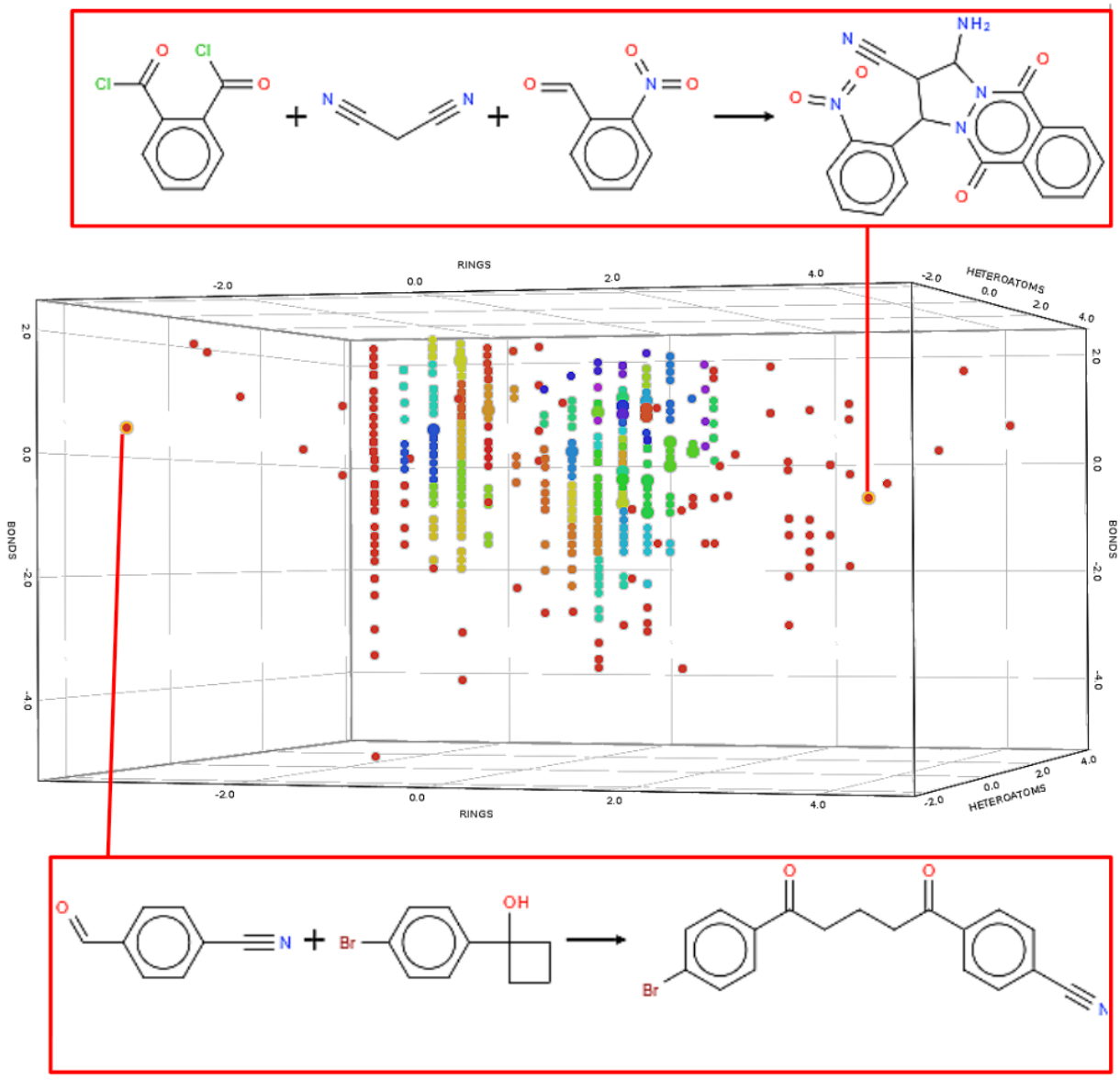

Fig. S24. Chemical reaction space for reactions starting with aldehydes and involving water as solvent in the Reaxys database. Two examples are reported in the boxes coloured according to the respective cluster.

Application to reaction starting with primary amines

For adapting the workflow to the Reaxys data set of primary amines, few changes were necessary. Firstly, reactions in which the amine functionality was part of an amide or amidine group were excluded because their reactivity would greatly change. The reactants were split via a *Cell Splitter* node and each reactant was processed by a *Column List Loop Start* node, converted in

SMILES via a *Molecule Type Cast* node and submitted to substructure search with a *MarvinSketch* node and the *RDKit Substructure Counter* node. The following SMARTS patterns were utilized as substructures: [#6][#6](=,:[#7])-[#7]([H])[H], [H][#7]([H])-[#6]=O, [H][#7]([H])-[#6], [#7][#6](=,:[#7])-[#7]([H])[H]. This combination of node was functional for counting the substructures and then subtract the amines from the undesired functionalities. At first, a *Rule-based Row Splitter* distinguished reactions where multiple amino groups were present in the same reactants or in two or more different ones. This distinction was necessary to differentiate between bifunctional reactants that could be necessary to the reaction, and scenarios in which more reactants show the same functional group, which is not acceptable in a combinatorial library asset. These two data sets were neamed differently via two *Constant Value Column* nodes. The number of identified amino group was summed up for all reactants, via a *Column Aggregator* node, as well as the number of amines. The "iteration" columns deriving from the loop were removed via a *Column Splitter* node and the difference was calculated with a *Math Formula* node with the following expression: *"$Sum_amides_amidines$-Sum_amines*". The reactions for which this difference was null were excluded by a *Row Splitter* because it would mean that the number of amines identified with the number of undesired functionality. The rest of the reactions was filtered by a *Rule-based Row Splitter* with the following expression: *"$amines$ = "mono" OR ($amines$ = "multi" AND $amides_amidine-amines$ = -1) => TRUE".* In this expression, "mono" indicates amines on the same reactant and "multi" amines on two different reactants. The result includes reactions wherein either the amines belong to the same reactants or, if not, the number of amines must be bigger by one unit than the number of undesired functionalities. With such procedure, approximately 1,000 reactions were excluded, the remaining reactions were submitted to the rest of the workflow and the resulting chemical reactions space with examples is depicted in Figure S25.[37,38,39]

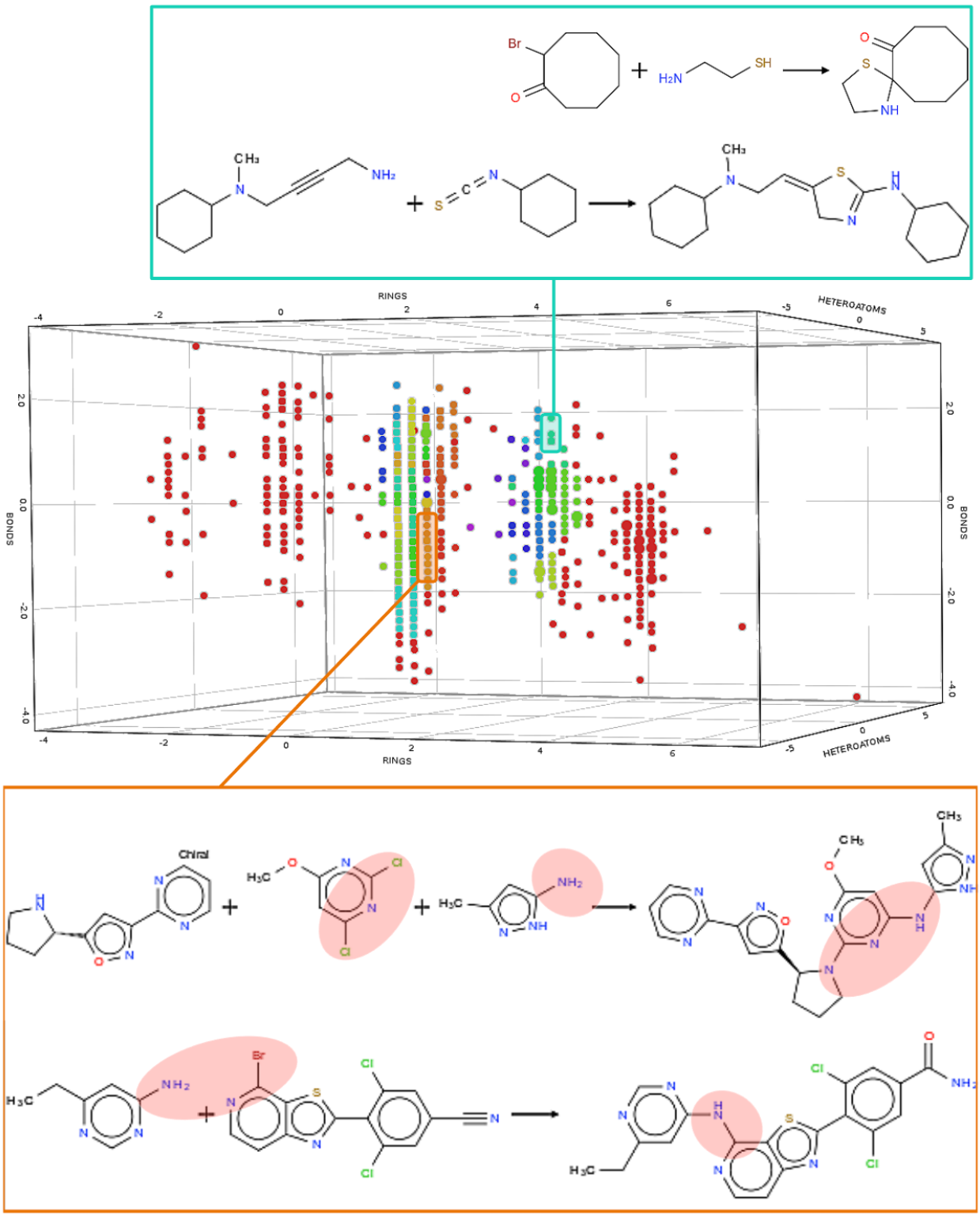

Fig. 25. Chemical reaction space for reactions starting with primary amines in the Reaxys database. Four examples from two clusters are reported in the boxes coloured according to the respective cluster and the reaction cores are highlighted in red.

Application to the USPTO database

Two samples of 10,000 reactions starting with aldehydes and primary amines were extracted from the database of US patents compiled in SMILES format by Daniel Lowe. [5] Some parts of the workflow were slightly modified for adaptability, while the filtering by conditions step was skipped due to the insufficient organization of the data in this data set. Two nodes were added to the *Reaction Navigator* to handle this data set: a *Cell Splitter* to divide the reaction SMILES from the US patent, and a *Molecule Type Cast* node for converting strings into SMILES. Such data was submitted to the rest of the workflow taking care of splitting them by functional group with the *RDKit Functional Group Filter* node and sampling them via the *Row Sampling* node. An additional step was necessary in this case, namely the extraction of the patent number in order to easily identify the reactions at the end of the workflow. For this a *String Manipulation* node was employed with the expression: "*substr($ReactionSmiles PatentNumber ParagraphNum Year TextMinedYield CalculatedYield_Arr[1]$,0 ,23)*". The species above the arrows were eliminated by redrawing the reaction schemes with another *String Manipulation* node with the following expression: "*join($reactants$, ">>", $products$)*". After converting the string to SMILES with a *Molecule Type Cast* node, the rest of the workflow was applied unchanged. The leaving group treatment confirmed to be the bottle neck of the procedure, reducing the drastically the number of reactions. At the end, 1445 reactions starting with aldehydes (15% of the initial sample) and 995 reactions starting with primary amine (10% of the initial sample) were clustered, showing the scatter plots in Figure S25 and S27.

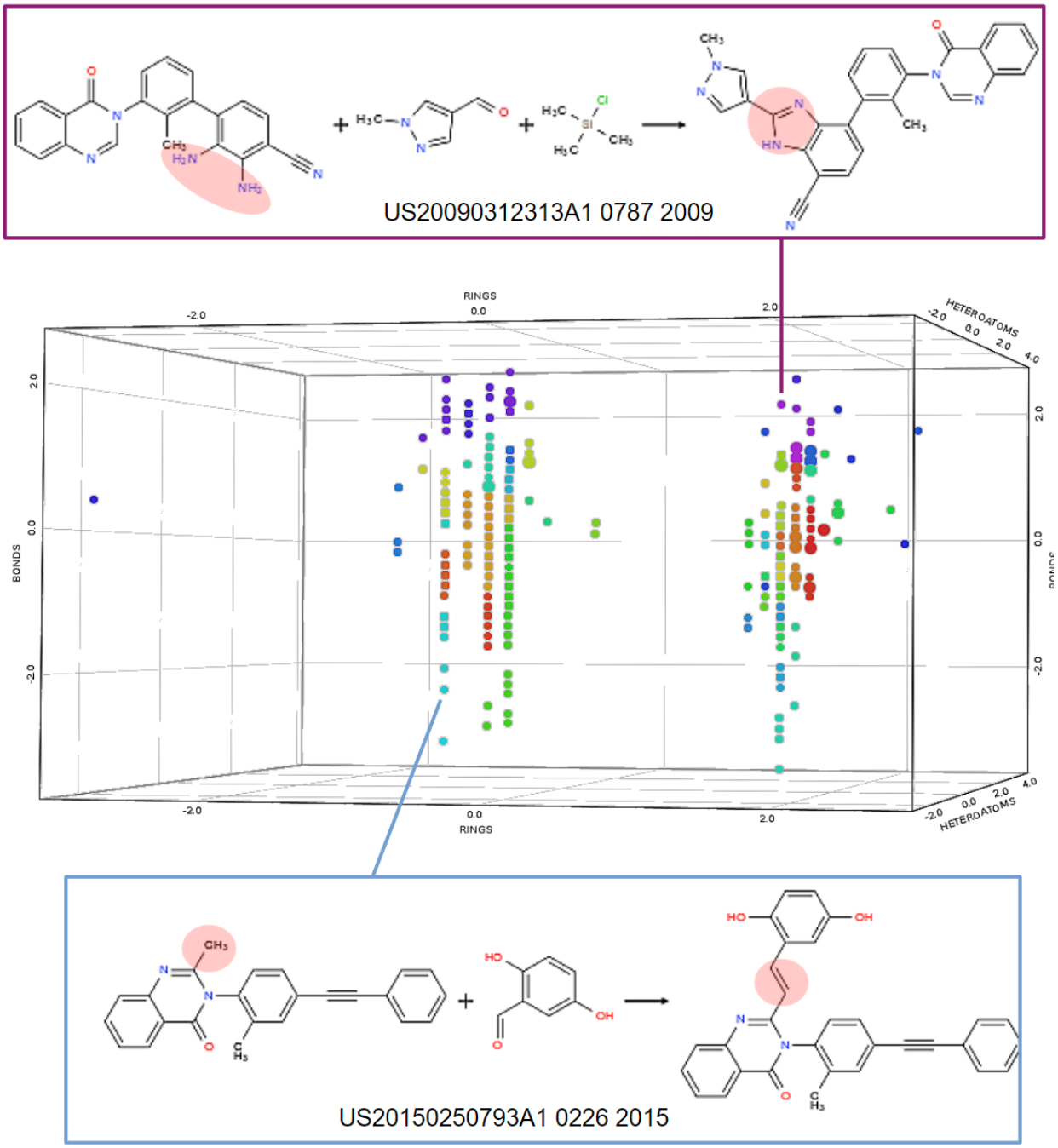

Fig. 26. Chemical reaction space for reactions starting with aldehyde in the USPTO database. Two examples are reported in the boxes coloured according to the respective cluster together with the patent number.

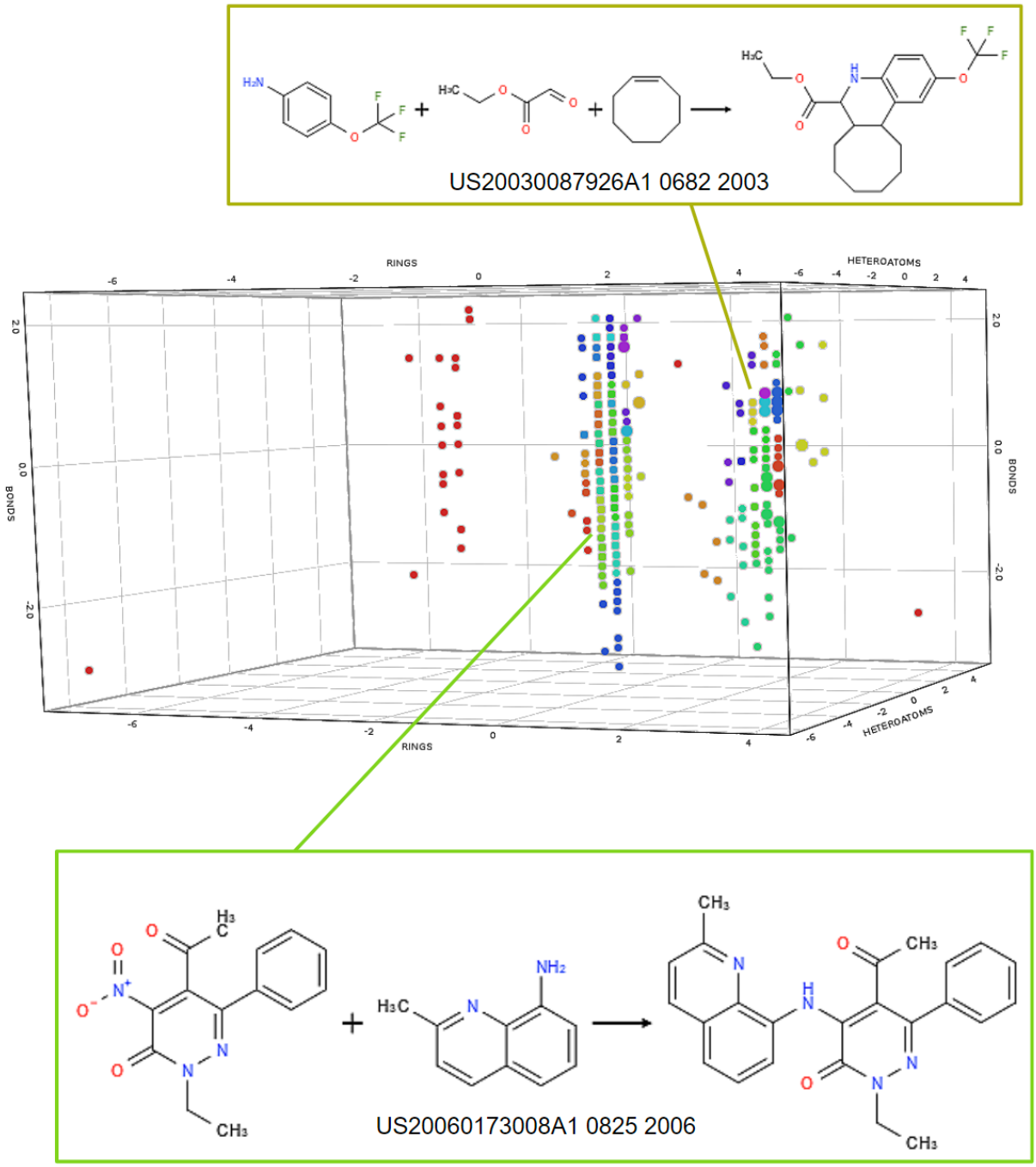

Fig. 27. Chemical reaction space for reactions starting with primary amines in the USPTO database. Two examples are reported in the boxes coloured according to the respective cluster together with the patent number.

References

S1 S. Touil and E. Chebil, *HETEROCYCLES*, 2012, **85**, 2765.
S2 P. Gunasekaran, S. Indumathi and S. Perumal, *RSC Adv.*, 2013, **3**, 8318.
S3 X.-Y. Chen, J.-W. Xiong, Q. Liu, S. Li, H. Sheng, C. von Essen, K. Rissanen and D. Enders, *Angew. Chem. Int. Ed.*, 2018**, 57**, 300–304.
S4 S. Kumari, R. Singh and R. Walia, *Orient. J. Chem*, 2014, **30**, 1293–1302.
S5 Suchand and G. Satyanarayana, *Eur. J. Org. Chem.*, 2018, **19**, 2233–2246.
S6 WO2003/105237 (2003).
S7 T.-S. Jin, G.-Y. Du, Z.-H. Zhang and T.-S. Li, *Synt. Commun.,* 1997, **27**, 2261–2266.
S8 H. Park, J. Choi, M. Kim, S. Choi, M. Park, J. Lee, Y.-G. Suh, H. Cho, U. Oh, H.-D. Kim, Y. H. Joo, S. S. Shin, J. K. Kim, Y. S. Jeong, H.-J. Koh, Y.-H. Park and S. Jew, *Bioorganic Med. Chem. Lett.*, 2005, **15**, 631–634.
S9 M. Hajimohammadi, Z. Ahmadi Khamesi and P. Nosrati, *Transit. Met. Chem.*, 2019, **44**, 167–173.
S10 R. Radhakrishnan, A. Demurov, H. Herzog and B. L. Trout, *Energy Convers. Manag.*, 2003, **44**, 771–780.
S11 R. Karimi and A. Khodadadi, *Tetrahedron Lett.,* 2012, **53**, 5223–5226.
S12 Pérez, N. Gimeno, F. Vera, M. B. Ros, J. L. Serrano and M. R. De la Fuente, *Eur. J. Org. Chem.*, 2008, **5**, 826–833.
S13 J. B. Bharate, S. B. Bharate and R. A. Vishwakarma, *ACS Comb. Sci.*, 2014, **16**, 624–630.
S14 J. Illesinghe, E. M. Campi, W. R. Jackson and A. J. Robinson, *Aust. J. Chem.*, 2004, **57**, 531.
S15 Roy, E. Das, A. Roy and D. Mal, *Org. Biomol. Chem.*, 2020, **18**, 3697–3706.
S16 M. Potowski, F. Losch, E. Wünnemann, J. K. Dahmen, S. Chines, A. Brunschweiger, *Chem. Sci.*, 2019, 10, 10481-10492.
S17 M. Klika Škopic, K. Götte, C. Gramse, M. Dieter, S. Pospich, S. Raunser, R. Weberskirch, A. Brunschweiger, *J. Am. Chem. Soc.,* 2019, 141, 26, 10546-10555.
S18 M. Klika-Škopić, F. Losch, A.E. McMillan, N. Willeke, M. Malenica, L. Bering, J. Bode, A. Brunschweiger, *Org. Lett.*, 2022, 24(6), 1383-1387.
S19 V. B. K. Kunig, C. Ehrt, A. Dömling, A. Brunschweiger, *Org. Lett.* ,2019, 21, 7238-7243.
S20 M. Potowski, R. Lüttig, A. Vakalopoulos, A. Brunschweiger, *Org. Lett.* ,2021, 23, 5480–5484.
S21 M. Klika Škopic, H. Salamon, O. Bugain, K. Jung, A. Gohla, L. J. Doetsch, D. dos Santos, A. Bhat, B. Wagner, A. Brunschweiger, *Chem. Sci.* , 2017, 8, 3356-3361.
S22 M. Potowski, V. B. K. Kunig, F. Losch, A. Brunschweiger, *Med. Chem. Commun.*, 2019, 10, 1082-1093.
S23 M. Potowski, R. Esken, A. Brunschweiger, *Bioorg. Med. Chem.,* 2020, 28, 115441.
S24 RDKit: Open-source cheminformatics; http://www.rdkit.org.
S25 E.L. Willighagen, J.W. Mayfield, J. Alvarsson, J. et al. *J Cheminform.* 2017,**9**, 33.
S26 Indigo toolkit, GGA Software Services, http://ggasoftware.com/.
S27 S. Steenken, S.V. Jovanovic, *J. Am. Chem. Soc.*, 1997, **119**(3), 617-618.
S28 N. Wongsa, U. Sommart, T. Ritthiwigrom, A. Yazici, S. Kanokmedhakul, K. Kanokmedhakul, A. C. Willis and S. G. Pyne, *J. Org. Chem.*, 2013, **78**, 1138–1148.
S29 Franche, C. Imbs, A. Fayeulle, F. Merlier, M. Billamboz and E. Léonard, *Chinese Chemical Letters*, 2020, **31**, 706–710.
S30 R. Ćwiek, P. Niedziejko and Z. Kałuża, *J. Org. Chem.*, 2014, **79**, 1222–1234.
S31 J. Wu, Y. Peng, B. Ouyang, J. Yuan, Q. Yang and Q. Ding, *HETEROCYCLES*, 2010, **82**, 1239.
S32 M. Shekouhy and A. Khalafi-Nezhad, *Green Chem.*, 2015, **17**, 4815–4829.
S33 R. Kordnezhadian, M. Shekouhy, S. Karimian and A. Khalafi-Nezhad, J. *Catal.*, 2019, **380**, 91–107.
S34 B. T. Golding, P. K. Slaich, G. Kennedy, C. Bleasdale and W. P. Watson, *Chem. Res. Toxicol.,* 1996, **9**, 147–157.
S35 M. Sako and I. Yaekura, *Tetrahedron*, 2002, **58**, 8413–8416.
S36 C. Che, Z. Qian, M. Wu, Y. Zhao and G. Zhu, *J. Org. Chem.*, 2018, **83**, 5665–5673.
S37 C. V. Kumar, S. Kavitake, S. S. Kumar, P. Cornwall, M. Ashok, S. Bhagat, S. G. Manjunatha and S. Nambiar, *Org. Process Res. Dev.*, 2012, **16**, 1416–1421.
S38 M. Matsushita, T. T. Takahashi, T. Utsukihara, Y. Shimizu, R. J. Jansen and C. A. Horiuchi, *Tetrahedron*, 2007, **63**, 8932–8938.
S39 J. Maffrand, D. Frehel, F. Eloy, D. Aubert, J. Ferrand, Europ. J. Med. Chem. 1975, 10(5), 528-532.
S40 D. Lowe, 2017.

KNIME Report I - manually scored mediators

Knime report *powered by Birt*

"column1"	"Min*(Score)"
potentially damaging the DNA	0
unknown (to be tested)	1
probably compatible with DNA	2
proven to be compatible	3
((R)-2,2'-bis(3,5-tBu2-2-HO-C6H2CH=N)-1,1'-binaphthyl)AlCl]	3
((S)-(PhCH(Me))N=C(Me)(Rp-OH[2,2-paracyclophane])	1
((S)-(PhCH(Me))N=C(Phe)(Rp-OH[2,2-paracyclophane])	1
(+)-(1S)-camphor-10-sulphonic acid	3
(+)-(3,2,10-eta-pinene)palladium(II) chloride	0
(+)-1-t-Bu-2-TsO-2H-[1,2]azaborolyl*(CO)2*Me3Si*iron	0
(+)-diisopinocampheylboron triflate	3
(+/-)-MIB	2
(-)-1,2-bis((2R,5R)-2,5-dimethylphospholano)benzene	2
(-)-MIB	2
(-)-N-methylephedrine	1
(-)-diisopinocampheylboron triflate	3
(-)-sparteine	1
(1,1'-bis(diphenylphosphino)ferrocene)palladium(II) dichloride	0
(1,2-bis(diphenylphosphanyl)ethane)dichloridopalladium(II)	0
(1,2-dimethoxyethane)dichloronickel(II)	3
(1,3-dimesitylimidazol-2-ylidene)gold(I) chloride	3
(10,10-dimethyl-5-(pyridin-2-yl)-6-azatricyclo[7.1.1.02,7]undeca-2(7),3,5-trien-8-yl)diphenylmethanol	2
(11aR)-(+)-10,11,12,13-tetrahydrodiindeno[7,1-de:1',7'-fg][1,3,2]dioxaphosphocin-5-bis[(R)-1-phenylethyl]amine	1
(11bR)-2,6-di-9-phenanthrenyl-4-hydroxy-dinaphtho[2,1-d:1?,2?-f][1,3,2]-dioxaphosphepin-4-oxide	1
(1R)-1-[(1R)-1-[bis[3,5-bis(trifluoromethyl)-phenyl]phosphino]ethyl]-2-[2-]bis(4-methoxy-3,5-dimethyl-phenyl)phosphino]-phenyl]ferrocene	1
(1R)-3-di-(3,5-dimethylphenyl)phosphino-(4-diphenylphosphino-2,5-dimethylthienyl-3)-1,7,7-trimethylbicyclo[2.2.1]heptene-2	2
(1R,2R)-2-[(diphenylphosphoroso)amino]-1,2-diphenylethyl](propan-2-yl)amine	1
(1R,2S)-(+)-2-(N,N-di-n-butylamino)-1-phenylpropan-1-ol	1
(1R,2S)-(-)-2-[N-(3?,5?-di-tert-butylsalicylidene)amino]-1,2-diphenylethanol	1
(1R,2S)-1-phenyl-2-(1-pyrrolidinyl)-1-propanol	2
(1R,2S)-2-(4-methylbenzenesulfonylamino)-1,3-diphenyl-1-propanol	2
(1R,2S)-2-Amino-1,2-diphenylethanol	1
(1S)-1-((S)-1-methylpropyl)-(2-morpholin-4-ylethyl)amine	3

"column1"	"Min*(Score)"
(1S)-10-camphorsulfonic acid	3
(1S,2R)-(+)-N-methylephedrine	1
(1S,2R)-(-)-2-(N,N-di-n-butylamino)-1-phenylpropan-1-ol	3
(1S,2R)-(-)-2-(N,N-di-n-propylamino)-1-phenylpropan-1-ol	3
(1S,2S)-2-N,N-dimethylamino-1-(p-nitrophenyl)-3-(tert-butyldimethylsilyloxy)propan-1-ol	1
(1S,2S,4S,5S)-N2,N2,N5,N5-tetramethylbicyclo[2.2.1]heptane-2,5-diamine	1
(2,7-dimethyl-1,8-biphenylenedioxy)bis(dimethoxyaluminum)	1
(2-hydroxy-ethyl)ammonium acetate	2
(2-methylpropyl)lithium	0
(2R)-(+)-3,3'-diphenyl-[2,2'-dinaphthalene]-1,1'-diol	1
(2R)-(+)-3-exo-N-morpholinoisoborneol	3
(2R,3R)-1,4-dioxaspiro[4.5]decane-alpha,alpha,alpha',alpha'-tetrakis(1-naphthyl)-2,3-dimethanol	3
(2R,3R)-4-dimethylamino-3-methyl-1,2-diphenyl-butan-2-ol	1
(2R,3R)-tartaric acid-derived bis-benzimidazole	3
(2R,3S,3aS,4aR,6R,8aS)-2-isopropyl-6,9,9-trimethyl-3-phenyldecahydro-4aH-pyrrolo[2,1-b][1,3]benzoxazin-3-ol	1
(2S)-(-)-3,3'-diphenyl-(2,2'-binaphthalene)-1,1'-diol	2
(2S)-(?)-3-exo-(morpholino)isoborneol	3
(2S)-2-{diphenyl[(trimethylsilyl)oxy]methyl}pyrrolidine	2
(2S)-N-(2-pyrrolidine-2-carbonyl)-benzenesulfonamide	2
(2S,3S)-2,3-bis(diphenylphosphino)butane	2
(2S,5R)-2-(methylaminomethyl)-1-methyl-5-phenylpyrrolidine	2
(3,5-dioxa-4-phospha-cyclohepta[2,1-a;3,4-a']di-naphthalen-4-yl)-bis-(1-phenyl-ethyl)-amine	1
(3S)-(+)-2,2'-diphenyl-(3,3'-biphenanthrene)-4,4'-diol	1
(3aR)-1-methyl-3,3-diphenyl-tetrahydro-pyrrolo[1,2-c][1,3,2]oxazaborole	1
(4R,4'R)-2,2'-(propane-2,2'diyl)bis(4-phenyl-4,5-dihydrooxazole)	1
(4R,5R)-2,2-dimethyl-alpha,alpha,alpha?,alpha?-tetra(naphthalen-1-yl)-1,3-dioxolane-4,5-dimethanol	3
(4R,5R)-2-bromo-1,3-bis[(4-methylphenyl)sulfonyl]-4,5-diphenyl-1,3,2-diazaborolidine	3
(4R,5R)-Ph2-1,3-Me2-2-oxo-2-(CH2)5N-1,3,2-diazaphospholidine	1
(4S)-Bn-3-(4-FPhSO2)-2-PhCH2CH2-[1,3,2]-oxazaborolidin-5-one	2
(4S,4'S)-2,2'-(3,6-diphenyl-9H-carbazole-1,8-diyl)bis(4-methyl-4,5-dihydrooxazole)	1
(4S,4'S)-2,2'-(4-chloropyridine-2,6-diyl)bis(4-tert-butyl-4,5-dihydrooxazole)	3
(4S,4S')-(-)-2,2'-(1-methylethylidene)bis[4,5-dihydro-4-(phenylmethyl)oxazole]	1
(4S,5S)-1,3-dimethyl-4,5-diphenyl-2-(1-piperidinyl)-1,3,2-diazaphospholidine 2-oxide	0
(4S,5S)-2-bromo-1,3-bis[(4-methylphenyl)sulfonyl]-4,5-diphenyl-1,3,2-diazaborolidine	3

"column1"	"Min*(Score)"
(5S)-5-benzyl-2,2,3-trimethylimidazolidin-4-one trifluoroacetic acid salt	3
(5aR,10bS)-2-mesityl-5a,10b-dihydro-4H,6H-indeno[2,1-b][1,2,4]triazolo[4,3-d][1,4]oxazin-2-ium tetrafluoroborate	0
(5aS,10bR)-5a,10b-dihydro-2-(2,4,6-trimethylphenyl)-4H,6H-indeno[2,1-b]-1,2,4-triazolo[4,3-d]-1,4-oxazinium chloride	1
(6,8,15,17-tetramethyldibenzo[b,i][1,4,8,11]-tetraazacyclo-tetradecinato)nickel(II)	3
(C2H5)2AlSnClF2	0
(E)-1,1-bis(3,5-dimethylphenyl)-N-(pyridin-2-yl-methylene)methanamine iron(II) chloride dichloromethane solvate	3
(E)-diazene-1,2-diylbis(cyclohexylmethanone)	1
(IPr)Au(NTf2)	0
(R)-((4,4?-bi-1,3-benzodioxole)-5,5?-diyl)bis(bis(3,5-di-t-butyl-4-methoxyphenyl))phosphine	1
(R)-(-)-3,3?-bis(3,5-diphenylphenyl)-1,1?-binaphthalene-2,2?-sulfonimide	2
(R)-(3,3'-bis(1-naphthyl)-1,1'-binaphthanele-2,2'-yl)phosphoric acid	2
(R)-(?)-1-[(R)-2-(2?-diphenylphosphinophenyl)ferrocenyl]ethylbis(di-3,5-trifluoromethylphenyl)phosphine	2
(R)-1,1'-Bi-2-naphthol	0
(R)-1,1'-binaphthalene-2,2'-diol lithium salt	1
(R)-1,1'-binaphthyl-2,2'-phosphoric acid	3
(R)-1-{(RFc)-2-[2-(diphenylphosphino)phenyl]ferrocenyl} ethylbis[3,5-bis-(trifluoromethyl)phenyl]phosphine	2
(R)-10-camphorsulfonic acid	3
(R)-2,2'-bis(diphenylphosphanyl)-1,1'-binaphthyl	3
(R)-2,2'-bis[bis(3-methylphenyl)phosphino]-1,1'-binaphthyl	3
(R)-2,2'-dihydroxy-1,1'-binaphthyl	3
(R)-2,2?-diphenyl-(4-biphenanthrol)	3
(R)-2,6-bis(naphthalen-2-yl)-4-oxo-3,5-dioxa-4lambda5-phosphacyclohepta[2,1-a;3,4-a']dinapthalen-4-ol	1
(R)-2-(diphenyl(trimethylsilyloxy)methyl)pyrrolidine	2
(R)-2-methyl-1-(2-(3,3-dimethylbut-1-ynyl)pyrimidin-5-yl)propan-1-ol	2
(R)-3,3',6,6'-tetraiodo-1,1'-binaphthalene-2,2'-diol	2
(R)-3,3'-bis(2,4,6-triisopropylphenyl)-1,1'-binaphthyl-2,2'-diylhydrogenphosphate	3
(R)-3,3'-bis(2,4,6-triisopropylphenyl)binol phosphoric acid	3
(R)-3,3'-bis(4-trifluoromethylphenyl)-1,1'-binaphthyl-2,2'-diylphosphoric acid	3
(R)-3,3'-bis(9-anthracenyl)-1,1'-binaphthyl-2,2'-diyl hydrogenphosphate	3
(R)-3,3'-bis(dimethylphenylsilyl)-1,1'-binaphthyl-2,2'-dicarboxylic acid	3
(R)-3,3'-bis(triphenylsilyl)-1,1'-bi-naphthyl-2,2'-diyl	3

"column1"	"Min*(Score)"
(R)-3,3'-di(anthracen-9-yl)-5,5',6,6',7,7',8,8'-octahydro-[1,1'-binaphthalene]-2,2'-diyl hydrogen phosphate	2
(R)-3,3'-dibromo-1,1'-bi-2-naphthol	0
(R)-3,3'-dichloro-1,1'-binaphthalene-2,2'-diol lithium salt	1
(R)-3,3'-diiodo-2,2'-dihydroxy-1,1'-binaphthyl	3
(R)-3,3?-bis(2,4,6-triisopropylphenyl)-BINOL-phosphoric acid	0
(R)-3,3?-difluoro-1,1'-bi-2-naphthol	0
(R)-3-(3,5-diphenylphenyl)-2,2'-dihydroxy-5,5',6,6',7,7',8,8'-octahydro-1,1'-binaphthyl	3
(R)-3-diphenylhydroxymethyl-2,2'-dihydroxy-1,1'-bi-naphthalenyl	2
(R)-BINAPHANE	1
(R)-DHTP	2
(R)-SEGPHOS-I	0
(R)-methylaluminum beta-binaphthoxide	0
(R)-p-Tol-BINAP*AgF	0
(R)-segphos	0
(R)?2,2'?bis(diphenylphosphoryl)?1,1'?binaphthyl	3
(R,R')-N,N'-bis(5-tert-butyl-2-hydroxybenzylidene)-1,2-cyclohexanediamine	1
(R,R)-1,2-bis(2,5-diphenylphospholanyl)ethane	2
(R,R)-1,2-diphenylethandiol (2-methoxy)ethyldiether	1
(R,R)-N,N'-dimethylstilbene-1,2-diamine chiral phosphoramide	1
(R,R)-TADDOL	0
(R,R)-hydroxybenzoin	2
(R,R)-walphos	2
(R,S)-2-OH-3,5-Cl2-C6H2-SO2-NH-CH(CH2Ph)-CH(Ph)OH	1
(Ra)-5,6,7,8,5',6',7',8'-octahydro-[1,1']binaphthalenyl-2,2'-diol	2
(Ra)-N-[(1S,2R)-1,2-diphenyl-2-hydroxyethyl]-3,5-dihydro-4H-dinaphtho[2,1-c:1',2'-e]-azepine	2
(Re(CO)3(THF)Br)2	0
(RhCl(diene*))2	0
(S)-(-)-2,2'-dihydroxy-1,1'-binaphthalene	2
(S)-(-)-2,2'-dihydroxy-1,1'-binaphthyl	3
(S)-(1,1'-binaphthalene)-2,2'-diylbis(diphenylphosphine)	2
(S)-1,1'-binaphthalene-2,2'-diylbis(diphenylphosphineoxide)	2
(S)-1-methyl-2-(1-naphthylaminomethyl)pyrrolidine	2
(S)-2'-methoxy-2-methylthio-1,1'-binaphthalene	2
(S)-2,2',5,5'-tetramethyl-4,4'-bis-(diphenylphoshino)-3,3'-bithiophene oxide	1
(S)-2-(((tert-butyldimethylsilyl)oxy)diphenylmethyl)pyrrolidine	2
(S)-2-(1-pyrrolidinylmethyl)pyrrolidine	2
(S)-2-(diphenyl((triethylsilyl)oxy)methyl)pyrrolidine	2
(S)-2-[bis(3,5-bis(trifluoromethyl)phenyl)-triethyl-siloxy-methyl]-pyrrolidine	2
(S)-3,3'-bis(2,4,6-tri-iso-propylphenyl)-1,1'-bi-naphthyl-2,2'-diyl hydrogenphosphate	3

"column1"	"Min*(Score)"
(S)-3,3'-bis(4"-tert-butylphenyl)-2,2'-(2,2-bisbromo-2-stannopropane-1,3-diyl)-1,1'-binaphthyl	3
(S)-3,3'-diiodo-2,2'-dihydroxy-1,1'-binaphthyl	3
(S)-3,3'-dimethyl-[1, 1'-binaphthalene]-2, 2'-diol	2
(S)-3,3?-bis(9-anthracenyl)-1,1?-binaphthyl-2,2?-diyl N-triflyl-phosphoramide	3
(S)-3,5-dichloro-N-(6-(4-isopropyl-4,5-dihydrooxazol-2-yl)-2,3-dimethoxyphenyl)benzenesulfonamide	2
(S)-5-benzhydryl-2-(perfluorophenyl)-6,7-dihydro-5H-pyrrolo[2,1-c][1,2,4]triazol-2-ium tetrafluoroborate	0
(S)-5-benzyl-2-(2,6-dimethoxyphenyl)-6,6-dimethyl-6,8-dihydro-5H-[1,2,4]triazolo[3,4-c][1,4]oxazin-2-ium tetrafluoroborate	0
(S)-5-benzyl-2-mesityl-6,6-dimethyl-5,6-dihydro-8H-[1,2,4]triazolo[3,4-c][1,4]oxazin-2-ium tetrafluoroborate	0
(S)-6,6'-bis(2,4,6-triisopropylphenyl)-1,1'-spirobiindane-7,7'-diyl hydrogenphosphate	1
(S)-6,6'-di(naphthalen-1-yl)-1,1'-spirobiindane-7,7'-diyl phosphate	1
(S)-AlCl[2,2'-[O-3,5-(t-Bu)2-C6H2-CH=N)]2-1,1'-binaphthyl]	3
(S)-N-((3-methylpyridin-2-yl)carbamothioyl)pyrrolidine-2-carboxamide	3
(S)-[1,1'-binaphthalen]-2-yldiphenylphosphine	2
(S)-[1,1']-binaphthalenyl-2,2'-diol	2
(S)-bis(4-fluorophenyl)(1-methylpyrrolidin-2-yl)methanol	2
(S, S)-6,6?-bis(1-hydroxy-2,2-dimethylpropyl)-2,2?-bipyridine	2
(S,R)-N-PINAP	1
(S,S)-(+)-2,6-bis[2-(hydroxydiphenylmethyl)-1-pyrrolidinyl-methyl]-4-methylphenol	2
(S,S)-1,1'-(6,6',7,7'-tetrahydro-5H,5'H-[1,1'-bi(cyclo-penta[c]pyridine)]-3,3'-diyl)bis(2,2-dimethylpropan-1-ol)	3
(S,S)-2,2'-methylenebis(4-tert-butyl-2-oxazoline)	1
(S,S)-4-tBu-2,6-bis[2-(HOPh2C-)pyrazolidin-1-ylmethyl]phenol	1
(S,S)-Bn-bod	1
(carbonyl)chloro(hydrido)tris(triphenyl-phosphine)ruthenium(II)	0
(eta6-toluene)Ni(1,3-bis(2,6-diisopropylphenyl)imidazolin-2-ylidene)	3
(lIpc)2BH	1
(methyl benzoate)chromium tricarbonyl	0
(mu3,eta2,eta3,eta5-acenaphthylene)Ru3(CO)7	3
(o,o'-biphenylenedioxy)methylaluminium	0
(oxydi-2,1-phenylene)bis(diphenylphosphine)Pd(pi-allyl)Cl	0
(pi-allyl)palladium chloride	0
(polyallyl)scanduium trifylamide ditriflate	3
(tricyclohexylphosphine)gold(I) chloride	3
(triphenyl phosphite)gold(I) chloride	3
(triphenylphosphine)gold(I) chloride	3
(±)N,N?-bis(3,5-di-tert-butylsalicylidene)-1,2-cyclohexanediami nocobalt(II)	0
1,1'-(1,2-ethanediyl)bisbenzene	1

"column1"	"Min*(Score)"
1,1'-bi-2-naphthol	3
1,1'-binaphthyl-2,2'-diyl hydrogenphosphate	3
1,1'-biphenyl-2,2'-diyl hydrogen phosphate	1
1,1'-bis(di-tertbutylphosphino)ferrocene	1
1,1'-bis(dicyclohexylphosphinocyclopentadienyl iron	3
1,1'-bis(diisopropylphosphino)ferrocene	1
1,1'-bis-(diphenylphosphino)ferrocene	2
1,1'-carbonyldiimidazole	2
1,1,1,3',3',3'-hexafluoro-propanol	1
1,1,1,3,3,3-hexamethyl-disilazane	0
1,1,3,3-tetramethylguanidine	3
1,1-dicyclohexyl-N-(dicyclohexylphosphino)-N-methylphosphinamine	1
1,1-dimethoxyethane	1
1,10-Phenanthroline	1
1,1?-bi-2-naphthol	3
1,1?-binaphthalene-2,2?-diylbis[bis(4-methylphenyl) phosphine]	2
1,2,2,6,6-pentamethylpiperidine	3
1,2,3-Benzotriazole	3
1,2-bis(2,5-dimethylphospholano)benzene	2
1,2-bis(dimethylphosphanyl)ethane	1
1,2-bis(diphenylphosphino)ethane nickel(II) chloride	3
1,2-bis-(diphenylphosphino)ethane	2
1,2-bisethane	1
1,2-dichloro-ethane	3
1,2-dimethyl-3-[4-(1,2-dimethyl-1H-imidazol-3-ium-3-yl)butyl]-1H-imidazol-3-ium dibromide	3
1,3,4,6,7,8-hexahydro-2H-pyrimido[1,2-a]pyrimidine	2
1,3-bis(2,4,6-trimethylphenyl)-4,5-dihydro-imidazolium chloride	3
1,3-bis(2,6-(i-Pr)2-phenyl)-4,5-dihydroimidazolin-2-ylidene	3
1,3-bis(2,6-diethylphenyl)-1H-imidazol-3-ium chloride	1
1,3-bis(cyclohexyl)imidazolium tetrafluoroborate	0
1,3-bis(mesityl)imidazolium chloride	3
1,3-bis-(diphenylphosphino)propane	2
1,3-bis[2,6-diisopropylphenyl]imidazolium chloride	3
1,3-dibenzyl-1H-benzo[d]imidazol-3-ium chloride	1
1,3-dimethyl-2-imidazolidinone	3
1,3-dimethyl-3,4,5,6-tetrahydro-2(1H)pyrimidinone	2
1,3-dimethylimidazolim iodide	3
1,4-di(diphenylphosphino)-butane	2
1,4-diaminobutane	3
1,4-diaza-bicyclo[2.2.2]octane	1

"column1"	"Min*(Score)"
1,4-dimethyl-1,2,4-triazolium iodide	3
1,4-phenylenediacetic acid	3
1,5-diazabicyclo[5.4.0]-undec-7-ene	3
1,5-diazabicyclo[5.4.0]undecene	3
1,8-diazabicyclo[5.4.0]undec-7-ene	3
1-(2,6-diisopropylphenyl)-3-(2-(phenylthio)phenyl)-4,5-dihydroimidazolinium chloride	3
1-(3,5-Bis-trifluoromethyl-phenyl)-3-((1R,2R)-2-dimethylamino-cyclohexyl)-thiourea	2
1-(3,5-Bis-trifluoromethyl-phenyl)-3-[(S)-quinolin-4-yl-((2R,4S,5R)-5-vinyl-1-aza-bicyclo[2.2.2]oct-2-yl)-methyl]-thiourea	2
1-(3,5-bis(trifluoromethyl)phenyl)-3-((1R)-(6-meth-oxyquinolin-4-yl)(3-vinylquinuclidin-7-yl)methyl)urea	1
1-(3,5-bis(trifluoromethyl)phenyl)-3-((1R,2R)-2-(piperidin-1-yl)cyclohexyl)thiourea	2
1-(3,5-bis(trifluoromethyl)phenyl)-3-((1R,2R)-2-(pyrrolidin-1-yl)cyclohexyl)thiourea	2
1-(3,5-bis(trifluoromethyl)phenyl)-3-((1S)-(6-hydroxyquinolin-4-yl)((5R)-5-vinylquinuclidin-2-yl)methyl)thiourea	2
1-(3,5-bis(trifluoromethyl)phenyl)-3-((1S)-(6-meth-oxyquinolin-4-yl)(5-vinylquinuclidin-2-yl)methyl)thiourea	1
1-(3,5-bis(trifluoromethyl)phenyl)-3-((S)-(6-meth-oxyquinolin-4-yl)((2S,4S,8R)-8-vinylquinuclidin-2-yl)methyl)thiourea	1
1-(phenylsulfonyl)propyne	1
1-(tert-butoxycarbonyl)-L-proline	3
1-[3,5-bis(trifluoromethyl)phenyl]-3-[(1S,2S)-2-(dimethylamino)cyclohexyl]thiourea	2
1-[3,5-bis(trifluoromethyl)phenyl]-3-phenyl-2-thiourea	2
1-[bis(trifluoromethanesulfonyl)methyl]-2,3,4,5,6-pentafluorobenzene	1
1-acetoxy-1,2-benziodoxol-3-one	2
1-butyl-3-methylimidazolium Tetrafluoroborate	0
1-butyl-3-methylimidazolium hydroxide	0
1-fluoro-2,4,6-trimethylpyridin-1-ium tetrafluoroborate	0
1-hydrosilatrane	1
1-hydroxy-3H-benz[d][1,2]iodoxole-1,3-dione	1
1-methoxy-2-methyl-1-trimethylsiloxy-1-propene	1
1-methyl-1H-imidazole	3
1-methyl-2,3,4,6,7,8-hexahydro-1H-pyrimido[1,2-a]pyrimidine	2
1-methyl-3-(2,4,6-trimethylphenyl)-3H-benz-imidazol-1-ium iodide	3
1-methyl-3-(4-sulfobutyl)-1H-imidazol-3-ium hydrogensulfate	3
1-methyl-3-methylimidazol-3-ium dimethyl phosphate	1
1-methyl-piperazine	1
1-methyl-pyrrolidin-2-one	2
1-methylimidazole-3-sulfonic acid hydrochloride	3
1-n-butyl-3-methylimidazolim bromide	3
1-naphthalenesulfonic acid	0
1-pyrroline	2

"column1"	"Min*(Score)"
1-{3,5-bis(trifluoromethyl)phenyl}-3-{(1R,2R)-2-(dimethylamino)cyclohexyl}thiourea	2
1-{3,5-bis(trifluoromethyl)phenyl}-3-{(1R,2R)-2-(pyrrolidin-1-yl)cyclohexyl}urea	2
10 percent chiral ammonium fluoride	0
10 wt\% Pd(OH)2 on carbon	0
10-camphorsufonic acid	3
10-camphorsulfonic acid	3
10-methyl-9-(2,4,6-trimethylphenyl) acridinium tetrafluoroborate	0
10V/SiO2-25	3
15-crown-5	0
18-crown-6 ether	0
18O-labeled water	3
1H-imidazole	3
2,2'-bis(diphenylphosphino)-5,5',6,6',7,7',8,8'-octahydro-1,1'-binaphthyl	3
2,2'-bis-(diphenylphosphino)-1,1'-binaphthyl	3
2,2,2-trifluoroethanol	3
2,2,6,6-Tetramethyl-1-piperidinyloxy free radical	0
2,2,6,6-tetramethyl-piperidine	3
2,2,6,6-tetramethyl-piperidine-N-oxyl	0
2,2,6,6-tetramethylpiperidinyl-lithium	0
2,2,6,6-tetramethylpiperidinylmagnesium chloride	3
2,2,6,6-tetramethylpiperidinylmagnesium chloride lithium chloride complex	3
2,2-dimethylthiolane	1
2,2?-azobis(4-methoxy-2,4-dimethyl)valeronitrile	3
2,2?-methylene bis[(4R,5S)-4,5-diphenyl-2-oxazoline]	1
2,3,4-trimethoxy-N-((R)-quinolin-4-yl((1S,2S,4S,5R)-5-vinylquinuclidin-2-yl)methyl)benzenesulfonamide	2
2,3-dicyano-5,6-dichloro-p-benzoquinone	0
2,3-dihydro-1H-1,3-dimesylimidazole-2-carbene	3
2,4,6-trimethyl-pyridine	3
2,4,6-tripropyl-1,3,5,2,4,6-trioxatriphosphinane-2,4,6-trioxide	0
2,4-dinitrobenzoic acid	2
2,5-dimethyl-piperazine	1
2,6-bis((R)-4-phenyl-4,5-dihydrooxazol-2-yl)pyridine	3
2,6-bis(bis(3,5-bis(trifluoromethyl)phenyl)(hydroxy)-methyl)-dinaphtho-[2,1-d:1',2'-f][1,3,2]dithiazepine 3,3,5,5-tetraoxide	2
2,6-bis(hydroxybis(3-(trifluoromethyl)phenyl)methyl)dinaphtho[2,1-d:1',2'-f][1,3,2]dithiazepine 3,3,5,5-tetraoxide	2
2,6-bis(pyrazole)pyridine	3
2,6-bis-(4-chloro-phenyl)-4-oxo-3,5-dioxa-4-lambda5-phospha-cyclohepta[2,1-a;3,4-a']di-naphthalen-4-ol	1
2,6-bis<5',5'-diphenyl-4'-(S)-isopropyl oxazolin-2'-yl>pyridine	3
2,6-bis[(R,R)-4-(1-TPSO-ethyl)-2-oxazolin-2-yl]pyridine	3

"column1"	"Min*(Score)"
2,6-bis[4?-(S)-(tert-butyl)oxazolin-2?-yl]pyridine	3
2,6-di-tert-butyl-4-methylpyridine	3
2,6-di-tert-butyl-pyridine	3
2,6-dimethylpyridine	3
2,7-dimethyl-1,8-biphenylenediol	1
2-(((1R,2R)-2-(3-(3,5-bis(trifluoromethyl)phenyl)thioureido)cyclohexyl)carbamoyl)-3,4,5,6-tetrabromobenzoic acid	2
2-(((2,6-diisopropylphenyl)imino)methyl)pyridine	3
2-(2-hydroxyethyl)-3,4-dimethylthiazolium iodide	3
2-(3-(cyclopropylmethoxy)phenoxy)-4-fluorobenzaldehyde	2
2-(4-bromophenyl)-acetic acid	3
2-(5,5-dimethyl-1,3,2-dioxaborinan-2-yl)-5,5-dimethyl-1,3,2-dioxaborinane	1
2-(N,N-dimethylamino)athanol	1
2-(aminomethylcyclohexyl)ethylamine	1
2-(di-tert-butylphosphino)-1,1'-biphenylgold(I) chloride	3
2-(diphenylphosphino)-N-((S)-((1S,2S,4S,5R)-5-ethyl-quinuclidin-2-yl)(6-methoxyquinolin-4-yl)methyl)benzamide	2
2-(tert-butylethynyl)pyrimidine-5-carbaldehyde	2
2-(trimethylsilyl)phenyl trifluoromethanesulfonate	1
2-Methylpiperidin	3
2-amino-2-hydroxymethyl-1,3-propanediol	2
2-aminopyridine	3
2-chloropyridine	3
2-cyano-2-(hydroxyimino)acetic acid methylester	2
2-fluoro-2-iodo-1,3-benzodithiole-1,1,3,3-tetraoxide	1
2-hydroxy-p-toluic acid	0
2-hydroxyethanethiol	1
2-iodoxybenzoic acid	3
2-isopropoxy-4,4,5,5-tetramethyl-2-vinyl-1,3,2-dioxasilolane	1
2-mesityl-2,5,6,7-tetrahydropyrrolo[2,1-c][1,2,4]triazolium chloride	3
2-mesityl-6,7-dihydro-5H-pyrrolo[2,1-c][1,2,4]triazol-2-ium chloride	1
2-mesityl-6,7-dihydro-5H-pyrrolo[2,1-c][1,2,4]triazol-2-ium tetrafluoroborate	0
2-methyl-but-2-ene	3
2-nitropropane	3
2-pentafluorophenyl-6,7-dihydro-5H-pyrrolo[2,1-c][1,2,4]triazol-2-ium tetrafluoroborate	0
2-phenyl-6,7-dihydro-5H-pyrrolo[2,1-c][1,2,4]triazol-2-ium tetrafluoroborate	0
2-tert-butylanthraquinine	0
2.9-dimethyl-1,10-phenanthroline	0
20% palladium hydroxide-activated charcoal	0
20percent iron-modified mesoporous silica SBA-15	3
2ClO4(1-)*7.25H2O*Fe(2+)	3

"column1"	"Min*(Score)"
2V/SiO2-500	3
3 A molecular sieve	0
3 Angstroem MS	0
3,3'-(1,4-phenylenebis(methylene))bis(5-(2-hydroxyethyl)-4-methyl-thiazol-3-ium) bromide	2
3,3'-bis-pyrrolidin-1-ylmethyl-[1,1']binaphthalenyl-2,2'-diol	1
3,3?-di(9-phenylanthryl)BINOL phosphoric acid	0
3,3?-dibromo-2,2?-dihydroxy-1,1'-binaphthyl	3
3,4,5,6-tetrahydropyrimidin-2(1H)-one	2
3,4-dimethyl-2-(alpha-hydroxybenzyl)thiazoliumiodide	3
3,4-dimethyl-5-(2-hydroxyethyl)thiazolium iodide	3
3,5,3',5'-tetra-tert-butyl-4,4'-diphenoquinone	0
3,5-difluoropyridine	3
3,6-di(2'-pyridyl)-1,2,4,5-tetrazine	1
3,6-di-tert-butyl-9,10-dimesitylacridinium tetrafluoroborate	0
3,6-dioxocyclohexa-1,4-diene-1,2-dicarbonitrile	0
3-((3,5-bis(trifluoromethyl)benzyl)amino)-4-(((1S)-(6-methoxy-quinolin-4-yl)((2S,4S,5R)-5-vinylquinuclidin-2-yl)methyl)amino)cyclobut-3-ene-1,2-dione	2
3-Dimethylamino-1-propanol	1
3-Methyl-1-phenyl-2-phospholene 1-oxide	0
3-Methylpiperidine	3
3-amino propanoic acid	3
3-azapentane-1,5-diamine	0
3-benzyl-4,5-dimethylthiazol-3-ium bromide	2
3-benzyl-5-(2-hydroxyethyl)-4-methyl-1,3-thiazol-3-ium chloride	2
3-chloro-benzenecarboperoxoic acid	1
3-ethyl-5-(2-hydroxyethyl)-4-methyl-1,3-thiazolium bromide	3
3-ethyl-5-(2-hydroxymethyl)-4-methyl-1,3-thiazolium bromide	3
3-iodo-2-methylcyclohexenone	1
3-nitrobenzoic acid	3
4 A molecular sieve	0
4 A molecular sieves	0
4 Angstroem M.S	1
4 Angstroem MS	0
4 Angstroems MS	0
4'-(4-methylphenyl)-2,2':6',2'-terpyridine	3
4,4'-di-tert-butyl-2,2'-bipyridine	3
4,4'-di-tert-butylbiphenyl	1
4,4'-dibromobpy-NiCl2	3
4,5-bis(diphenylphos4,5-bis(diphenylphosphino)-9,9-dimethylxanthenephino)-9,9-dimethylxanthene	2
4-[(5S)-3-ethyl-4-oxa-1-azatricyclo[4.4.0.03,8]decan-5-yl]quinolin-6-yl (2,2,2-trichloroacetyl)carbamate	2
4-fluorobenzylic alcohol	3

"column1"	"Min*(Score)"
4-hydroxy-2,6-di(naphthalen-2-yl)dinaphtho[2,1-d:1',2'-f][1,3,2]dioxaphosphepine 4-oxide	1
4-methoxy-2,2,6,6-tetramethylpiperidin-1-oxyl radical	0
4-methoxy-N-(pyridin-4-ylmethylene)benzenamine	2
4-methoxy-N-[(E)-phenylmethylidene]aniline	3
4-methoxy-aniline	3
4-methoxy-phenol	2
4-methyl-morpholine	3
4-methylpiperidin	3
4-morpholineethanesulfonic acid	3
4-nitraminopyridine N-oxide	3
4-nitro-benzoic acid	3
4-toluenesulfonyl azide	0
4A MS	0
5 wtpercentFe-H-Beta-SiO2/Al2O3=150 zeolite	3
5%-palladium/activated carbon	0
5,10,15,20-tetrakis(p-chlorophenyl)porphyrin iron(III) chloride	3
5,5'-dimethyl-2,2'-bipyridine	3
5,5?-bis[di(3,5-di-tert-butyl-4-methoxyphenyl)phosphino]-4,4?-bi-1,3-benzodioxole	1
5-(2-hydroxy-ethyl)-3,4-dimethyl-thiazolium chloride	3
5-ethyl-2-methylpyridine borane complex	3
5-iodo-2,3-dihydrobenzofuran	1
5-methoxy-1H-benzimidazole	1
5A molecular sieve	0
5a(S),10b(R)-5a,10b-dihydro-2-(pentafluorophenyl)-4H,6H-indeno[2,1-b][1,2,4]triazolo[4,3-d][1,4]oxazinium tetrafluoroborate	0
5percent iron-modified mesoporous silica SBA-15	3
7b-phenyl-7bH-oxazirino<2,3-b><1,2>benz-isothiazole 3,3-dioxide	1
9,10-phenanthrenequinone	0
9-BBN triflate	3
9-benzylfluorene lithium salt	1
AD-mix-beta	1
ATP	3
Adam?s catalyst	0
Ag*ClO4(1-)=AgClO4(1-)	3
AlPO4 supported ethylenediamine-chromium(III)-salen complex nanoparticles	0
Amberlite G-50 ion-exchange resin	0
Amberlite IRA-400	0
Amberlyst 15	0
Amberlyst A-21 ion-exchange resin	0
Ambersep 900 OH resin	0
Au(OAc)3	0

"column1"	"Min*(Score)"
B-(trifluoromethanesulfonyloxy)-9-borabicyclo[3.3.1]nonane	2
BCl(C6H11)2	1
BF3*(OEt)2	1
BF4(1-)*2C8H12*Rh(1+)	0
BF4(1-)*C18H13Cl3N3O(1+)	1
BF4(1-)*C18H17F5N3O(1+)	1
BF4(1-)*C21H22N3O(1+)	1
BF4(1-)*Cu(2+)*6H2O	1
BIPHEP-I	1
Bis<2-(N,N-dimethylamino)aethyl>aether	1
Bromotrichloromethane	3
Bu3SnN(Ph)C(OMe)=NPh	0
BuLi	0
C42H63AuO3P(1+)*C2F6NO4S2(1-)	0
C49H68AuNP(1+)*F6Sb(1-)	0
C5H5BrMnO5	0
CH3BN(1-)*C10H15NPol(1+)	0
CH3BN(1-)*H(1+)*H2NPol	0
Candida rugosa lipase	1
Carbonate buffer	3
Celite	3
Cinchonin	1
Cl(3)HO4	1
Co(3,5-DitBu-Ibu-Phyrin)	0
Co(meso-tetraphenylporphyrin) tetrakis[3,5-bis(trifluoromethyl)phenyl]borate	0
Coenzyme A	3
CrCl2*(THF)1.4	0
CrCl2*DMF	0
CuCl*2LiCl	0
CuF(PPh3)3 methanol solvate	0
CuF*(R)-tolBinap	0
CuF-(R)-DTBM-SEGPHOS	0
CuI*2LiBr	0
CyJohnPhos	1
D-Prolin	3
DBN	1
DIMCARB	1
DL-dithiothreitol	1
DTBP	1
Dess-Martin periodane	0

"column1"	"Min*(Score)"
Diethoxy-methyl-(6-amino-hexylaminomethyl)-silan	1
Difluoroacetic acid	3
Diphenyl(N-methyl-2-pyrrolidinyl)methanol	2
Eaton?s reagent	0
Echavarren's catalyst	3
Ethyl diphenylphosphinite	2
Ethyl propionate	2
Fe(TCP)Cl	3
GeCl2*dioxane	0
GeCl2-dioxane	0
Grotjahn?s catalyst	3
H2SO4-SiO2	0
HATU	3
Hexamethylbenzene	0
Hexamethyldisiloxane	1
Hexamethylphosphorous triamide	0
Hf(OTf)4	0
Hoveyda-Grubbs catalyst second generation	2
In(OSO2CF3)3	0
Indion-130 resin	3
Iron(III) nitrate nonahydrate	3
Isopropyl acetate	3
K10 montmorillonite clay	3
L-(+)-diisopropyl tartrate	3
L-Cysteine	3
L-Leucine supported on superparamagnetic silica encapsulated gamma-Fe2O3 nanoparticles	3
L-Tartaric acid	3
L-diisopinocampheylborane	0
L-proline	3
L-prolinium sulfate	3
Lawessons reagent	0
Lewatit S 100 ion exchange resin	3
Li(2,2,6,6-tetramethylpiperidide)*Al(iBu)3	0
LiHMDSA	0
Lindlar's catalyst	3
MANDELIC ACID	0
MIL-101-SO3H	1
MP-BH(OAc)3 resin	3
MP-BH3CN	1
MP-CNBH3	1

"column1"	"Min*(Score)"
MP-cyanoborohydride	0
MP-triacetoxyborohydride	0
MP-triacetoxyborohydride resin	3
MS 4 Angstroem	0
Mesitol	3
Methyltrichlorosilane	0
Mg-Al hydrotalcite	1
Mn89Cr11	0
MnBr(CO)5	0
Mo(CO)3(CN-t-Bu)3	0
Montmorillonite K 10	3
Montmorillonite K10 clay	3
Montmorillonite KSF	0
N+C5Ala2C16	1
N,N'-((11bS,11b'S)-azanediylbis(2,6-bis(3,5-bis(pentafluoro-lambda6-sulfanyl)phenyl)-4lambda5-dinaphtho[2,1-d:1',2'-f] [1,3,2]dioxaphosphepine-4-yl-4-ylidene))bis(1,1,2,2,2-pentafluoroethane-1-sulfonam ide)	1
N,N'-((11bS,11b'S)-azanediylbis(2,6-bis(3,5-bis(perfluoropropyl)phenyl)-4lambda5-dinaphtho[2,1-d:1',2'-f] [1,3,2]dioxaphosphepine-4-yl-4-ylidene))bis(1,1,1-trifluoromethanesulfonamide)	0
N,N'-Dimethylurea	2
N,N'-dimethylpiperazine	1
N,N,N',N'',N'''-pentamethyldiethylenetriamine	1
N,N,N',N'-Tetraethylethylenediamine	3
N,N,N',N'-tetramethyl-1,4-butanediamine	1
N,N,N',N'-tetramethyl-1,8-diamin onaphthalene	3
N,N,N',N'-tetramethyl-1,8-diaminonaphthalene	3
N,N,N',N'-tetramethylguanidine	3
N,N,N,N,-tetramethylethylenediamine	3
N,N,N,N,N,N-hexamethylphosphoric triamide	0
N,N,N-triethyl-N-(propanesulfonic acid)ammonium hydrogensulfate	0
N,N,N?,N?-tetramethyl-N?-tert-butylguanidine	3
N,N-di(propan-2-yl)-4H-1,3,2-benzo-dioxaborinin-2-amine	1
N,N-dibutyl amino-2 ethanol	0
N,N-diisopropyl-1,2-ethanediamine	1
N,N-dimethyl acetamide	3
N,N-dimethyl-aniline	3
N,N-dimethyl-ethanamine	1
N,N-dimethyl-formamide	3
N,N-dimethylalanine	3
N,N-dimethylammonium chloride	0
N,N-dimethylethylenediamine	3
N,N?-bis(2,6-diisopropylphenyl)imidazol-2-ylidene hydrochloride	3
N,N`-dimethylethylenediamine	3

"column1"	"Min*(Score)"
N,O-bis-(trimethylsilyl)-acetamide	3
N-(2-acetamido)-3-iminodiacetic acid	3
N-(3,5-bis(trifluoromethyl)phenyl)-3-((2-(((S)-(6-methoxy-quinolin-4-yl)((1S,2S,4S,5R)-5-vinylquinuclidin-2-yl)methyl)amino)-3,4-dioxocyclobut-1-en-1-yl)amino)-5-(trifluoromethyl)benzamide	2
N-(p-toluenesulfonyl)-L-valine	3
N-(tert-butyl)benzenesulfinimidoyl chloride	1
N-3,5-(CF3)2-C6H3-N'-[9-dehydroxy-quinidin-9(S)-yl]thiourea	2
N-Bromosuccinimide	3
N-[3,5-bis(trifluoromethyl)phenyl]-N'-[(9R)-6'-methoxycinchonan-9-yl]thiourea	1
N-benzyl-N,N,N-triethylammonium chloride	0
N-benzyl-trimethylammonium hydroxide	0
N-benzylidenephenylsulfonamide	1
N-butylamine	1
N-chloro-succinimide	3
N-cyclohexyl-cyclohexanamine	1
N-ethyl-N,N-diisopropylamine	2
N-ethylmorpholine	3
N-fluorobis(benzenesulfon)imide	1
N-iodo-succinimide	3
NAD	3
Na(1+)*HSO4(1-)*SiO2 = NaHSO4*SiO2	0
Na(OAc)3BH loaded resin	0
Na2H2S2O5	0
Ni(acetylacetate)2	3
NiCl(o-tolyl)(tetramethylethylenediamine)	3
Noyori's catalyst	3
O,O-Diethyl hydrogen phosphorodithioate	0
O-(1H-benzotriazol-1-yl)-N,N,N',N'-tetramethyl-uronium hexafluorophosphate	0
O-(4-nitrobenzoyl) hydroxylamine	0
O4S(2-)*2Al(3+)*4CH3(1-)	1
Oxone	0
P(p-C6H4F)3	1
P(p-CH3OC6H4)3	1
PL-cyanoborohydride resin	3
PS-CNBH3	1
PS-Trisamine	0
PS-cyanoborohydride	0
PS-diisopropylethylamine	3
PS-isocyanate scavenger resin	3
PS-p-toluensulfonyl hydrazide scavenger resin	3
PS-triacetoxyborohydride	0

"column1"	"Min*(Score)"
PYRIMIDINE	2
PdCl(dppb)(C3H5)	0
Pentafluorobenzoic acid	3
Pic-BH3	1
Quinuclidine	0
Rh2(OAc)4	0
Rh2(esp)2	0
Rh2(trifluoroacetate)4(1,3-bis(2,6-diisopropylphenyl)imidazol-2-ylidene)2	0
Rh2[3S-3-(1,3-dioxobenzo[f]isoindol-2-yl)-2-piperidinonate]4	0
RhHCl2(PPh3)3	0
Ru(2 wt\%)/CeO2	3
Ru2(OAc)4	3
RuBr(CO)3(eta-C3H5)	3
S-pyrrolidine-2-carbaldehyde	2
SL-J009-1	1
SPhosAuNTf2	0
Schwartz's reagent	1
Selectfluor	0
TEA	3
Tetrakis(dimethylamino)ethylen	1
Tosyl isocyanate	0
Tri(p-tolyl)phosphine	0
Trifluoromethanesulfonamide	0
Triisopropyl borate	0
Trimethyl borate	0
Trimethyl orthoacetate	3
Trimethylacetic acid	3
Trimethylmethoxysilane	0
Triphenylphosphine oxide	0
Tris(3,6-dioxaheptyl)amine	1
Tris(4-methoxyphenyl)phosphine oxide	1
TurboGrignard	1
VANOL-B3	2
W(CO)5	1
WA30 basic resin	0
Wilkinson's catalyst	0
XPhos	1
Yb(OTf)3 immobilized on sodium propylsulphonate and phenyl group co-functionalized magnetic core?mesoporous silica shell composite	3
Yb(hfc)3(+)	2
YerE from Yersinia pseudotuberculosis	1

"column1"	"Min*(Score)"
Zn(2+)*CF3O3S(1-)*C6H18NSi2(1-)	3
[(1,3-bis(2,4,6-trimethylphenyl)imidazol-2-ylidene)3Zn3(H)4(THF)][BPh4]2	0
[(1,3-bis(diphenylphosphino)propane)Pd(H2O)2](BF4)2	0
[(1,5-cyclooctadiene)(OH)iridium(I)]2	0
[(C6H6)(PCy3)(CO)RuH]+*BF4	3
[(DPEphos)Rh(COD)]BF4	0
[(R)-(+)-1,1'-bi(2-naphthol)]Ti(Oi-Pr)2	1
[(eta5-C5Me5)RuCl(mu2-SMe)2Ru(eta5-C5Me5)Cl]	3
[1,1'-bis(diphenylphosphino)ferrocene]nickel(II) chloride	3
[1,3-bis(2,6-diisopropyl-phenyl)imidazol-2-ylidene] silver(I) chloro	0
[1,3-bis(2,6-diisopropylphenyl)imidazol-2-ylidene]gold bis(trifluoromethanesulfonyl)imidate	0
[2,2]bipyridinyl	3
[3,5-bis(trifluoromethyl)phenyl]-3-{(2S)-3,3-dimethyl-1-[(triphenylphosphoranylidene)amino]butan-2-yl}thiourea	2
[AuCl(IPr)]	0
[Cd2(tren)2(dl-alaninato)](ClO4)3*H2O	0
[Cp(P-iPr3)Ru(CH3CN)2](1+)*B(C6F5)4(1-)	3
[Cp*Co(C6H6)][B(C6F5)4]}2	0
[Cp*Rh(CH3CN)3](BF4)2	0
[Cp*Rh(CH3CN)3][SbF6]2	0
[D3]phosphoric acid	0
[D]-sodium hydroxide	0
[Fe(5,10,15,20-tetraphenylporphyrin)]BF4	3
[Fe(5,10,15-triphenylcorrole)]BF4	3
[Fe{N(SiMe3)2}2]2	3
[In(S,S)-iPr-pybox](OTf)3	0
[Ir(1,5-cyclooctadiene)2]triflate	3
[Ir(2-(2,4-difluorophenyl)-4-(trifluoromethyl)pyridine)2(5,5'-bis(trifluoromethyl)-2,2'-bipyridine)]PF6	3
[Ir(COD)2]BF4	0
[IrH2(thf)2(PPh2Me)2]PF6	0
[MoO2Cl2(dmf)2]	0
[Ni(dimethylglyoxime)Cl2]	3
[Rh(OH)(cod)]2	0
[Rh(dppe)]ClO4	0
[Rh(dppp)]BF4	0
[Rh(nbd)(R,R)-Me-Duphos]ClO4	0
[Rh2(S-BPTPI)4]*3H2O	0
[Ru(kappa1-OAc)(kappa2-OAc)(kappa3-1,1,1-tris(diphenylphosphinomethyl)ethane)]	2
[bis(acetoxy)iodo]benzene	2
[bis(trifluoromethanesulfonyl)imidate](triphenylphosphine)gold(I)	3
[iridium(CH2CHCH2)(C6H2(Cl)(NO2)COO)((R)-2,2'-bis(diphenylphosphino)-5,5'-dichloro-6,6'-dimethoxy-1,1-biphenyl)]	2

"column1"	"Min*(Score)"
[ruthenium(II)(eta6-1-methyl-4-isopropyl-benzene)(chloride)(mu-chloride)]2	3
[{(R)-H8-BINOLate}Ti(O-i-Pr)2]x	1
acetaldehyde	3
acetamide	3
acetic acid	3
acetic acid hydrazide	0
acetic anhydride	3
acetonitrile	3
acetophenone	3
acetyl chloride	3
acetylacetonatodicarbonylrhodium(l)	0
acetylhydroxamic acid	0
acidic ion exchange resin	0
acidic ion-exchange resin P-SO3H	0
air	3
alkali hydroxide	0
allyl(cyclopentadiene)palladium(II)	0
alpha cyclodextrin	1
alpha-picoline borane	0
alpha-picoline-borane	0
alumina*KF supported on silica	0
alumina-supported iron(III) chloride	0
aluminium	0
aluminium oxide hydroxide	0
aluminium trichloride	0
aluminium tris(2,6-diphenylphenoxide)	0
aluminium(III) triflate	3
aluminum (III) chloride	0
aluminum oxide	0
aluminum tri-bromide	0
aluminum tri-tert-butoxide	0
amberlyst-15	0
aminosulfonic acid	0
ammonia	0
ammonium acetate	3
ammonium bicarbonate	0
ammonium bromide	3
ammonium cerium(IV) nitrate	1
ammonium chloride	3
ammonium fluoride	0

"column1"	"Min*(Score)"
ammonium formate	0
ammonium hexafluorophosphate	0
ammonium hydroxide	0
ammonium iodide	3
ammonium metavanadate	0
ammonium peroxydisulfate	3
aniline	3
antimony pentafluoride	1
aqueous extract of the tamarind fruits	1
askanite-bentonite clay	0
barium dihydroxide	0
barium hydroxide monohydrate	0
barium hydroxide octahydrate	0
barium manganate	0
barium permanganate	0
barium(II) hydroxide	0
barium(II) iodide	0
barium(II) oxide	0
bathophenanthroline	0
benzaldehyde	3
benzaldehyde dimethyl acetal	2
benzenesulfonic acid	0
benzo[1,3,2]dioxaborole	0
benzoic acid	3
benzotriazol-1-ol	3
benzotriazol-1-yloxyl-tris-(pyrrolidino)-phosphonium hexafluorophosphate	2
benzotrifuroxan	0
benzylamine	2
benzylmagnesium chloride	0
benzyltriethylammonium	2
benzyltriethylammonium bromide	2
beta-Zeolite	0
biphenyl	1
bis(1,5-cyclooctadiene)diiridium(I) dichloride	0
bis(1,5-cyclooctadiene)iridium(I) tetrafluoroborate	0
bis(1,5-cyclooctadiene)nickel (0)	3
bis(1,5-cyclooctadiene)nickel(0)	3
bis(1,5-cyclooctadiene)rhodium(I) tetrafluoroborate	0
bis(1,5-cyclooctadiene)rhodium(I) trifluoromethanesulfonate	0
bis(1-methyl-1-phenylethyl)peroxide	0

"column1"	"Min*(Score)"
bis(2,2'-diamino-1,1'-binaphthyl)-based chiral phosphoramide	0
bis(2,2,6,6-tetramethylpiperidin-1-yl)magnesium-bis(lithium chloride) complex	3
bis(2,6-diisopropylphenyl)imidazol-2-ylidene	2
bis(acetonitrile)(1,5-cyclooctadiene)rhodium(I) tetrafluoroborate	0
bis(acetylacetonate)nickel(II)	3
bis(benzonitrile)palladium(II) dichloride	0
bis(bis(trimethylsilyl)amido)zinc(II)	3
bis(cyclohexanyl)borane	1
bis(cyclopentadienyl)titanium dichloride	0
bis(dibenzylideneacetone)-palladium(0)	0
bis(dicyclohexylphosphino)methane	0
bis(diethylamino)cyclopropenium tetraphenylborate	0
bis(eta3-allyl-mu-chloropalladium(II))	0
bis(ethylene)rhodium(I) chloride dimer	0
bis(norbornadiene)rhodium(l) tetrafluoroborate	0
bis(pinacol)diborane	0
bis(tertbutylcarbonyloxy)iodobenzene	3
bis(tri-n-butyltin)	0
bis(tricarbonyl(eta-cyclopentadienyl)tungsten)	0
bis(trifluoromethane)sulfonimide lithium	0
bis(trifluoromethanesulfonyl)amide	1
bis(triphenylphosphine) palladium (Il) acetate	0
bis(triphenylphosphine)copper(I) tetrahydroborate	0
bis(triphenylphosphine)nickel(II) chloride	3
bis-diphenylphosphinomethane	2
bis-triphenylphosphine-palladium(II) chloride	0
bis[-(R)-MeCH-O-CH2-2-yl-pyridine-6-yl-CH2-O-(R)-MeCH-]	3
bis[2-(diphenylphosphino)phenyl] ether	2
bis[dichloro(pentamethylcyclopenta-dienyl)iridium(III)]	0
bisacetonitrile[norbornadiene]rhodium(I) hexafluoroantimonate	0
bismuth(III) bromide	2
bismuth(III) chloride	2
bismuth(III) iodide	2
bismuth(lll) trifluoromethanesulfonate	2
bis{rhodium[3,3'-(1,3-phenylene)bis(2,2-dimethylpropanoic acid)]}	0
borane pyridine	3
borane pyridine complex	3
borane tert-butylamine	0
borane-THF	0
borane/tetrahydrofuran	3

"column1"	"Min*(Score)"
boric acid	3
boric acid tributyl ester	3
boric anhydride	0
boron tribromide	0
boron trichloride	0
boron trifluoride	0
boron trifluoride diethyl etherate	0
boron trioxide	0
brominated hydroxymethylbenzoic acid resin	3
bromine	1
bromopentacarbonylmanganese(I)	0
brucine N-oxide	1
buta-1,3-diene	1
butyl magnesium bromide	0
caesium carbonate	0
calcium carbonate	0
calcium carbonate pentahydrate	0
calcium chloride	3
calcium hydride	0
calcium oxide	1
calcium sulfate	0
calcium(II) bis-(trifluoromethanesulfonimide)	1
calcium(II) trifluoromethanesulfonate	1
camphor-10-sulfonic acid	3
carbocationic species *B(C6F5)4(-)	1
carbon dioxide	3
carbon monoxide	3
carbon tetrabromide	3
carbon-SO3H	3
carbonic acid dimethyl ester	1
carbonochloridic acid 1-chloro-ethyl ester	0
carbonyl bis(hydrido)tris(triphenyl-phosphine)ruthenium(II)	0
carboxypolystyrene	1
cellulose sulphuric acid	0
cerium(III) chloride	1
cerium(III) chloride heptahydrate	1
cesium acetate	3
cesium fluoride	3
cesium hydroxide	0
cesium pivalate	3

"column1"	"Min*(Score)"
cetyltrimethylammonim bromide	2
cetyltrimethylammonium chloride	2
chiral amino alcohol ligand	1
chiral bis(1-naphthyl)methyl-amine-derived ligand	1
chiral bis-pyridino-18-crown-6	0
chiral camphor-derived [2.2.1] bicyclic sulfide	0
chiral catalyst	1
chiral deriv. of [2-thiabicyclohept-3-yl]bicycloheptanone	1
chiral dipeptide N-acylethylenediamine-based ligand	0
chiral phosphoramide catalyst	1
chiral thiazolyl-L-threonine-derived catalyst	1
chiral triazolium salt	1
chloranil	0
chloro(1,3-bis(2,6-di-i-propylphenyl)imidazol-2-ylidene)gold(I)	3
chloro(1,5-cyclooctadiene)rhodium(I) dimer	0
chloro(triphenylphosphine)gold(I)	3
chloro-trimethyl-silane	1
chloro[1,3-bis(2,6-di-i-propylphenyl) imidazol-2-ylidene]copper(I)	0
chloro[1,3-bis(2,6-diisopropylphenyl)imidazol-2-ylidene]gold(I)	3
chloro[tris(2,3,4,5,6-pentafluorophenyl)phosphine]gold(I)	3
chlorobis(ethylene)rhodium(I) dimer	0
chlorodicarbonyl(eta5-pentaphenylcyclopentadienyl)ruthenium(II)	3
chloroform	2
chlorosulfonic acid	0
chlorosulfonic acid supported piperidine-4-carboxylic acid functionalized Fe3O4 nanoparticles	0
cholin hydroxide	3
chromium chloride	0
chromium dichloride	0
chromium tricarbonyl	0
chromium(VI) oxide	0
cis-dichlorobis(triphenylphosphine)platinum(II)	0
citric acid	2
clay	0
cobalt(II) bromide	0
cobalt(II) bromide-[1,2-bis(diphenylphosphino)ethane]	2
cobalt(II) chloride	0
cobalt(II) phthalocyanine	0
cobalt(III) acetylacetonate	0
copper	0
copper (I) acetate	1

"column1"	"Min*(Score)"
copper (I) trifluoromethane sulfonate benzene	0
copper (II) trifluoroacetate hydrate	3
copper acetylacetonate	3
copper diacetate	3
copper dichloride	3
copper(I) 3-metthylsalicylate	1
copper(I) bromide	1
copper(I) bromide dimethylsulfide complex	1
copper(I) oxide	0
copper(I) trifluoromethanesolfonate toluene complex	1
copper(I) trifluoromethanesulfonate * 1/2 toluene	1
copper(II) 2-ethylhexanoate	3
copper(II) acetate monohydrate	3
copper(II) acetylacetonate	3
copper(II) bis(trifluoromethanesulfonate)	3
copper(II) choride dihydrate	3
copper(II) ferrite	3
copper(II) iodide	3
copper(II) nitrate hexahydrate	3
copper(II) oxide	3
copper(II) sulfate	3
copper(l) chloride	1
copper(l) cyanide	1
copper(l) iodide	1
copper(ll) bromide	3
copper(ll) sulfate pentahydrate	3
cucurbituril	1
cyanoborane	0
cyclo-octa-1,5-diene	1
cyclohexanone	1
cyclohexylamine	3
cyclohexyldiphenylphosphine	2
cyclopentyl methyl ether	1
cyclopentylmagnesium chloride	0
d-Ipc2BH	1
d8-isopropanol	1
dacarbazine	1
decacarbonyldirhenium(0)	0
deuteriated sodium hydroxide	0
di(n-butyl)(iodo)tin hydride	0

"column1"	"Min*(Score)"
di-isopropyl azodicarboxylate	1
di-mu-bromobis(tri-tert-butylphosphino)dipalladium(I)	0
di-mu-chlorobis(norbornadiene)dirhodium(I)	0
di-n-butylboryl trifluoromethanesulfonate	1
di-n-butyliodotin hydride	0
di-n-butylzinc	0
di-tert-butyl dicarbonate	0
di-tert-butyl peroxide	0
di-tert-butyl(1,1'-biphenyl)-2-ylphosphinegold(I)bis(trifluoro-methanesulfonimidate)	3
di-tert-butyl(methyl)phosphonium tetrafluoroborate salt	0
di[(eta-1,2,5,6)-1,5-cyclooctadiene]rhodium hexafluoroantimonate	0
diallyl 1,4-dihydro-2,6-dimethylpyridine-3,5-dicarboxylate	3
diammonium sulfide	3
diazomethyl-trimethyl-silane	0
dibenzo-18-crown-6	0
dibenzoyl peroxide	0
dibenzylamine	2
diboron trioxide	0
dibromoborane	3
dibutyl tin diiodide	0
dibutylamine	3
dibutylbis(cyclopentadienyl)zirconium	0
dibutyldimethoxytin	0
dibutyltin chloride	0
dibutyltin diacetate	0
dicarbonylacetylacetonato rhodium (I)	0
dichloro bis(acetonitrile) palladium(II)	0
dichloro(1,1'-bis(diphenylphosphanyl)ferrocene)palladium(II)*CH2Cl2	0
dichloro(pentamethylcyclopentadienyl)rhodium (III) dimer	0
dichlorogallane	1
dichloromethylsilane	3
dicyclohexyl-(2',6'-dimethoxybiphenyl-2-yl)-phosphane	1
dicyclohexyl-carbodiimide	3
dicyclohexylboron chloride	0
dicyclohexylphenylphosphine	0
dicyclopentylboron trifluoromethanesulfonate	0
diethyl 2,6-dimethyl-1,4-dihydropyridine-3,5-dicarboxylate	3
diethyl chlorophosphate	0
diethylaluminum iodide	0
diethylamine	1

"column1"	"Min*(Score)"
diethylamino-sulfur trifluoride	0
diethylazodicarboxylate	0
diethylzinc	0
dihydrogen peroxide	0
diiodomethane	1
diisobutylaluminium acetylacetonate	0
diisobutylaluminium hydride	0
diisopinocamphenylborane	0
diisopinocampheylborane	0
diisopropoxy(eta2-propene) titanium(II) complex	0
diisopropyl zinc	0
diisopropyl-carbodiimide	3
diisopropylamine	2
dilithium (R)-3,3'-diphenylbinaphtholate	0
dilithium tetra(tert-butyl)zincate	1
dimesitylmagnesium	3
dimethyl sulfoxide	3
dimethyl zinc(II)	0
dimethylaluminum chloride	0
dimethylfumarate	3
dimethylphenyl(4,4,5,5-tetramethyl-1,3,2-dioxaborolan-2-yl)silane	1
dimethylsulfide	3
dimethylsulfide borane complex	0
dimethylsulfide gold(I) chloride	3
diphenyl hydrogen phosphate	0
diphenyl hydrogen phosphite	0
diphenyl((R)-1-((S)-1-phenylethyl)aziridin-2-yl)methanol	3
diphenyl((S)-1-((S)-1-phenylethyl)aziridin-2-yl)methanol	3
diphenyl(methyl)phosphine	0
diphenyl-((S)-1-((S)-1-phenylethyl)aziridin-2-yl)-methanol	3
diphenylborinic acid	3
diphenylboronchloride	0
diphenylsilane	0
dipotassium hydrogenphosphate	0
dipotassium peroxodisulfate	0
dirhodium tetraacetate	0
dirhodium(II) tetrakis(perfluorobutyrate)	0
dirhodium(II) tetrakis<(3S)-phthalimido-2-piperidinonate>	0
dmap	3
dodecacarbonyl-triangulo-triruthenium	3

"column1"	"Min*(Score)"
dysprosium	0
dysprosium(III) trifluoromethanesulfonate	1
epi-cinchonidine	1
epiCDT	1
erbium triisopropoxide	0
ethanol	3
ethanolamine	3
ethoxy(potassiosulfanyl)methanethione	0
ethyl 2-[2-(4-chlorophenyl)-2-oxoethyl]sulfonylacetate	3
ethyl acetate	3
ethyl bromide	2
ethyl iodide	1
ethylacrolein	1
ethylaluminum dichloride	0
ethylene dibromide	2
ethylene glycol	3
ethylenediamine	0
ethylenediamine diacetate	3
ethylenediamine diacetic acid	3
ethylenediaminediacetic acid	3
ethylenediaminetetraacetic acid	3
ethylmagnesium bromide	0
ethylmagnesium chloride	0
ethyltriphenylphosphonium bromide	0
europium(III) trifluoromethanesulfonate	1
ferric(III) bromide	3
fluoride	0
fluorous reverse-phase silica	0
formaldehyd	3
formamide	3
formic acid	3
furan	3
gadolinium(III) isopropoxide	0
gadolinium(III) trifluoromethanesulfonate	0
gallium(III) trichloride	3
gallium(III) triflate	3
germanium(II) chloride dioxane	3
girard's reagent T	0
glycine	3
gold bromide	3

"column1"	"Min*(Score)"
gold(I) chloride	3
gold(III) bromide	0
gold(III) chloride	0
gold(lll) acetate	0
gold-on-silver film	3
graphene?mesoporous anatase nanocomposite	1
guanidine hydrochloride	3
hex-3-yne	1
hexafluorophosphoric acid	0
hexamethyldisilathiane	0
hydrazine	0
hydrazine hydrate	0
hydrazinium sulfate	0
hydrochloric acid diethyl ether	0
hydrogen	0
hydrogen bromide	0
hydrogen cation	0
hydrogen fluoride	0
hydrogen sulfide	0
hydroquinidein 1,4-phthalazinediyl diether	1
hydroquinine 2,5-diphenyl-4,6-pyrimidinediyl diether	1
hydroquinone	1
hydroxyapatite-encapsulated-gamma-Fe2O3 supported sulfonic acid nanoparticles	0
hydroxylamine	0
hydroxylamine acetate	3
hydroxylamine hydrochloride	0
hydroxylamine potassium salt	0
hypophosphorous acid	0
i-Pr2Et	1
iPr2NCOO (R)-2-[(S)-CH(4-Br-C6H4)OH]-2-Bu-cC6H8-(Z)=CH ester	1
iPr2NCOO (R)-2-[(S)-CH(C6H5)OH]-2-Bu-cC6H8-(Z)=CH ester	1
immobilized Co(II) Schiff base complex supported on multi?wall carbon nanotubes	0
indium	0
indium (III) iodide	0
indium iodide	0
indium tribromide	0
indium(I) bromide	0
indium(II) bromide	0
indium(III) bromide	0
indium(III) chloride	0

"column1"	"Min*(Score)"
indium(III) triflate	3
iodine	1
iodosylbenzene	1
iron	0
iron oxide	3
iron(II) chloride	3
iron(II) dodecylsulfate	3
iron(II) triflate	3
iron(II,III) oxide	3
iron(III) chloride	3
iron(III) chloride adsorbed on silica gel	3
iron(III) chloride hexahydrate	3
iron(III) paratoluenesulfonate	3
iron(III) trifluoromethanesulfonate	3
isopropyl alcohol	3
isopropyl bromide	1
isopropyl chloride	0
isopropyl magnesium chloride - lithium chloride complex	0
isopropyl magnesium lithium chloride	0
isopropyllithium	0
isopropylmagnesium bromide	0
isopropylmagnesium chloride	0
lanthanium (III) chloride bis(lithium chloride) complex	3
lanthanum(lll) triflate	3
lead	0
lead dioxide	0
lead(II) chloride	0
lead(II) iodide	0
lead(IV) acetate	0
lithium	0
lithium (10R)-9-dihydro-10-trimethylsilyl-9-borabicyclo[3.3.2]decane diethyl etherate	0
lithium (S)-B-H2-(10)-trimethylsilyl-9-borabicyclo[3.3.2]decane	0
lithium acetate	3
lithium aluminium tetrahydride	0
lithium borohydride	0
lithium bromide	3
lithium bromide monohydrate	3
lithium carbonate	0
lithium chloride	3
lithium cyanide	0

"column1"	"Min*(Score)"
lithium di-n-butylcuprate	0
lithium dihydronaphthylide radical	0
lithium diisopropyl amide	0
lithium ethoxide	0
lithium fluoride	3
lithium hexamethyldisilazane	0
lithium hydroxide	0
lithium hydroxide monohydrate	0
lithium iodide	3
lithium methanolate	0
lithium n-propoxide	0
lithium pentane-2,4-dionate	0
lithium tert-butoxide	0
lithium tetrafluoroborate	0
lithium triethylborohydride	0
lithium trifluoromethanesulfonate	0
lithium-B-H2-(10R)-trimethylsilyl-9-borabicyclo[3.3.2]decane	0
macroporous cyanoborohydride	0
magnesia	0
magnesium	0
magnesium bromide	3
magnesium bromide ethyl etherate	3
magnesium chloride	3
magnesium hydrogen sulfate	3
magnesium iodide	3
magnesium methanolate	0
magnesium oxide	3
magnesium sulfate	3
magnesium sulphate	3
magnesium triflate	3
maleic acid	0
manganese	0
manganese(II) chloride hexahydrate	0
manganese(II) sulfate	0
manganese(IV) oxide	0
manganese(ll) chloride	0
mercaptoacetic acid	3
mercury dichloride	0
mercury(II) diacetate	0
mesitylcopper(I)	0

"column1"	"Min*(Score)"
mesityllithium	0
meso-tetraphenylporphyrin iron(III) chloride	3
mesoporous aluminosilicate Al-MCM-41	0
mesoporous silica supported copper nano catalyst	0
methanesulfonamide	0
methanesulfonic acid	0
methanesulfonyl chloride	0
methanol	3
methoxide	0
methoxy(cyclooctadiene)rhodium(I) dimer	0
methyl iodide	1
methyl magnesium iodide	0
methyl zinc (1+); methylate	0
methyl-((R)-1-phenyl-2-piperidin-1-yl-ethyl)-amine	1
methylamine	3
methylcyclopentadienyl manganese(I) tricarbonyl	0
methyllithium	0
methyllithium lithium bromide	0
methylmagnesium bromide	0
methylmagnesium chloride	0
methylthioninium chloride hydrate	0
methyltin(IV) trichloride	0
modified germanium	3
modified silica-supported 1-propyl-3-methyl- imidazolium?HSO4 catalyst	0
molecular sieve	0
montmorillonite K 10	0
montmorillonite K 10 clay	0
montmorillonite K-10	0
montmorillonite K10	0
montmorillonite K10 Clay	0
montmorillonite K10 clay	0
montmorillonite clay K10	0
morpholine	3
morpholinium acetate	3
mutant sperm whale myoglobin Mb(F43V,V68F)	1
n-Bu2SnClH	0
n-butanethiol	1
n-butylammonium acetate	3
nano-Fe3O4	3
naphthalen-1-yl-lithium	0

"column1"	"Min*(Score)"
naphthalene	0
neodymium	0
neodymium(III) trifluoromethanesufonate	0
neopentylmagnesium bromide	3
nickel	0
nickel dibromide	3
nickel dichloride	3
nickel(II) acetate tetrahydrate	3
nickel(II) bromide dimethoxyethane	3
nickel(II) chloride hexahydrate	3
nickel(II) nitrate hexahydrate	3
nickel(II) perchlorate hexahydrate	3
nickel(II) triflate	3
nido-decaborane	0
niobium pentachloride	3
niobium(V) oxide	3
nitrobenzene	1
nitromethane	1
octylmagnesium bromide	0
ortho-(diphenyl-phosphino)-benzene sulphonic acid	0
ortho-diphenylphosphinobenzoic acid	2
ortho-ethylaniline	0
ortho-methylbenzoic acid	3
ortho-methylphenyl iodide	1
ortho-nitrobenzoic acid	3
orthoformic acid triethyl ester	0
oxalic acid	0
oxone	0
oxygen	1
oxygen-18	1
ozone	0
p-benzoquinone	1
palladium 10\% on activated carbon	0
palladium dichloride	0
palladium on activated carbon	0
palladium on activated charcoal	0
palladium on calcium fluoride poisoned with lead	0
palladium(II) chloride benzonitrile complex	0
palladium(II) hexafluoroacetylacetonate	0
palladium(II) iodide	2

"column1"	"Min*(Score)"
palladium(II) trifluoroacetate	0
palladium(II)[(1,3-bis(diphenylphosphino)propane) (C6H5CN)2]*2BF4	0
pepsin from porcine gastric mucosa [EC 3.4.23.1]	1
per-rhenic acid	0
perchloric acid	0
phenol	1
phenylborondichloride	0
phenylboronic acid	3
phenyllithium	0
phenylmagnesium bromide	0
phenylmagnesium chloride	0
phenylphosphinic acid	0
phenylsilane	0
phenyltrimethylammonium tribromide	2
phosphate buffer	3
phosphazene base-P4-tert-butyl	0
phosphomolybdic acid	0
phosphonic acid diethyl ester	0
phosphoric acid	0
phosphorus pentachloride	0
phosphorus pentoxide	0
phosphorus tribromide	0
phosphotungstic acid	0
phthalic anhydride	0
pi-allyl-palladium chloride	0
picoline-borane complex	1
pipecolic Acid	3
piperazine	1
piperdinium acetate	3
piperidin-2-one	3
piperidine	3
pivalaldehyde	3
platinum(II) chloride	0
platinum(IV) oxide	0
poly(methylhydrosiloxane)	1
polyethylene supported arsine	0
polymer-bound dimethylaminopyridine	0
polymer-bound trimethyl ammonium cyanoborohydride	0
polymer-supported 1,8-diazabicyclo[5.4.0]undec-7-ene	0
polymer-supported BH(OAc)3	0

"column1"	"Min*(Score)"
polymer-supported chiral lithium amide	0
polymer-supported cyanoborohydride	0
polymethylhydrosiloxane	1
polyphosphoric acid	0
polyphosphoric acid containing 84percent of P2O5	0
polystyrene cyanoborohydride	0
polystyrene-bound 4-(N-benzyl-N-methylamino)pyridine	0
polystyrene-bound super Broensted acid	1
polystyrene-supported sulfonic acid	0
potassium	0
potassium 2-methylbutan-2-olate	0
potassium 3,7-dimethyloctan-3-olate	0
potassium acetate	3
potassium bromide	3
potassium carbonate	0
potassium chloride	3
potassium cyanide	0
potassium diazodicarboxylate	1
potassium dihydrogenphosphate	0
potassium ethoxide	0
potassium fluoride	3
potassium fluoride 18-crown-6	0
potassium fluoride on aluminum oxide	0
potassium fluoride on basic alumina	0
potassium formate	0
potassium hexacyanoferrate(III)	3
potassium hexafluorophosphate	3
potassium hexamethylsilazane	2
potassium hydride	0
potassium hydrogen bifluoride	0
potassium hydrogen difluoride	0
potassium hydrogencarbonate	0
potassium hydrogenfluoride	0
potassium hydrogensulfate	0
potassium hydroxide	0
potassium iodide	3
potassium methanolate	0
potassium peroxymonosulfate	0
potassium phosphate	3
potassium sulfate	3

"column1"	"Min*(Score)"
potassium tert-butylate	0
potassium tetrachloroaurate(III)	0
potassium thioacetate	3
potassium titanium oxalate dehydrate	1
potassium triethylborohydride	0
potassium trifluoroacetate	3
potassium trimethylsilonate	0
praseodymium(III) isopropoxide	0
praseodymium(III) trifluoromethanesulfonate	1
propan-1-ol	1
propionic acid	3
propylamine	3
propylene diammonium diacetate	3
pyridine	3
pyridine N-oxide	3
pyridine hydrochloride salt	3
pyridine hydrogenfluoride	3
pyridinium chlorochromate	0
pyridinium p-toluenesulfonate	3
pyridinium triflate	3
pyrrole	3
pyrrolidine	2
quinindine	3
quinine	3
rac-Ala-OH	3
rac-Pro-OH	3
racemic BINOL derived phosphoric acid catalyst	0
racemic TBAT	0
resin Amberlyst A-31	0
rhenium(I) pentacarbonyl chloride	0
rhodium (II) octanoate dimer	0
rhodium(II) acetate	0
rhodium(II) pivalate	0
rhodium(III) chloride hydrate	0
rubidium hydroxide	0
ruphos	1
salicylic acid	3
samarium	0
samarium diiodide	1
scandium(III) acetate	1

"column1"	"Min*(Score)"
sec.-butyllithium	0
selenium	0
silica gel	0
silicon carbide	3
silicon-supported cyanoborohydride reagent	0
silicotungstic acid hydrate	0
silver	0
silver (II) carbonate	0
silver carbonate	0
silver fluoride	3
silver hexafluoroantimonate	1
silver nitrate	3
silver tetrafluoroborate	0
silver trifluoroacetate	3
silver trifluoromethanesulfonate	3
silver(I) acetate	3
silver(I) hexafluorophosphate	3
silver(I) triflimide	3
silver(l) oxide	3
silver-graphite	3
sodium	0
sodium (triacetoxy)borohydride	0
sodium acetate	3
sodium amalgam	0
sodium amide	0
sodium azide	2
sodium bis(2-methoxyethoxy)aluminium dihydride	0
sodium bis(trifluoromethanesulfonyl)imide	1
sodium borohydride acetate	0
sodium butanolate	0
sodium carbonate	0
sodium chloride	3
sodium chlorite	1
sodium cyanide	1
sodium cyanoborohydride	0
sodium cyanoborohydride resin	3
sodium cyanotrihydroborate	0
sodium deuterium cyanoborohydride	0
sodium diacetoxy(acetyl)boranuide	0
sodium dihydrogen phosphate	3

"column1"	"Min*(Score)"
sodium dihydrogen phosphate monohydrate	3
sodium dihydrogenphosphate	3
sodium disulfate	0
sodium disulfite	0
sodium dithionate	3
sodium dithionite	0
sodium dodecyl-sulfate	3
sodium ethanolate	0
sodium formate	0
sodium hexafluoroantimonate	1
sodium hexamethyldisilazane	0
sodium hydride	0
sodium hydrogen sulfate	0
sodium hydrogencarbonate	0
sodium hydrogensulfite	0
sodium hydroxide	0
sodium iodide	0
sodium metabisulfite	0
sodium methoxide	0
sodium methylate	0
sodium nitrite	0
sodium ortho-iodobenzoate	1
sodium perborate	0
sodium perborate tetrahydrate	0
sodium periodate	0
sodium persulfate	0
sodium phenoxide	0
sodium phosphate	3
sodium pyrosulfate	3
sodium salt of sulphur oxide	1
sodium sulfate	3
sodium sulfide	0
sodium sulfite	0
sodium t-butanolate	0
sodium tert-pentoxide	0
sodium tetrachloroaurate(III) dihyrate	0
sodium tetrahydroborate	0
sodium tetrakis[(3,5-di-trifluoromethyl)phenyl]borate	0
sodium tri(benzoyloxy)borohydride	0
sodium triacetoxy borohydride	0

"column1"	"Min*(Score)"
sodium triacetoxyborane hydride	0
sodium triacetoxyborohydride	0
sodium tris(acetoxy)borohydride	0
solid phase supported Sc(III)	1
stannic bromide	0
succinic acid	1
sulfonated graphene	1
sulfonic acid supported on hydroxyapatite-encapsulated-gamma-Fe2O3	0
sulfur	0
sulfuric acid	0
suspension of male Wistar rat liver mitochondria	1
t r i s (4 , 4 ?-methoxydibenzylideneacetone)dipalladium(0)	0
t-butoxide	0
t-butyldimethylsiyl triflate	3
tBu4ZnLi2	1
tbepc	1
tellurium	0
tert-Butyl peroxybenzoate	0
tert-butyl (2S,3R)-2-amino-3-hydroxybutanoate	1
tert-butyl alcohol	3
tert-butyl carbazate	1
tert-butylammonium hexafluorophosphate(V)	0
tert-butyldimethylsilyl chloride	0
tert-butyldimethylsilyl triflate	3
tert-butyldiphenylphosphine	2
tert-butyldiphenylsilyloxy 4-hydroxyproline	3
tert-butylhypochlorite	0
tert-butylisonitrile	0
tert-butylmagnesium chloride	0
tert.-butyl lithium	0
tert.-butylhydroperoxide	0
tetra(4-chlorophenyl)porphyrin iron chloride	3
tetra(n-butyl)ammonium hydrogensulfate	1
tetra(n-butyl)ammonium hydroxide	0
tetra-(n-butyl)ammonium iodide	1
tetra-N-butylammonium tribromide	1
tetra-n-butylammoniumfluoride trihydrate	0
tetrabutoxytitanium	1
tetrabutyl ammonium fluoride	0
tetrabutyl-ammonium chloride	0

"column1"	"Min*(Score)"
tetrabutylammomium bromide	1
tetrabutylammonium acetate	3
tetrabutylammonium borohydride	0
tetrabutylammonium triphenyldifluorosilicate	3
tetrabutylammonium triphenyldifluorostannate	0
tetrachlorobis(tetrahydrofuran)titanium(IV)	2
tetrachloromethane	3
tetrachlorosilane	1
tetraethoxy orthosilicate	3
tetraethylammonium fluoride	0
tetraethylammonium iodide	1
tetrafluoroboric acid	0
tetrafluoroboric acid diethyl ether	0
tetrafluoroboric acid diethyl ether complex	0
tetrahydrofuran	3
tetrakis(4-phenyl)methane-benzimidazole containing porous organic polymer	3
tetrakis(acetato)dimolybdenum(II)	0
tetrakis(acetonitrile)copper(I)tetrafluoroborate	0
tetrakis(acetonitrile)palladium(II) bis(tetrafluoroborate)	0
tetrakis(acetonitrile)palladium(II) tetrafluoroborate	0
tetrakis(actonitrile)copper(I) hexafluorophosphate	0
tetrakis(trifluoroacetato)rhodium(II)	0
tetrakis(triphenylphosphine) palladium(0)	0
tetramethlyammonium chloride	3
tetramethoxymethane	3
tetramethylammonium triacetoxyborohydride	0
tetramethylenebis(magnesium chloride)	3
tetramethylpiperidyl MgCl LiCl	0
theophylline	3
thiamine diphosphate	3
thiazolium bromide	3
thionyl chloride	1
thiophene	3
thiophenol	1
tin	0
tin(II) chloride dihdyrate	0
tin(II) iodide	0
tin(II) trifluoromethanesulfonate	0
tin(IV) chloride	0
tin(ll) chloride	0

"column1"	"Min*(Score)"
titanium tetra-n-propoxide	0
titanium tetrachloride	0
titanium tetraisopropoxide	0
titanium tris(diethylamido)chloride	1
titanium(III) triisopropoxide	0
titanium(IV) bromide	1
titanium(IV) dichlorodiisopropylate	1
titanium(IV) iodide	1
titanium(IV) isopropylate	2
titanium(IV) tetraethanolate	0
titanium(IV) trichloride isopropoxide	0
titanium(IV)isopropoxide	0
titanocene(III) chloride	1
tol uene-4-sulfonic acid	0
toluene-4-sulfonic acid	0
toluene-4-sulfonic acid hydrazide	0
tri tert-butylphosphoniumtetrafluoroborate	0
tri-1-napthylphosphine	0
tri-n-butyl-tin hydride	0
tri-n-butyltin lithium	0
tri-tert-butyl phosphine	0
triacetoxy sodium borohydride	0
triacetoxyborane	1
tributyl borane	0
tributyl-amine	3
tributylphosphine	0
tricarbonylcyclopentadienyltungsten(II) chloride	0
trichloroacetic acid	3
trichloroacetonitrile	3
trichlorophosphate	0
trichlorosilane	0
tricyclohexylphosphine	0
tricyclohexylphosphine[1,3-bis(2,4,6-trimethylphenyl)-4,5-dihydroimidazol-2-ylidine][benzylidene]ruthenium(II) dichloride	3
tricyclopentylphosphine	0
triethanolamine	0
triethyl borane	0
triethyl borate	0
triethyl gallium	3
triethyl phosphate	0
triethyl phosphite	0

"column1"	"Min*(Score)"
triethyl-sulfopropylammonium dihydrogen phosphomolybdate	0
triethylamine	3
triethylamine hydrochloride	3
triethylammonium methylpolystyrene triacetoborohydride	1
triethylbutylammonium chloride	3
triethylphosphine	0
triethylsilane	2
triethylsilyl trifluoromethyl sulfonate	1
trifluoroacetic acid-d1	3
trifluoroacetic anhydride	3
trifluoroborane diethyl ether	1
trifluoromethylsulfonic anhydride	0
trifluorormethanesulfonic acid	0
trifuran-2-yl-phosphane	1
triisopropoxytitanium(IV) chloride	1
triisopropyl phosphite	0
triisopropylsilyl chloride	0
trimethoxysilane	0
trimethyl orthoformate	3
trimethylaluminum	0
trimethylamine	3
trimethylamine-N-oxide	0
trimethylphenylsilane	0
trimethylphosphane	2
trimethylsilyl acetate	3
trimethylsilyl bromide	0
trimethylsilyl iodide	0
trimethylsilyl trifluoromethanesulfonate	0
trimethylsilylazide	0
trimethylsilylmethyllithium	0
trimethylsilylphosphate	0
trimethylsilyltributyltin	0
triphenyl phosphite	0
triphenyl-arsane	1
triphenylacetic acid	3
triphenylborane	0
triphenylphosphine on polystyrene	0
triphenylsilyl perrhenate	0
tris hydrochloride	3
tris(2,4-di-tert-butylphenyl)phosphite gold(I) chloride	3

"column1"	"Min*(Score)"
tris(acetonitrile)(eta5-pentamethylcyclo-pentadienyl)rhodium(III) hexafluoroantimonate	0
tris(dibenzylideneacetone)dipalladium (0)	0
tris(dibenzylideneacetone)dipalladium(0) chloroform complex	0
tris(dimethylamino) sulphonium bifluoride	0
tris(dimethylamino)sulfonium trimethylsilyldifluoride	0
tris(ethoxy)monochloro titanium	1
tris(methoxyethoxyethyl)amine	3
tris(p-bromophenylammoniumyl) hexachloroantimonate	1
tris(pentafluorophenyl)borate	0
tris-(2,2'-bipyridine)ruthenium(II) chloride	3
tris-(2-carboxyethyl)-phosphine hydrochloride	3
tris-(dibenzylideneacetone)dipalladium(0)	0
tris-(m-sulfonatophenyl)phosphine	0
tris-(o-tolyl)phosphine	0
tris-(triphenylsiloxy)-vanadium oxide	0
trityl tetrakis(pentafluorophenyl)borate	0
tungstosilicic acid hydrate	0
urea	2
vanadyl acetylacetonate	0
vanadyl triflate	3
water	3
water-d2	3
ytterbium(III) triflate	3
ytterbium(III) trifluoromethanesulfonate hydrate	2
ytterbium(III) trifluoromethanesulfonate nonohydrate	2
yttrium(III) chloride	0
yttrium(III) trifluoromethanesulfonate	0
yttrium(lll) nitrate hexahydrate	0
zinc	0
zinc acetate dehydrate	3
zinc chloride diethyl ether	1
zinc diacetate	3
zinc dibromide	3
zinc dichloro(N,N,N?,N?-tetramethylethylenediamine)	3
zinc trifluoromethanesulfonate	3
zinc(II) chloride	3
zinc(II) hydroxide	0
zinc(II) iodide	3
zinc(II) oxide	3
zinc(II) sulfate	3

"column1"	"Min*(Score)"
zinc(II) tetrahydroborate	3
zirconium (IV) butoxide	0
zirconium complex of (R)-3,3'-diiodo-BINOL on 3 A MS	0
zirconium triflate	3
zirconium(IV) chloride	0
zirconium(IV) tert-butoxide	0
zirconocene dichloride	0
{(2-methyl-2-phenyl-propylidene)((2,6-dimethylphenyl)imido)molybdenum(VI)bis(hexafluoro-tert-but oxide)}	0
{(2-methyl-2-phenyl-propylidene)((2,6-dimethylphenyl)imido)molybdenum(VI)bis(hexafluoro-tert-butoxide)}	0
{(R)-H8-BINOL}Ti(O-i-Pr)2	2
(S)-3,3'-bis(4''-trifluoromethylphenyl)-2,2'-(2,2-bisbromo-2-stannapropane-1,3-diyl)-1,1'-binaphthyl	0
(1,4,7,10-tetraoxacyclododecane)	3
(1,3,5-triaza-7-phosphaadamantane)	2
(3R,5R,7R)-N-((S)-(6-methoxyquinolin-4-yl)((1S,2S,4S,5R)-5-vinylquinuclidin-2-yl)methyl)adamantane-1-sulfamide	2
(R)-(+)-(4,4'-bi-1,3-benzodioxole)-5,5'-diylbis(di(3,5-dimethylphenyl)phosphine)	1
(R)-2-(piperidin-1-yl)-1,1,2-triphenylethanol	3
1,2-bis-(dicyclohexylphosphino)ethane	3
1,3,5-trichloro-2,4,6-triazine	3
1,3-bis-(2,6-diisopropylphenyl)-imidazol-2-ylidene	3
1-(2,6-diisopropylphenyl)-3-(3-sulfonatopropyl)imidazolium	2
1-ethyl-(3-(3-dimethylamino)propyl)-carbodiimide hydrochloride	3
1-ethyl-3-methylimidazolium hexafluorophosphate	2
2,2'-azobis(isobutyronitrile)	1
2,2'-iminobis[ethanol]	3
2,2-bis[(4S)-4-isopropyloxazolin-2-yl]propane	2
2,3-diazobicyclo[2.2.1]heptane bis-hydrochloride	3
2,3-dimethyl-buta-1,3-diene	2
2,4,6-triisopropyl-N-((S)-(6-methoxy-2-phenylquinolin-4-yl)((1S,2S,4S,5R)-5-vinylquinuclidin-2-yl)methyl)benzenesulfonamide	1
2,6-di-tert-butyl-4-methyl-phenol	3
3-butyl-1,2-dimethyl-1H-imidazol-3-ium hydroxide	2
3-methyl-N-(3-methylbutyl)-1-butanamine	3
3-quinuclidinol	3
4-(benzyloxy)-N-(2-{1-[(4-fluorophenyl)methyl]piperidin-4-yl}ethyl)benzamide	2
4-chloro-benzenesulfonic acid	1
4-chlorobenzophenone	3
4-hydroxy-4-[2-(2,2,2-trifluoro-ethanoyl-amino)-ethyl]-piperidine-1-carboxylic acid tert-butyl ester	3
9-bora-bicyclo[3.3.1]nonane	2

"column1"	"Min*(Score)"
9-borabicyclo[3.3.1]nonane	2
9-borabicyclo[3.3.1]nonane dimer	2
Acetyl bromide	3
(1R,2R)-1,2-bis[(2-diphenylphosphanyl)benzoylamino]cyclohexane	1
1,4-dichlorocyclohexane	2
p-toluenesulfonic acid monohydrate	1
p-toluenesulfonyl chloride	2
triphenylphosphine	1

KNIME Report II - salt table

Knime report *powered by Birt*

"salt string"	"salt smiles"
[Cl-]	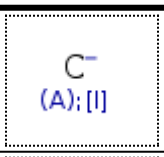
[Br-]	
[Br]	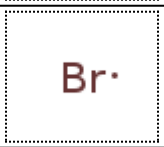
[BH4-]	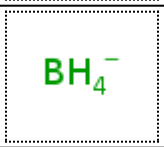
[Cl]	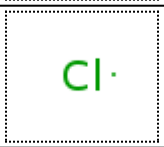
[F-]	
[F-][B+3]([F-])([F-])[F-]	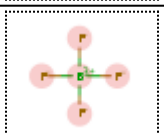
[F-][P+5]([F-])([F-])([F-])([F-])[F-]	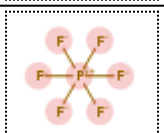
[H][N]([H])([H])[H]	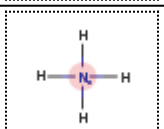
[I-]	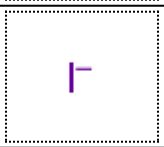
[I]	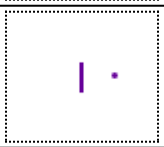

"salt string"	"salt smiles"
[N]	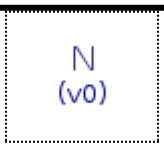
[N](=O)(O)O	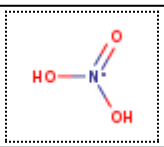
[NH4]	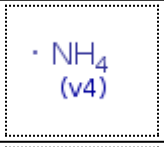
[NH4+]	
[O-][Cl]=O	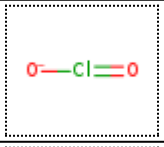
[O-]Cl(=O)(=O)=O	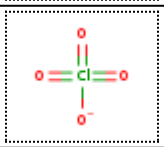
[O-]Cl=O	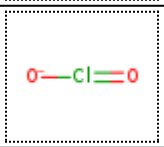
[O-]N(=O)=O	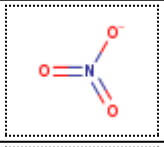
[O-]P([O-])([O-])=O	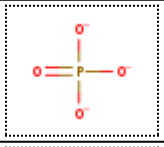
[O-]S([O-])(=O)=O	
[O-]S(=O)(=O)C(F)(F)F	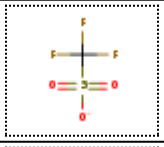
[O-]S(O)(=O)=O	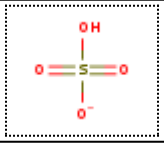

"salt string"	"salt smiles"
[O-2]	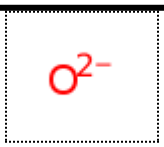
[OH-]	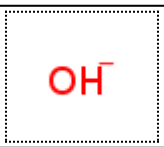
[O]	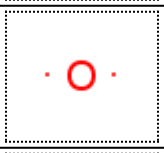
[P](=O)(O)(O)O	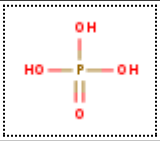
[P](F)(F)(F)(F)(F)F	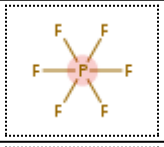
[S-2]	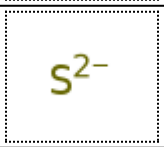
[S](=O)(=O)(O)O	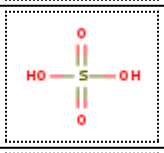
B	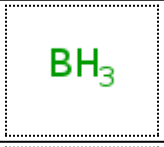
Br	
C[Si](C)(C)[O-]	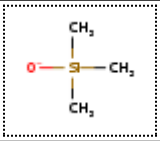
Cl	
Cl.Cl	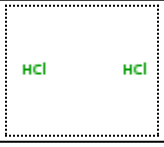

"salt string"	"salt smiles"
Cl[Sb](Cl)(Cl)(Cl)(Cl)Cl	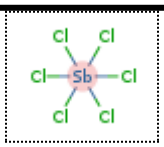
Cl[Sn](Cl)(Cl)Cl	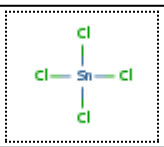
ClCCl	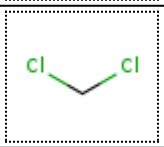
F	
F[B-](F)(F)F	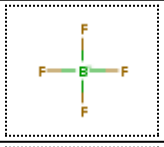
F[B](F)(F)F	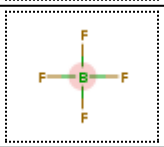
F[B](F)(F)F	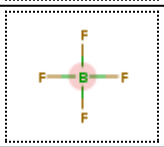
F[P-](F)(F)(F)(F)F	
F[P](F)(F)(F)(F)F	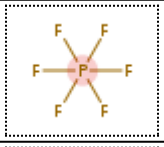
F[Sb-](F)(F)(F)(F)F	
F[Sb](F)(F)(F)(F)F	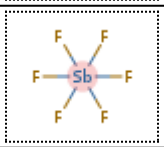
I	

"salt string"	"salt smiles"
N	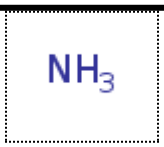
NO	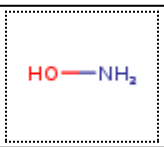
O	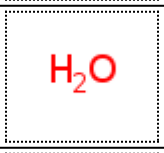
O[Cl](=O)(=O)=O	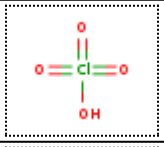
O=S(=O)([N-]S(=O)(=O)C(F)(F)F)C(F)(F)F	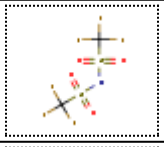
O=S(=O)([N-]S(=O)(=O)C(F)(F)F)C(F)(F)F	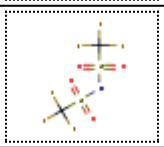
O=S(=O)(O)O	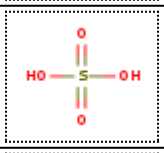
OC(=O)C(F)(F)F	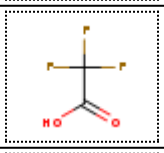
OCl(=O)(=O)=O	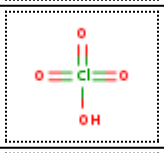
ON(=O)=O	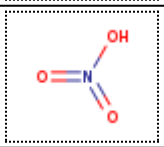
S	
[Ag+]	

"salt string"	"salt smiles"
[57Fe++]	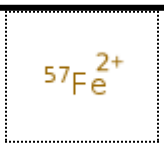
[Al+3]	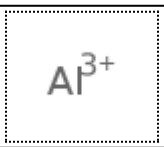
[Ba+2]	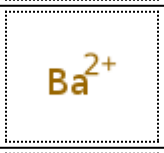
[Bi+3]	
[Ca]	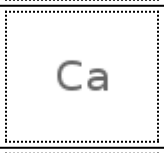
[Ca++]	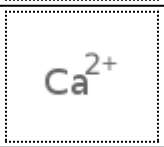
[Cd]	
[Cd+]	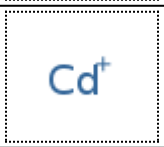
[Cd+2]	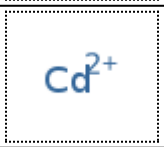
[Ce]	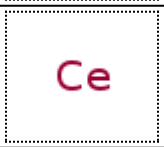
[Ce+4]	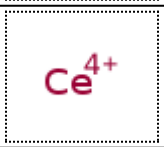
[Cl-][Fe+3]([Cl-])([Cl-])[Cl-]	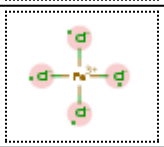

"salt string"	"salt smiles"
[Co]	
[Co++]	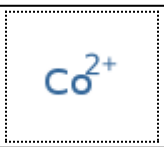
[Co+2]	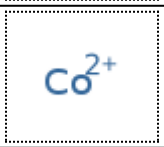
[Co+3]	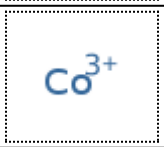
[Cs+]	
[Cu]	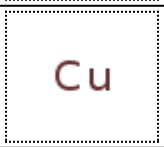
[Cu+]	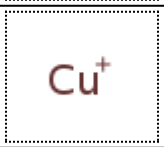
[Cu++]	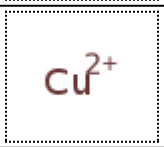
[Cu+2]	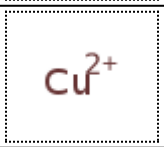
[Er+3]	
[Eu+3]	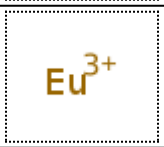
[Fe]	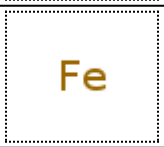

"salt string"	"salt smiles"
[Fe++]	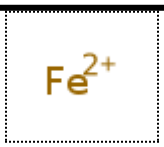
[Fe+2]	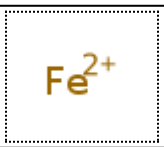
[Fe+3]	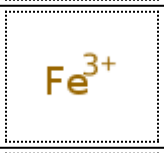
[Ga+2]	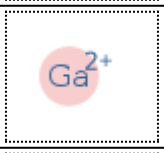
[Ga+2]Ga+2]	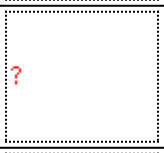
[Gd+3]	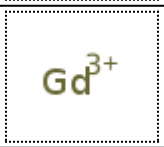
[H]	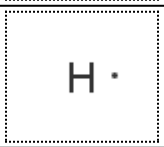
[H+]	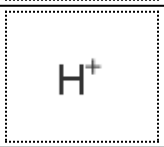
[H-]	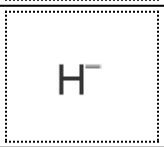
[I-][Zn++]([I-])([I-])[I-]	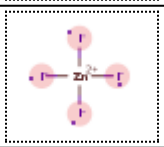
[I-][Zn+2]1([I-])[I-][Zn+2]([I-])([I-])[I-]1	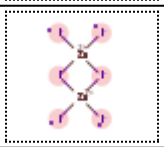
[Ir+3]	

"salt string"	"salt smiles"
[K]	
[K+]	
[KH]	
[La]	
[La+3]	
[Li]	
[Li+]	
[LiH]	
[Lu+3]	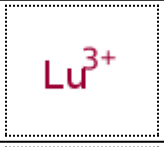
[Mg]	
[Mg++]	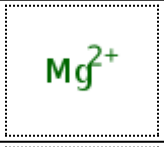
[Mg+2]	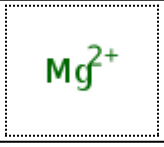

"salt string"	"salt smiles"
[Mn]	
[Mn+2]	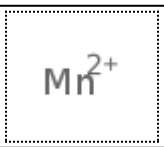
[Mo]	
[Mo+6]	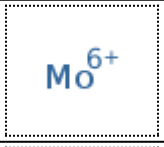
[Mo+6][Mo+6]	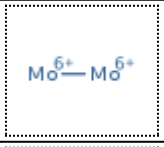
[Na]	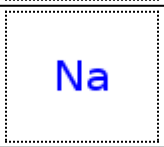
[Na+]	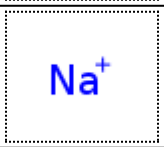
[NaH]	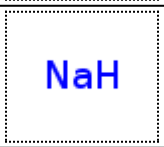
[Ni]	
[Ni+2]	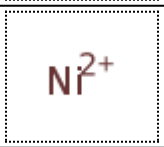
[Pb+2]	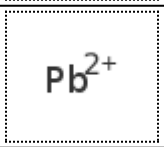
[Pd]	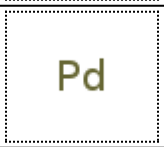

"salt string"	"salt smiles"
[Pd++]	
[Pd+2]	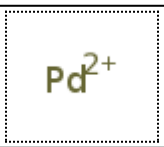
[Pt+2]	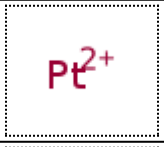
[Re+]	
[Ru]	
[Sn]	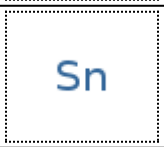
[Sn+4]	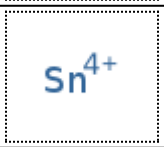
[Sr]	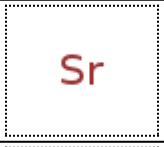
[SrH2]	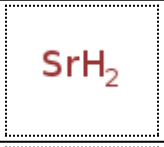
[Ta+5]	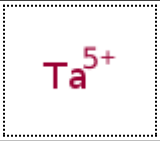
[Tc+2]	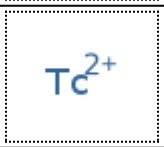
[Ti]	

"salt string"	"salt smiles"
[Ti+4]	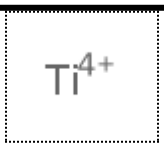
[Tm+3]	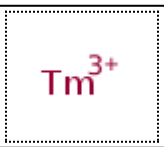
[Yb+3]	
[Zn]	
[Zn]	
[Zn+2]	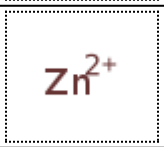
[Zr+4]	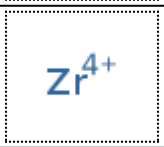
C[N+](C)(C)C	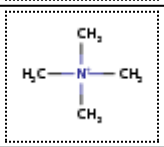
F[As](F)(F)(F)(F)F	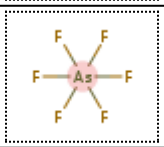
Mo	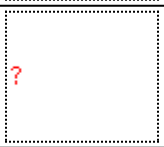
Ni	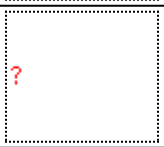
O=[Mo++]=O	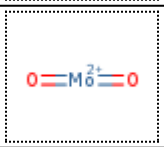

"salt string"	"salt smiles"
O=[Mo+2]=O	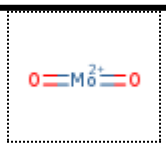
O=[Tc-](Cl)(Cl)(Cl)Cl	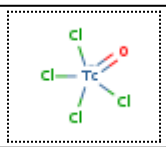
O=[U+2]=O	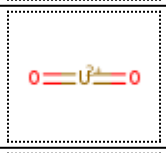
O=[V+2]	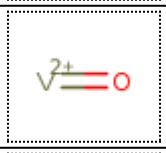
[C]	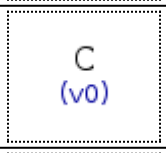
[cH-]1cccc1	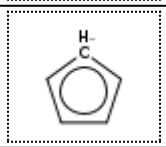
[CH3][S](=O)(=O)(O)	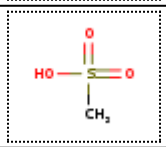
[CH3]C(=O)O	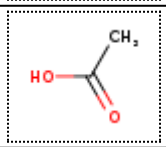
[O-]C	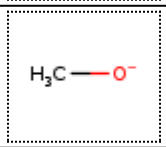
[O-]C=O	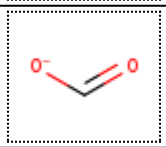
C	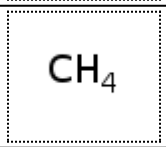
C(=O)(C(=O)[O-])[O-]	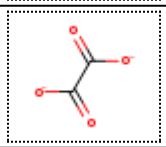

"salt string"	"salt smiles"
C(C(=O)[O-])C(CC(=O)[O-])(C(=O)[O-])O	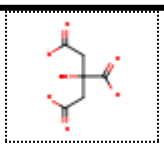
C[O-]	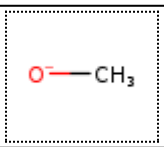
c1cc([CH3])ccc1[S](=O)(=O)(O)	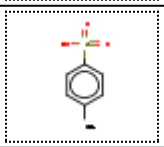
CC(=O)[O-]	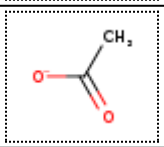
CC(O)C(=O)O	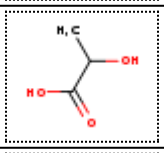
CC[O-]	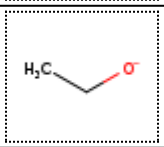
CCCCCCCCCCCCCCCCCC(O[Al](O)O)=O	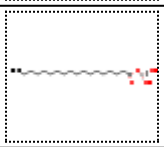
ClCCl	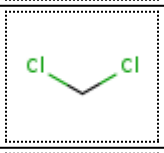
COC([S-])=S	
COC([S-])=S	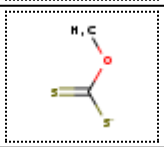
COS(O)(=O)=O	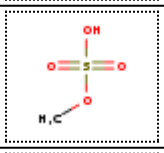
CS([O-])(=O)=O	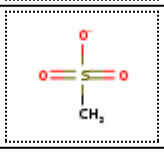

"salt string"	"salt smiles"
FC(F)(F)C(=O)O	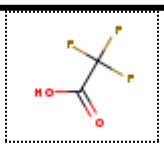
[Dy]	
[Zn++]	
[Cl-]	
[Hg++]	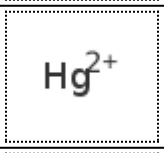
[Hg]	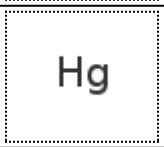
[Dy+++]	
S([O-])(=O)=O	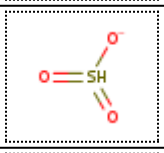
Cc1ccc(cc1)S([O-])(=O)=O	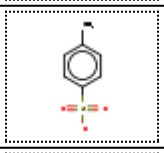
COS([O-])(=O)=O	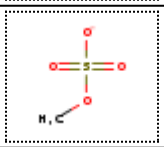
S([O-])(=O)=O	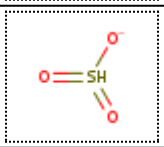
Cc1ccc(cc1)S([O-])(=O)=O	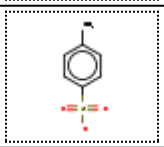

"salt string"	"salt smiles"
COS([O-])(=O)=O	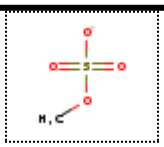
[O-]S(=O)(=O)c1ccccc1	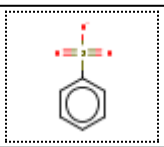
CS(O)(=O)=O	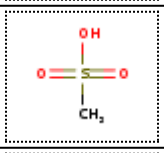
OS(O)(=O)=O	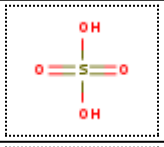
Cc1cc(C)c(c(C)c1)S([O-])(=O)=O	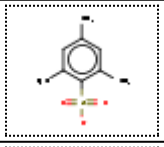
OS(=O)(=O)C(F)(F)F	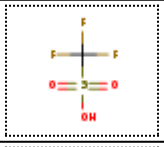
Cc1ccc(cc1)S(O)(=O)=O	
CC[S+](CC)CC	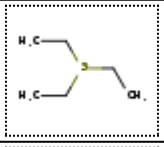
OS([O-])(=O)=O	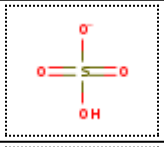
COS(=O)(=O)OC	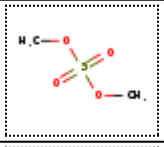
O=[S-](=O)c1ccccc1	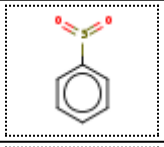
CS(C)=O	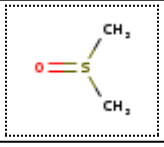

"salt string"	"salt smiles"
C[S+](C)(C)=O	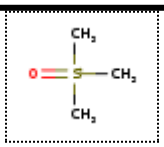
Fc1c(F)c(F)c(c(F)c1F)[B-](F)(c1c(F)c(F)c(F)c(F)c1F)c1c(F)c(F)c(F)c(F)c1F	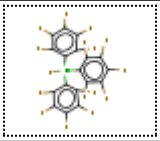

KNIME Report IV - LGs list

Knime report *powered by Birt*

"LGs"	"LGs rendered with Marvin"
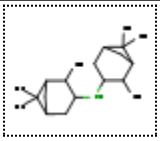	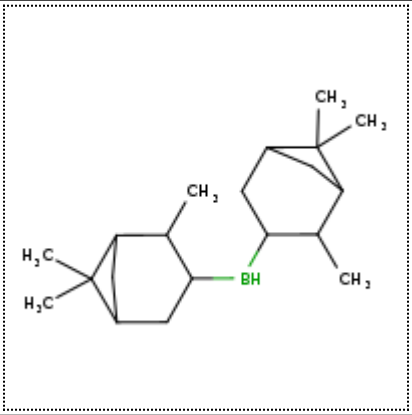
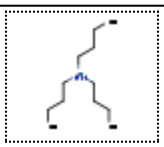	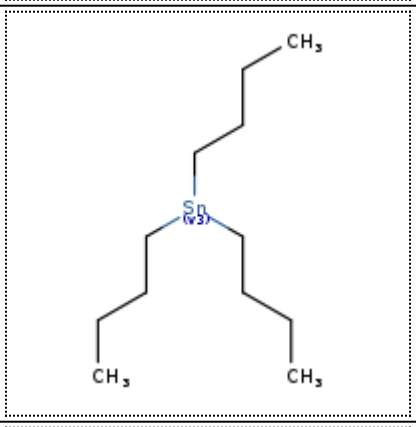
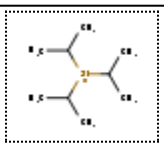	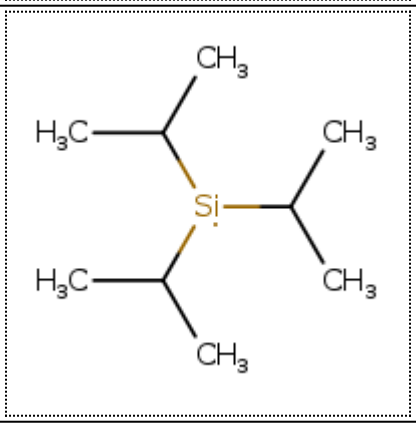

"LGs"	"LGs rendered with Marvin"
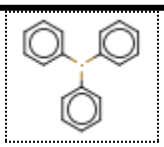	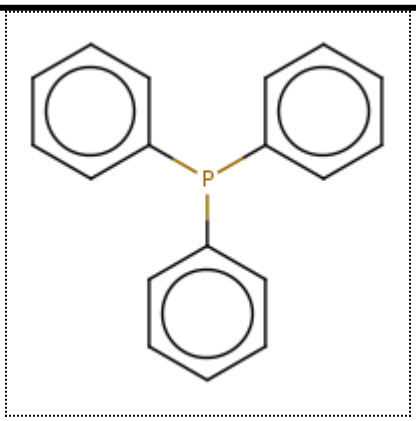
	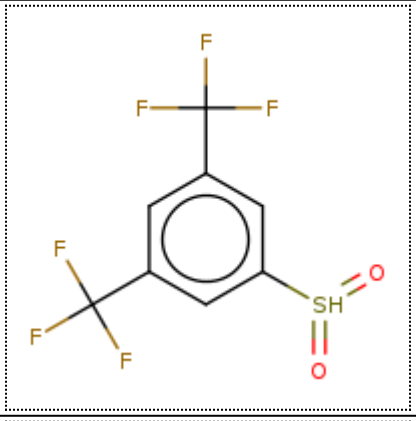
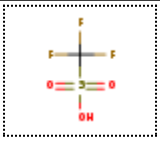	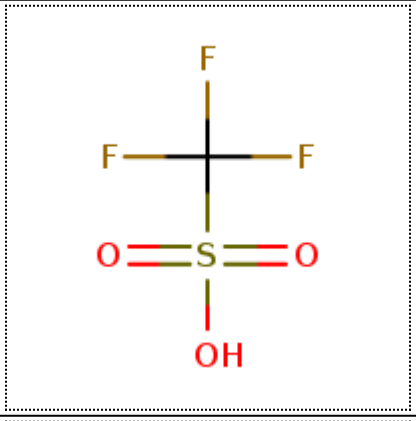
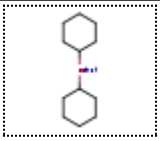	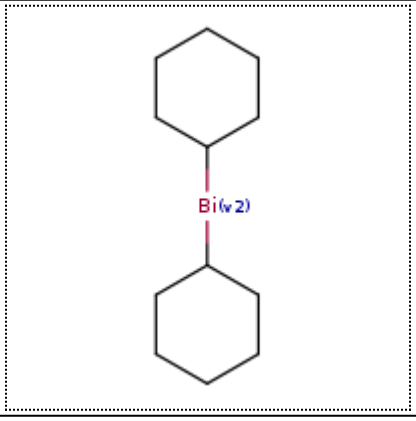

"LGs"	"LGs rendered with Marvin"
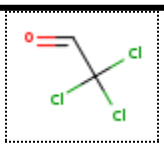	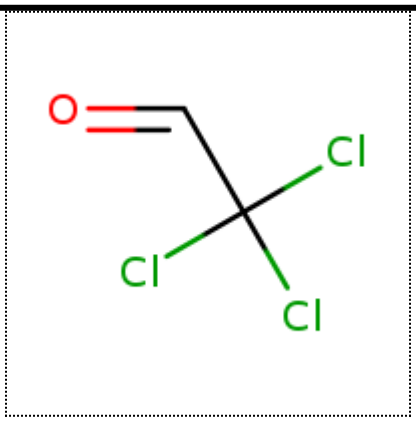
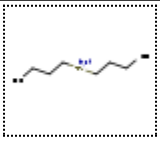	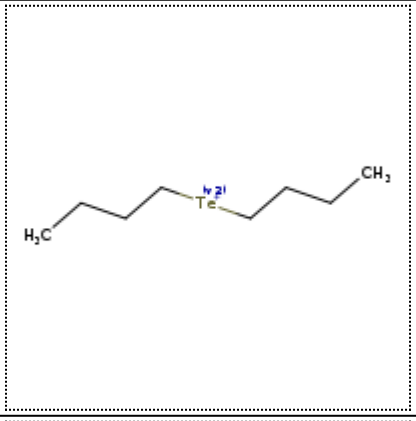
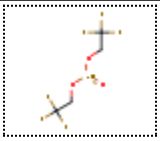	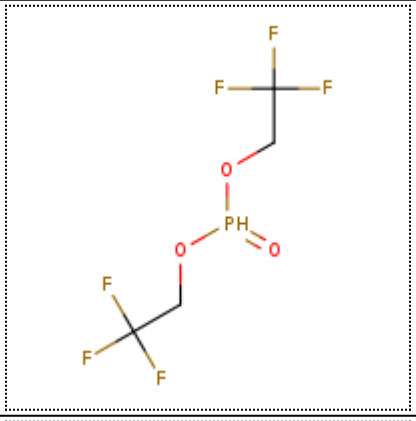
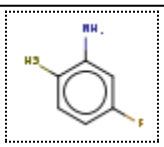	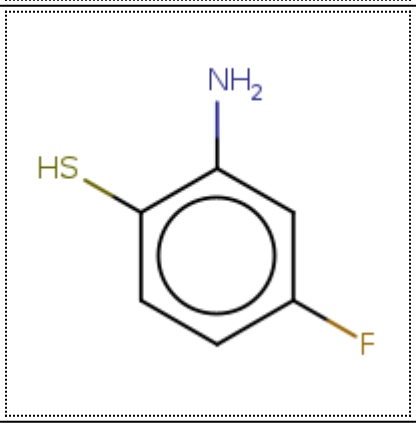

"LGs"	"LGs rendered with Marvin"
	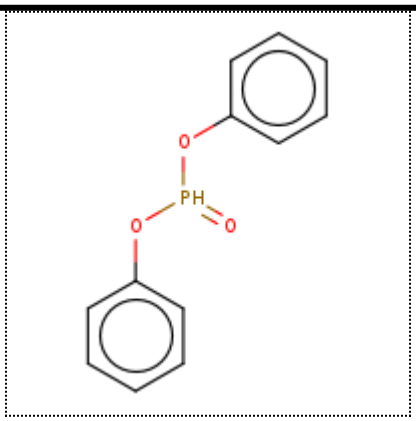
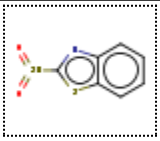	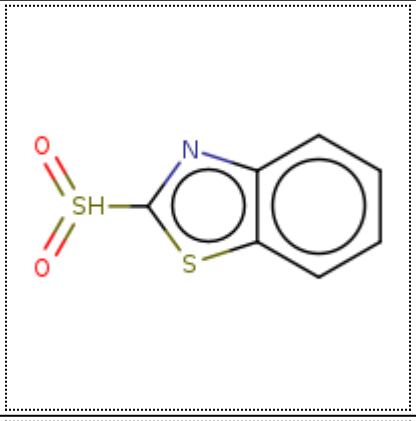
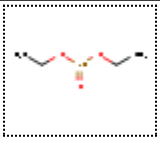	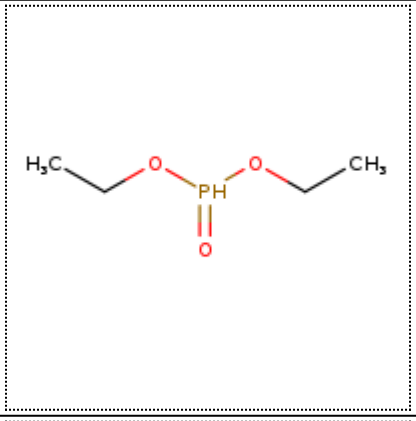
	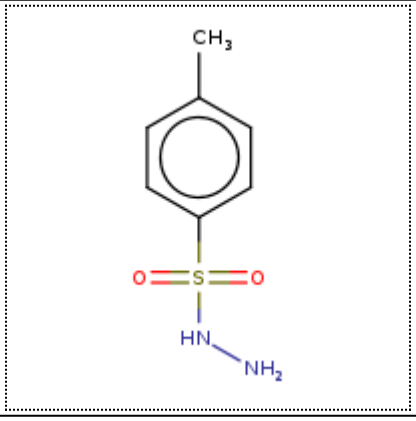

"LGs"	"LGs rendered with Marvin"
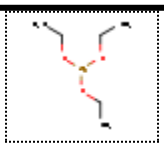	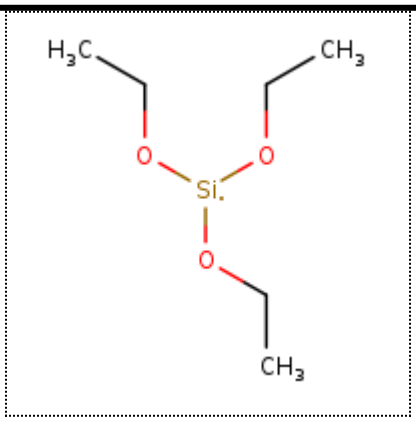
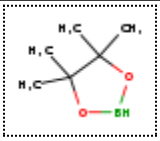	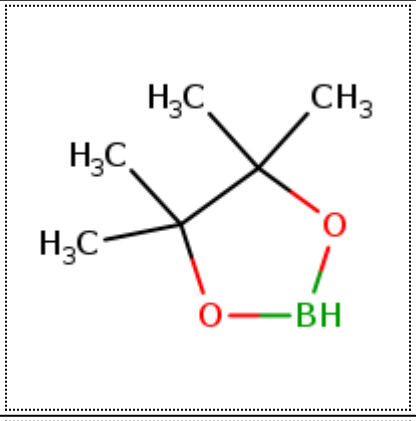
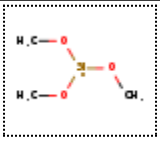	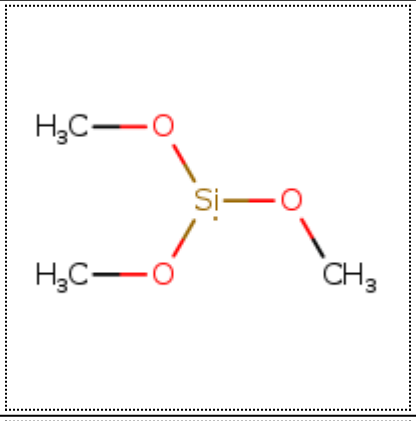
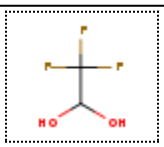	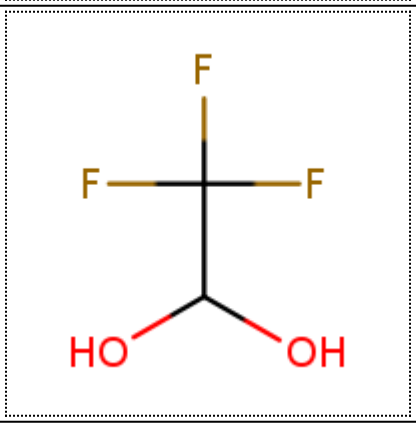

"LGs"	"LGs rendered with Marvin"